Synthesis of Novel Antimicrobial Chlorhexidine Particles for Biomedical Application

By

Rui Sun

DDS (China) MSc (UK)

A thesis submitted in fulfilment of the requirements for the degree of Doctor of Philosophy in Institute of Dentistry, Queen Mary University of London

Institute of Dentistry, Bart's and The London School of Medicine and Dentistry

Queen Mary University of London

17/1/2022

Barts and The London
School of Medicine and Dentistry

Statement of Originality

I, Rui Sun, confirm that the research included within this thesis is my own work or that where it has been carried out in collaboration with or supported by others, that this is duly acknowledged below, and my contribution indicated. Previously published material is also acknowledged below.

I attest that I have exercised reasonable care to ensure that the work is original and does not to the best of my knowledge break any UK law, infringe any third party's copyright or other Intellectual Property Right, or contain any confidential material.

I accept that the College has the right to use plagiarism detection software to check the electronic version of the thesis.

I confirm that this thesis has not been previously submitted for the award of a degree by this or any other university.

Signature: Rui Sun

Abstract

Aims: To synthesize and characterize calcium, strontium, zinc and fluoride containing CHX particles and incorporate them into gels for antibacterial applications, as well as explore the surface crystallisation of the particles.

Methods: Novel chlorhexidine (CHX) particles were synthesized by mixing CHX diacetate (CHXD) with $CaCl_2$, $SrCl_2$, $ZnCl_2$, NaF or NaCl-NaF mixtures to harvest CHX-$CaCl_2$ / CHX-$SrCl_2$ / CHX-$ZnCl_2$ / CHX-$ZnCl_2$ / CHX-NaF / CHX-NaF-NaCl particles, which were characterized using; SEM, FTIR, XRD and UV-Vis. Antibacterial ability was evaluated by incubating three major sub-gingival bacteria (*Porphyromonas gingivalis*, *Fusobacterium nucleatum* and *Aggregatibacter actinomycetemcomitans*) and cytotoxicity was measured using mouse fibroblast L929 cells. Alkaline phosphatase activity and bone-like mineral nodules expression of MC3T3-E1 cells were carried out.

The synthesized CHX-$CaCl_2$, CHX-$SrCl_2$ and CHX-$ZnCl_2$ particles (1%) were incorporated into HPMC gels or used for surface coating via a rinse method. A CHX digluconate (1%) HPMC gel and Corsodyl® were used as comparison gels. Gels were immersed in deionized water, phosphate-buffered saline (PBS) and artificial saliva (AS) to characterize drug release behaviour. The released samples were examined against *P. gingivalis* (strain 381) using the zone of inhibition method.

The synthesized CHX-$CaCl_2$ particles were coated on the surface of the human teeth and medical devices including polymethyl methacrylate denture base, a regular neck implant (ø3.3mmRN, 8mm, lot RA221, Straumann) and orthodontic brackets (Victory Series, 3M Unitek, Monrovia, Calif). The coated bracket was immersed in AS to characterize drug release kinetics.

Results: The CHX-$CaCl_2$, CHX-$SrCl_2$ and CHX-$ZnCl_2$ particle sizes were controlled via processing time and temperature and were as safe as CHXD, with antibacterial activity against a range of oral pathogens. CHX-$ZnCl_2$ particles gave pH-responsive release of Zn^{2+} ions. XRD and FTIR indicated a unique crystal structure for the novel particles (CHX-$CaCl_2$ / CHX-$SrCl_2$ / CHX-$ZnCl_2$ / CHX-$ZnCl_2$ / CHX-NaF / CHX-NaF-NaCl) compared with CHXD. Alkaline phosphatase activity and bone-like mineral nodules of MC3T3-E1 cells were not significantly promoted in the CHX-$SrCl_2$ and CHX-$ZnCl_2$ particles when compared with the cell only group.

CHX release of CHX-$CaCl_2$ / CHX-$SrCl_2$ / CHX-$ZnCl_2$ gels was via a sustained release throughout the assay period in all mediums (PBS and DW). The CHX digluconate gel in contrast showed phases of burst CHX release in DW and PBS. All test and comparison gels displayed lower cumulative CHX release when immersed in PBS compared to deionised water. Dialysates from novel CHX HPMC gels (PBS) exhibited inhibition of P. gingivalis at all time points. Corsodyl® gel failed to inhibit *P. gingivalis* at 2 weeks. SEM / digital images revealed rapid crystallisation of dendritic CHX-$CaCl_2$ on teeth, titanium implants and brackets. The amount of CHX loaded into the CHX-$CaCl_2$ particles and coated onto brackets was controlled by adjusting the concentration of CHXD.

Conclusions: Novel CHX particles containing calcium/strontium/zinc and fluoride were synthesized, which had a sustained drug release and were effective against a range of oral pathogens, with reduced cytotoxicity, and a smart pH-responsive drug/ ion release. Novel CHX particles were incorporated into gels or surface-coated on a range of medical devices and teeth, showing sustainable and antimicrobial efficacy.

These particles show great potential for the prevention or reversal of caries and infections in Medicine and Dentistry.

Acknowledgements

This research would not have been possible without the sponsorship from my parents and care from the family.

I would like to thank my supervisors Dr Mike Cattell, Dr Robert Whiley Prof Gleb Sukhorukov for their excellent guidance and invaluable assistance which enable me to complete my thesis successfully. I am particularly grateful to Dr Mike Cattell for his dedicated supervision and inspiration, without his selfless advice, guidance and constant feedbacks and discussions, this PhD would not be achieved. I would like to thank Professor Ama Johal, Dr David J Gould and Dr Simon C.F. Rawlinson for their help in my experimental works, for which I am much obliged. An especially thankful is expressed to Dr Natalia Karpukhina and Dr Hong Wan for their massive supports and advice besides the research.

I am very grateful to all my fellow students in the Blizard institute and SEMS for all the fun and memorable time we had in the PhD office and all the help you offered in the laboratory room. I thank especially Dr Mei Huang, Dr Rebecca Yuan, Dr Jutams Uttagomol, Miss Yunying Huang, Mr Usama Sharif Ahamd, Miss Javeria Khalid, Mr Haoran Chen and Miss Qian Guo. My PhD journey would not have been so enjoyable without all of you.

Last but not least, I would like to thank my parents for their love and unconditional support, my friend Miss Keren Wang for all the happiness that she brings to me and my boyfriend Dr Jiaxin Zhang for his love, encouragement, which all make me motivated, confident and strong.

Table of Contents

List of Figures

List of Tables

Abbreviations

CHX; Chlorhexidine

CHXD; Chlorhexidine diacetate

PBS; Phosphate buffered saline

AS; Artificial saliva

SRP; Scaling and root planning

RSD; Root surface debridement

BI; Bleeding index

UV/Vis; Ultraviolet-Visible spectroscopy

XRD; X-ray diffraction

SEM; Scanning electron microscopy

ISE; Ion selective electrode

EDX; Elemental dispersive X-ray analysis

Chapter 1. Literature Review of Common oral diseases

1.1 Periodontal Disease

Periodontal disease is characterized by chronic inflammatory lesions and destruction of the supporting periodontal tissues [1]. The periodontium including the gingiva, the periodontal ligament, the alveolar bone and the root cementum comprises the tissues which support the tooth [2]. During the process of periodontal disease, the bacteria may attach to tooth surfaces, to epithelial surfaces of the gingival crevice or periodontal pocket [3]. Additionally, this disease may be caused by adverse changes in the composition of the local microbiota. Local area conditions change in the subgingival region such as increased GCF (Gingival crevicular fluid) flow during inflammation which allows the proliferation of anaerobic microbiota switching from aerobic microbiota [4]. Thus, increased flow of GCF causes the microbiota to shift from Gram-positive community to Gram-negative periodontal pathogens [5]. Gingivitis is the early stage of gingival inflammation which have been associated with the increased prevalence of serval bacteria including *F.nucleatum, Prevotella, and capnocytophaga* [6]. However, in the later stages (periodontitis), the gram-negative bacterial including *P. gingivalis, A. actinomycetemcomitans and Tannerella forsythensis* will be observed [7]. In the final stages of periodontitis, it may cause damage to connective tissues and even tooth loss [8].

1.1.1 Oral microbial morphology

Evidence exists indicating that the specific gram-negative oral bacteria play an important role in progression of periodontal disease [9]. Oral bacteria reproduce quickly

and can tolerate a wide range of environmental conditions. They are complex and highly variable microbes [10]. Different types of microbes have different shapes. Normally they come in four basic shapes including spherical (cocci), rod-shaped (bacilli), arc shaped (vibrio), and spiral (spirochete) [11]. The basic bacterial structure includes the cell wall, cell membrane, cytoplasm, nuclear material, ribosome, plasmid, etc. Special structures like flagellum, pilus, capsule or spores are only found in some bacteria [12].

The cell membrane is a selectively permeable biological membrane which is made of a lipid bilayer. The lipid bilayer is embedded with carrier proteins which possess specific functions. The cytoplasm is the gel-like substance within the cell membrane. Plasmids are small, circular, double-stranded DNA molecules and are genetic material. They are able to replicate independently of chromosomal DNA and transmit genes from one bacterium to another. It is also able to stain these bacteria using different colours (crystal violet and safranin). The gram-positive bacteria have a thick peptidoglycan layer and no outer lipid membrane while gram-negative bacteria have a thin peptidoglycan layer and an outer lipid membrane [13]. Thus, the gram-positive bacteria stain violet due to the presence of a thick layer of peptidoglycan can retain the crystal violet. And the decolourized gram-negative cells will be stained red [14]. The bacterial nuclear material is termed nucleoid. The function of the nucleoid is similar to the nucleus such as growth, metabolism, reproduction etc. [12].

1.1.2 Periodontal Plaque

Dental plaque can be defined as the diverse community of micro-organisms found on the tooth surface as a biofilm, embedded in an extracellular matrix of polymers of host

and microbial origin [15]. Löe (1965) established that the key aetiological factor in the development of gingival inflammation was the accumulation of plaque [16]. If initial gingival inflammation continues, periodontitis will develop on the hard root surface adjacent to the soft tissues of the supporting periodontium. Periodontal disease may be confined to the gingiva (gingivitis) or extend to the deeper supporting structures. Specifically, the periodontal ligament and the alveolar bone that supports the teeth (periodontitis) can be deconstructed. In addition, the associated periodontal pocket would form and ultimately lead to loosening and loss of the affected teeth. Periodontitis threatens tooth retention affecting 10 - 15% of adults in the UK, with different degrees of bone loss needing treatment [2]. In this process, plaque plays an important role in the development and pathogenesis of periodontal disease [17].

In conclusion, gingivitis and periodontitis are the same chronic inflammatory processes [18]. A similar cause-effect relationship between the accumulation of plaque and the development of peri-implant mucositis was seen in an experimental study on implants [19]. It had been found that peri-implant mucositis is the precursor for peri-implantitis [20]. There is clear evidence that the accumulation of plaque is the key factor in both periodontal and peri-implant disease. So, the treatment of those diseases should focus on plaque control.

It is important to understand plaque and the bacterial environment so that the drug will be required to act against it. Plaque is a specific type of sticky biofilm formed by the interaction of salivary coating. These microorganisms are adherent to each other and/or to surfaces or interfaces [17], as a result of the dynamic balance between microbial attachment processes [15].

The crucial survival strategy for the microorganisms is the ability of plaque to adhere to the tooth or implant surface. The bacteria in the plaque can not only adhere to the hard tissue, but also deep periodontal tissues such as periodontal pockets and co-aggregate to other bacteria within the biofilm.

There are over 1000 different species of bacteria at 10^8 to10^9 bacteria per ml of saliva. There are around 1.7×10^{12} bacteria in 1g plaque [21], which consists of different species [22]. In the beginning, the initial colonisation of plaque is mostly by aerobic and facultative anaerobes. Specific surface receptors on gram-positive cocci and rods allow the adherence of gram-negative bacteria, which otherwise lack the ability to attach directly to the pellicle. With prolonged accumulation and maturation of plaque and the progression of the periodontitis, the microflora shifts from gram-positive to gram-negative organisms. Socransky (1998) proposed that bacterial species exist in complexes in sub-gingival plaque and identified five of these complexes that were repeatedly found together in periodontitis [23]. Those complexes are grouped as the red complex because of their shared strong association with periodontitis (i.e. high numbers of these usually means period is active). The red complex species are the relatively last microorganisms to establish in the plaque biofilm.

The status and pocket depth will affect the composition of sub-gingival biofilms [24]. Further, the severity and progression of periodontitis are also influenced by host factors and environmental factors such as obesity, smoking and IL-1 polymorphism [25,26]. The studies have all shown increased proportions of red complex species in worsening states of periodontitis. The major pathogens responsible for advancing periodontitis have been identified as *Porphyromonas gingivalis, Tannerella forsythia,*

and Treponema denticola [27]. Multiple studies indicate the high prevalence of A. actinomycetemcomitans in patients with aggressive periodontitis [28,29].

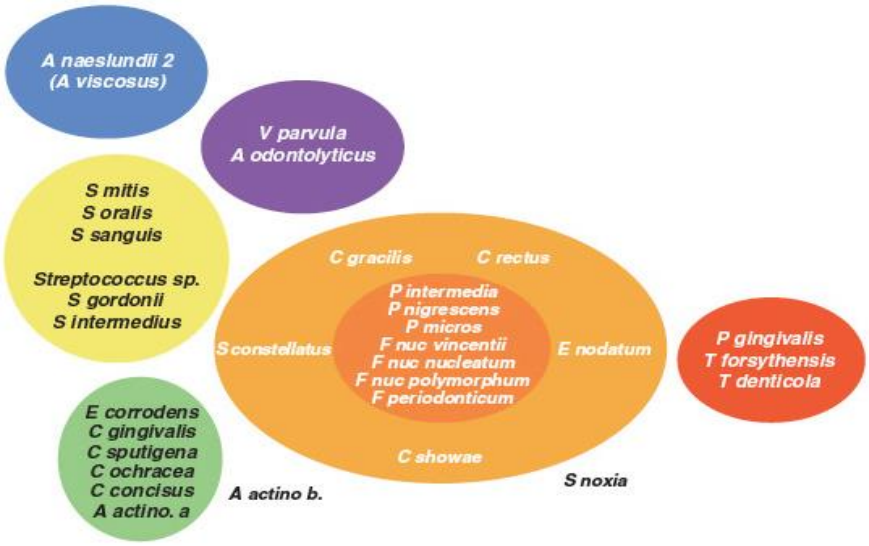

Figure 1. Subgingival microbial complexes [23].

1.1.3 Major Pathogens in Advancing Periodontitis and Peri-implantitis

There is a strong correlation between *A. actinomycetemcomitans* and initiation and progression of aggressive periodontitis [30]. *A. actinomycetemcomitans* is a gram-negative, anaerobic coccobacillus bacterium. It is able to produce a variety of virulence factors to modulate the host immune system, including tissue destruction and inhibiting tissue repair [31]. *A. actinomycetemcomitans* can produces cryptolectal distending toxin (CDT) and leukotoxin which are exotoxins to cause death of the host issues by blocking cell proliferation and inducing cell death [31,32].

It has been reported that *Porphyromonas gingivalis* has been frequently associated with and periodontal disease activities [33]. Although this anaerobe species is a late colonizer in bacterial plaque, it can rapidly and actively invade gingival sulcus epithelial cells, and potentially the underlying soft and hard tissues [8]. As a key pathogen,

Porphyromonas gingivalis can survive, replicate, and disseminate from cell to cell through the actin cytoskeleton bridge, and affect cell-cycle pathways after the intracellular invasion. After its invasion, it can block the epithelial cell interleukin-8(IL-8) response to other oral bacteria, indicating the host may not detect other bacterial colonization and cannot direct leukocytes to remove them [34]. Thus, the other species may rapidly establish the subgingival biofilms, enhancing the progression of the disease. This may be the reason that *Porphyromonas gingivalis* is frequently associated with active tissue destruction.

A previous study indicated that *Porphyromonas gingivalis, Tannerella forsythia*, and *Treponema denticola* are now regarded as the major pathogens in advancing periodontitis [27]. The prevention of periodontal diseases is traditionally targeted at mechanical or non-specific control of the plaque biofilm because this is the precipitating factor. The use of antimicrobial agents such as CHX represents a valuable complement to mechanical plaque control [35]. The strategies should ideally prevent plaque without markedly affecting the oral environment. However, actual periods of exposure to antimicrobial agents during mouth rinsing can be very short, amounting to about 1 minute [36].

Several implant systems are now in use to replace missing teeth, and most integrate with bone without complications. In peri-implantitis, anaerobic Gram-negative organisms predominate [37]. Further, in peri-implant inflammation, *Aggregatibacter actinomycetemcomitans, Porphyromonas gingivalis* and *Preevotella intermedia* is playing an important role. However, *Tannerella forsythensis, Fusobacterium nucleatum, Parvimonas micra* and spirochetes can often also be isolated from failing implants [38,39]. Microorganisms primarily not associated with periodontitis, such

as *Staphylococcus* spp., *enteric rods* and *Candida* spp., can also be found [40]. Compared with this, clinically healthy implants show a microflora that resembles the flora of periodontal healthy conditions [41].

1.2 Dental Caries

Dental caries is an infectious microbiological disease of the teeth that can lead to localized dissolution and destruction of the calcified tissues [42]. Bacteria play an important role in the genesis of caries. Especially, Streptococci predominate which is one of the gram-positive bacteria in the oral microbiota are frequently isolated from all areas of the oral cavity [43]. *Streptococcus mutans*, *Streptococcus sobrinus* and *Lactobacillus acidophilus* are the major cariogenic bacteria [44]. Apart from that, ingested carbohydrates will help bacteria to produce organic acids rapidly such as lactic and acetic acids. Those bacteria activate especially lactic acid leading to demineralization of tooth structures. Therefore, the constant intake of sugary food is one of the risk factors for dental caries [15]. Tooth structure defects such as enamel hypoplasia are also a risk factor, as they make the tooth more susceptible to acid challenge [45]. Further, the longer the period that the tooth is in acidic conditions, the more destructive the dental lesion will be [46]. Thus, the etiology of caries is the complex interaction of various factors within the dental plaque.

It is a dynamic process between demineralization and remineralization that is affected by both tooth structure and the oral environment. The mineral composition of enamel and dentine is hydroxyapatite (HAP) (($Ca_{10}(PO_4)_6(OH)_2$) which is at equilibrium at neutral pH 6-7 [47]. However, whenever the acidity of saliva is below the neutral pH of HAP (below pH 5.5 for HAP), it becomes under-saturated concerning enamel

minerals, leading to dental demineralization [48]. The demineralization process, however, is reversed by the buffering effect of HAP dissolution products and the actual value depends on the concentrations of Ca^{2+}, PO_4^{3-}, and OH^- in the solution. Further, environmental pH neutralization above the critical level enhances precipitation of Ca^{2+} and PO_4^{3-} within demineralized tooth structures [49] which is known as remineralization.

1.3 Periodontal Treatment

Currently, the main therapy for periodontal disease is to control the oral biofilm by improving oral hygiene and removing plaque to arrest inflammation and create conditions for healing and regeneration of the periodontium. The treatment plan is normally divided into several phases including emergency, nonsurgical, surgical, restorative and maintenance phases. Traditional mechanical methods involve scaling and root planning (SRP). However, mechanical debridement may be ineffective in eliminating pathogenic bacteria from periodontal pockets [50]. Because dental plaque has a strong association with periodontitis, reducing the perio-pathogens is one of the important steps in the treatment plan. It is difficult to reach the base of pockets with curettes and reach the plaque may be hindered due to access to root area. It has been pointed out that insufficient eradication of pathogens may be the cause of chronic lesions to not heal [51]. Thus, after SRP, anti-bacterial drugs may help reduce microbial species in the biofilm.

1.3.1 Systemic Antibiotics

Systemic antibiotics such as amoxicillin or metronidazole can be used during the treatment of periodontal disease which may enhance tissue healing after SRP [52]. The study showed that tetracycline, systemically administered over a period of at least 6

weeks, in combination with supragingival plaque control, decreased the probing pocket depths and resulted in gains in clinical attachment for up to at least 24 months[53,54]. However, it might have side effects including hypersensitivity and gastrointestinal disturbances [55]. Furthermore, mechanically reducing the subgingival bacteria will always come first, otherwise, it may inhibit or degrade the antimicrobial agent [56]. Therefore, the structured bacteria aggregates should be mechanically disrupted because it can protect the bacteria from the agent.

1.3.2 Local Antimicrobials

The reason for using local antimicrobials is based on antibiotic resistance and the possibility to achieve maximum antibacterial concentrations and the reduction of systemic side effects. A study showed that after a 6-month follow-up in 10 patients who have periodontitis, using tetracycline fibers resulted in statistically significant additional probing pocket-depth reductions of 0.6mm and in gains of clinical attachment of 0.7mm [57]. Similarly, Kaner (2007) et al found that using chlorhexidine chop with systemically administered amoxicillin and metronidazole, resulted in clinical improvements over a 6-month observation period [58]. It was reported by Guarnelli (1995) et al. in a crossover clinical trial study, that using mouth rinse was effective for reducing the amount of supragingival plaque deposits [58]. Thus, using antiseptics to support oral hygiene as part of supportive periodontal therapy is attractive.

Chapter 2. Literature Review of Chlorohexidine and additional metal ions

Although some bacteria are beneficial to the health of humans, infection by pathogenic bacteria remains one of the major causes of hospitalization and mortality [59]. A wide variety of agents with antibacterial activities exist such as metal ions (e.g. silver, strontium) and chlorhexidine as well as antibiotics [60,61]. This review mainly focuses on the application of chlorhexidine, strontium, zinc and fluoride.

2.1 Physicochemical Properties of Chlorhexidine

CHX is a synthetic broad-spectrum antimicrobial agent effective against gram-positive and gram-negative microbes, facultative anaerobes, aerobes, yeast and enveloped viruses [62,63]. Given chlorhexidine has a strong antimicrobial activity [64], it has been used widely in antiseptic and safe disinfectant applications [65]. The molecular structure of CHX (Figure 2) is a bis-biguanide that uses a hexamethylene chain to connect two chloroguanide chains.

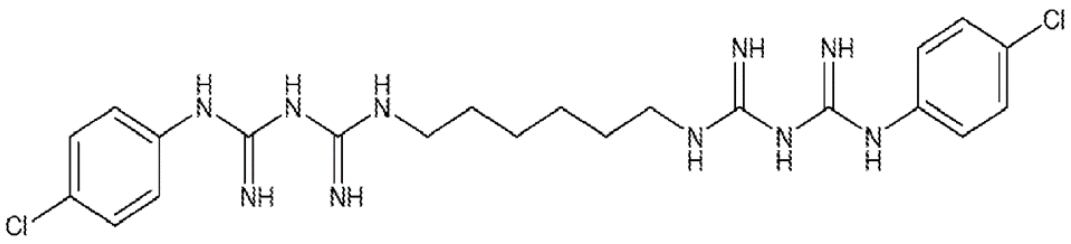

Figure 2. The chemical structure of chlorhexidine.

CHX is assumed that the guanidium group from the structure have a strong coordinating ability, which might bind to bacterial cell membranes, causing disruption of cell function [66]. At lower concentrations, CHX is bacteriostatic while at higher

concentrations it is bactericidal [67]. As a result of it being practically insoluble in water (8mg/ml at 20^{o}C) [68], it is normally used as salt solutions such as CHX diacetate, CHX digluconate, and CHX dihydrochloride.

The non-specific bactericidal mechanism of CHX is thought to endow it with a broad range of antimicrobial activity and to be responsible for the low microbial resistance observed. In clinical use, at suitable concentrations, the CHX cation is a highly potent, fast-acting antibacterial agent [69]. CHX can eliminate nearly 100% of Gram-positive and Gram-negative bacteria within half a minute *in vitro* [70]. Moreover, chlorhexidine activity is also influenced by pH range (5.5 to 7.0) [71,72]. The pH of the normal oral environment average is around 6.9 and will decrease if there were infections [73].

There is some research concentrated on the modification of CHX formulations in order to bring extra functionality to chlorhexidine. Several studies have found an enhanced antimicrobial activity when incorporating some metal ions such Zn^{2+}, Sr^{2+}, and Ag^{+} [74–76] because the biguanidines of CHX have strong coordination capability with those ions. It has been confirmed that when new copper (II) complex compounds were utilized, the biguanidine of chlorhexidine coordinated with Cu^{2+} (Figure 3) to produce a new CHX formulation with comparable antibacterial properties [66,77]. In this structure, CHX is expected to act as a tetradentate ligand where possible coordination sites are the four nitrogen atoms. Thus, it is able to generate metal-ligand complexes 1:1[78].

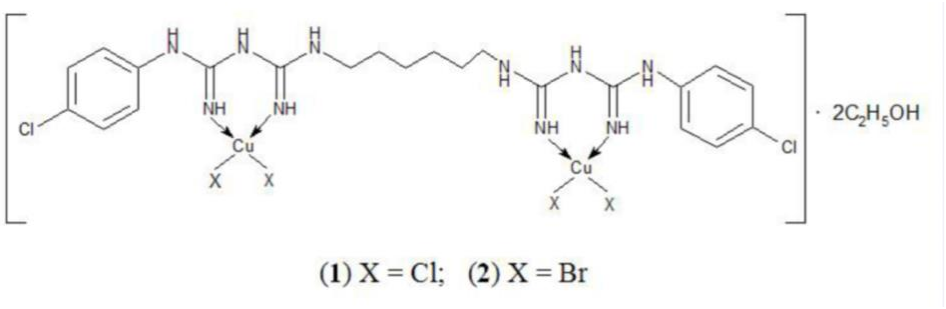

(1) X = Cl; (2) X = Br

Figure 3. Proposed structures for the copper (II) CHX complexes [66].

2.1.1 Chlorhexidine - Hexametaphosphate Nanoparticles

Barbour et al., (2013) used chlorhexidine digluconate to react with sodium hexametaphosphate and produced a new formulation of chlorhexidine-hexametaphosphate nanoparticles (CHX-HMP NPs) [79]. The reaction of these two reagents formed a white precipitate of CHX-HMP NPs and sodium gluconate in solution. The chlorhexidine digluconate and the NaHMP were reacted in a 3:1 ratio because CHX carried $^{+2}$ charge and HMP carried $^{-6}$ charge. Instead of a linear reaction, it was more likely to be an equilibrium shift because of the slow solubility of the HMP molecule. The CHX-HMP NPs described are around 80-90nm in diameter and has negative surface charges [79]. It tended to form a larger aggregate in suspension. Recently, CHX-HMP NPs have been developed as a coating for titanium implants, dental silicone, and as a component added to glass ionomer cements [80,81]. It indicated that the CHX-HMP NPs can deliver a steady release of CHX over a period of 4-22 months [82,83]. All the samples were however placed in 2 ml of water. Then all the solutions for CHX concentration solutions were measured over a 60-day period [79,80]. These experiments, however, did not demonstrate the behaviour of the sample in a simulated oral circulation environment, as samples were submerged in the same solution without media changes. Additionally, it had a bactericidal effect against

Streptococcus and *Candida* species *in vitro* in the presence of a salivary pellicle [80,84]. It was also shown to prevent colonisation by *Enterococcus faecalis* whilst allowing normal wound healing at 7 days in a murine wound healing model. Compared with chlorhexidine digluconate, these CHX-HMP NPs have reduced cytotoxicity to human cells *in vitro* [85].

2.1.2 Novel CHX-$CaCl_2$ Spherical Particles

Luo et al., (2016) synthesized novel CHX-$CaCl_2$ particles by the co-precipitation of CHXD with $CaCl_2$ [86]. This was possible due to the coordination ability of the CHX biguandines which may have coordinated with Ca^{2+}. Instead of being physically absorbed on the particle surface, Ca^{2+} was bound in the structure. The presence of Cl^- in solution accelerated the precipitation because CHX has low solubility in water. Therefore, the novel spherical CHX particles are a combined function of Cl^- and the counterpart cations Ca^{2+}. The chloride may help to reduce the solubility of CHX and the rate of formation of the interconnected structures, while the Ca^{2+} are responsible for the assembly of a more compact spherical structures. The mechanism for this formation of the radiating interconnected structures is still unclear, but similarly, the chelation mechanism of Cu^{2+} coordinated CHX complexes was studied [77]. The outcome of this synthesis was the creation of homogeneous and interconnected spherical CHX-$CaCl_2$ particles whose CHX content within the particles were around 90%. The size of the CHX -$CaCl_2$ particle was controlled by the temperature (0 -25 °C) of the solution and the size of particles was in a range from 5.6 μm to over 20 μm.

In order to provide a more sustained CHX delivery system against bacteria, gold nanorods have been added and combined with novel CHX-$CaCl_2$ spherical particles

[87]. There are two main stages in the process of CHX-$CaCl_2$ particle growth including rapid nucleation to form primary seeds, and sustained growth of precursors on the primary seeds. It is a very rapid process for novel CHX-$CaCl_2$ particle formation, which may depend on the type and concentration of ions and temperature of the bulk solution [86]. However, the addition of gold nanorods in the solution encouraged surface crystallization to produce more primary crystallites. Furthermore, the gold nanorods in the solution were a key factor to determine the CHX-$CaCl_2$ particle size and number. The negatively charged gold nanorods may have a high affinity to positively charged CHX molecules, which encourage crystallization of CHX on their surface. For the second stage, the growth of nano CHX particles proceeded via the continuous deposition of monomers on the primary particles. Therefore, when the primary particles were transferred into solution with monomers, crystal growth continued until the CHX monomers were depleted.

The novel CHX-$CaCl_2$ spherical particle was further encapsulated with different polymers including polyelectrolytes, PLA and HEMA-UDMA resins using different techniques [88,89]. Using the layer-by-layer (LbL) technique, the needle-like particle structure was covered by the polymers which provided an increased sustained-release (7h) in water. Additionally, both uncoated and LbL coated CHX-$CaCl_2$ spherical particles were electrospun into PLA fibres, to enable fibres with sustained antibacterial properties. The incorporation of CHX-$CaCl_2$ particles into fibres improved the drug loading ratio. Both fibres indicated no cytotoxicity to L929 fibroblasts cells at low CHX concentrations (0.5%. to 1% wt). After encapsulating the particles, the biocompatibility was significantly improved to 5 wt% CHX concentration [89]. An antibacterial assay was also conducted with *E. coli,* which showed good bacterial inhibition and a sustained antibacterial effect via broth transfer experiments at 5 wt % CHX [89].

The novel CHX-$CaCl_2$ spherical particles were also incorporated into HEMA-UDMA resin discs, and the CHX release was controlled using ultrasound treatment. The longer ultrasound treatment led to increased and controlled CHX release. In addition, chlorhexidine diacetate and CHX-$CaCl_2$ particles appear to have different dissolution processes. For the chlorhexidine diacetate incorporated in HEMA-UDMA resin, the dissolution of CHX started from the crystal boundaries. In contrast, dissolution of the CHX-$CaCl_2$ particles started at the centre of the interconnected particle [88].

In summary, the synthesis of the CHX-$CaCl_2$ particles is simple and has the potential to make further ion functionalization to the structure to create particles with additional properties. The CHX-$CaCl_2$ particles appear hydrophilic and can be encapsulated or embedded into polymer matrices, to provide further sustained release and antibacterial effects. Therefore, this shows huge potentials and possibilities to be applied in medicine and dentistry.

2.2 Mode of Action

As a broad-spectrum antimicrobial, various CHX concentrations can contribute to diverse results. It has both bacteriostatic and bactericidal mechanisms of action. At concentrations in the range of 1-100μg/ml CHX inhibits cellular respiration and solute transportation [90,91]. The disruption of the cell membrane structure is caused by the connection between the cationic CHX molecule and the negatively charged bacterial cell envelope, thereby increasing permeability and efflux of intracellular solutes including potassium (Figure 4). However, in bacteriostatic levels of CHX, bacteria can recover from damage despite losing up to 50% of their potassium storage. When the concentration of CHX is increased (100 to 500 mg/L), this results in cellular

components such as nucleotides denaturing, leading to cell death [92]. There is a comparative study that examined the response of how cell morphology of both gram-positive and gram-negative bacteria are affected when exposed the bacteria to CHX. It has been proved both gram-positive and gram-negative bacterium's cell wall has been affected, however, compared with gram-positive bacteria, gram-negative bacteria can enter the bloodstream and showed more interaction with serum cationic proteins when viewed under the scanning electron microscopy due to the distributed lipids in gram-negative bacterial cell membranes [93].

Gram-negative bacteria can enter the bloodstream and interact with serum cationic proteins. The character of interaction will depend on the surface characteristics of bacterial cells, which are determined by bacterial chemotype and density of lipopolysaccharide (LPS) packing in the cell wall. Thus, CHX cations are more effective against Gram-positive bacteria. Table 1 and Table 2 shows typical MIC's for a range of Gram-positive and Gram-negative bacteria [94].

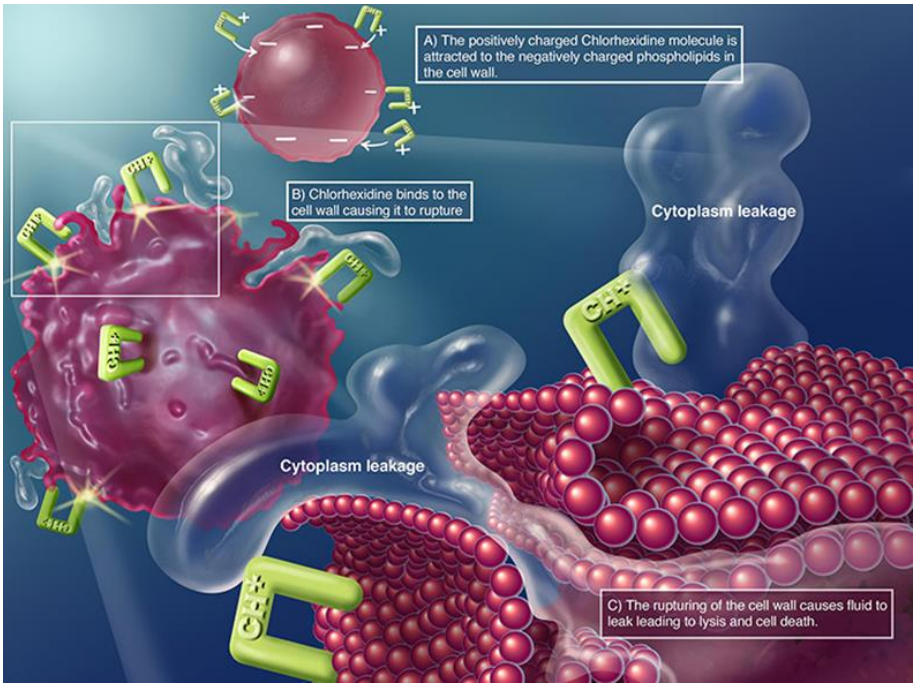

Figure 4. Mechanism of action of CHX. (Image from www.chlorhexidinefacts.com)

Table 1. MIC of CHX against Gram-positive bacteria [94].

Microorganism	MIC (µg/mL) (µg/ml)
Bacillus species	1.0 – 3.0
Clostridium species	1.8 – 70.0
Corynebacterium species	5.0 – 10.0
Staphylococcus species	0.5 – 6.0
Enterococcus faecalis	2.0 – 5.0
Streptococcus species	0.1 – 7.0

Table 2. MIC of CHX against Gram-negative bacteria [94].

Microorganism	MIC (µg/mL) (µg/ml)
Escherichia coli	2.5 – 7.5
Klebsiella species	1.5 – 12.5
Proteus species	3 - 100
Pseudomonas species	3 - 60
Serratia marcescens	3 - 75
Salmonella species	1.6 - 15

The cell membrane enters a liquid-crystalline state, losing its structural and functional integrity and allowing irreversible leakage of cellular materials leading to cell death when the CHX concentrations are higher than 100μg/mL[95]. CHX can get through the broken cytoplasmic membrane and causes sediments with intracellular adenosine triphosphate as well as nucleic acid [96,97]. Phospholipids are bonded by CHX in the inner membrane leading to leakage of low-molecular-weight molecules causing precipitation of bacterial cytoplasm and cell death [98,99]. In contrast to antibiotics, CHX has the ability to cause the collapse of the bacterial cell membrane potential without targeting specific ATP inactivation, with the latter a cause of bacterial resistance. This is the reason for CHX antimicrobial activity [100].

It is noteworthy to address the CHX as substantivity is desired property of CHX. Substantivity is the ability of the drug to bind to soft and hard tissues. A previous finding indicated that CHX's substantivity was for a period of approximately 10-12 hours [98]. However, concerning dental hygiene applications, the cationic nature of CHX enables to it bind to tooth surfaces and oral mucosa. This is because the positively charged ions released by CHX can adsorb into dentine and mucosa [101,102]. This ability to adhere to the tooth surface also gives CHX plaque inhibitory abilities by interfering with bacterial adhesion, strongly inhibiting plaque regrowth [103,104], and preventing gingivitis [105,106]. Moreover, it also can attach to the hydroxyapatite in dentine. An earlier study demonstrated that when using CHX in the endodontic application, it may bind to hydroxyapatite, causing the release to last around 12 weeks within a closed environment [107]. This will give CHX long term antibacterial effectiveness. Besides, oral treatment of human volunteers with CHX (0.2%) resulted in a 30 to 50% reduction in total bacterial counts, with an associated reduction in counts of *Streptococcus mutans* [108].

2.3 Limitations of Chlorhexidine

2.3.1 Staining

CHX has limitations when used in dental applications. The common side effect when using CHX mouthwash is it causes a brownish discoloration of teeth, which is called the Maillard reaction[109]. Clinically, tooth staining observed was correlated with the volume of CHX, with higher volumes above 20 ml of CHX rinse (commercial CHX mouth rinses dosage) increasing staining [102]. Nevertheless, the staining is associated with its concentration and interaction with chromogenic factors including red wine, coffee and tea [110]. It can be minimized if the patients avoid the above-mentioned products. CHX mouthwashes may also cause an increase in the tartar on the teeth and taste problems such as taste sensation [111]. Furthermore, it was recommended to avoid using CHX mouthwash immediately after brushing the teeth, because its antimicrobial response may be reduced by the reaction between CHX and toothpaste [112]. Compatibility between cationic charges on the CHX and anionic charges on sodium lauryl sulphate have been reported, and with a reduced plaque inhibitory efficacy in vivo. It has also been reported that sodium mono fluorophosphate and CHX form through the precipitation of insoluble salts in vitro [113].

2.3.2 Sensitivity

Clinicians may have concerns that CHX may be hypersensitive to patients. Both Type I (anaphylaxis) and Type IV (delayed) CHX induced sensitivity reactions have been reported [114]. Type IV reactions commonly appeared in healthcare workers and in patients who have CHX containing dressings or venous catheters [115]. Although CHX has been shown to induce both immediate and delayed hypersensitivity reactions [116],

CHX anaphylaxis is considered very rare. There are only 65 reports of it worldwide between 1994 to 2014, which indicates it is not always considered as a potential allergen [117].

However, a Type I hypersensitivity reaction to CHX can be fatal. There have been two reported cases of death after irrigation of dental extraction sockets with a CHX containing mouth rinse [116]. Thus, in UK hospitals, CHX allergies will be screened and tested before medical intervention for patients. When comparing with some commonly used antibiotics like penicillin (around 10% allergic response), the prevalence of CHX sensitivity is much lower [118]. The prevalence of CHX contact allergy by performing a patch test was 0.5-1% of patients [119,120]. Thus, CHX is still an attractive option, especially for the treatment of infections, as it is a broad-based antimicrobial.

2.3.3 Bacterial Resistance

In recent years there has been increasing evidence that oral bacteria can develop tolerance, adaptations or resistance to CHX, which may reduce its antibacterial effectiveness [121]. Bacterial resistance can be intrinsic or acquired. Bacterial adaptation can also occur, which is transient. It can be reversed upon removing the antimicrobial agent. Moreover, bacteria can also display tolerance. For example, bacteria can survive by reduction in metabolic rate, instead of genetic changes when increasing dose [121]. However, monitoring of this effect is challenging because there is no accepted point to define the concentration of CHX when the bacteria have developed resistance [122].

Prolonged exposure to CHX may cause resistance or adaptation to CHX in various oral bacteria. It has been reported that the patients who used a CHX containing

toothpaste for 6 months, subsequently produced isolated plaque bacteria with higher minimum inhibitory concentrations (MICs) to CHX ($p<0.05$) [123]. It has been demonstrated that some repeated passage of various oral bacteria has been proved to increase MICs to CHX containing agar *in vitro* including *P. gingivalis*, *A. actinomycetemcomitans*, *F. nucleatum* and various oral *streptococc*. However, tolerance disappeared in some cases [124,125]. The wide use of CHX containing products may contribute to increased CHX tolerance or resistance. Therefore, current research into the use of CHX is focused on site-specific delivery to minimize the chance of increasing bacterial resistance to CHX, compared with the widespread use of CHX containing products. Reformulations of different CHX compounds or nanoparticles also use other carriers including micro or nano capsules, gels, and coatings to control the release and sustained release of the drug [81,86–88,126–128].

2.3.4 Nitrate-Nitrite-NO Pathway

It is reported that there is a correlation between periodontal disease and hypertension [129]. Through nitrate-nitrite reduction, some commensal oral bacteria can supply bioactive nitric oxide (NO), which is essential for endothelial cell function and regulation of arterial blood pressure (BP) [130]. Some research indicates using CHX may cause a decreased quantity of oral nitrate-reducing bacteria and an increased quantity of pathogenic bacteria. These bacteria are responsible for a correlation between chronic periodontitis and periimplantitis.

In the oral environment, nitrate is reduced to nitrite by the anaerobic bacteria [131]. In the stomach, nitrite is non-enzymatically reduced to NO by the acidity of the gastric milieu. Then the nitrate and the remaining nitrite pass into the intestines and are

absorbed. Nitrite in the circulation can be further reduced to NO, whereas nitrate enters the salivary loop [132].

During the nitrate-nitrite-NO pathway the components of NO production are active uptake of nitrate in saliva and then reduction of nitrate to nitrite. There are some clinical trials with CHX mouthwash that have associated nitrate reduction with increased blood pressure. It has been pointed out that 0.12% CHX mouth wash can kill nearly 94% of the oral bacteria, that reduce nitrate and can decrease the proportion of nitrate by 85% [133,134]. Tribble (2019) found that a twice-daily mouthwash using a 0.12% chlorhexidine solution for a week increased blood pressure in healthy subjects [135]. However, there is some evidence to suggest that dietary nitrate supplementation does not modify blood pressure and cardiac output at rest and during exercise in older adults [136].

Preshaw (2018) pointed that using mouthwash twice daily or more had around a 50% increased risk of developing prediabetes or diabetes combined, compared to those who used mouthwash less than two times daily [137]. However, this paper did not record recruited overweight and obese adults (BMI) $\geqslant$25 kg/m^2) aged 40–65. There was also no measurement of salivary or plasma levels of nitrate, nitrite or NO bioavailability. It is obvious that this population was already at high risk of developing diabetes (56.7% had prediabetes at baseline).

Nevertheless, many non-CHX antiseptic mouthwashes are effective against nitrate-reducing oral bacteria, which should decrease the NO bioavailability [132]. Additionally, other agents can also disrupt the nitrate-nitrite-NO pathway such as smoking, antibiotics and high concentrations of ascorbates [138]. Thus, CHX is still a common antibacterial agent used in dentistry and medicine.

2.4 Application of Chlorhexidine in Dentistry

CHX is widely used in the disinfection of skin and hands. It has also been extensively applied in dental products such as toothpaste, mouthwash, dental gels, gelatine chips [139]. For example, CHX di-gluconate is used in mouth rinses (0.2% or 0.12%) [140] and wash solutions which are used for disinfecting operation sites and root canals (2%) [107]. CHX has also been used in plaque control for the prevention and management of both caries and periodontal disease [141]. For example, CHX has been used in resin-modified glass ionomer cement (GIC) as a filler material for its antimicrobial properties [142]. However, it will increase in working and setting times and decrease compressive strength. Normally the digluconate form will be used under this condition because it is water-soluble and will be easy to dissociate at physiological pH. Although CHX is already used in many treatments, there remains a need for a suitably effective sustained delivery of CHX based compounds against microbes. Especially during the wound healing process and in the placement of a dental implant or endodontic infections, providing longer-term antimicrobial therapy were necessary [143]. For example, in the treatment of periodontal or peri-implant disease, when mechanical plaque control is difficult such as disabled patients [144] or immediately after periodontal surgery, chlorhexidine has been extensively used. The periodontal diseases can involve both the soft and hard tissues which are initiated by components of the plaque biofilm, which developed on the hard root surface adjacent to the soft tissues of the supporting periodontium [27]. It may extend to the deeper supporting structures with the destruction of alveolar bone. Chlorhexidine is efficacious in the treatment of periodontal and peri-implant disease. However, for it to be effective against the pathogens involved, chlorhexidine must reach the site of infection in sufficient concentration and for a long enough period.

The traditional prevention of periodontal disease is the mechanical removal of the plaque biofilm, removing the precipitation factor. Mousquéegs and Cugini (1983, 2000) pointed that [145,146], after scaling and root planning, the subgingival microflora is reduced. However, after one session of scaling and root planning (SRP), it may take approximately 42 days for the proportions of certain bacteria in the periodontal sub-gingival flora to return to baseline levels [147]. Although SRP helped control periodontal disease, it still has limitations, especially in the deep periodontal pocket. In this area, there is difficulty using instruments because of access to surgical treatment. Therefore, the use of antimicrobial agents such as CHX products is used to complement mechanical plaque control [148]. In which case, it is useful to design a stable and sustained effective chlorhexidine release system, which may have antimicrobial effects in sub-gingival periodontal and peri-implant pockets. Many delivery systems have been designed to deliver sustained CHX, which are based on gels, micro-particles, and even nano-particles [149].

2.4.1 Mouthwashes

Mouthwashes are the most common chlorhexidine commercial product. Normally, the available chlorhexidine mouth rinse products concentration is 0.12%-0.2% CHX digluconate [150]. Corsodyl mouth rinse as an example of CHX di-gluconate has been proved its antibacterial effect [151]. The previous study showed that chlorhexidine digluconate mouthwashes were significantly effective for dental plaque and gingival inflammation [152,153]. However, it has fewer effects on plaque-covered surfaces [154]. Thus, chlorhexidine mouthwash is not effective in poor oral hygiene patients compared with treated patients. Therefore, professional removal of plaque is still necessary. Although it may not penetrate an existing structured biofilm, it will prevent plaque on a

clean tooth surface [152]. Therefore chlorhexidine mouthwash can be used during periodontal therapy which may help in controlling plaque [155], having clinical and microbiological benefits [156].

Although there is literature showing clinical benefits of using chlorhexidine formulations in a mouth disinfection approach [157], chlorhexidine mouthwashes may not have a significant effect on periodontal disease. For example, the major treatment for peri-implant mucositis (an inflammatory lesion limited to the surrounding mucosa of an implant) and peri-implantitis (an inflammatory lesion of the mucosa that affects the supporting bone with resulting loss of osseointegration) is antimicrobial therapy. It also comprises; antiseptic rinsing, mechanical debridement, irrigation with antiseptics and local, systemic application of antibiotics and dental lasers [158]. Antiseptic rinsing is one of the easiest treatments for periodontal disease. However, because the gingival crevicular fluid is replaced every 90 seconds, the drug does not stay in the pocket for enough time, and the effects of antiseptic irrigation are transient [155]. Irrigation of Chlorhexidine mouthwash solution into deep periodontal pockets has been shown to be ineffective in the treatment of chronic periodontitis, peri-implant mucositis and peri-implantitis [159,160].

2.4.2 Local Antimicrobial Devices in Dentistry

Sustained or controlled released antibacterial agents provide obvious benefits especially during disease management. Compared with systemic antibiotics, it has reduced systemic side effects. They do not depend on patients' compliance with dosing regimens and a required dose can be delivered to the required area [161]. Some local antimicrobial agents such as CHX containing gels, fibres, microparticles or chips

are used in the management of periodontal defects [162]. Those devices may help CHX release over a period of days or weeks [163,164]. However, the gingival crevicular fluid (GCF) flow may cause the concentration of CHX to reduce or even lose the drugs [165]. Thus, a controlled release device that can provide sustained release, and give a steady drug release in the required site is important.

2.4.2.1 PerioChip®

A commercial product known as PerioChip® [166] showed in Figure 5 is available for the treatment of periodontal disease, and it consists of chlorhexidine digluconate and cross-linked gelatine. It is a degradable gelatine chip that contains 2.5g chlorhexidine gluconate [23]. In the beginning 24 hours, it has an initial chlorhexidine burst release, followed by 7-10 days of slow constant release [167].

When the periodontal patients' pockets are ≥ 5mm, PerioChip® can be used as an adjunct to root surface debridement (RSD). This adjunctive efficacy had been provided by many studies. Previous studies proved that adjunctive PerioChip® to be more effective than when using only using scaling and root planning (SRP) alone, especially when measuring pocket depth (PD), clinical attachment loss (CAL) and bleeding index (BI) [168]. Furthermore, the deeper pockets (>7mm) were shown to have the greatest response [169]. However, the low efficiency of drug loading, as well as preloaded drug release, are problematic with these kinds of carriers.

Figure 5. PerioChip® [167]

2.4.2.2 Polymethyl Methacrylate

Many delivery systems have been developed to for use with chlorhexidine. For instance, the organic carrier polymethyl methacrylate (PMMA) was used in conjunction with chlorhexidine to enable sustained CHX release. However, due to the strong binding formed between the drug and the polymeric matrix, chlorhexidine is poorly released from the structure, showing a sharp decrease in CHX release rate after the first few hours [170]. Thus, a CHX delivery system that has a sustained release behavior and maintains the bacterial inhibitory concentration for the desired time to reduce the viability of microbes is therefore needed.

2.4.2.3 Gels

There is a variety of gels that have been used as a carrier for CHX, showing mucoadhesive properties. For example, chlorhexidine digluconate (1-2%) can be combined with carboxymethyl cellulose (CMC), hydroxypropyl cellulose (HPC) or xanthan gum-based gels in order to increase the retention of the CHX in the oral environment [171,172]. Furthermore, the cellulose derivative displays mucoadhesive properties because they have an affinity to water. It allows them to form hydrogen bonds and be easily dispersed and bond with the oral mucus [173]. The gel's viscosity also enhances its firmness in the periodontal pocket. The gel can also be placed more

easily to administer CHX, than cross-linked gelatine chip carriers, and reduces potential tissue damage during the treatment procedure [71].

CMC, HPC and Hydroxypropyl methylcellulose (HPMC) is commonly used to prepare the mucoadhesive gels to enhance drug release property [174]. Carboxymethyl cellulose (CMC) is a mucoadhesive, ionizable, semi-synthetic water-soluble polymer that is affected by ionic strength and pH. The CH_2COOH groups in the CMC are substituted on the glucose units of the cellulose chain through an ether linkage [175]. Hydroxypropyl cellulose (HPC) is a non-ionic water-soluble cellulose ether with a remarkable combination of properties. It has the thickening and stabilizing properties characteristic of other water-soluble cellulose polymers. Hydroxypropyl methylcellulose (HPMC) is a mixed alkyl/hydroxyalkyl cellulose ether containing methoxyl and hydroxypropyl groups which are frequently used in hydrophilic matrix drug delivery systems [175]. It is also used as a gel base to provide drug sustained-release [176].

2.4.2.3.1 Hydroxypropylmethyl Cellulose Gels

Hydroxypropylmethyl cellulose gels (HPMC) belongs to the group cellulose (Figure 6) [177]. It is the most commonly used matrix polymer due to its biocompatibility, non-pH dependence and global regulatory acceptance [178]. It has been a hydrophilic vehicle widely used in drug controlled release systems because of its non-toxicity and capacity to accommodate high levels of drug loading [179]. Furthermore, different viscosity grades of HPMC are commonly used, blended to achieve matrices with improved physical characteristics in order to achieve the desired drug release profile [180]. It is well known that HPMC gel has good mucoadhesive properties. When in contact with liquid, the fluid diffuses into the HPMC gel, resulting in polymer chain relaxation leading to volume expansion. The incorporated drug will therefore come out from the gel system

at a required rate [181]. This makes the HPMC gel able to carry out a effective release control. Thus, incorporated drugs into the HPMC gel may decrease the release rate of the drug and provide a sustained release.

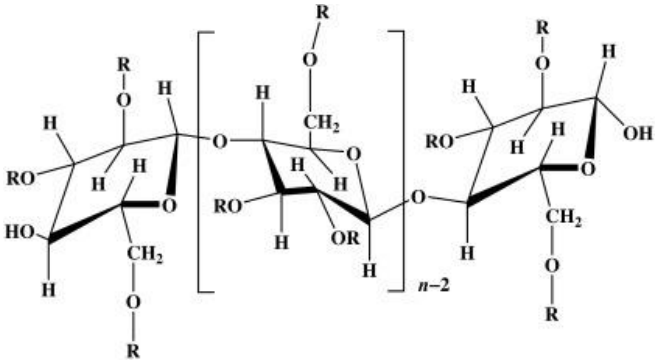

Figure 6. Chemical structure of hydroxypropyl methylcellulose. R=H, -CH_3 or –$(OCH_2CHCH_3)_xOH$ [177].

When preparing HPMC, the powder first needs to be dispersed in hot water, heated above 90 ^oC. Then complete dissolution takes place, and the remaining water portion is added as cold water to lower the temperature of the dispersion. As the temperature is lowered, HPMC becomes water-soluble; the solution resulting in increased viscosity [182]. Water-soluble drugs are released primarily by diffusion of dissolved drug molecules across the gel layer, whilst poorly water-soluble drugs are released predominately by erosion mechanisms [183]. CHX as a poorly water-soluble drug has been incorporated with HPMC, showing decreased releasing rate of the drug because of absorption of water by the polymer and forming a gelatinous barrier layer at the surface of the tablet matrix [184].

In practice, due to mechanical stress generated during tooth brushing or eating, the major problem for the local release of drugs is to avoid accidental expulsion of the drug from the site of action. The HPMC gel may help to overcome this problem

because of its viscosity. It has been demonstrated that HPMC gel can provide improved textural properties and enhanced adhesion to the treatment area, such as teeth or gingival pockets [185,186].

2.4.2.3.2 Xanthan Gum Gels

Chlosite® is a product containing 2.5g of Xanthan gum, devised to increase the retention of CHX gels in the periodontal pocket. Xanthan gum is a polysaccharide that increases the viscosity of a liquid and is stable over a wide range of temperatures and pHs. It contains two CHX formulations, 0.5% CHX digluconate and 1% CHX dihydrochloride. The gel undergoes a progressive process of imbibition and is physically removed in 10-13 days. The digluconate salt is liberated from the gel on the first day (>100µg/ml) and is maintained for 6-9 days. The dihydrochloride salt was then released over 2 weeks, maintaining bacteriostatic and bactericidal concentrations [187].

Results from RCTs have shown adjunctive Chlosite® gives significantly greater improvements in the PD, CAL, gingival index and BI of chronic periodontitis patients compared with SRP alone [172].

2.4.2.4 Cervitec ™

Cervitec varnish is a vehicle that can deliver antimicrobial in the management of oral infections [188]. It can retain the dosage at the site of action, prolonging direct contact of the drug with the affected tissue, and minimizing the associated adverse effects [189]. Thus, varnishes may be promising as vehicles for local delivery of antibacterial drugs in periodontal treatment.

Chlorhexidine varnishes available contain CHX concentration at 1% (Cervitec), 10% (chlorozoin), 35% (EC 40), and 20% (Bio C) [190]. Cervitec is one varnish contains 1% chlorhexidine acetate, 1% thymol and 10%poly vinyl butyral in water [191]. Most Thymol belongs to the phenols family and displays an antimicrobial effect combined with pronounced fungistatic properties. It can decrease bacterial colonization on the teeth by disrupting bacterial metabolism and decreasing the formation of lactic acid. This varnish (Vinyl acetate polymer) creates a mechanical barrier after drying and effectively seals the dentinal tubules, which may be valuable in the treatment of dentine hypersensitivity [192]. Further, the Cervitec and cervitec plus has also been used in a controlled double-blind study, which demonstrated both Cervitec and cervitec plus is capable of reducing cervical tooth hypersensitivity [193]. It has been pointed out that *Porphyromonas gingivalis,* and *Aggregatibacter actinomycetemcomitans* as being the most sensitive bacteria to the chlorhexidine–thymol varnish (Cervitec) in a invitro study [194]. It has been recommended to increase the frequency of applications in order to retain the antibacterial effect for a longer time [195]. In order to achieve a reservoir of CHX on the tooth surface, CHX concentration may need to be high enough, otherwise, multiple applications are required if the varnishes are contained a low concentration of drugs like cervitec. Thus, the multiple applications of chlorhexidine varnish have benefits over a single application in the treatment in dentistry [191].

2.5 Additional metal ions

2.5.1 Strontium

Strontium (Sr) has taken on an added importance due to its effects on bone metabolism [196]. Therapeutic effects of Sr ions on bone metabolism have been

extensively investigated, which suggest that an appropriate concentration of Sr is able to stimulate osteoblast proliferation and differentiation while inhibiting osteoclast activity [197]. Additionally, it has been reported that Sr has mild antimicrobial properties against certain bacterial strains, including *E. coli, S. aureus, and Lactobacillus* [198].

Further, Sr rapidly oxidises due to the formation of strontium oxide. Sr is chemically and physically closely related to calcium (Ca). Both Sr and Ca are incorporated into the bone at the same rate [199]. Sr has an ionic radius of 1.16 Å close to Ca at 0.94 Å. The small size difference allows the substitution of Sr for Ca in many crystal lattices. In some materials such as bio-glass, calcium has already been replaced by Sr [200]. They act to waken the glass network by creating non-bridging oxygen atoms, to reduce the glass stability and make it more reactive. It easily forms a divalent cation in biological fluids such as blood. In the serum or plasma of the human body, the connection between protein and strontium has the same order of magnitude as that of Ca [201].

Sr has beneficial biological activities and assists in bone regeneration [202]. For example, strontium ranelate is a strontium compound that is made of combining Sr with renelic acid reveals its efficiency in treating postmenopausal osteoporosis [203,204]. One study on this showed that those who have taken 680 mg of strontium daily for two years can reduce vertebral fractures and alteration in bone metabolism [205]. Strontium has been shown to stimulate cell replication of pre-osteoblasts, causing an enhancement in the rate of new bone formation [206]. Strontium is mainly incorporated by exchange into the crystal surface. In newly formed bone, only a few Sr may be incorporated into the crystal by ionic substitution of Ca.

Further, it is found that in order to improve the bone condition in the treatment of osteoporosis, some minerals such as strontium, calcium, and zinc can be used as supplements [207,208]. Osteoporosis is due to an imbalance between bone deposition and bone resorption during the bone remodelling process [209].

In addition, strontium may improve cartilage formation. It is reported that strontium may enhance the metabolism of cartilage in patients who were diagnosed with osteoarthritis. In this study, it was found that strontium could stimulate the production of proteoglycan which plays an important role in promoting cartilage growth [210].

Sr salt has been widely used in desensitising toothpaste formulations for treating dentine hyper sensitisation [211]. The reason for this is that Sr ions may help with apatite formation and form Sr containing apatite [212]. Sr is able to reach the bone extracellular fluid and may be absorbed into the bone surface or replaces the Ca positions in the lattice. Thus, Sr can be substituted for Ca to form strontium hydroxyapatites [213].

Strontium as a re-mineralizing agent is related to rescued caries [214]. The prevalence of caries has an inverse relationship with strontium levels in the water, plaque, and enamel [215], indicating that strontium can exhibit cariostatic properties [216]. Previous studies showed that moderate doses of strontium could prevent rat's caries [217]. Thus, understanding how this element behaver in the dental area becomes important.

Additionally, both fluoride and strontium encourage the remineralisation process of dental tissue and combining fluoride and strontium will improve the apatite crystallinity and reduce the acid reactivity of synthetic carbonated apatite [218]. Moreover, strontium shows a more significant ability to mineralise than adjacent untreated dentine in vitro

[219] while the re-mineralising effect of F^- is also reported to be enhanced by the presence of Sr^{2+} [220].

Therefore, the above merits enable to the strontium be particularly beneficial in the treatment of implant and surgical associated infections and will potentially help to treat caries, and periodontal diseases as well. Thus, the introduction of strontium into the CHX particles may potentially improve the regeneration of bone.

2.5.2 Zinc

Zinc acts as a co-factor for over 400 enzymes, including ALP, which is an important enzyme for hard tissue formation and mineralisation [221]. Similar to Sr, it has a stimulatory effect on bone formation [222]. Depending on the intake amount, Zn can improve the alkaline phosphatase activity and DNA content in the bone tissue [223]. Thus, both *in vitro* and *in vivo*, Zn has a stimulatory effect on bone formation [224]. Zinc is also an antibacterial agent which helps wound healing [225]. It is capable of leaching into the growth medium and impeding the metabolism of sugars while disrupting enzyme systems of the plaque[226]. Zn-containing products such as Zn oxide eugenol (ZOE) and Zn polyphosphate (ZOP) are widely used in dentistry due to their bacteriostatic and cariostatic properties [227].

Additionally, Zn has the ability to decrease the bacterial production of acids by inhibiting the action of glycosyltransferase enzyme [228]. It has been added to toothpaste in order to help inhibit bacterial infections, and plaque and gingivitis can be controlled and prevented [229]. When infection occurs, the pH value is reduced [230]. Ideally, if zinc can only release from zinc-containing antibacterial material when needed, i.e., during an infection, where that area pH is low, it is attractive for dental and medical

applications. It is reported that zinc has smart release properties depending on pH [223,231], making it particularly useful as pH changes are prevalent during infections [232]. Therefore, Zn^{2+} has been wildly applied to dental products like bioactive glasses [233]. Consequently, introducing zinc into CHX particles will potentially improve its antibacterial effect and change the ion release behaviour in different pH environments.

2.5.3 Fluoride

As mentioned previously, fluoride plays a significant role in the reduction of dental caries. It is an element that occurs in the human diet and is biologically available in the human body [234]. In human saliva, the concentration of fluoride is around 1μM [235]. Basically, fluoride interacts with mineralized tissues in a biphasic manner [234]. At lower doses, it is passively incorporated into bone and teeth to form fluorapatite (Fap) [236]. It has been reported that F^- (1μg/ml) is necessary to prevent the tooth demineralization process. Thus, 1μg/ml of F^- was incorporated into the water supply (fluoridated water) of most of the UK regions [237], to reduce the incidence of dental caries. However, at higher concentrations, fluoride induces the occurrence of skeletal and dental fluorosis, which is characterized by the increased fracture risk, and marked mottling and discoloration in the teeth [238]. The combined effect of fluoridated drinking water and fluoride dental products may cause dental fluorosis. It has been reported by Beltran-Aguilar (2005) that the daily consumption of a 1450μg/ml fluoride toothpaste can cause dental fluorosis [239].

Fluoride has been used in dentistry because it can inhibit the growth of caries and decrease the demineralization process. Fluoride mouth rinses for preventing dental caries are used in children and adolescents[240]. The hydroxyl group (OH^-) in

hydroxyapatite ($Ca_{10}(PO_4)_6(OH)_2$) is replaced by fluoride in the oral saliva to form fluorapatite ($Ca_{10}(PO_4)_6F_2$), which makes the crystal lattice more compact and stable [241]. In addition, when pH is below 5.5, hydroxyapatite is susceptible to dissolution and replaced by fluorapatite, which has superior resistance to subsequent demineralization due to its decreased solubility [242].

Fluoride is also able to enhance re-mineralization and to bring positive effects on bone, and has effective anti-microbial properties [243]. Fluoride can affect bacterial metabolism through a spectrum of actions with fundamentally different mechanisms [244]. On the one hand, fluoride is able to act directly as a bacterial enzyme inhibitor, such as irreversibly inhibiting the glycolytic enzyme enolase. Further, fluoride can bind directly to heme then inhibits the heme-based peroxidases of bacteria. Fluoride can also form metal-fluoride complexes such as AlF^{4-}, which interact with bacterial proton-translocating F-ATPase and nitrogenase enzymes. Mimicking phosphate to form complexes with ADP at the enzyme reaction centers. This will lead to bacterial activity inhibition [245]. For example, it has been reported that 0.1 mM of fluoride can cause the complete arrest of glycolysis by intact *S.mutans* cells [244]. Generally, fluoride antibacterial effects involve both direct and indirect actions on bacteria.

In this study, fluoride has been added to the novel CHX particles to prevent the tooth demineralization process and may enhance the antibacterial effect.

2.6 Aims and Objectives

Aim 1: Synthesis and Characterisation of the novel calcium, strontium, zinc and fluoride containing CHX particles.

Hypothesis: CHXD can react with $CaCl_2$, $SrCl_2$ or $ZnCl_2$ individually and produce precipitation of CHX salts.

Objectives: Particle concentration and composition ($CaCl_2$, CHX-$ZnCl_2$, CHX-$SrCl_2$, CHX-NaF-NaCl and CHX-NaF) was investigated in response to temperature, pH and reaction time using SEM, FTIR, XRD and FTIR analysis. Solubility was explored using UV/Vis and ICP-OES.

Aim 2: In vitro effects of CHX-$ZnCl_2$, CHX-$SrCl_2$ particles in 2D cell models.

Hypothesis: CHX-$ZnCl_2$, CHX-$SrCl_2$ particles have less cytotoxicity compared with CHXD in the same concentration and shows effects on pre-osteoblasts (MC3T3-E1 cells).

Objectives: Cytotoxicity study of different concentrations of CHX-$ZnCl_2$, CHX-$SrCl_2$ particles on cultured fibroblast-like L929 after different exposure times and compared with CHXD.

Investigation of CHX-$ZnCl_2$, CHX-$SrCl_2$ particle function in the regulation of MC3T3-E1 cell behaviour, including ALP activity, odontogenic differentiation, and mineralisation.

Aim 3: Efficacy of CHX particles on antimicrobial release profiles using a gel and medical device model.

Hypothesis: Novel particles are able to crystallize on the surface of a medical devices and release from medical grade gels and devices.

Objectives: Synthesis of CHX-$CaCl_2$, CHX-$ZnCl_2$ and CHX-$SrCl_2$ containing gels and investigating CHX /ion release kinetics and the antibacterial efficacy against periodontal pathogens.

Surface crystallisation of CHX-$CaCl_2$ particles onto medical devices and teeth and proof of concept CHX release study.

Chapter 3. Synthesis, Characterization and Stability of CHX Particles

3.1 Introduction

Antiseptics are widely applied for preventing and reducing wound and surgical infections, which continue to be a major problem in health care [246]. This can be particularly difficult to manage in developing countries due to lack of resources, high costs, and special storage conditions of antibacterial agents [247]. Lack of suitable antibacterial agents can however lead to high infection rates and even death [248], due to ventilator-associated pneumonia and sepsis [249]. An effective, affordable, and safe intervention for preventing infections and improving public health is therefore in high demand.

Chlorhexidine (CHX) is an antibacterial agent [250–252] widely applied in medicine and dentistry [253,254]. It has been used for daily bathing of critically ill patients in intensive care units [255] or as a neonatal wipe for cord care [256]. In the dental field, it is used to control dental plaque [257] and reduce surgical/recurrent infections (e.g., periodontal disease and endodontic disease) [258–261]. As a broad-spectrum antibacterial agent, CHX provides both bactericidal and bacteriostatic effects by producing non-specific binding to the negatively charged membrane phospholipids of the bacteria. This leads to alteration in bacterial osmotic equilibrium. When the CHX concentration is increased, the cytoplasm contents precipitate, causing cell death [63,207].

Many systems have been proposed for chlorhexidine delivery, where the direct addition of chlorhexidine gluconate solution (4%) [262] is used for burns and wounds, or 0.12–0.3% CHX in mouthwash as a common method for reducing bacterial load [140,263].

Generally, the incorporation of CHX gluconate into loading systems involves gels and varnishes. Biodegradable chips or incorporation into polymers are also feasible methods [166,264]. The low drug loading capacity, burst drug release, and strong binding formed between the drug and the polymeric matrix, however, limits its antibacterial efficacy [1,170]. Furthermore, the main limitations of the majority of formulations and delivery methods that have been used are the difficulties of maintaining bacteriostatic concentrations in the oral environment for a significant time [257,265] and the inability to reach and remain in the periodontal or peri-implant pocket.

To achieve effective chlorhexidine delivery, modification of the chlorhexidine formulation is one of the promising and feasible strategies. Previous studies suggested the co-precipitation of CHXD with $CaCl_2$ to produce CHX-$CaCl_2$ spheres, which demonstrated sustained release behaviour and high CHX content (95%) [86]. It is also possible to substitute Ca^{2+} ions within the structure with other ions, to bring additional therapeutic benefits. Good candidates for this particle substitution are ions such as Zn^{2+}, Sr^{2+} or F^- to optimize antimicrobial activity and re-mineralization [66,266–268].

The presence of strontium (Sr) would be beneficial to perform the dual action of bone stimulation and bone resorption suppression [208,269]. Numerous studies have demonstrated strontium is able to promote pre-osteoblast proliferation, osteoblast differentiation, bone matrix mineralization, and stimulate type I collagen protein levels [270] while inhibiting osteoclast differentiation [271]. Therefore, strontium inclusion would be particularly useful in the treatment of implant and surgical associated infections (peri-implantitis) found in dentistry. Strontium has also been shown to significantly enhance the remineralizing effect of fluoride ion (F^-) [220] and to help remineralize dentine in vitro [219]. Zinc (Zn) has various positive characteristics, such as angiogenic,

osteogenic, and antimicrobial properties [272]. Zn^{2+} is attracted to the negatively charged microbe cell membrane, penetrates it, and reacts with sulfhydryl within it. Thus, the activity of synthetase in the microbe is damaged and the cells lose the ability of mitosis, which leads to the death of the microbe [273]. In practice, owing to its bacteriostatic properties, zinc is incorporated in dental filling materials, mouth rinses, and toothpastes [274]. The release rate of Zn increases dramatically under acidic conditions in Zn containing silicate glasses, enabling Zn release during bacterial infections at low pH value (pH = 4.5) [232]. This particular property would also be very attractive in the development of a smart release antiseptic.

Therefore, the aim of the work is to use low-cost reagents and energy-saving synthesis to develop a novel drug delivery particle that can pH responsively release antibacterial agents of CHX and metal ions to take advantage of their therapeutic functions, thus providing a safe and effective antimicrobial environment for dental and medical applications.

3.2 Materials and Methods

All the chemicals were listed in Table 3 below, which were used directly without further purification. All the solutions were prepared using deionized (DI) water (Milli-Q, Millipore Co., Bedford, MA, USA) with an 18.2 MΩ·cm resistance.

Table 3. Reagents used in the experiment.

Chemical reagent	Manufacturer	Batch No.
Chlorhexidine Diacetate	Sigma-Aldrich Gillingham, Dorset, The UK.	4G013891
Strontium Chloride hexahydrate		MKC131848V
Calcium Chloride dihydrate		SLBT9639
KH_2PO_4		BCBC2041
Hepes		SLBW8459
KCl		BCBZ4557
$CaCl_2 \cdot 2H_2O$		060M0027V
Acetic acid		6776070
phosphate-buffered saline (PBS)		1762519
Zinc Chloride		MKCC2307
NaF		SLCB1955
NaCl		1540269

3.3 Synthesis of CHX particles

3.3.1 Synthesis of Calcium, Strontium, Zinc Containing CHX particles

Calcium, zinc and strontium ions were selected as the positive cations to be released from CHX particles. The chlorhexidine (CHX) particles were synthesised by coprecipitation of 0.024M chlorhexidine diacetate (CHXD) with 0.33M $CaCl_2$, $ZnCl_2$ or $SrCl_2$ mixed at 1:1 by volume at room temperature. The mixtures were left for 1 min and then centrifuged at 2400 rpm for 1 min (Eppendorf centrifuge 5417C, Germany). The precipitates were washed with 1ml deionized water (three-stage Millipore Milli-Q 185 water purification system, Millipore, USA), placed into liquid nitrogen for 30 minutes, and then transferred to a freeze dryer (ScanVac CoolSafe Freeze Drying, Denmark) at -107°C, 0.009 mBar for 24 hours. Particles were stored at 4°C and wrapped in aluminium foil paper to exclude the light.

3.3.2 Analysis of Temperature and Time on Particle Synthesis

To evaluate the influence of temperature on CHX-$SrCl_2$ and CHX-$ZnCl_2$ particle formation, both CHXD and $SrCl_2$/$ZnCl_2$ solutions were kept in a temperature-controlled water bath or ice bath (IKA RET basic C, UK) at selected temperature points of 0, 5, 10, 15, 20, and 25 °C. The coprecipitation process was then carried out at these selected temperatures using the same procedures and freeze-dried as previously. To demonstrate the influence of the reaction times on the formation of both particles, 20 µL CHXD solution (0.024M) was added onto glass slides and left for one minute, and 20 µL $SrCl_2$ or $ZnCl_2$ (0.33 M) was further added and reacted for 15 s, 30 s, 45 s, and 60 s. Then the excess liquid was carefully removed with fuzz-free lab wipes. The samples were then freeze dried as previously.

After gold coating, SEM images (detailed in section 3.4.1) of the temperature and reaction time samples were captured (the experiment was performed triplicate with each sample taking three pictures) and particles were analysed using quantitative image analysis (Nanoparticle measurer).

3.3.3 Synthesis of Fluoride Containing CHX Particles

Fluoride as a common ion used in dentistry was selected as the negative cation incorporated into CHX particles. The CHXD concentration was at 0.024M. The 0.66 M NaCl solution was mixed with the NaF concentrations of 0.125, 0.25, 0.33, 0.5, 0.66 and 0.68 M. then with the CHXD solution at 1:1 by volume at room temperature.

The mixtures were left for 1 min and then centrifuged at 2400 rpm for 1 min (Eppendorf centrifuge 5417C, Germany). The precipitates were washed with 1ml deionised water (three-stage Millipore Milli-Q 185 water purification system, Millipore, USA), and the precipitates were placed into liquid nitrogen for 30 minutes, and then transferred to a freeze dryer (ScanVac CoolSafe Freeze Drying, Denmark) at -107°C, 0.009 mBar for 24 hours. Particles were stored at 4°C and wrapped in aluminium foil paper to exclude the light.

The 0.024M CHXD was mixed with the concentrations of 0.96 M NaF solution at 1:1 by volume at room temperature. The mixtures were left for 20, 40, 60, 80, 100, 120, 140 minutes and then centrifuged at 2400 rpm for 1 min (Eppendorf centrifuge 5417C, Germany). The precipitates were washed with 1ml deionised water (three-stage Millipore Milli-Q 185 water purification system, Millipore, USA), and the precipitates were placed into liquid nitrogen for 30 minutes, and then transferred to a freeze dryer

(ScanVac CoolSafe Freeze Drying, Denmark) at -107°C, 0.009 mBar for 24 hours. Particles were stored at 4°C and wrapped in aluminium foil paper to exclude the light.

3.4 Characterisation of the CHX Particles

The freeze-dried novel CHX-$CaCl_2$, CHX-$SrCl_2$, CHX-$ZnCl_2$ and fluoride containing particles were characterized using scanning electron microscopy (SEM, FEI inspect-F, Hillsboro); Energy-Dispersive Spectroscopy (EDS) (FEI Inspect F, NanoPort, Eindhoven, The Netherlands) and analysed using Fourier Transform Infrared Spectroscopy (FTIR, Bruker, Billerica, MA) and X-ray diffraction (XRD) (Panalytical, Almelo, The Netherlands).

3.4.1 Scanning Electron Microscopy (SEM)

Scanning Electron Microscopy (SEM) is an instrument used for the examination and analysis of the microstructural characteristics of a specimen which can carry out the specimen dimensional topography and elemental analysis [275]. Specimens are coated with a thin layer of a conductive metal such as gold or carbon to make them electrically conductive [276]. The basic principle of the SEM has an electron beam excited from an electron gun and its passage through the microscope [277]. These electrons are accelerated towards the anode, where they are emitted into the microscope column (under vacuum), via a circular hole and as a high-energy beam of monochromatic electrons. The condenser lens in conjunction with selected accelerating voltage focuses the electron beam via an aperture, which is used to control the depth of field and brightness. Magnetised coils surround the electron beam as it scans over the surface of the specimen. The incident electrons impart energy to lower energy electrons in the K shell and they are emitted as a secondary electron that is picked up

by an electron collector linked to an amplifier [278]. When bulk objects are examined, secondary electron imaging (SEI) can give high-surface resolution detail in the order of 2 to 5 nm [279].

The powder samples (CHX-$CaCl_2$, CHX-$SrCl_2$, CHX-$ZnCl_2$, and CHX-NaF-NaCl and CHX-NaF) were prepared on a carbon tape and coated with gold in an automatic sputter coater (Agar Scientific Ltd, U.K.) under vacuum for 60 seconds. The samples were viewed using scanning electron microscopy (FEI Inspect F, NanoPort, Eindhoven, The Netherlands) in the secondary electron imaging mode. The accelerating voltage used was 10 kV, spot size set at 3.0, and working distance 8-10 mm. SEM was used to evaluate three random positions (triplicate), in order to assess and confirm the different morphology and size ranges of the CHX-$CaCl_2$, CHX-$SrCl_2$, CHX-$ZnCl_2$, and CHX-NaF-NaCl and CHX-NaF particles obtained.

3.4.2 Energy-Dispersive Spectroscopy (EDS)

The components of the specimen can be investigated in the SEM by using energy-dispersive X-ray spectroscopy (EDS or EDX) which is commonly attached to the SEM dedicated to quantitative chemical characterization of sample [280]. The main principle of EDS is that different elements reflect a special atomic structure which could result in a critical electromagnetic spectrum when they are emitted [281]. The EDS experiment of a specimen is investigated by using a high energy electron beam that can excite an electron from an inner shell, knocking it out from its original orbit while creating an empty position for electrons. An electron from outer orbit would jump from a higher energy shell to a lower energy state and fill the position and emit X-rays to conserve energy because of the electron jumps. Because the magnitude of the signal is

proportional to the energy of the X-ray, the EDS spectrum can be illustrated as X-ray counts versus energy. This can offer a rapidly evaluating the elemental constituents of a specimen and can further provide an accurate quantitative analysis. Based on the identification of peaks in the spectrum, the excited volume of the elements present in the sample was determined, which gives the result of qualitative analysis[282]. Therefore, the EDS attachment is used for analysis of the elemental composition by measuring the amount and the energy of the captured X-rays [280].

The powder samples were prepared on a carbon tap and coated with carbon in an automatic sputter coater (Agar Scientific Ltd, U.K.) under vacuum for 60 seconds. The samples were viewed using scanning electron microscopy (FEI Inspect F, NanoPort, Eindhoven, The Netherlands). The accelerating voltage used was 20 kV, spot size set at 5.0, and working distance 8-10 mm. Ca^{2+} / Zn^{-} / Sr^{2+} / F^{-}/ Cl^{-} in the sample was analysed using energy-dispersive spectroscopy (EDS).

3.4.3 Fourier Transform Infrared Spectroscopy (FTIR)

Fourier Transform Infrared Spectrometer (FTIR) is a basic technique for chemical structure analysis, functional groups of molecules identification and detection of certain compounds. It can test organic or inorganic in their status of solid, gas and even liquid, although the interference from water is not favoured [283]. It is sensitive to the mid-region electromagnetic spectrum (4000-200 cm^{-1}), and is an effective method to identify the molecule structures with their characteristic absorption of infrared radiation. FTIR (Bruker, Billerica, MA) was used to analyze the chemical structure of the CHX-$SrCl_2$ and CHX-$ZnCl_2$ particles. A small amount of CHX-$SrCl_2$ or CHX-$ZnCl_2$ particles was placed on the stage in such a way that the particles covered the IR

window. Afterwards, the data was collected in the absorbance mode from 1500 to 500 cm^{-1}. The CHXD was also analysed by FTIR as a compared group.

3.4.4 X-ray Diffraction (XRD)

X-ray Powder Diffraction (XRD) can be utilized for determining different crystalline phases and the crystal structure in materials. This process determines unit cell size at the atomic level. It is routinely used for phase determination for eutectics mixtures and determining structural parameters [76]

Synthesized CHX-$CaCl_2$, CHX-$SrCl_2$, CHX-$ZnCl_2$, CHX-NaF-NaCl and CHX-NaF compounds were placed in a holder of an Xpert-Pro X-ray Diffractometer (Paralytical, B.V., Almelo, Netherlands). Flat plane geometry and Cu Ka radiation Theta1=1.5405980 Å and Theta = 1.5444260 Å were used. Data were collected from 5 to 70 2 Theta, with the Xpert- Pro X-ray Collector in a continuous mode. Data were plotted using Excel software (Microsoft office 365).

3.4.5 UV-Vis Spectrometry

3.4.5.1 UV/Vis Standards Preparation for CHX Release

The Ultra-Violet/ Visible Spectrometer can quantitatively analyse the concentration of a tested specimen by comparing the different light absorption behaviour of organic solutions separated by two equal intensity beams [284]. Thus, it can be used in pharmaceutical drug formulation studies. It is distinct from other techniques such as electron energy loss and X-ray absorption spectroscopy since it uses photons to excite

particles and can induce electronic transitions without changing the incoming radiation [285].

The detectable light ranges from Ultraviolet to infrared (190 nm to 780 nm) is shown in Figure 7 [286]. To produce the spectrum range, the lights are produced by two bulbs which include ultra-violet spectrum (deuterium lamp) and visible light spectrum (tungsten/ halogen lamp) [287]. The visible and ultraviolet light beam is divided into its component light by a dispersion device which happens in the monochromator.

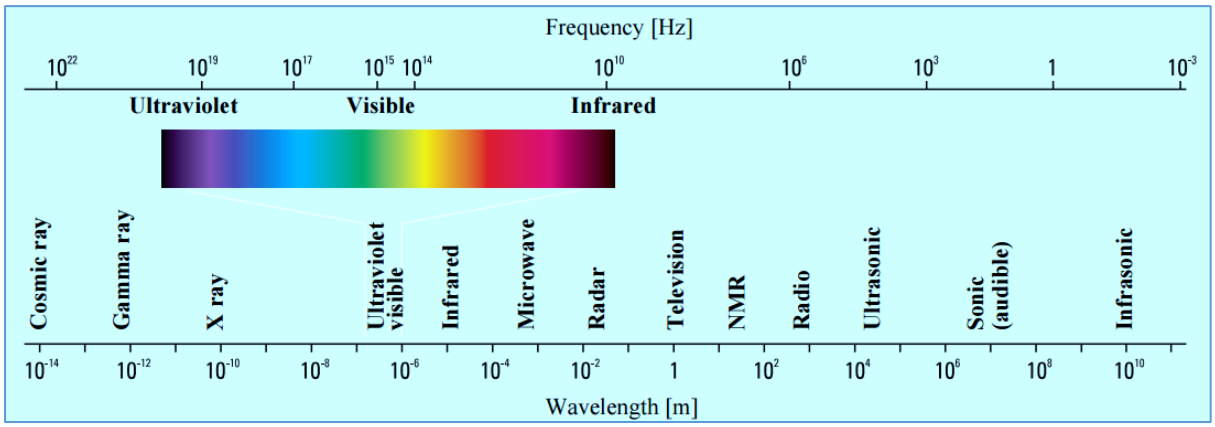

Figure 7. The electromagnetic spectrum [286].

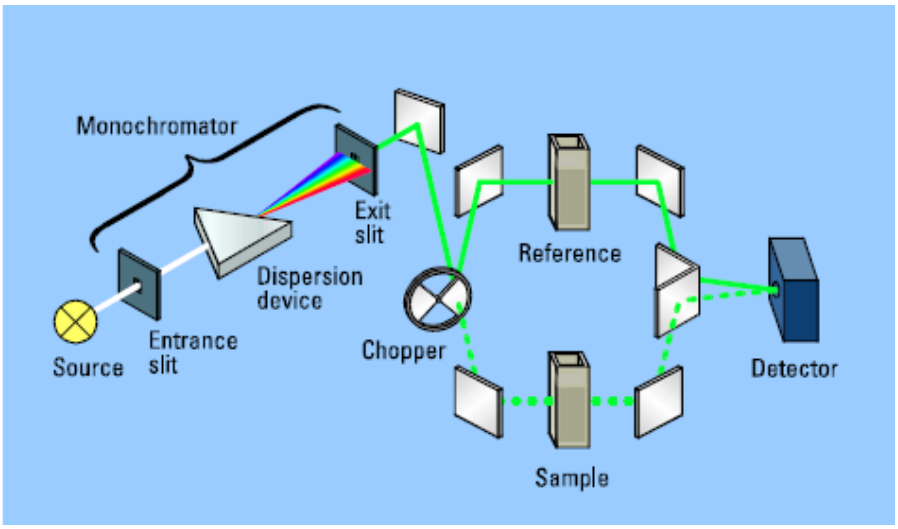

Figure 8. The optical system of a double-beam spectrophotometer [286].

Figure 8 shows an illustrated diagram of the double-beam spectrophotometer. Test sample and reference are placed in the quartz cuvette which has two of its side grooved, preventing light to travel through while the other two sides allow lights to pass through. Then the sample is placed into the UV/Vis spectrometer's sample slot while the reference sample is placed in the reference slot. The energy supplied by the light source of a single beam and the absorbance of the ultraviolet light causes the excitation of photons, which leads to electron collisions to occur from a lower vibrational state to a higher vibrational state within the orbitals. It is then transmitted through the cuvette where light is dispersed into different wavelengths by the dispersion device prism in the monochromator. A beam of light is separated into two equal intensity beams by a half-mittore device. One beam has to pass through a small transparent cuvette which includes the test sample. The other beam passes through a cuvette containing a reference sample (i.e., distilled water). Following this, the spectrophotometer will automatically scan all component wavelengths during a short period [287]. Generally, the ultraviolet region scanned is normally from 190 to 400 nm, and the visible portion is from 400 to 780nm. Furthermore, in order to obtain higher accuracy in measuring the absorbance, calibrated data from a series of standard solutions of serial dilutions of known concentrations of chemical reagent for any quantitative analysis should be used [288]. The concentration of the sample can then be calculated from the calibration curve [286]. The concentrations of the sample could be determined within the concentration limits of the curve using the equation of the slope ($y = mx + y_0$).

In previous studies, the UV/Vis technique was used to measure the chlorhexidine diacetate released in drug delivery systems. Chlorhexidine diacetate was measured using a wavelength of 257.5 nm in PMMA/PEM [289], 220 nm was used in a PEM/THFM

chlorhexidine diacetate system [290] and 260 nm was used as a reference wavelength for chlorhexidine diacetate released in HEMA [291]. Normally, wavelength selections are based on the cuvette containing only the dissolved components involved. This technique can therefore be used in drug detection in solutions [292].

Various chemicals have diverse absorption maxima and absorbance in UV/Vis spectroscopy. Intensely absorbing compounds should be diluted into less concentrated solutions to facilitate the critical light energy receiving of the detector. UV/Vis spectroscopy can only provide non-specific information quantitatively, mainly because it cannot accurately identify species of chemical reagents [286]. Thus, in order to obtain higher accuracy in measuring the absorbance, calibrated data consisting of a series of standard solutions, in the form of serial dilutions of a known concentration of chemical reagent are prepared [288]. These sample solvents are used as a reference to analyse the sample. This might be helpful in the correction of and interference caused by a component with a second wavelength [293].

The CHX release of the CHX particles 0.024M (CHXD and 0.33M $CaCl_2$, $ZnCl_2$ or $SrCl_2$) was measured by using UV-Vis absorption (Lambda 35, Perkin Elmer, USA). For concentration determination, the number of molecules in the solution was calculated based on the calibrated relationship. Initially, a series of CHXD standard solutions with a concentration of 1, 3, 5, 10, 20, 30 and 50 µg/ml were prepared and used to obtain a linear relationship between the absorbance peak (254nm) and the CHX concentration. All the released solution concentration was measured and calculated with the linear calibration curve. In this experiment, the reference cuvette filled with 3ml of deionized water was placed into the spectrometer before the CHX sample. The spectrometer scan was run at the absorbance value of 254nm. Figure 9 showed an

example of the calibration curves for UV/Vis spectrometry. A calibration curve plotting absorbance versus concentration in µg/ml showed a good correlation (r^2 value = 1). The concentrations of the sample could be determined within the concentration limits of the curve using the equation of the slope.

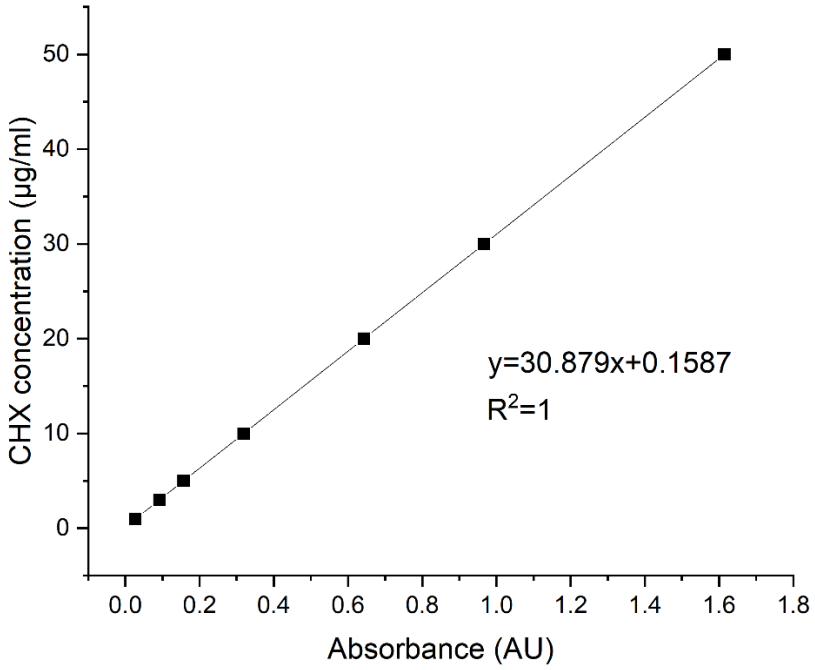

Figure 9. The UV/Vis results of calibration curve for CHX diacetate.

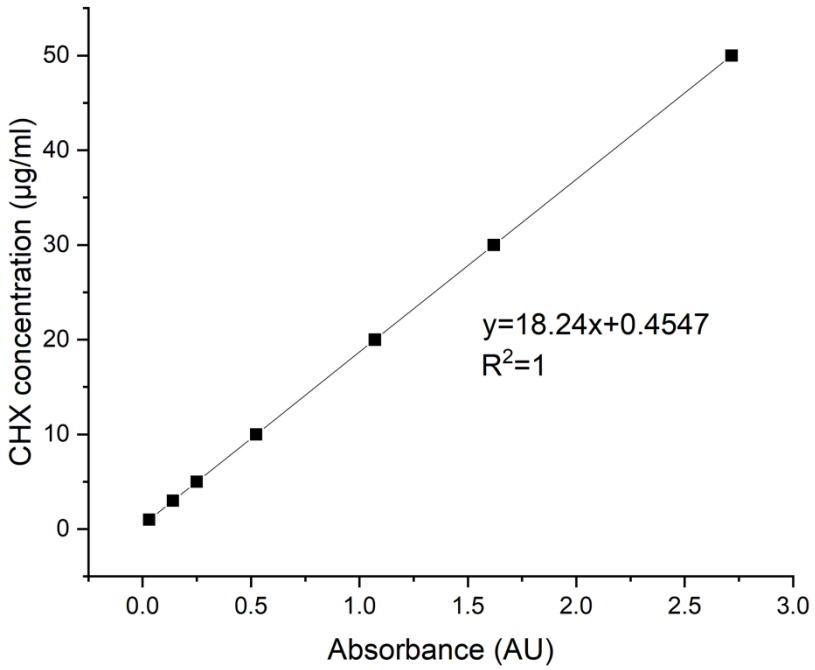

Figure 10. The UV/Vis results of calibration curve for CHX digluconate.

3.4.5.2 CHX-$CaCl_2$, CHX-$ZnCl_2$ or CHX-$SrCl_2$ Particle Release Assays

The content of chlorhexidine in the compounds was determined by using the UV-Vis spectrometer. The release kinetics was tested weighting 0.01g CHX-$CaCl_2$, CHX-$ZnCl_2$ or CHX-$SrCl_2$ particles (n=3) stored in 2ml centrifuge tubes with either 2ml phosphate-buffered saline (PBS) or artificial saliva (AS; pH=7). At specified time points (Table 4), the samples were centrifuged, and supernatant was collected for UV-Vis absorption measurement. A further, 2ml fresh PBS or artificial saliva (AS; pH=7) was added again and this procedure was repeated until CHX release measured was below MIC. The cumulative release was calculated using a calibration curve.

Table 4. UV/Vis schedule for the release assay

Week	Day	Time interval (minutes/hours) (PBS/AS)	Time interval (minutes/hours) (water)
1st Week	1st Day (Monday)	5 minutes	6 minutes
		10 minutes	8 minutes
		20 minutes	10 minutes
		40 minutes	15 minutes
		60 minutes (1 hour)	20 minutes
		120 minutes (2 hours)	25 minutes
		180 minutes (3 hours)	30 minutes
		240 minutes (4 hours)	40 minutes
		300 minutes (5 hours)	50 minutes
		360 minutes (6 hours)	60 minutes
		420 minutes (7 hours)	70 minutes
		------	80 minutes
		------	90 minutes
	2nd Day (Tuesday)	2 readings (10:00 and 16:00)	------
	3rd Day (Wednesday)	2 readings (10:00 and 16:00)	------
	4th Day (Thursday)	2 readings (10:00 and 16:00)	------
	5th Day (Friday)	2 readings (10:00 and 16:00)	------
	6th Day (Saturday)	1 reading (12.00)	------
	7th Day (Sunday)	1 reading (12.00)	------
2nd Week	Monday	1 reading (12.00)	------
	Friday	1 reading (12.00)	------
3rd Week	Monday	1 reading (12.00)	------
	Friday	1 reading (12.00)	------
4th Week	Monday	1 reading (12.00)	------
	Friday	1 reading (12.00)	------

3.4.6 Ion Release Analysis

To analyse Sr, Zn ions from the particles, the supernatant from the release experiments in section 3.4 were collected and analysed.

The fluoride concentration of synthesized CHX-NaF-NaCl particles was measured using F^- electrodes attached to an ELIT 9808 ion analyser (Nico2000, UK) and ELIT electrochemical software (Nico2000, UK). Calibration curves were performed before ion analyses of supernatant samples using known concentrations of F^- ions. The 1000 µg/ml F^- the stock solution was diluted to different concentrations to calibrate the electrode (1000µg/ml , 100µg/ml ,10µg/ml ,1µg/ml and 0.5pµg/ml). The voltage recorded at each point was used to plot a calibration curve which was used to calculate the concentrations of samples. In order to analyse the amount of fluoride in the fluoride containing particles, 0.03g of CHX-NaF-NaCl particles from the range 0.33M to 0.66M and 0.03g of CHX-NaF particles were dissolved in 30ml of DI water and run for ion-Selective Electrode (ISE).

3.4.7 Inductively Coupled Plasma-Optical Emission Spectroscopy

Inductively coupled plasma–optical emission spectroscopy (ICP-OES) is a sensitive technique used to measure ion [294] (Sr^{2+}, Zn^{2+}) concentrations even at very low concentrations (0.1 µg/ml)[295]. Additionally, ICP provides a simple sample preparation. It is reported that ICP is a chemical element imaging technique of high sensitivity which has multi-element capability, allowing multiple elements to be measured in the same analysis [296]. Within this technique, the contained sample solution is first nebulized in the sample introduction system, converting to an aerosol that is subsequently transferred to the argon plasma. This enters the central tube of

the plasma. Because of the high temperature (10,000K) plasma, a large proportion of the atoms are ionized by losing its most loosely bound electrons. Thus, the generated ions are extracted through the interface region and into a set of electrostatic lenses [297]. The ions beam then into the quadrupole mass analyzer and are separated according to their mass-charge ratio. Thus, the detector is able to receive an ion signal in proportion to the concentration of the ion [298].

In this work, the concentrations of Zn were quantified using inductively coupled plasma-optical emission spectroscopy (ICP-OES; Varian Vista-PRO, UK). Before the sample measurement, a calibration for each element is performed with standards.

Elemental calibration standards prepared from element standards (1000µg/ml standards in deionized water, VWR), were diluted in deionized water to produce 0, 1, 5, 10, 50 and 100µg/ml concentrations of each ion. The zinc content of the calibration standards was measured using inductively coupled plasma-optical emission spectroscopy (ICP-OES; Varian Vista-PRO, Yarnton, UK).

The zinc or strontium content measurements were tested by ICP-OSE. The measured solution was prepared by adding 0.04g CHX-$ZnCl_2$ or CHX-$SrCl_2$ particles into 8ml deionized water. Calibrations were performed using diluted element stock solution. Data were plotted using Excel software (Microsoft office 365).

ICP-OSE was employed for measuring the zinc release curve of CHX-$ZnCl_2$ particles in AS of pH=4 and pH=7, according to the timepoints in Table 4 (up to 7 hours). At each time point, samples were centrifuged, and the supernatants were used for the analysis, before replacing with fresh AS. All the experiments were repeated in triplicate.

3.5 Results of Synthesis and Characterization of Ca, Sr and Zn Containing CHX Particles

3.5.1 Results of SEM Analysis for the Novel Particle Structure

The SEM images confirmed that the CHX-$CaCl_2$, CHX-$SrCl_2$ and CHX-$ZnCl_2$ particles produced a spherical morphology and dendritic microstructure, as illustrated in Figure 11 a - f. This unique structure differed from the original CHXD platelet morphology (Figure 11 g, h). The CHX particles showed a porous and inter-connected spherical structure (Figure 11 b, d, f) which grew dendritically from a nucleation site central to the structure, while the microstructure of CHXD appeared as a solid crystal with an angular shape (Figure 11 h). The Mean (SD) particle diameter was 15.7 (4.73) µm (CHX-$CaCl_2$), 17.5 (4.39) µm (CHX-$SrCl_2$) and 14.2 (4.71) µm (CHX-$ZnCl_2$) and CHXD 80 (30) µm at 25°C.

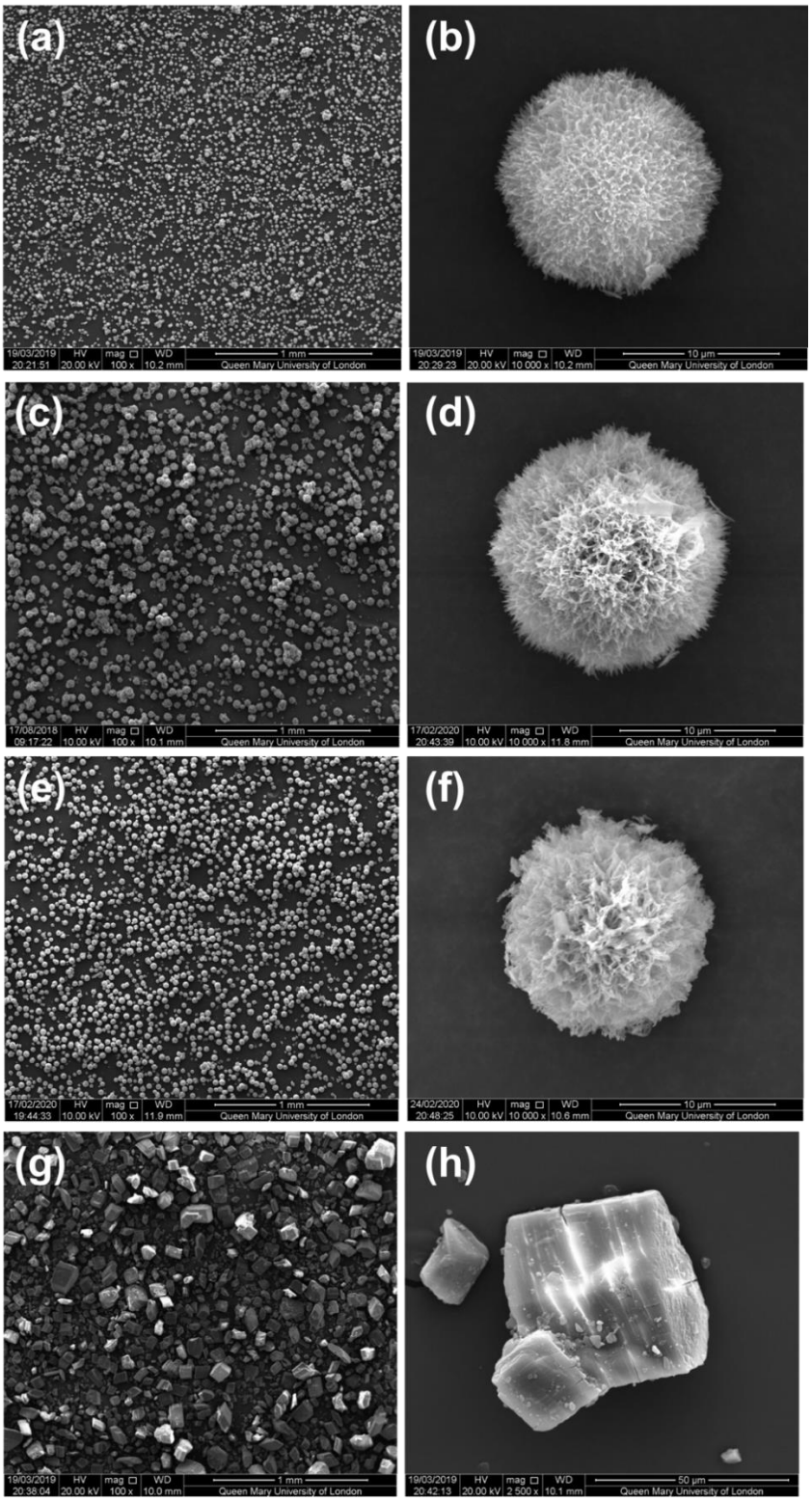

Figure 11. SEM images of (a)(b) CHX-$CaCl_2$ particles; (c)(d) CHX-$SrCl_2$ particles; (e)(f) CHX-$ZnCl_2$ particles; with a spherical / dendritic morphology and even distribution; (g)(h) CHX diacetate particles with an angular structure and larger size.

3.5.2 Results of SEM Analysis for the Novel Particle Reaction Time

The results of the SEM study for particle reaction time were illustrated in Figure 12 a, b. Inserted figures were higher magnification (10,000x) SEM images of novel CHX particles. Figure 12 a, b showed CHX-$SrCl_2$ and $ZnCl_2$ particles had a systematic increase in Mean particle diameter with increased reaction time. Figure 13 suggested the Mean diameter of the CHX-$SrCl_2$ and CHX-$ZnCl_2$ particles was correlated (r^2=0.96, r^2=0.99) with reaction time (15s to 60s). Both particles showed dendritic and spherical structures in Mean particle diameter between all reaction time groups.

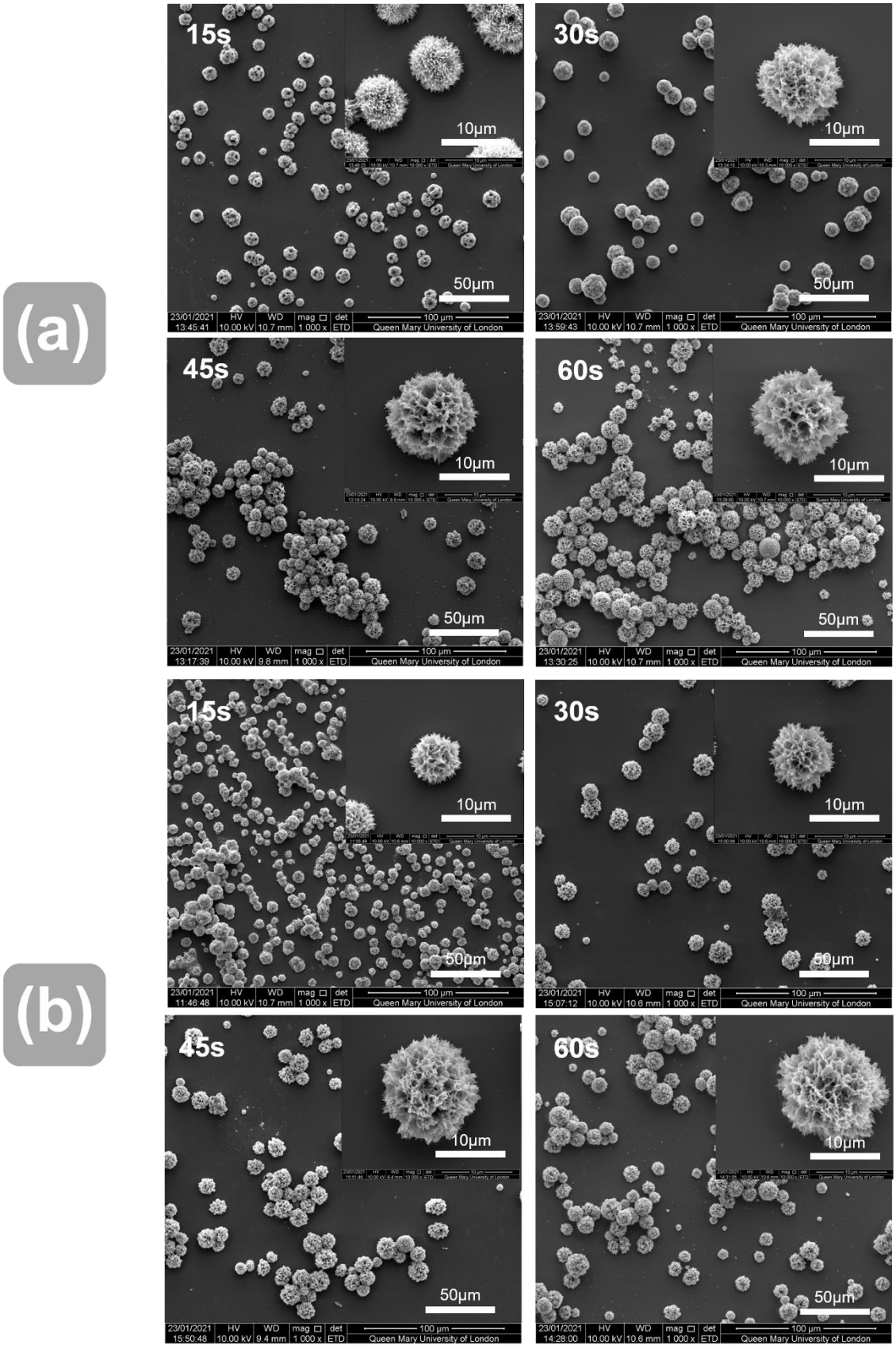

Figure 12. SEM images of: (a) CHX-$ZnCl_2$ particles; (b) CHX-$SrCl_2$ particles at different reaction times.

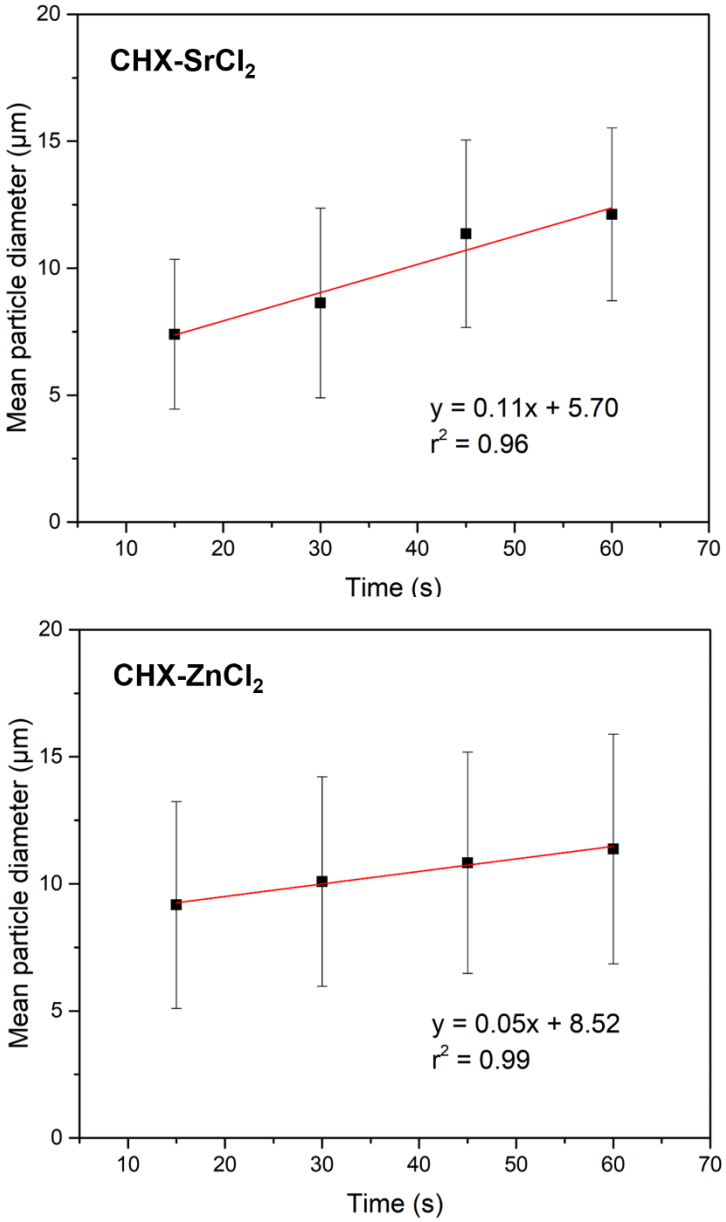

Figure 13. Plots showing the correlation between the Mean particle diameter and reaction time for both CHX-$SrCl_2$ and CHX-$ZnCl_2$ particles.

The CHX-$SrCl_2$ and CHX-$ZnCl_2$ crystallisation reactions were captured using HD video. Figure 14 demonstrated the instantaneous reaction of CHXD solutions with $SrCl_2$ or $ZnCl_2$ solutions. When $SrCl_2$/$ZnCl_2$ solutions contacted the CHXD solutions, the mixture immediately turned into a white colour, indicating a reaction progression.

The crystallization reaction of the two solutions appeared to be extremely rapid (some turbidity in 0.05 secs, and complete turbidity in 0.4 secs Figure 14

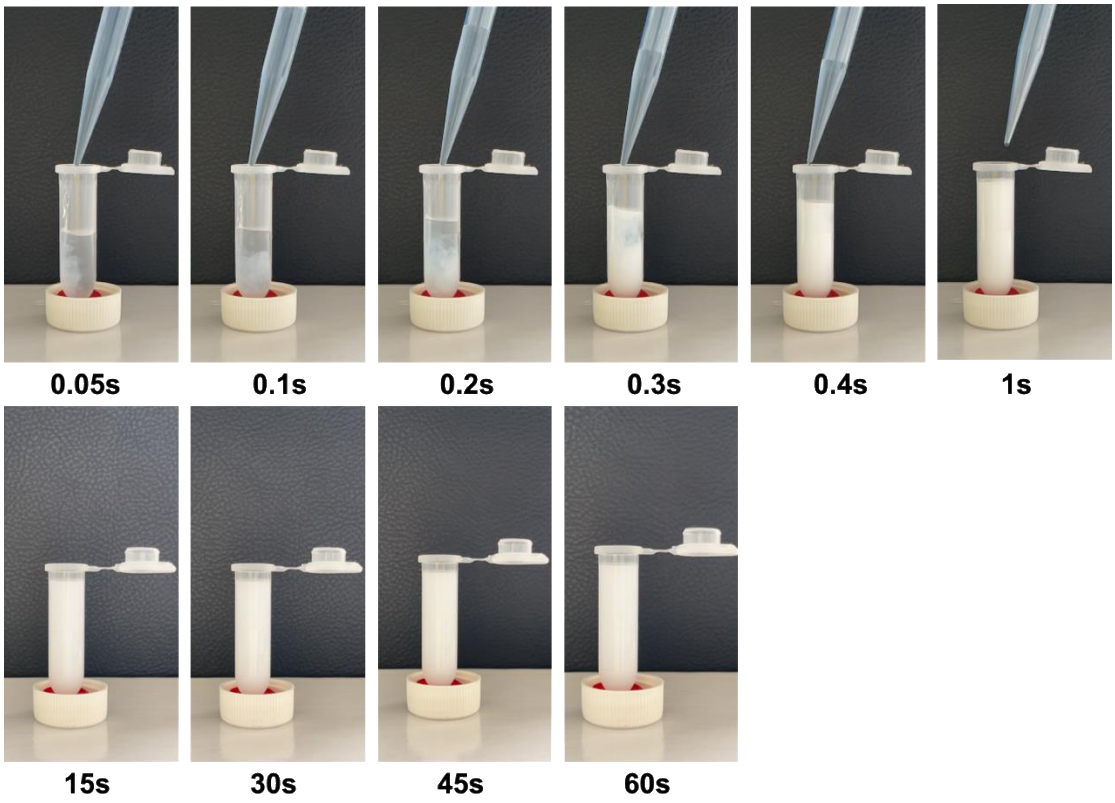

Figure 14. Digital photos showing CHX-$ZnCl_2$ particles at different reaction times.

3.5.3 Results of SEM Analysis for the Novel Particle Reaction Temperatures

The CHX-$SrCl_2$ and CHX-$ZnCl_2$ particles were also produced at selected temperature points (0°C to 25°C), and the results were shown in Figure 15. There was an increase in Mean particle diameter with an increase in synthesis temperature for both particles (Figure 16 a, b), with particle size correlated (r^2=0.98, r^2=0.99) with temperature (Figure 16). Both particles showed statistical differences in Mean particle diameter between all selected temperature groups ($P < 0.05$). As the temperature increased, the Mean diameter of CHX-$ZnCl_2$ particles was increased from 4.35 (1.94) μm (0°C) to 14.2 (4.71) μm at 25°C. Similar to the trends observed in the CHX-$ZnCl_2$, the size

of CHX-$SrCl_2$ particles were increased from 3.37 (1.71) μm at 0°C to 17.5 (4.39) μm at 25°C. The particle morphology had no individual structural difference in this temperature range between 0°C to 20°C. At 25°C there was a slightly more open particle structure.

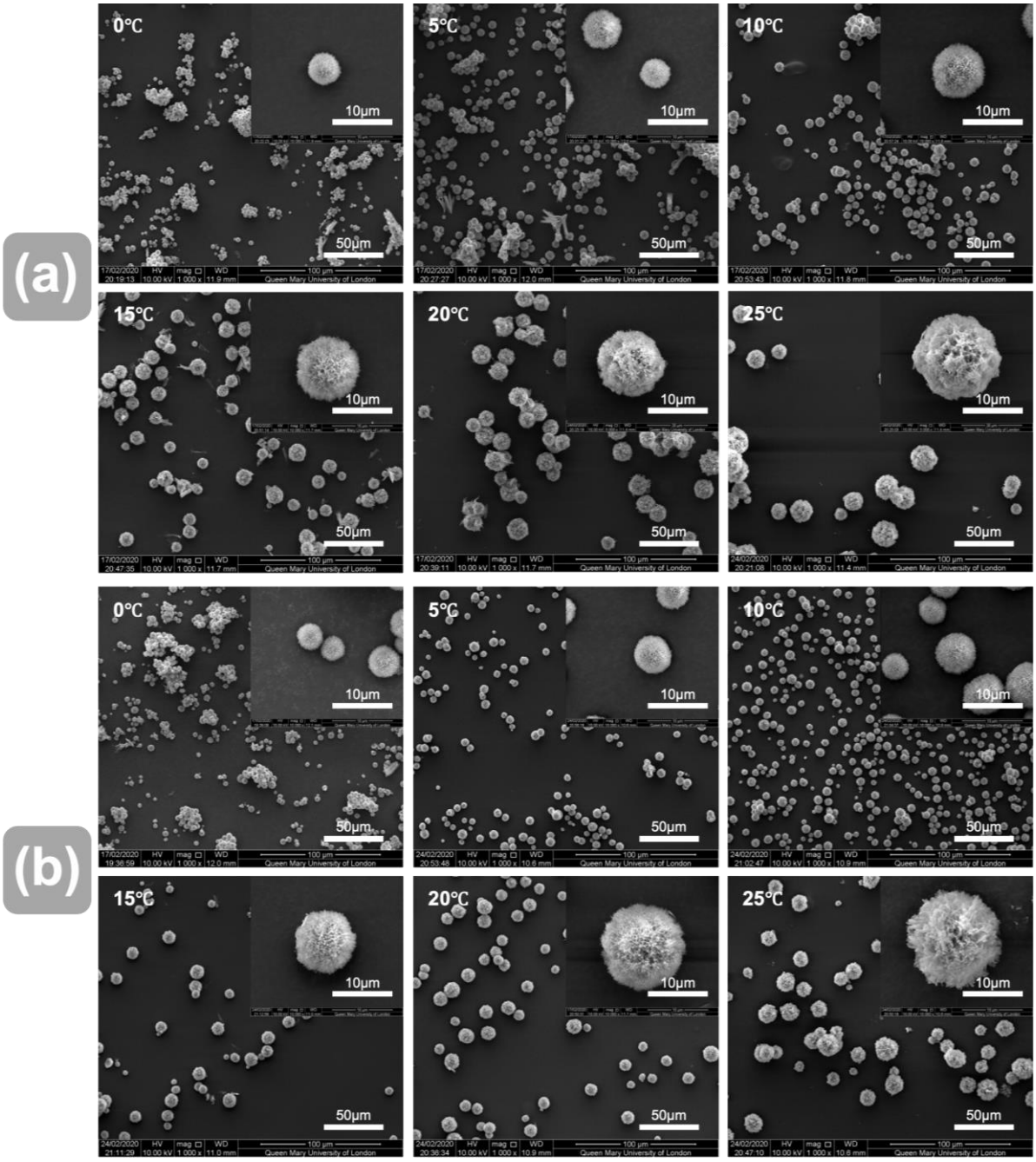

Figure 15. SEM images of: (a) CHX-$SrCl_2$ particles; (b) CHX-$ZnCl_2$ particles at different synthesis temperatures.

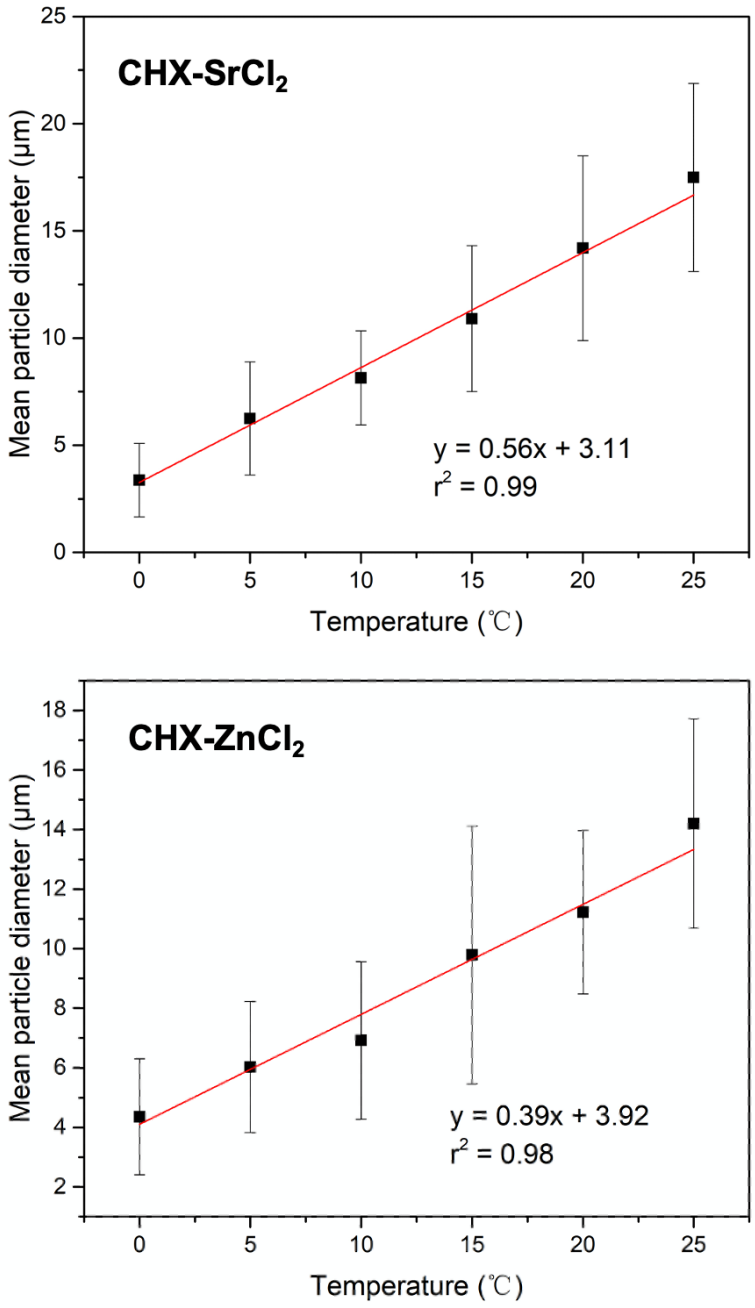

Figure 16. Plots showing the correlation between the Mean particle diameter and temperature for both CHX-$SrCl_2$ and CHX-$ZnCl_2$ particles.

3.5.4 Results of EDS Study

The electron photomicrographs of the CHX particles are shown in Figure 17 a - Figure 19 a. The EDS results of the CHX-Ca/Sr/$ZnCl_2$ particles (Figure 17 b, c - Figure 19 b, c) indicated an even distribution of calcium, strontium or zinc and chloride throughout the particles and associated with its structure. Quantitative elemental analysis indicated that the weight percentage of divalent ions incorporated in the CHX particles was 3.95wt% for strontium, 7.66wt% for zinc, and 17.47 wt% for calcium, respectively (Table 5 - Table 7).

EDS mapping images of Ca/ Sr/ Zn/ Cl results were shown in Figure 17 b, c to Figure 19 b, c. Among those images, Figure 17 b - Figure 19 b showed the chloride distribution in the particles. Figure 17 c - Figure 19 c respectively showed the Sr/ Ca/ Zn distribution in each particle. The CHX-$SrCl_2$ Particle (Figure 17 a) showed higher strontium and reduced chloride distribution (Figure 17 b, c) compared to the other two particles. The CHX-$CaCl_2$ Particle (Figure 18 a) indicated a higher chloride and reduced calcium distribution (Figure 18 b, c). The CHX-$ZnCl_2$ particle (Figure 19 a) illustrated an even zinc distribution and dense dispersion of chloride ions. The corresponding EDS spectra were shown in Figure 17 d and Figure 19 d. Moreover, the CHX-$SrCl_2$ or CHX-$ZnCl_2$ particles were able to release additional antibacterial ions. CHX-$SrCl_2$ (3.95 wt%, Table 5) and CHX-$ZnCl_2$ particles contain (7.66 wt%, Table 7,) potentially available for release as an antibacterial agent.

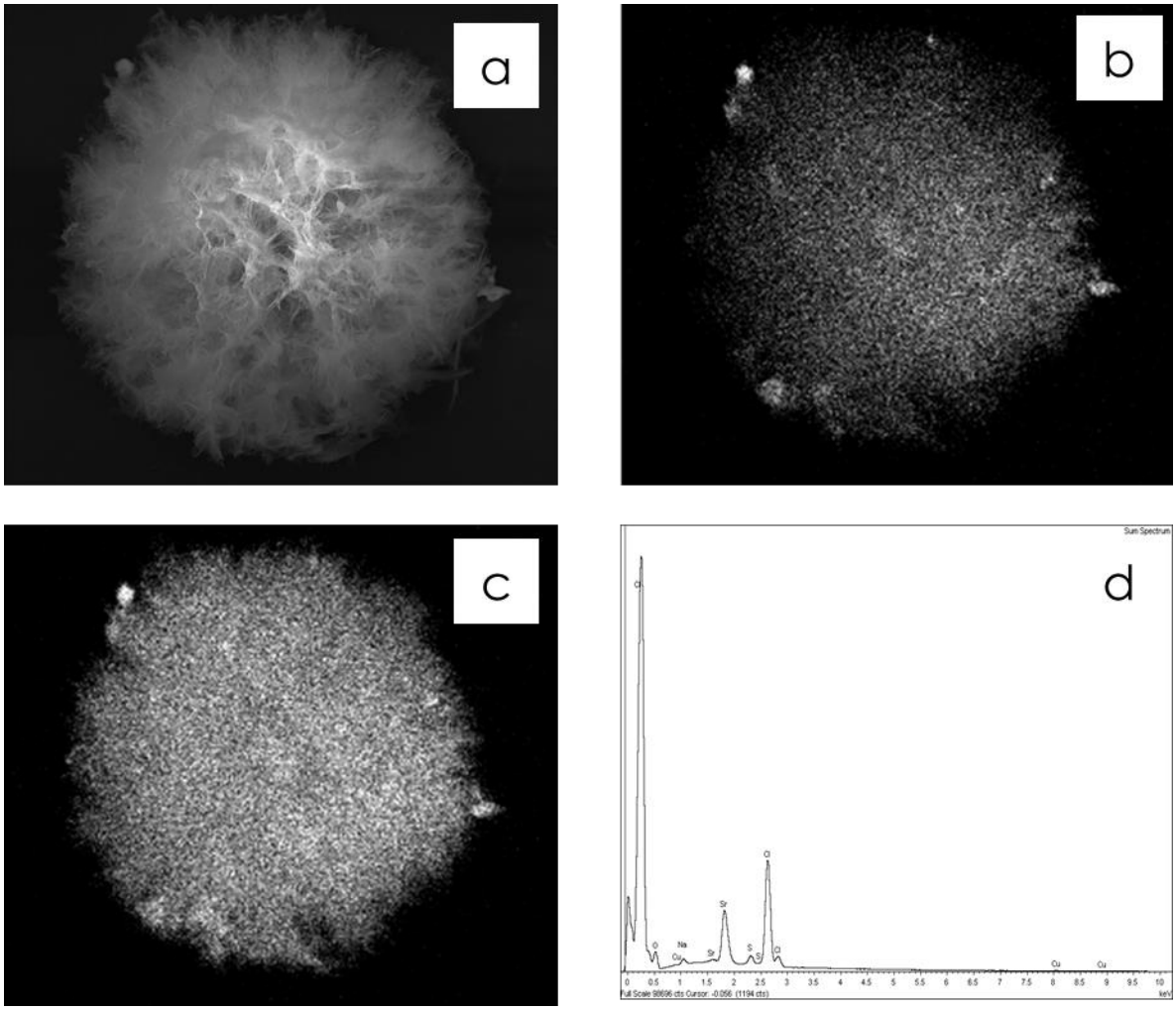

Figure 17. EDS results of the CHX-$SrCl_2$ Particle; (a) showing the distribution of (b) chloride and (c) Strontium and (d) the spectra.

Table 5. EDS element analysis for the CHX-$SrCl_2$ particle

Element	Weight%	Atomic%
O K	54.49	73.67
Cl K	41.56	25.36
Sr L	3.95	0.98
Totals	100.00	

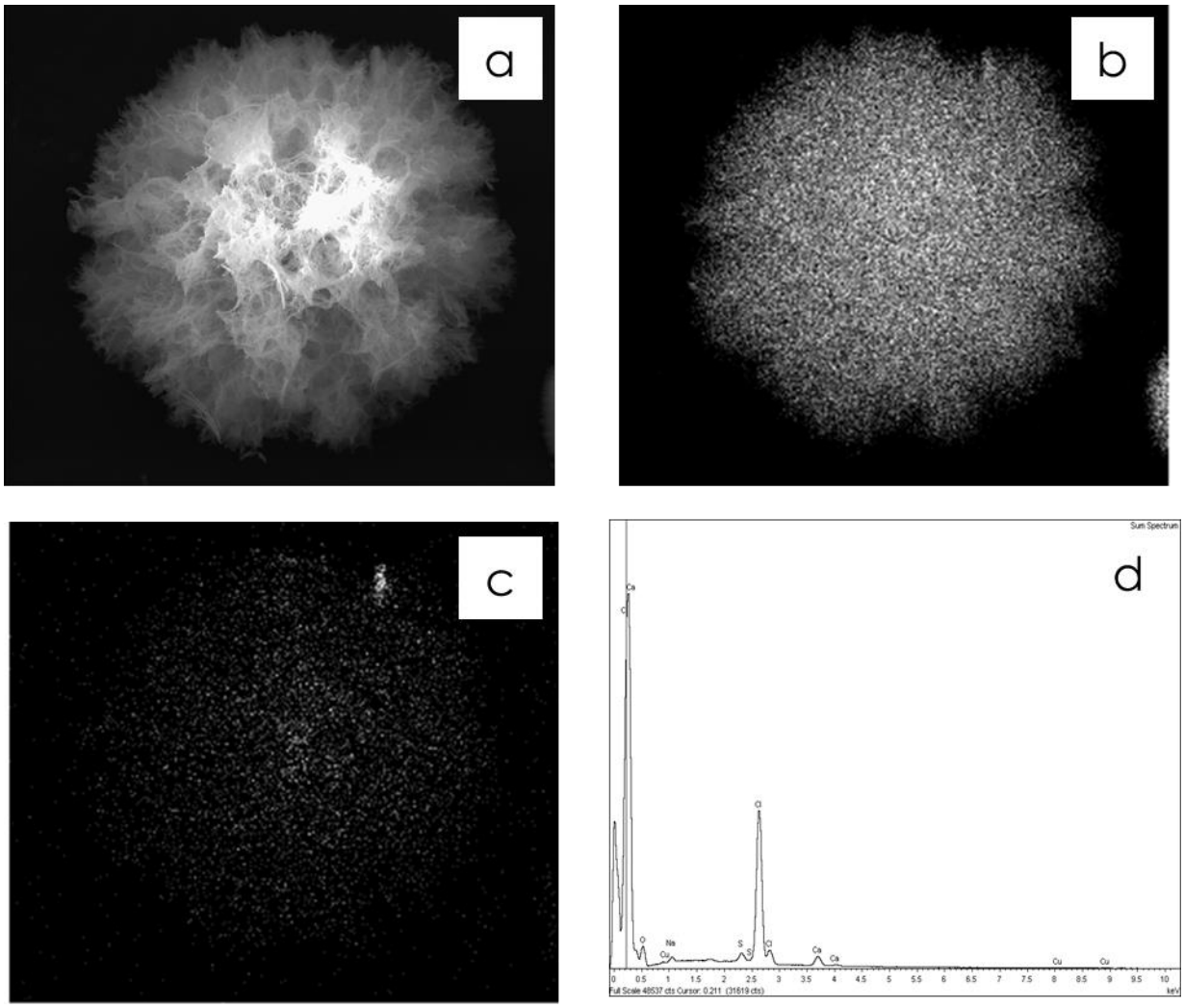

Figure 18. EDS results of the CHX-$CaCl_2$ Particle; (a) showing the distribution of (b) chloride and (c) Calcium and (d) the spectra.

Table 6. EDS element analysis for the CHX-$CaCl_2$ particle

Element	Weight%	Atomic%
O	48.39	69.03
Na	3.09	2.35
Cl	50.63	59.29
Ca	17.47	23.13
Totals	100.00	

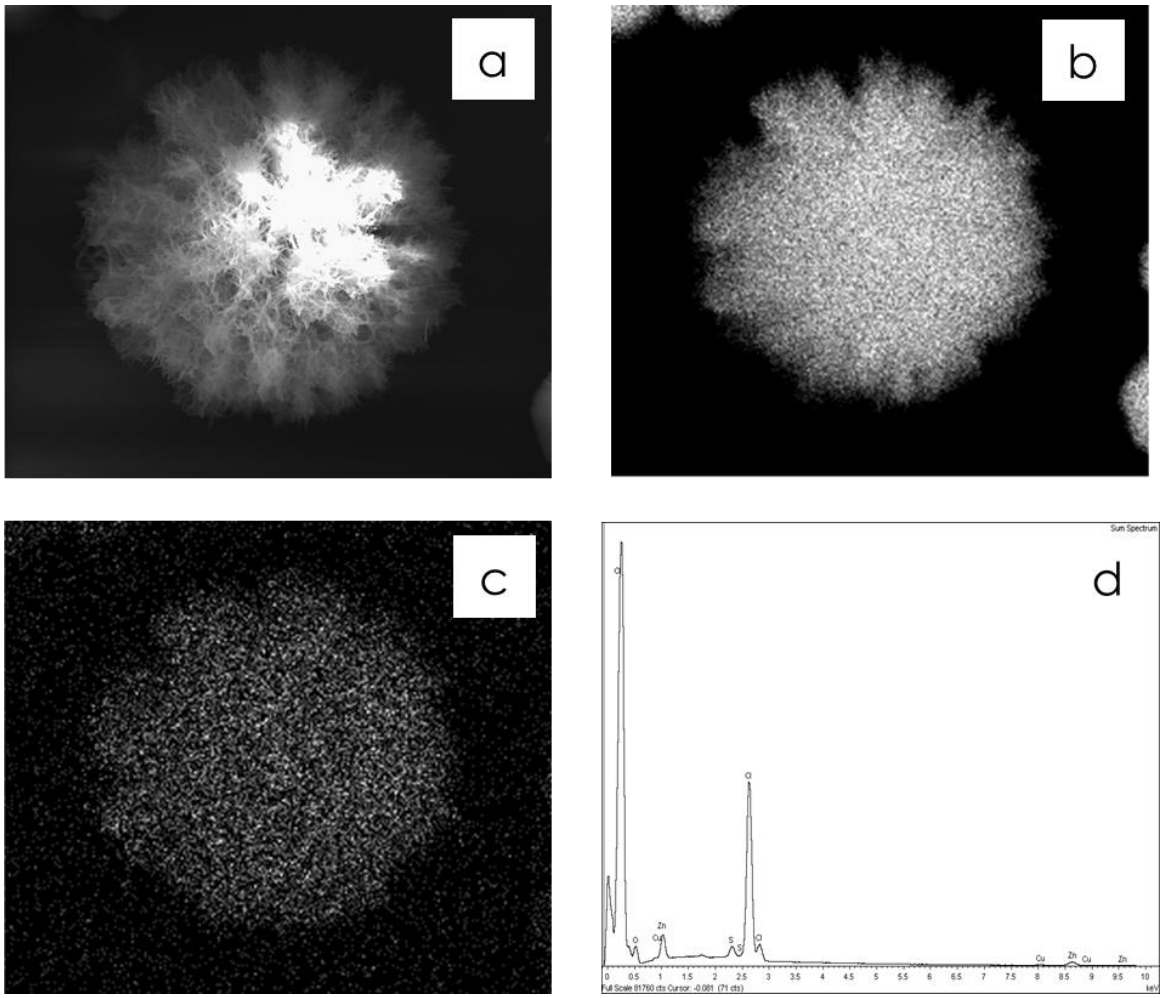

Figure 19. EDS results of the CHX-$ZnCl_2$ Particle; (a) showing the distribution of (b) chloride and (c) Zinc and (d) the spectra.

Table 7. EDS element analysis for the CHX-$ZnCl_2$ particle

Element	Weight%	Atomic%
O	48.39	69.03
Cl	43.95	28.29
Zn	7.66	2.68
Totals	100.00	

3.5.5 Results of the FTIR

The CHX-$SrCl_2$, CHX-$ZnCl_2$ and the CHXD powder were characterized and analysed with Fourier Transform Infrared Spectroscopy (FTIR) in order to confirm the presence and bonding of divalent ions. The FTIR results of the above samples were shown in Figure 20. FTIR results of chlorhexidine diacetate and CHX-ZnCl2 and CHX-SrCl2 particles.. In the infrared spectrum of the CHXD, there were three absorption peaks at 3325 cm^{-1}, 3120 cm^{-1}, and 3180 cm^{-1}. Additionally, when forming the novel CHX particles, those group showed shift to 3307 cm^{-1}, 3120 cm^{-1}, and 3190 cm^{-1} for CHX-$SrCl_2$ and 3307 cm^{-1}, 3119 cm^{-1}, and 3189 cm^{-1} for CHX-$ZnCl_2$ particles. The IR spectrum of the CHX-$SrCl_2$ and CHX-$ZnCl_2$ particles for the band of the imine group displayed a positive shift from 1612 cm^{-1} to 1623 cm^{-1}.

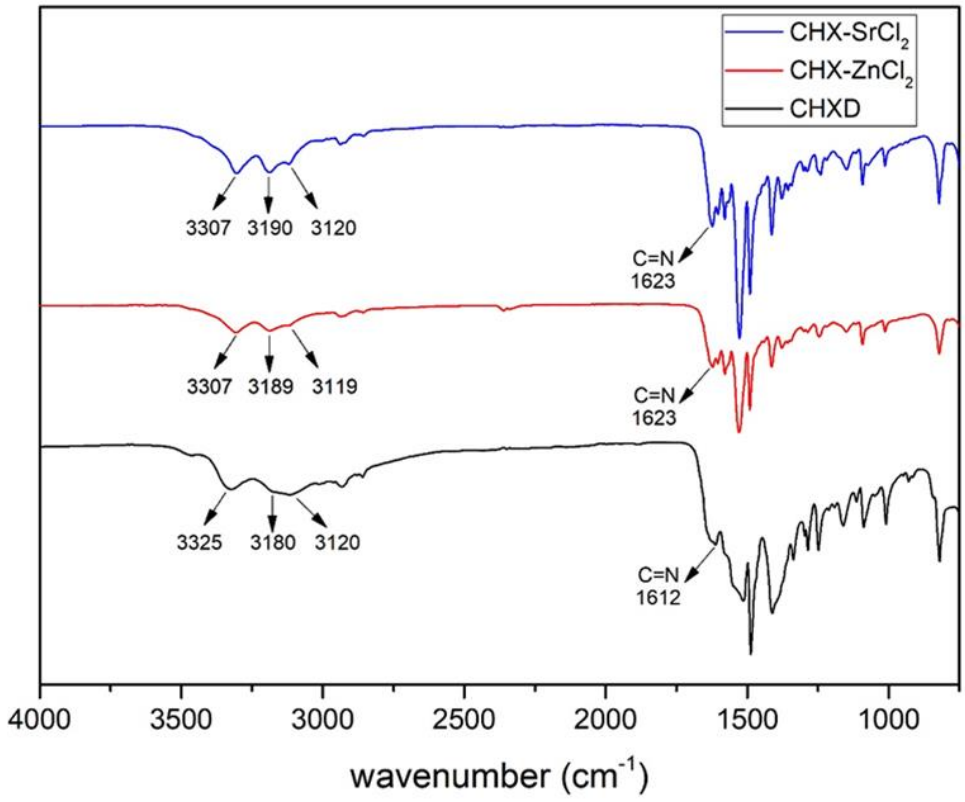

Figure 20. FTIR results of chlorhexidine diacetate and CHX-$ZnCl_2$ and CHX-$SrCl_2$ particles.

3.5.6 Results of the XRD

The structure of the spherical chlorhexidine particles was further analysed with XRD. The XRD plots of the CHX-$SrCl_2$ and CHX-$ZnCl_2$ particles indicated they had missing peaks at the 6.20, 11.40, 14.47, 16.18, 16.61, 19.09, and 36.27 degrees 2 theta positions, which were present in the CHXD XRD plot. There were also slight deviations in the 2 theta positions, changes in intensity for similar peaks for the CHXD and the novel particles, and signs of peak broadening (Figure 21. The X-ray diffraction patterns of CHXD/ CHX-Ca / Zn /SrCl2 particles.). The CHX-$SrCl_2$ and CHX-$ZnCl_2$ particles also displayed new peak positions (not in the CHXD plot) at 15.81, 15.85, 18.55, 20.02, 20.83, 21.56, 28.85, 28.88, 29.85, 29.88, 31.22, 35.43, and 35.46 degrees 2 theta. The CHX-$SrCl_2$ and CHX-$ZnCl_2$ particles displayed almost the same 2 theta positions.

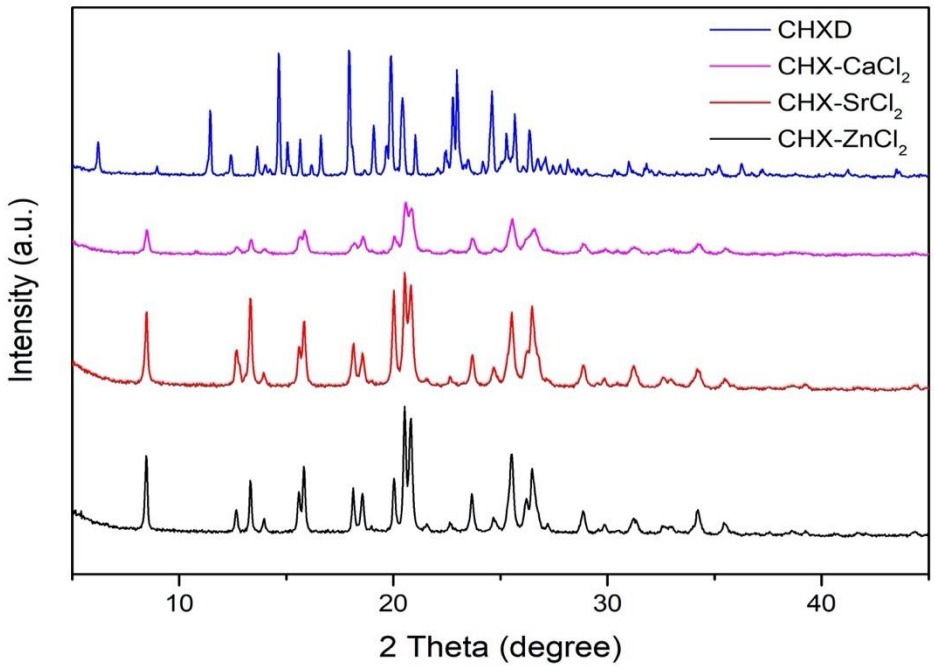

Figure 21. The X-ray diffraction patterns of CHXD/ CHX-Ca / Zn /$SrCl_2$ particles.

3.5.7 Release Assays for Sr and Zn Containing CHX Particles

3.5.7.1 Results of CHX Particle Release Experiments

The graphs below showed the results for the release assay for CHX particles and CHXD. The cumulative release curve for CHXD indicated a burst release at the beginning of the first day (Figure 22. CHX release curves for chlorhexidine diacetate (CHXD), CHX-CaCl2, CHX-SrCl2 and CHX-ZnCl2 particles in PBS (Arrows indicate where concentration is below MIC).), and with the concentration dropping below MIC (2.5 µg/ml) for *Porphyromonas gingivalis (strain- 381)* of CHXD particles at Day 7. In contrast, the CHX-$CaCl_2$, CHX-$SrCl_2$ and CHX-$ZnCl_2$ particles showed a reduced burst CHX release in the first day followed by a sustained release until 8 days for CHX-$SrCl_2$ and 12 days for CHX-$ZnCl_2$ and CHX-$CaCl_2$, before the CHX concentration was below MIC.

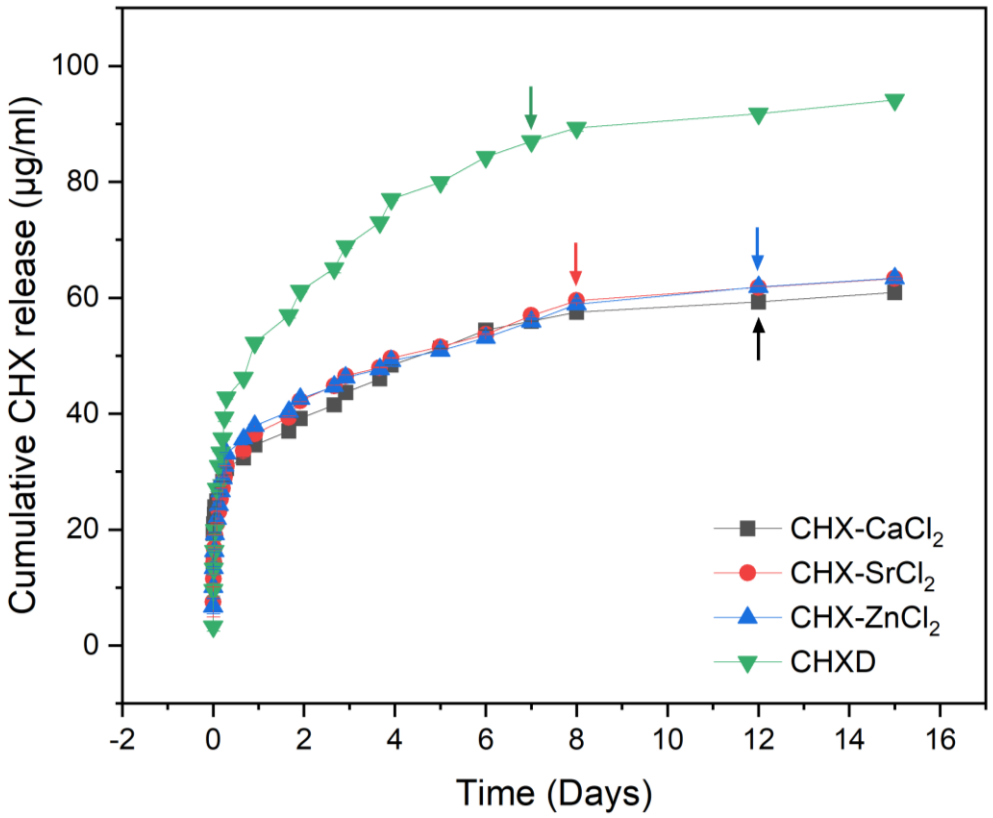

Figure 22. CHX release curves for chlorhexidine diacetate (CHXD), CHX-$CaCl_2$, CHX-$SrCl_2$ and CHX-$ZnCl_2$ particles in PBS (Arrows indicate where concentration is below MIC).

3.5.7.2 Results of the ICP-OES Experiments

The CHX-$ZnCl_2$ particles had a higher CHX and Zn release rate in artificial saliva (AS) pH=4, when compared to AS pH=7 (Figure 23 and Figure 24). Initially, both groups showed a burst Zn release (≤ 30 minutes). After 7 h storage, the overall amount of zinc released was 140 µg/ml for acidic artificial saliva (pH=4), which was double that released in neutral pH=7 artificial saliva (73 µg/ml). There was similarly an initial CHX burst release (Figure 23) in AS pH=4, and after 40 days of storage, the cumulative CHX released was 3888 µg/ml versus 281 µg/ml for AS pH=7. In acidic conditions (pH 4), the CHX can be rapidly released, providing an initial high dose of antibacterial

drug, followed by a sustained and effective CHX release up to 5 days. In addition, if there were no potential infections (pH 7 environment) CHX would be released in a sustained manner for 19 days (at MBC level Figure 24).

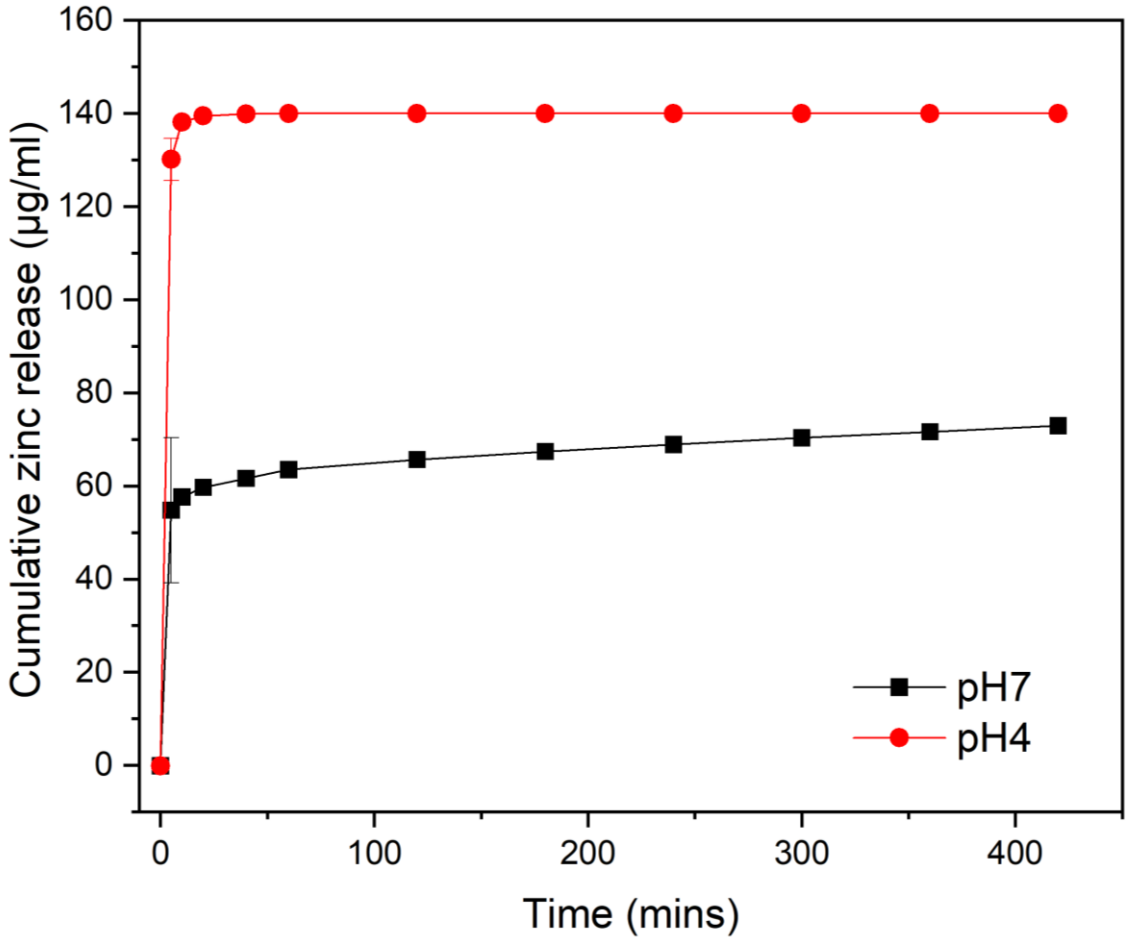

Figure 23. Cumulative zinc release from CHX-$ZnCl_2$ particles in artificial saliva (pH=4 or pH=7).

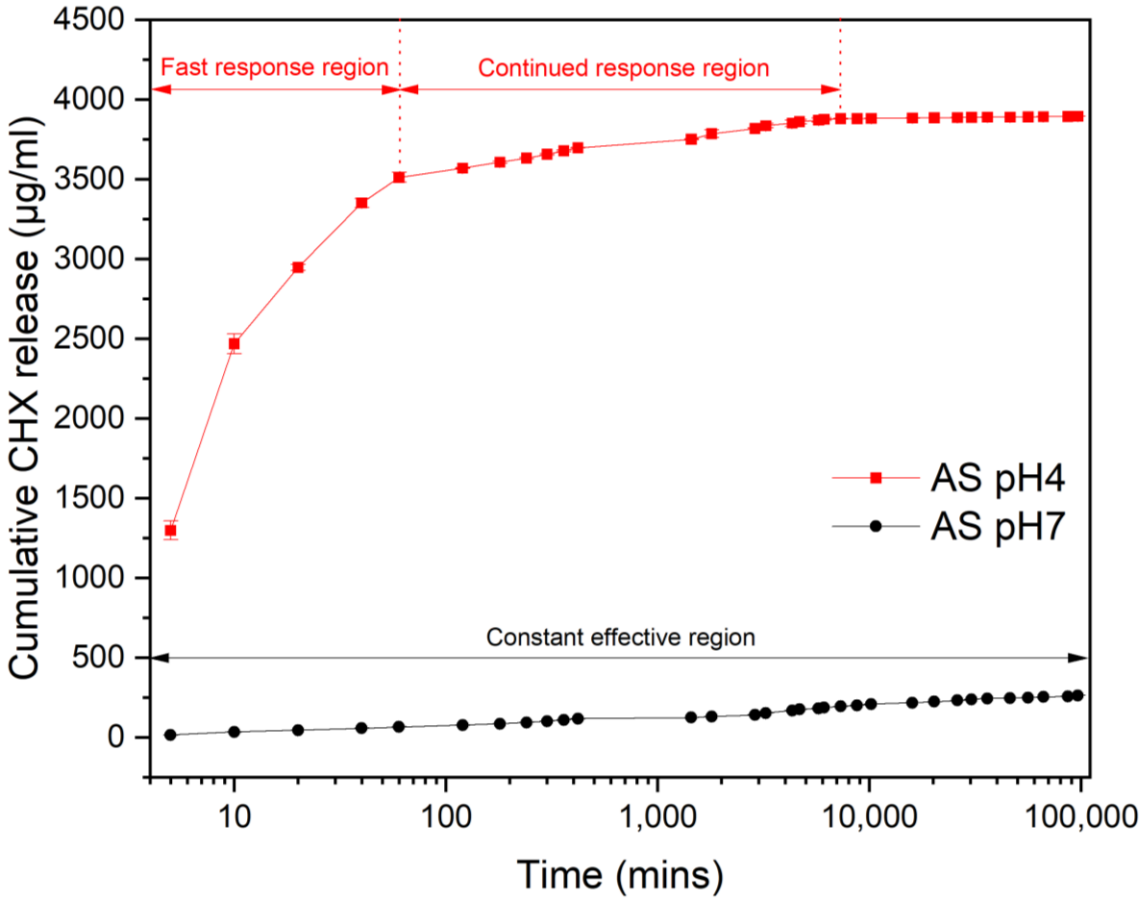

Figure 24. Cumulative CHX release curve for CHX-$ZnCl_2$ particles in AS (pH=7 or pH=4).

3.6 Results of Synthesis and Characterization of Fluoride Containing Particles

3.6.1 Results of SEM for CHX-NaF Particles

The results of the SEM study of the CHXD (0.024M) reacted with NaF (0.96 M) 1:1 by volume at different reaction times were shown in Figure 25 - Figure 27. The original (0.96 M) solution after dehydration was also imaged and shown in Figure 42 a, b as a comparison. Figure 42 a, b, after the dehydration of the NaF solution, therefore showed a large number of NaF crystals formed on the substrate. The NaF crystals showed a rhombic shape, with sharp geometric crystal edges clearly observed. After 1 min reaction time of the NaF with CHXD solutions the observed crystallites generally still displayed the rhombic shape, however, some imperfect morphology of the crystals was observed (Figure 25 a, b). With a longer reaction time (20 minutes) of NaF with CHXD solutions similar crystals were formed but with a more irregular shape, as demonstrated in Figure 25 e, f. After 40 minutes an agglomerated precipitate was formed, with some signs of rhomboidal crystals and primary dendrites (Figure 26 a, b). With an increased reaction time (60 minutes) spherical dendritic crystals and small rhomboidal crystals were present (Figure 43 c, d). Figures 43 e, f (80-minute reaction time) showed largely dendritic crystallites and partly formed sheaths. For increased reaction times of 100-120 minutes there was a high-volume fraction of spherical dendritic crystals (Figure 27 a-d).

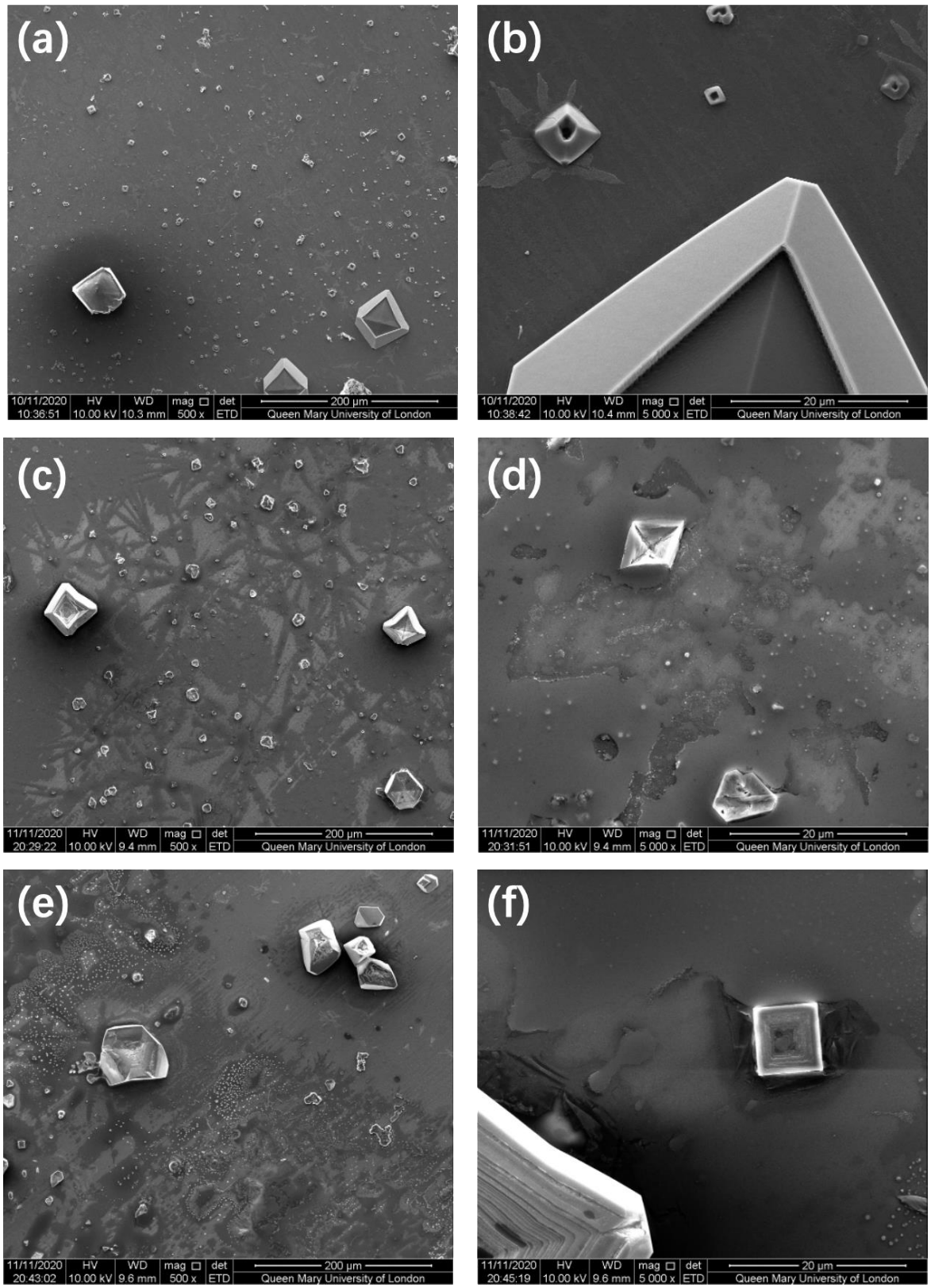

Figure 25. SEM images of CHX-NaF particles in different reaction times; (a)(b), NaF not reacted with CHXD; (c)(d), NaF reacted with CHXD solution for 1 min; (e)(f), NaF reacted with CHXD solution for 20 minutes.

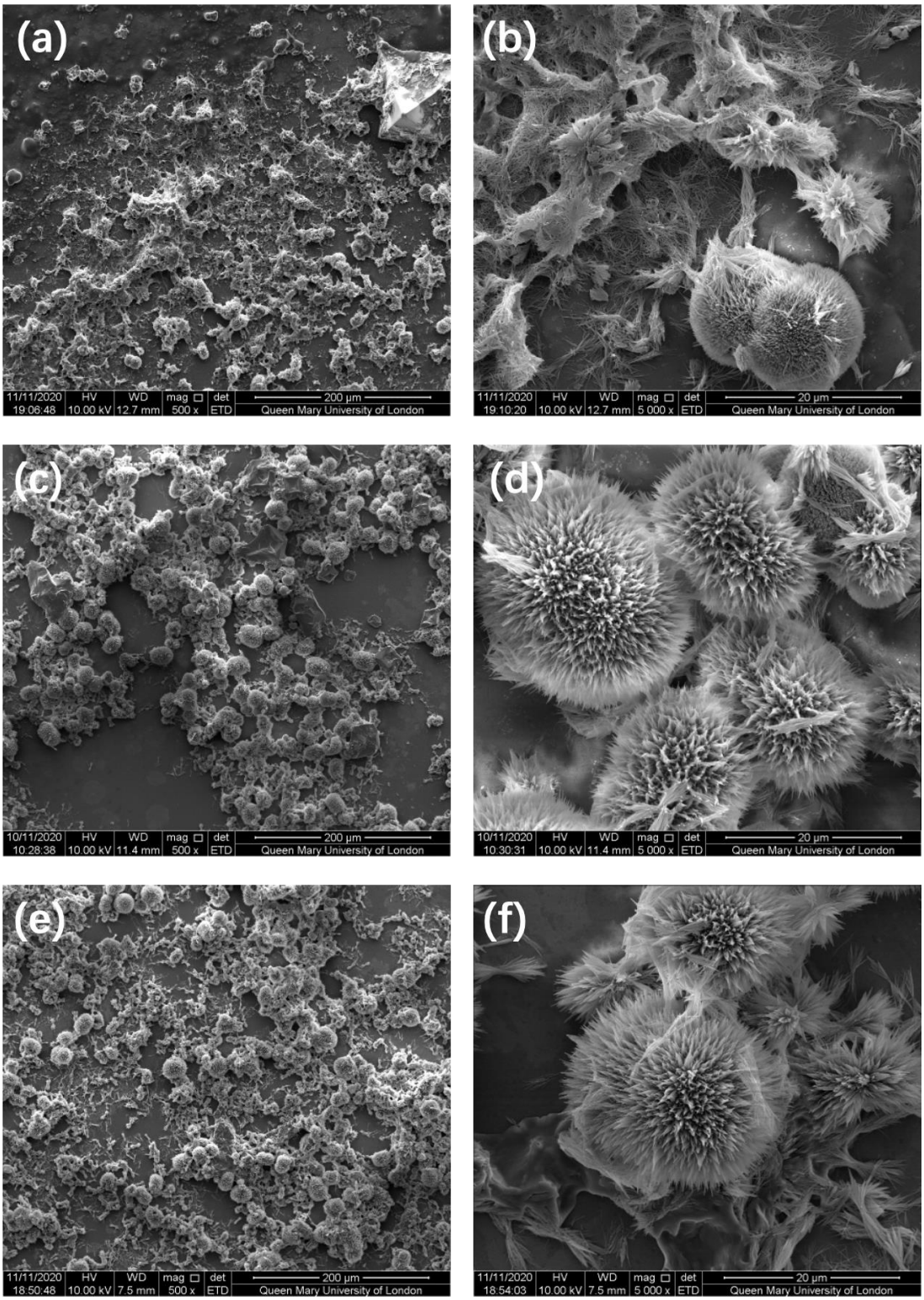

Figure 26. SEM images of CHX-NaF particles in different reaction times; (a)(b), NaF reacted with CHXD solution for 40 minutes; (c)(d), NaF reacted with CHXD solution for 60 minutes; (e)(f), NaF reacted with CHXD solution for 80 minutes.

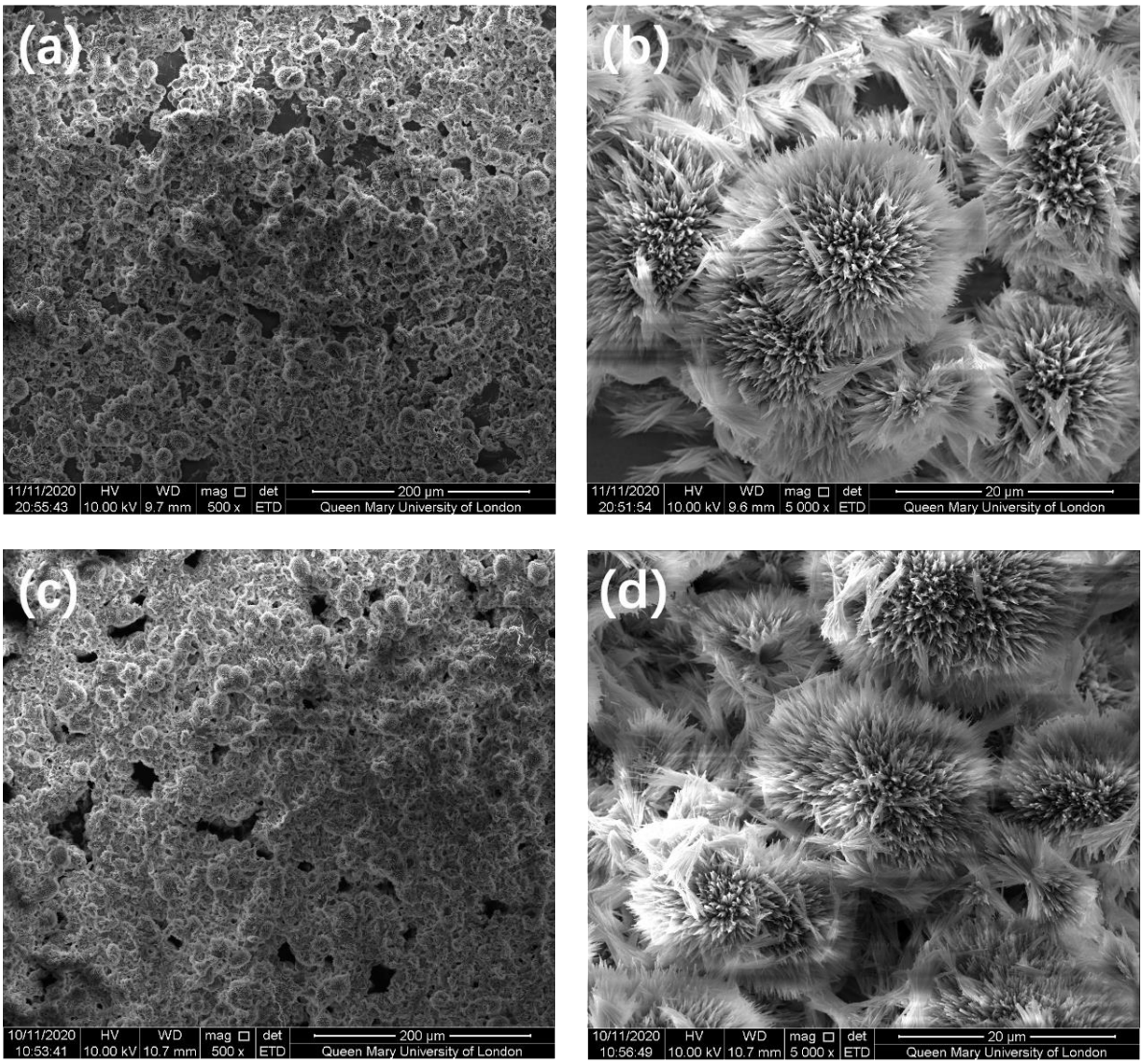

Figure 27. SEM images of CHX-NaF particles in different reaction times; (a)(b), NaF reacted with CHXD solution for 100 minutes; (c)(d), NaF reacted with CHXD solution for 120 minutes.

3.6.2 Results of SEM for the CHX-NaF-NaCl Particles

The SEM images of the CHX-NaF-NaCl particles synthesized by mixing 0.125 - 0.66M NaF and 0.66M NaCl salt solutions mixed with CHXD (0.024M) solution was demonstrated in Figure 29. Spherical particles were observed in all the concentration groups. Furthermore, all the CHX-NaF-NaCl particles demonstrated unique spherical

morphologies of a porous and interconnected dendritic structure, grown from a nucleation site central to the sphere, while the original chlorhexidine diacetate showed a platelet morphology (Figure 46 d). The novel CHX-NaF (0.125M-0.33M)-NaCl particles preserved spherical and dendritic fibrous morphologies (Figure 29 b, d, f), while the NaF concentration from 0.5M to 0.66 M demonstrated a more open structure (Figure 29 b and d).

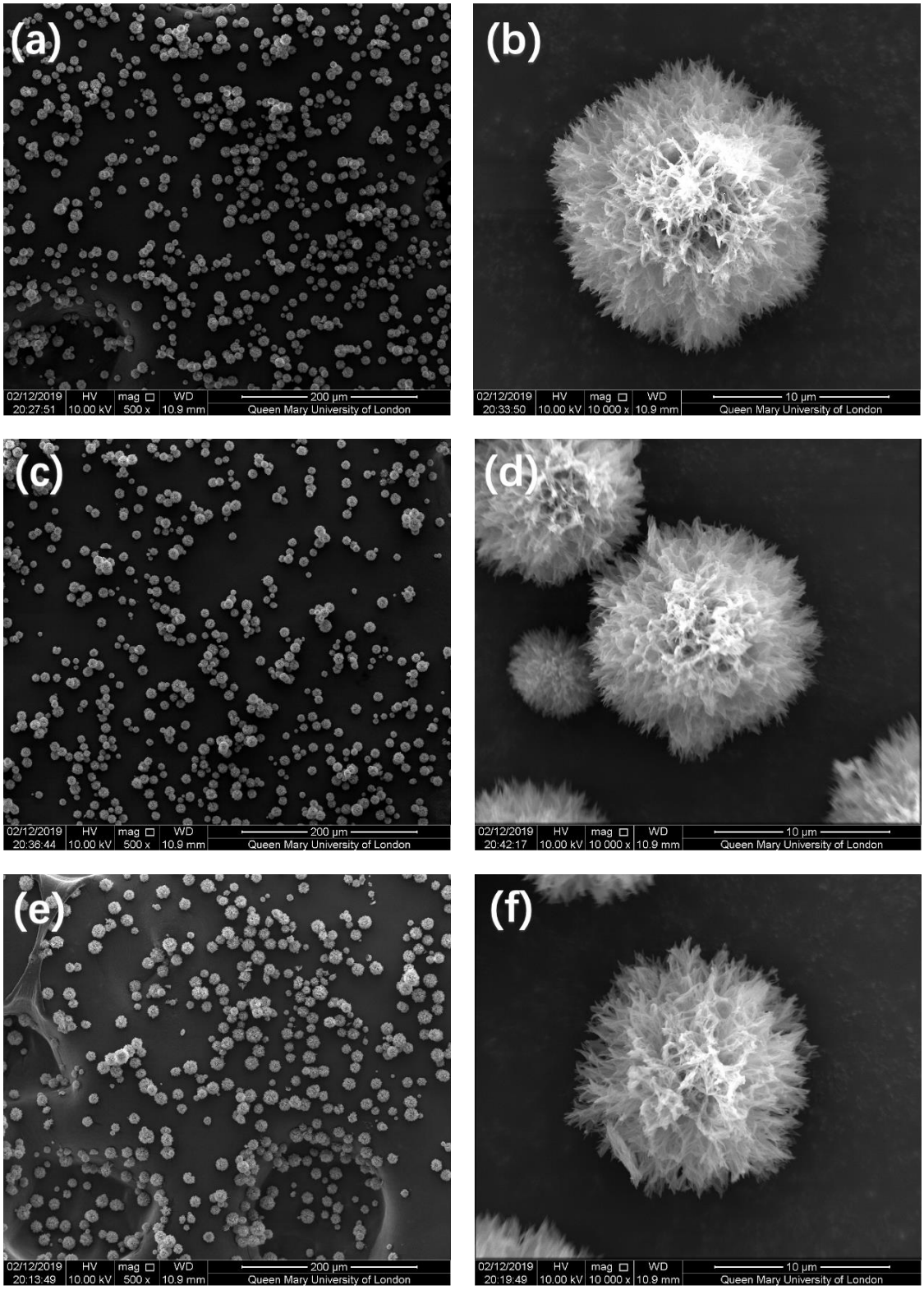

Figure 28. SEM images of 0.66M NaCl mixed with (a)(b). 0.125M NaF; (c)(d): 0.25M NaF; (e)(f): 0.33M NaF. All solution concentrations were further reacted with CHXD.

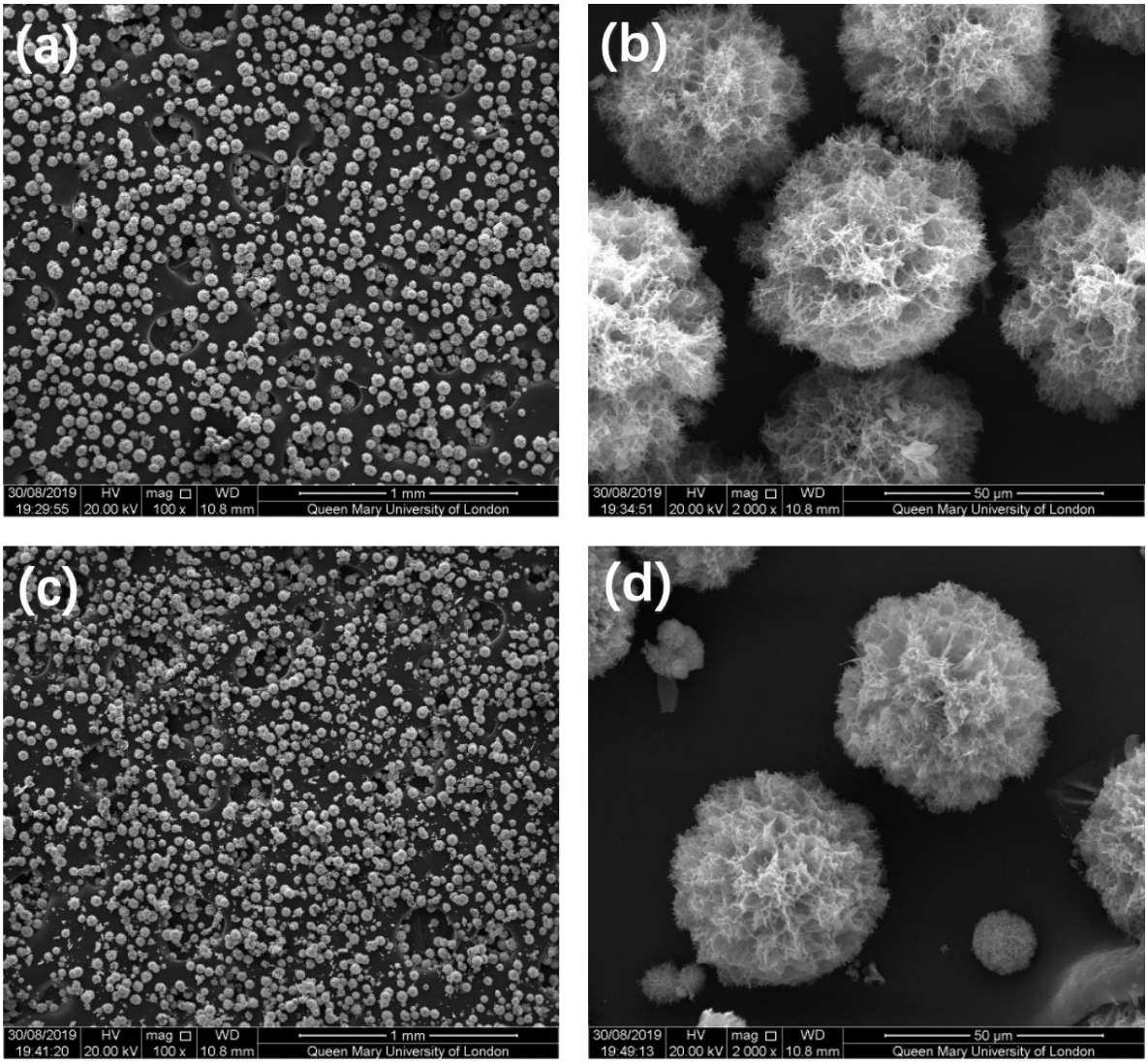

Figure 29. SEM images of 0.66M NaCl mixed with (a)(b). 0.5M NaF; (c)(d): 0.66M NaF. All solution concentrations were further reacted with CHXD.

3.6.3 Results of EDS for the CHX-NaF-NaCl Particles

The CHX-NaF-NaCl (0.66M NaF) was further analysed by EDS. Quantitative elemental analysis indicated that the weight percentage of fluoride ions incorporated in the particles (0.66M NaF sample) was 11.13 wt% fluoride (Table 8). Additionally, it is noteworthy to mention that the CHX-NaF-NaCl particles were washed with DI water to remove unreacted elements and any physically absorbed divalent metal ions as

much as possible. The corresponding EDS spectra was demonstrated in Figure 30 a, b.

Table 8. EDS element analysis for the CHX-NaF-NaCl particle

Element	Weight%	Atomic%
O	8.06	12.84
F	11.13	14.93
Na	36.26	40.20
Cl	44.54	32.02
Totals	100.00	

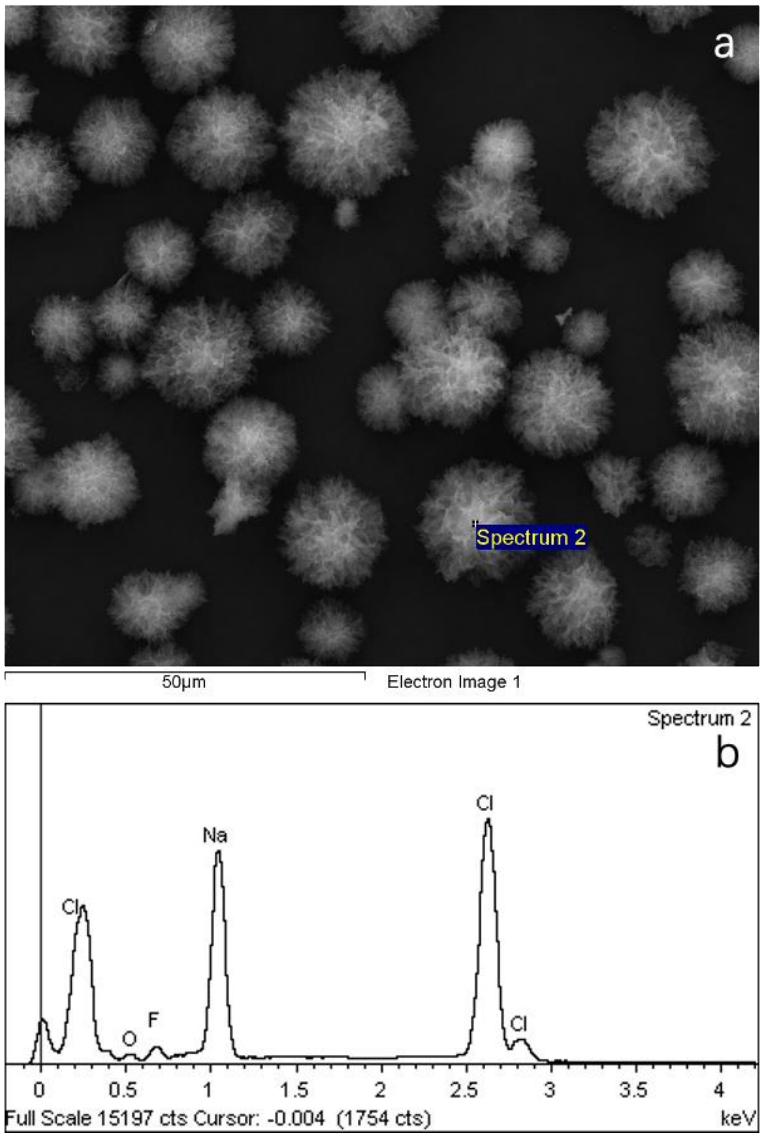

Figure 30. EDS results of the CHX-NaF-NaCl Particle; (a) spectrum position (b) the EDS spectra.

3.6.4 Results of XRD for Fluoride Containing CHX Particles

The structure of the CHX-NaF and CHX- NaF -NaCl particles was analysed with XRD which were demonstrated in Figure 31. All the CHX-NaF-NaCl particles displayed almost the same 2 theta positions which confirmed that a similar structure was formed by CHX-NaF-NaCl at different fluoride concentrations. The XRD plots of the CHX-NaF and CHX-NaF-NaCl particles indicated they had missing peaks at the 6.20, 11.40, 14.47, 16.18, 16.61, 19.09, and 36.27 degree 2 theta positions, which were present in the CHXD XRD plot. There were two peaks (31.7 and 45.45 degrees 2 theta) which were the same with NaCl [299] for CHX- NaF-NaCl particles (Figure 31. But all other peaks for NaCl were missing (27.4, 53.87, 56.48 and 66.23 degrees 2 theta) for CHX-NaF-NaCl particles. There were only two peaks confirmed at 38.78 and 56.03 [300] degrees 2 theta for NaF, which were similar with the two fluoride containing particles (Figure 46). The remaining peaks for NaF including; 27.37, 31.7, 45.48, 66.23 and 73.08 degrees 2 theta were missing.

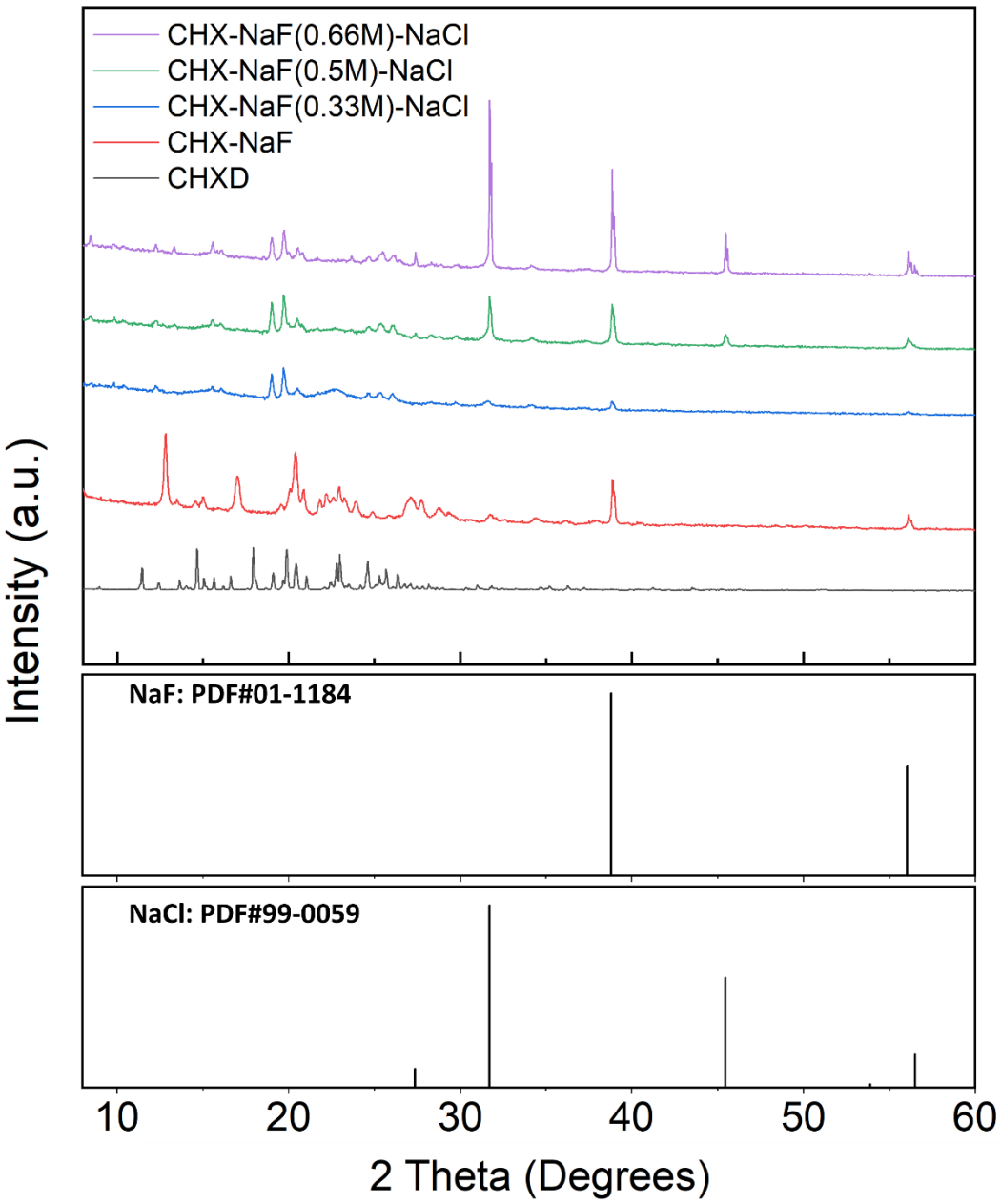

Figure 31. The X-ray diffraction patterns of CHXD/ CHX-NaF-NaCl/CHX-NaF particles.

3.6.5 ISE Results for the Fluoride Release of the CHX-NaF-NaCl Particles

The fluoride calibration curve from ISE (Figure 32) confirmed the fluoride concentration was highly correlated with the estimated mV of the fluoride standards (r^2= 0.99). The fluoride release for all groups was demonstrated in Figure 33 which showed that the amount of fluoride release was raised with increase in the concentration of NaF. The

fluoride content of CHX-NaF-NaCl particles (NaF concentration from 0.33M, 0.5M and 0.66M) are shown in Figure 33, and the fluoride released was 47.8 µg/ml, 69.3 µg/ml and 136.9µg/ml respectively. The fluoride content of the CHX-NaF particle (0.97M) was 86.1µg/ml .

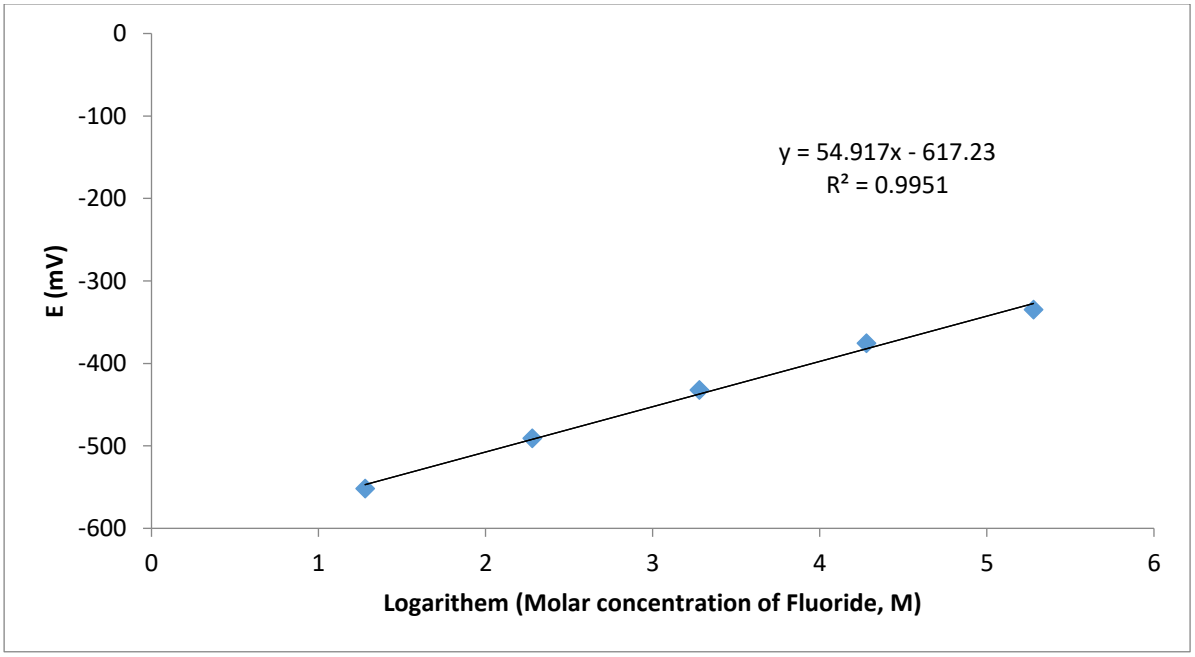

Figure 32. Fluoride ISE calibration curve.

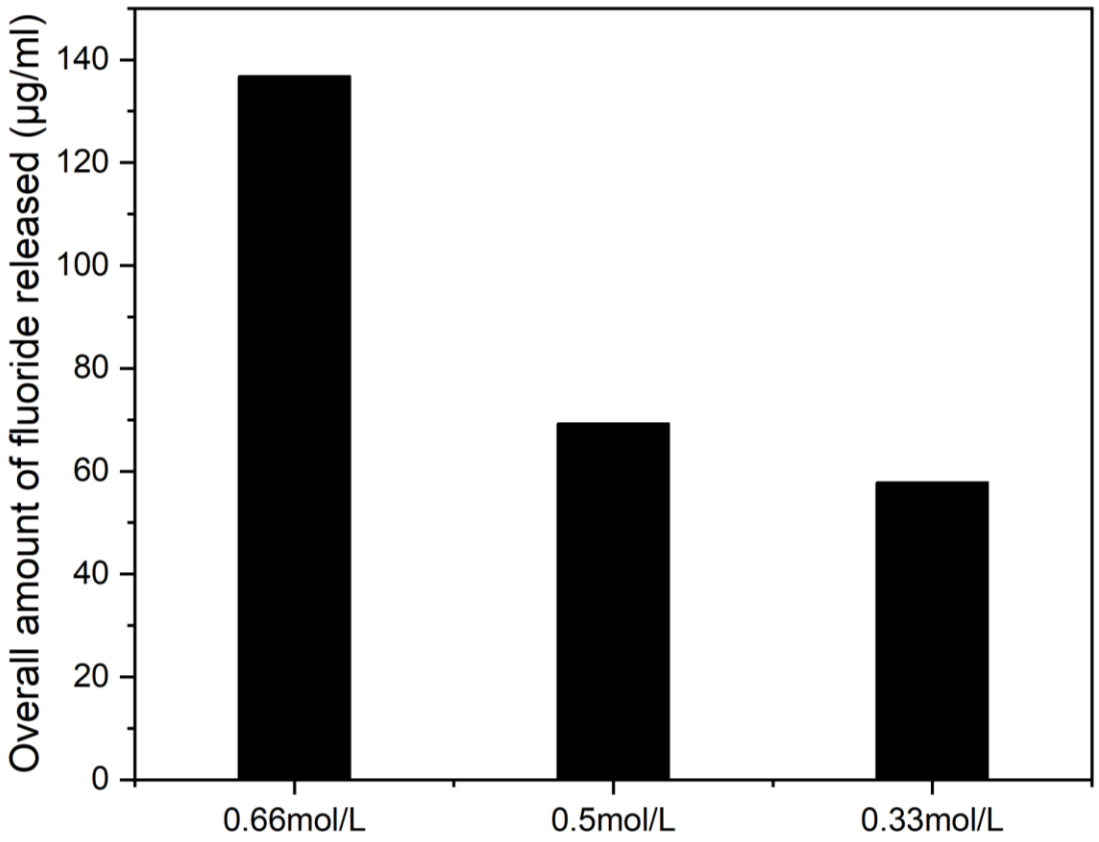

Figure 33. Fluoride release for the CHX-NaF-$NaCl_2$ particle for NaF concentration of 0.33M, 0.5M and 0.66M

Chapter 4. In vitro effects of Strontium, Zinc contained CHX particles in 2D cell model

4.1 Introduction

Osteoblasts form a closely packed sheet on the bone surface. It developed from the differentiation of osteoblasts progenitor population cells in the periosteal and endosteal. It is the main cells in the new bone formation process because it is responsible for the synthesis and secretion of bone matrix in mineralization [10].

Numerous study either in vitro or animal studies has demonstrated that zinc and strontium can regulate bone-forming cell activities [223,224,301]. Both zinc and strontium promotes the formation of new bone tissue [204,302]. Furthermore, zinc and strontium are able to be incorporated into novel CHX particles [303] which offers both an antibacterial agent and therapeutic functions. Thus, the addition of zinc into novel CHX particles with local delivery at appropriate concentrations would be beneficial for bone-forming cells in dental and medical applications.

However, in periodontal treatment, the bone defect healing outcome will not only depend on the osteoblast response but is also determined by the surrounding soft tissues, including epithelial cells and fibroblasts cells [304]. Thus, the surrounding soft tissues should not be adversely affected by the novel particles.

Therefore, the aim of this chapter is to investigate the osteogenic responses of osteoblast MC3T3-E1 to zinc and strontium-containing CHX particles and the cytotoxicity of mouse fibroblast cells.

4.2 Method and Materials

4.2.1 Antimicrobial Assay

4.2.1.1 Bacterial Strains and Growth Conditions

Porphyromonas gingivalis (strain - 381), *Fusobacterium nucleatum subspecies nucleatum* (strain-ATCC) and *Aggregatibacter actinomycetemcomitans* (strain-Y4) were used to test the antibacterial activity of CHX diacetate, CHX-$CaCl_2$, CHX-$SrCl_2$ and CHX-$ZnCl_2$ particles. Bacteria were grown on blood agar plates (Blood Agar Base No.2; Oxoid, UK) and 5% Defibrinated Horse Blood (TCS, UK) in an anaerobic atmosphere (10% H_2, 10% CO_2, and 80% N_2) at 37°C for 48 h. The resulting colonies were inoculated into 20 ml Brain Heart Infusion broth (BHI) (CM1135; Oxoid, UK) supplemented with 0.5μg/ml Vitamin K and 0.5μg/ml hemin. The bacterial culture was then grown for 24 hours anaerobically. Bacterial numbers in the BHI broth were determined and standardized by serial dilution and measured of colony-forming units (CFUs) on blood agar plates. After overnight incubation in an anaerobic environment, the bacterial suspensions were diluted 1:20 in pure BHI to achieve an optical density of 0.1 for *Porphyromonas gingivalis* and *Aggregatibacter actinomycetemcomitans* and 0.2 for *Fusobacterium nucleatum* subsp. *nucleatum* at 600nm (OD_{600}) to give approximately $6.36x10^7$ colony-forming units (CFU) per ml in order to standardize the bacterial inoculum used in these experiments.

4.2.1.2 MIC and MBC of CHX Particles Against Planktonic Bacterial Growth

0.08% CHX diacetate, CHX-$CaCl_2$, CHX-$SrCl_2$ or CHX-$ZnCl_2$ particle stock solutions were used to prepared fresh dilutions in sterile deionized water to obtain the final

concentrations of 0.004%, 0.002%, 0.001%, 0.0005%, 0.00025%, 0.000125%, and 0.0000625% wt/vol solutions. The MIC (minimum inhibitory concentration) was the lowest concentration of chlorhexidine spheres that inhibited the growth of microorganisms and MBC (minimum bactericidal concentration) was the lowest concentration that kills the bacteria. For determination of MICs and MBCs, the standardized inoculum of test bacteria was incubated in the presence of a series of dilutions ranging from 0.0000625–0.004% of CHX diacetate powder, CHX-$CaCl_2$, CHX-$SrCl_2$ or CHX-$ZnCl_2$ particles in sterile deionized water in 96 well microlitre plates. Controls included were; i) wells with 225µl BHI only + 25µl sterile water (no bacteria or CHX diacetate powder, CHX-$CaCl_2$, CHX-$SrCl_2$ or CHX-$ZnCl_2$ particles), and ii) wells with 225µl adjusted bacterial suspension plus 25µl sterile water (no CHX or CHX diacetate powder, CHX-$CaCl_2$, CHX-$SrCl_2$ or CHX-$ZnCl_2$ particles. The negative controls included were; bacterial inoculum only but no chlorhexidine particles and blank (medium only) wells. For test wells 225µl of diluted bacteria and 25µl of CHX diacetate powder, CHX-$CaCl_2$, CHX-$SrCl_2$ or CHX-$ZnCl_2$ particle dilution was mixed to give the final concentration range of 0.0000625% to 0.004% which was shown in Figure 34. The percentages of bacterial viability were calculated as: (absorbance of treated group/absorbance of the control group) *100%.

After incubation MBC was confirmed by transferring the microliter well contents to micro centrifuge tubes, centrifuging to pellet the bacterial cells, washing to remove any remaining chlorhexidine spheres or chlorhexidine diacetate and re-suspending the bacteria and incubating for 24 - 36 hours on blood agar plates. After incubation, bactericidal activity was confirmed by observation of any visible bacterial growth.

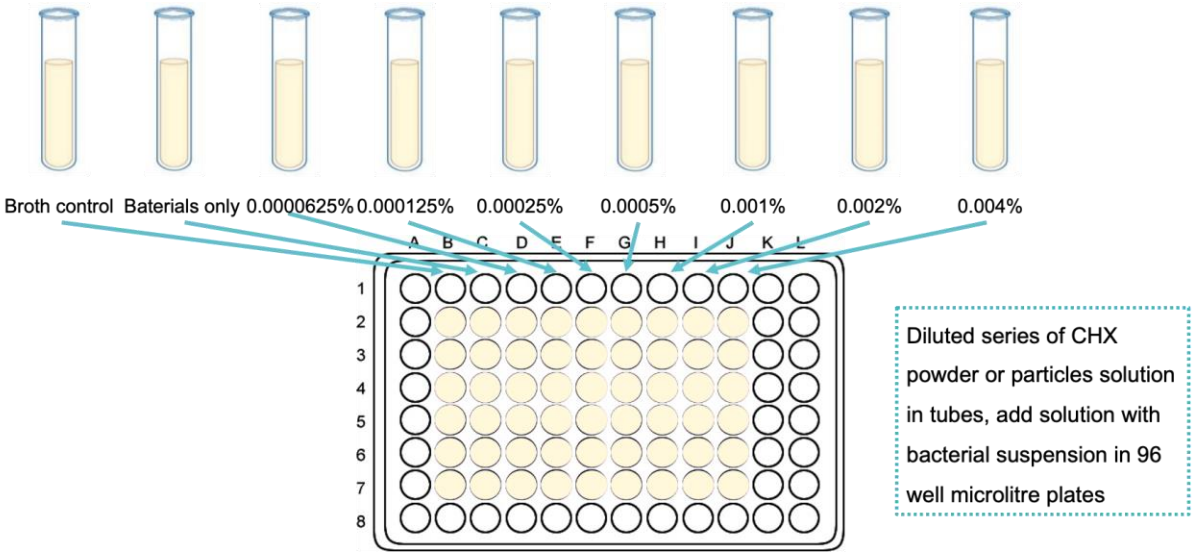

Figure 34. Diluted series of CHX particles in 96-well microlitre plates.

4.2.2 MIC and MBC of CHX Particles Against Preformed Biofilms

Dilutions of the periodontal pathogens and a series of dilutions ranging from 0.0000625–0.008% of dilutions treatment concentrations were prepared as above. The pathogens were diluted with fresh Brain Heart Infusion broth (BHI) (CM1135; Oxoid, UK) supplemented with 0.5μg/ml Vitamin K and 0.5μg/ml hemin to achieve an optical density at 600nm (OD_{600}) of 0.1 *P. gingivalis* and *A. actinomycetemcomitans* and 0.2 for *Fusobacterium nucleatum* subsp. BHI contain pathogens were added to 96 well plates and incubated in an anaerobic environment with an atmosphere of 10% H_2, 10% CO_2, and 80% N_2 at 37°C for 48 hours. After 48 hours of incubation, the supernatant was carefully removed from the wells by pipette and the biofilm was left at the bottom. The biofilm was then gently washed with sterile phosphate-buffered saline (PBS). A series of dilutions ranging from 0.0000625–0.004% of treatment solutions were added in each well following the order in Figure 34 and incubated for 24 hours and 48 hours. 50μl of 1mg/ml tetrazolium salt MTT solution (Sigma-Aldrich, Gillingham, UK) was added to each well including the blanks and incubated in an

anaerobic incubator for 2 hours. Then, the MTT solution was removed, and the biofilms were left in the wells. Formazan crystals generated by respiratory activity in bacteria were dissolved in 100 µl of isopropanol and the intensity of purple coloured reaction product was quantified by measuring the absorbance spectra at 570 nm. The percentages of biofilm viability were calculated as (absorbance of treated group/absorbance of the untreated control group) *100%.

4.2.3 Cell Culture

Two types of cells have been used in this study in order to understand the novel CHX particles affect gingival fibroblast viability and cell proliferation. For example, when increasing ZnO concentrations, the percentage of cell viability on L929 cells was decreased. The high doses ZnO (1 mM) caused a lethal effect on fibroblast cell line L929 where the cells possessed spherical shape and dull cells [305]. The pre-osteoblast cell line MC3T3-E1 were also used in this study because the cell was established from mouse calvaria with osteogenic potential to differentiate into osteoblasts and osteocytes and, has been demonstrated to form calcified bone tissue in vitro [306]. Thus, alkaline phosphatase activity and bone-like mineral nodules were evaluated.

4.2.3.1 Cell Culture Media Preparation

Mouse fibroblast L929 cell (ECACC 85011425) were cultured in dulbecco's minimum essential medium (DMEM, Lonza, UK) supplemented with 10% fetal bovine serum (FBS) and antibiotics (10 U/L penicillin and 100 mg/L streptomycins) in a humidified atmosphere containing 5% carbon dioxide (CO_2) in the air at 37 °C with medium change every two days.

Mouse osteoblastic MC3T3-E1 cell line cells were cultured in alpha-minimal essential medium (α-MEM, Lonza, UK) containing 10% FBS, antibiotics (10 U/L penicillin and 100 mg/L streptomycins), L-glutamine. 50 μg/ml L-ascorbic acid, 5 mM β-glycerophosphate and 10nM dexamethasone and maintained in an incubator at 37 °C with humidified air containing 5% CO_2. The medium was changed every two days.

4.2.3.2 Cell Growth

Passages 3 - 5 were used for all experiments. All the cells were cultured in 75 cm^2 flasks (Nunc, Thermo Scientific, UK) containing 15 – 20 ml of culture media in an environment of humidified air containing 5% CO_2 at 37 °C. The media was changed every two days until the cells grew to 70-80% confluence. Then, the cells were washed with 10ml phosphate-buffered saline (PBS) twice to remove the excess cell debris. In order to remove the cells from the culture flask, 3 - 5 ml of 0.25% trypsin solution in ethylenediaminetetraacetic acid (EDTA) (Sigma-Aldrich, UK) were added and incubated in a cell incubator for 2 minutes. Then the cells were checked under an inverted microscope (Nikon, TE 200-5, Tokyo, Japan) to make sure the cellular detachment and the morphology changed to a round shape. If not, the flask was shaken or incubated for a further minute then observed again. Once the cell detachment had been confirmed, 10 ml culture media was added to the flask to stop the action of trypsin. After this, the cell suspension was harvested into a 50ml centrifuged tube (Falcon, Thermo Scientific, UK) and centrifuged for 5 minutes at 800 rpm in a Sorvall Legend XTR Centrifuge (Thermo Scientific, UK) at room temperature. The supernatant was gently aspirated.

4.2.3.3 Cell Counting

The glass hemocytometer and coverslip (Thermo Scientific, UK) were used to count the density of harvested cell suspension. The number of cells was counted in each of the 16 grid squares in the glass hemocytometer. The mean number per ml was calculated by equation 1 [307]. Thus, the cell seeding density can be controlled to enable reproducibility.

$$Total\ cells/ml\ = Total\ cells\ counted * \frac{dilution\ factor}{number\ of\ squares} * 1 * 10^4\ cell/ml \qquad (1)$$

4.2.3.4 Freezing and Thawing Cells

In order to established cell line and keep using the same cell line, it is vital to thaw cells correctly and preserved for long term storage. Thus, the cell can maintain the viability of the culture and recover quickly. Briefly, after harvesting the cell into the centrifuged tube, 1 ml freezing media (10% Dimethyl Sulfoxide (DMSO, Sigma-Aldrich, UK) with 90% FBS) was added into the resuspended cell pellet. The mixed solution was then pipetted into 2ml cryogenic tubes (Thermo Scientific, UK) and placed in a freezing container (Thermo Scientific, UK) at -80 °C. After 24 hours, the cryogenic tubes were transferred to liquid nitrogen for long term storage.

Before the experiments, the cryogenic tubes (thawed cells) were transferred to a 37 °C water bath. Then the thawed cells were re-suspended in 5 ml general culture media and centrifuged at 800 rpm for 5 minutes in order to remove DMSO. After gently aspirating the supernatant, cells were rewashed with fresh media and expanded into the flasks.

4.2.4 Alkaline Phosphatase Activity Assay

Alkaline phosphates (ALP) is a membrane enzyme localized to the outer surface of the cells through a phosphatidylinositol-glycolipid anchor [308]. It was produced by osteoblasts and deposited in the matrix in bone. Thus, high amounts of ALP can be considered an indicator of early-stage osteoblast differentiation during the bone formation phase [309]. ALP activity assay is a colourimetric assay designed to measure ALP activity which is carried out to evaluate cell differentiation. ALP converts ρ-nitrophenyl phosphate into soluble yellow-coloured ρ-nitrophenyl (ρNP). Thus, in these experiments cell samples were washed in PBS and 100ml ALP reaction solution (20mg 4-Nitropheyl-phosphate disodium salt hexahydrate tableted dissolved in 8ml Tris buffer solution (pH=9.5) containing 15µl of 2 M $MgCl_2$) were added to generate cell lysate, incubated in the dark at 37 °C for 1 hour. The ALP standard solution were also be tested at the same time. Afterwards, the reaction was stopped by adding 50µl NaOH. The absorbance of the supernatant was measured at 405 nm and activity was calculated. The principle of this assay is that ALP can hydrolyse 4-Nitropheyl-phosphate, a colourless substrate, at alkaline pH values (pH= 9.5) and 37 °C and form p-nitro phenol (pNP). pNP is yellowish in basic solutions and its absorbance can be measured at 405 nm with the UV/visible spectrophotometer (Thermo Scientific, UK).

The ALP activity standard curve (Figure 35) indicated a linear relationship between absorbance and known amounts of pNP generated by ALP in the cells. Then ALP activity of the samples can then be calculated.

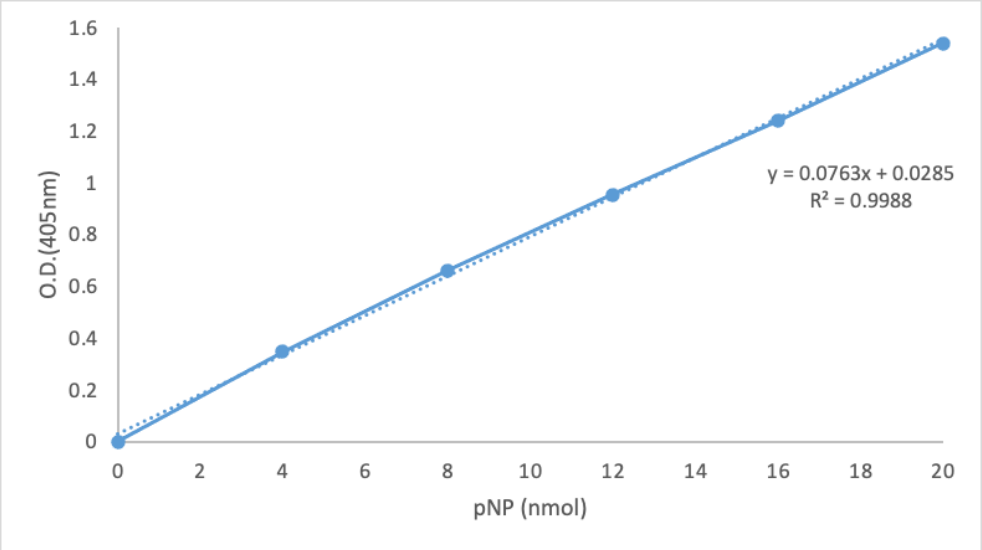

Figure 35. The ALP activity standard curve is constructed by adding 0, 4, 8, 12, 16 and 20 nmol pNP standard solution in a 96-well plate. Absorbance is measured at 405 nm.

4.2.5 Alizarin Red S Staining

The Alizarin Red S solution was prepared by dissolving 2g Alizarin Red S powder (Sigma-Aldrich, UK) in 100 ml deionized water and fully mixed. Afterwards, the pH was adjusted to 4.1 - 4.3 with hydrochloric acid (HCl) or sodium hydroxide (NaOH). Then the prepared dark-brown solution was filtered into a glass bottle and stored in a 4 °C refrigerator.

24 wells plates were used with 1 *10^4 cells/well cultured. The cells samples were collected after cell culture at 14 days, 21 days and 28 days and washed twice with PBS. After fixation the cell with 4% (w/v) glutaraldehyde (Sigma-Aldrich, UK) in each well, the cells were rinsed with PBS and stained with 2% (w/v) Alizarin Red S in deionized water at room temperature for 1 hour. Following three washes to remove

the unbound stain, the cells were photographed and imaged under an inverted microscope. The data were collected from three identical conditioned wells.

4.2.6 Cytotoxicity Assay

Cytotoxicity of CHX particles was evaluated with a standard 3-(4, 5 dimethylthiazol-2-yl)-2,5-diphenyltetrazolium bromide (MTT) assay with L929 cell (ECACC 85011425). The MTT activity reflects mitochondrial activity which can indicate viable cells. Initially, cells were cultured in Dulbecco's Modified Eagle's medium (DMEM, Lonza, Switzerland) supplemented with 10% fetal bovine serum (FBS) with 100 µg/ml penicillin, 100 µg/ml streptomycin in a humidified incubator atmosphere containing 10% CO_2 at 37°C were seeded in 96-well microliter plates at 10 000 cells per well. The negative controls included were; cell only group but no chlorhexidine particles and blank group (culture medium only). Following overnight incubation, the medium was removed, and cells were washed twice with PBS. Then the cells were treated with different concentrations (ranging from 0.0000625 to 0.004%) of CHXD as well as CHX Ca/Zn/$SrCl_2$ particles (n=3) for 24 and 48 h. After this, treatments were removed, and 50 µl of 5 mg/ml tetrazolium salt MTT was added to each well and incubated at 37 °C for 4 h. Then the medium was removed, and the formazan was solubilised in 100 µl isopropanol in each well. The absorbance of the supernatant was measured with a plate reader at 570 nm. The cells viability of the CHX-$CaCl_2$, CHX-$SrCl_2$, CHX-$ZnCl_2$, CHX-NaF-NaCl particles and CHX diacetate were tested with three independent experiments each and six replicate wells for all antimicrobial agent concentrations tested.

4.2.7 Tissue Adherence Study

To demonstrate the influence of novel CHX particle synthesis on tissue adherence, four tissue sections (10 mm length × 6 mm depth) were removed from the lingual wall of a lower jaw of a pig's head, at 2 mm from the gingival margins, using a scalpel (Swann Morton, Sheffield UK). The tissue sections were mounted onto metal SEM stubs using copper tape. Human saliva (20 ml) was collected from underneath the tongue of one person and placed in a 30 ml universal container (Star lab, UK) and stored at 37 °C in an incubator. A micro-brush (Stewmac #3101, UK) was dipped into a dappens pot containing 1 ml of human saliva and it was then applied to the surface of all the tissue-mounted samples.

One tissue section was used as a control group without any particle coating. The other three tissue sections were coated with either CHX-$CaCl_2$, CHX-$ZnCl_2$ and CHX-$SrCl_2$ particles, respectively. CHX particles were synthesized onto the surface of the moisturized tissue sections and also on a separate SEM stub (Figure S7), by the co-precipitation of 10µl CHXD solution (0.024M) and 10µl of 0.33 M of either $CaCl_2$, $ZnCl_2$ or $SrCl_2$ solutions. Then, the solution was removed by syringing with 2 ml human saliva drop by drop within 4 minutes.

4.3 Results

4.3.1 Antibacterial Results of CHX Particles Against Planktonic Bacterial

The antimicrobial tests showed that the concentration of CHX particles required to inhibit (Minimum Inhibitory Concentration- MIC) planktonic *P. gingivalis (strain-381)* and *A. actinomycetemcomitans (strain-Y4)* was 0.000025% at both 24 and 48-hour

time points, demonstrating its antibacterial efficacy in comparison to the CHX diacetate (Figure 36 a-d). The concentration of CHX particles required to inhibit (MIC) planktonic *F. nucleatum subsp. polymorphum (strain-ATCC)* was 0.0005% at 24 and 48-hour time points Figure 36 e-f), again consistent with the efficacy of the commercial CHX diacetate comparison antimicrobial.

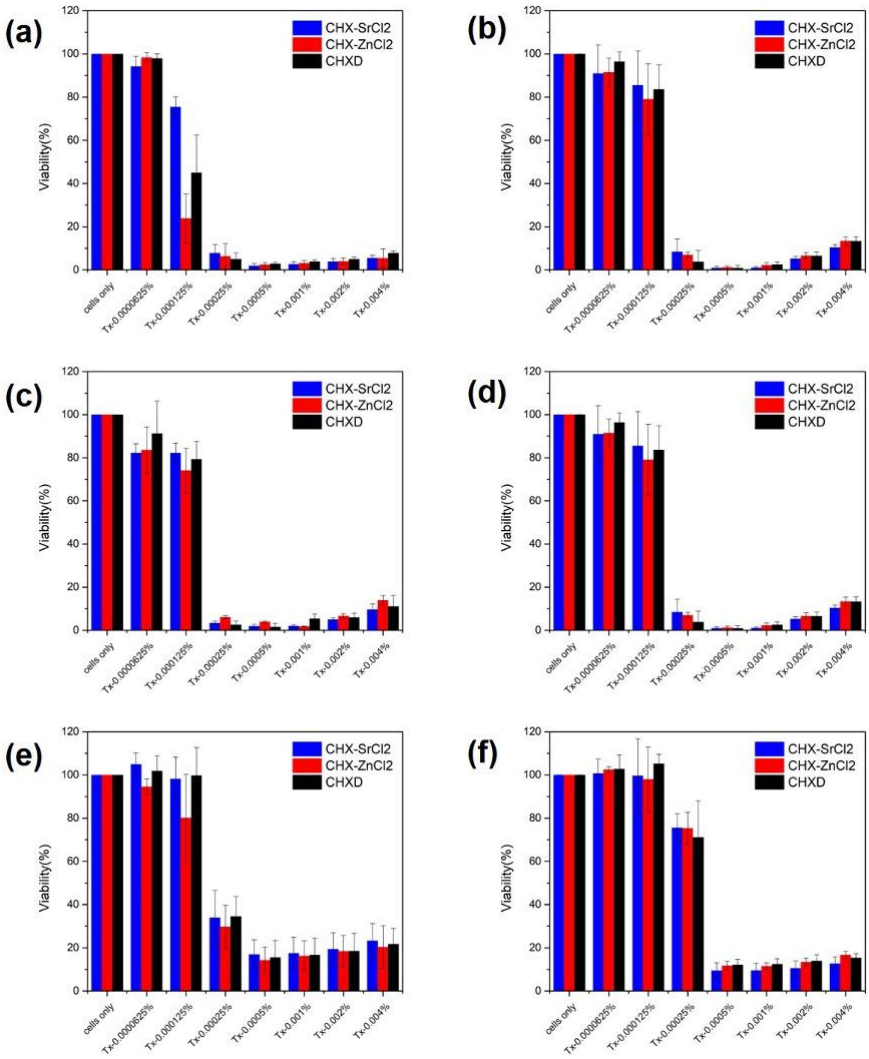

Figure 36. (a); Antimicrobial assays on Porphyromonas gingivalis (strain- 381) at 24 h (a); and 48h (b); Antimicrobial assay on A. actinomycetemcomitans (strain-Y4) at 24h and (c); 48h (d); Antimicrobial assays on F. nucleatum subsp. polymorphum (strain-ATCC) at 24h(e) and 48h(f). All the treated groups were normalized to the control groups.

Table 9. MIC and MBC of CHX-$ZnCl_2$ / CHX-$SrCl_2$ and Chlorhexidine Diacetate against *P. gingivalis* and *A. actinomycetemcomitans.*

Concentration of CHX-$ZnCl_2$ / CHX-$SrCl_2$ or CHXD	24 hours	48 hours
0.00025%	**MIC**	MBC
0.0005%	MBC	MBC
0.001%	MBC	MBC

Treated bacteria were harvested and re-incubated on agar plates to determine the Minimum Bactericidal Concentration (MBC) with the results are shown in Table 9 and for CHX diacetate at the same concentrations. When treated bacteria were harvested and re-incubated on agar plates to determine the Minimum Bactericidal Concentration (MBC), no visible bacterial growth was found at 0.0005% - 0.004% treated at 24-hour cultures, which indicated that after 24-hour treatment, 0.0005% chlorhexidine diacetate and chlorhexidine particles were all had a bactericidal effect on *P. gingivalis (strain-381)* and *A. actinomycetemcomitans (strain-Y4).* Bacterial growth was visible with 0.00025% chlorhexidine particles treated cultures for 24 hours suggesting an inhibition effect on the growth of *P. gingivalis (strain-381)* and *A. actinomycetemcomitans (strain-Y4)* but did not kill the organism. However, 48-hour treatment with 0.00025% chlorhexidine particles cultures did not demonstrate any visible bacterial growth. Thus, the MIC of CHXD and chlorhexidine particles was 0.00025% while MBC of CHX-$SrCl_2$ and CHX-$ZnCl_2$ particles and chlorhexidine diacetate for P. gingivalis/ A. actinomycetemcomitans was 0.0005% for 24h and 0.00025% for 48h demonstrating its antibacterial efficacy and consistent with commercial CHX diacetate. For F. nucleatum subsp. Polymorphum the MBC of both

CHX-$SrCl_2$ and CHX-$ZnCl_2$ particles was 0.001% at both 24 and 48h which was consistent with commercial CHX diacetate (Table 10).

Table 10. MIC and MBC of CHX-$ZnCl_2$ / CHX-$SrCl_2$ particles and Chlorhexidine Diacetate against *F. nucleatum subsp. polymorphum (strain – ATCC)*

Concentration of CHX-$ZnCl_2$ / CHX-$SrCl_2$ or CHXD	24 hours	48 hours
0.0005%	**MIC**	MIC
0.001%	MBC	MBC
0.002%	MBC	MBC

4.3.2 Results of CHX Particles Against Mature Biofilms

The antimicrobial activity of the CHX-$SrCl_2$, CHX-$ZnCl_2$ particles and CHX diacetate against mature biofilms of *P. gingivalis, Fusobacterium nucleatum subsp. Polymorphum and A. actinomycetemcomitans* were obtained and tested from all antimicrobial agent concentrations (Figure 37). The optical density (absorbance) of chlorhexidine treated cultures relative to that in the control (0%) were shown. A higher concentration of both chlorhexidine spheres (Zn/Sr) and chlorhexidine diacetate were required to inhibit biofilm growth. Further, the effect of CHX particles on these biofilms was similar to CHX diacetate demonstrating the antibacterial efficacy of the novel particle technology on biofilms.

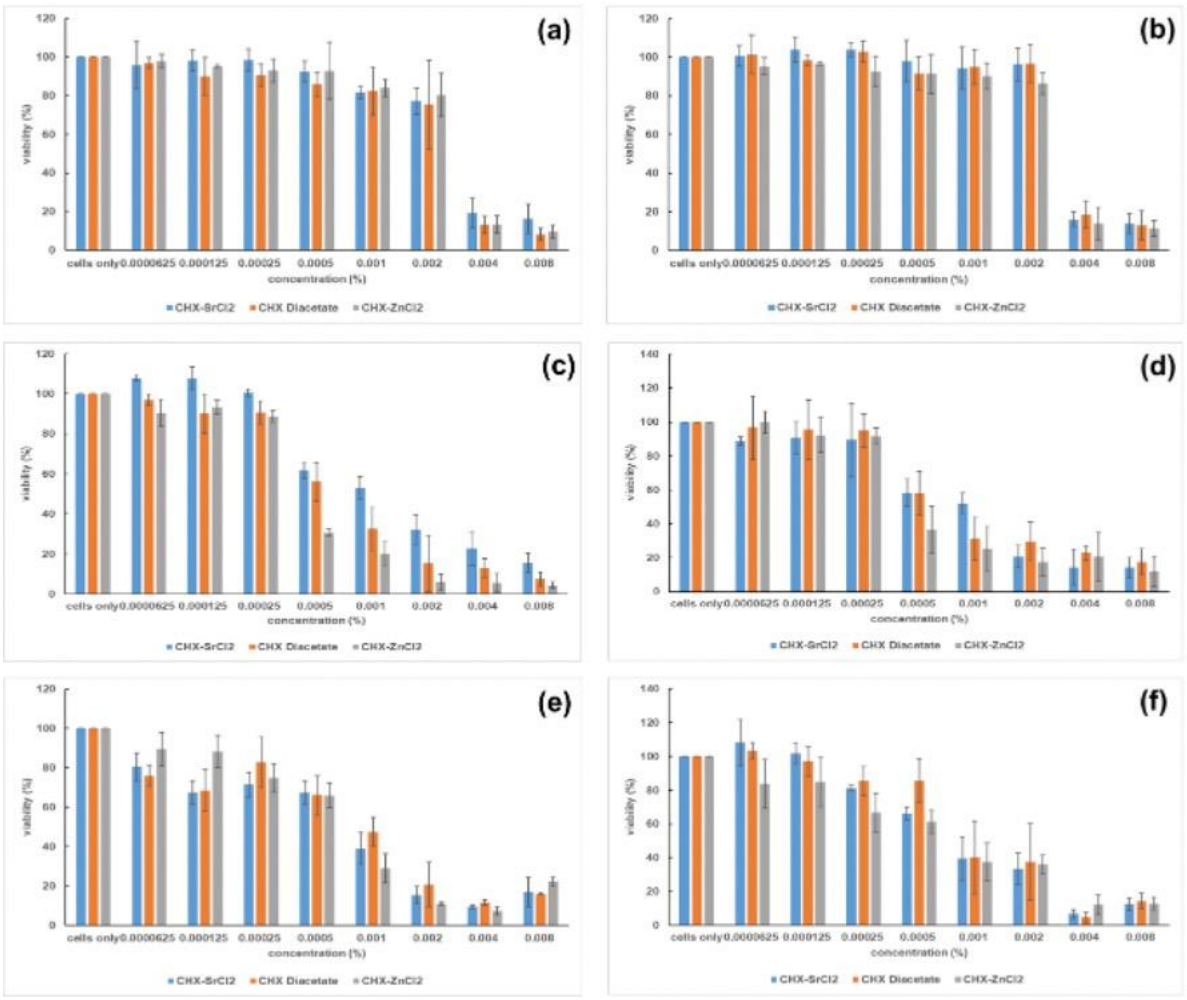

Figure 37. (a); Antimicrobial assays for biofilm on Porphyromonas gingivalis (strain-381) at 24 h (a); and 48h (b); Antimicrobial assay on A. actinomycetemcomitans (strain- Y4) at 24h and (c); 48h (d); Antimicrobial assays on F. nucleatum subsp. polymorphum (strain-ATCC) at 24h(e) and 48h(f). All the treated groups were normalized to the control groups.

The MBC of CHX-$SrCl_2$ and CHX-$ZnCl_2$ particles and chlorhexidine diacetate for P. gingivalis/ A. actinomycetemcomitans was 0.0008% for both 24h and 48 h demonstrating its antibacterial efficacy and consistent with commercial CHX diacetate (Table 11). For F. nucleatum subsp. Polymorphum the MBC of both CHX-$SrCl_2$ and CHX-$ZnCl_2$ particles was 0.008% at 48 h which was consistent with commercial CHXD (Table 12).

Table 11. MIC and MBC of CHX- $ZnCl_2$ and CHX- $SrCl_2$ particles and Chlorhexidine Diacetate against *Porphyromonas gingivalis (strain- 381)* and *A. actinomycetemcomitans (strain- Y4)*

Concentration of CHX Diacetate	24 hours	48 hours
0.004%	MIC	MIC
0.008%	MBC	MBC

Table 12**.** MIC and MBC of CHX- $ZnCl_2$ and CHX- $SrCl_2$ and Chlorhexidine Diacetate against *F. nucleatum subsp. Polymorphum*

Concentration of CHX Diacetate	24 hours	48 hours
0.008%	MIC	MBC

4.3.3 Results of Cytotoxicity Assay

Treatment with CHXD, CHX-$CaCl_2$, CHX-$SrCl_2$ and CHX-$ZnCl_2$ particles reduced the viability of the L929 cells in a dose- dependent manner but to different degrees (Figure 38). The potential cytotoxic effects and safe concentration levels of the novel particles were, therefore, evaluated.

Cell metabolic activity was investigated by measuring mitochondrial activity using a methyl-tetrazolium (MTT) assay when treated at the concentration of 0.0000625% for 24 hours, the relative cellular viability increased for all groups. While at higher concentrations of 0.000125% and 0.00025%, all groups demonstrated reduced relative viability to around 90% after 24 hours of treatment. However, the relative cellular viability showed a significant difference at 0.0005% for 24 hours points where the concentration was toxic for the CHXD treated cultures with about 60% viability while approximately 80% for all novel CHX groups. Relative cellular viability was reduced to approximately 40% when 0.001% of CHX-$CaCl_2$, CHX-$SrCl_2$, and CHX-

$ZnCl_2$ particles were used for 24 h, which was further decreased to around 2% after 48 h treatment.

Relative cellular viability was reduced to approximately 40% when 0.001% CHX-$SrCl_2$, CHX-$ZnCl_2$ particles were used for 24 hours, which was further decreased to around 2% after 48 hours of treatment. Lower concentrations of chlorhexidine particles ranging from 0.0000625% to 0.00025% showed approximately 90% and 60% of cellular viability at 24 and 48 hours, respectively. Although 0.0005% CHX-$CaCl_2$, CHX-$SrCl_2$, CHX-$ZnCl_2$ particles demonstrated above 80% of cellular viability at 24 hours, the viability was reduced to around 30% at 48 hours. Similar viability was observed in chlorhexidine diacetate treated cultures. When evaluating the cell structure of the fibroblast cells exposed to the current CHXD solutions (>0.01%), the shape of the cell became more rounded and less prolific (Figure 39).

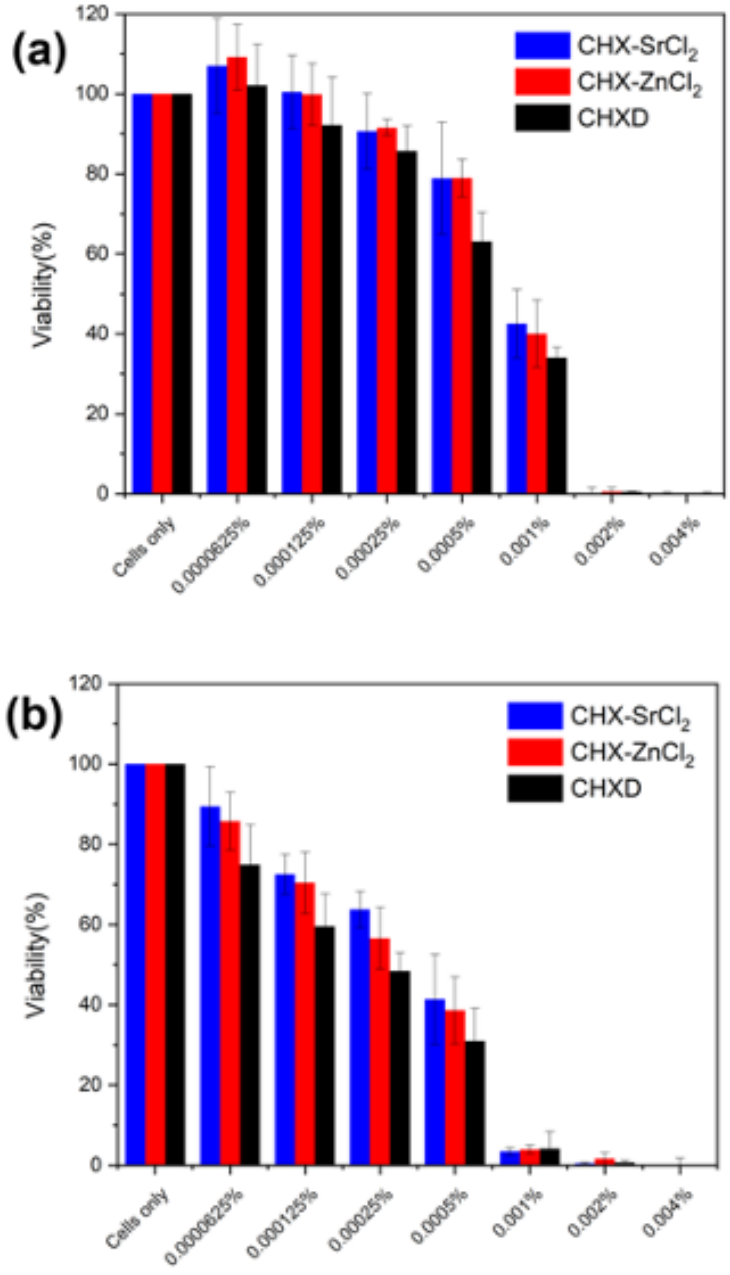

Figure 38. Effects of CHX-$CaCl_2$, CHX-$SrCl_2$, CHX-$ZnCl_2$, and CHXD particles on the relative viability of fibroblast (L929) cells at (a) 24h and (b) 48h. (n=3). All the treated groups were normalized to the control groups.

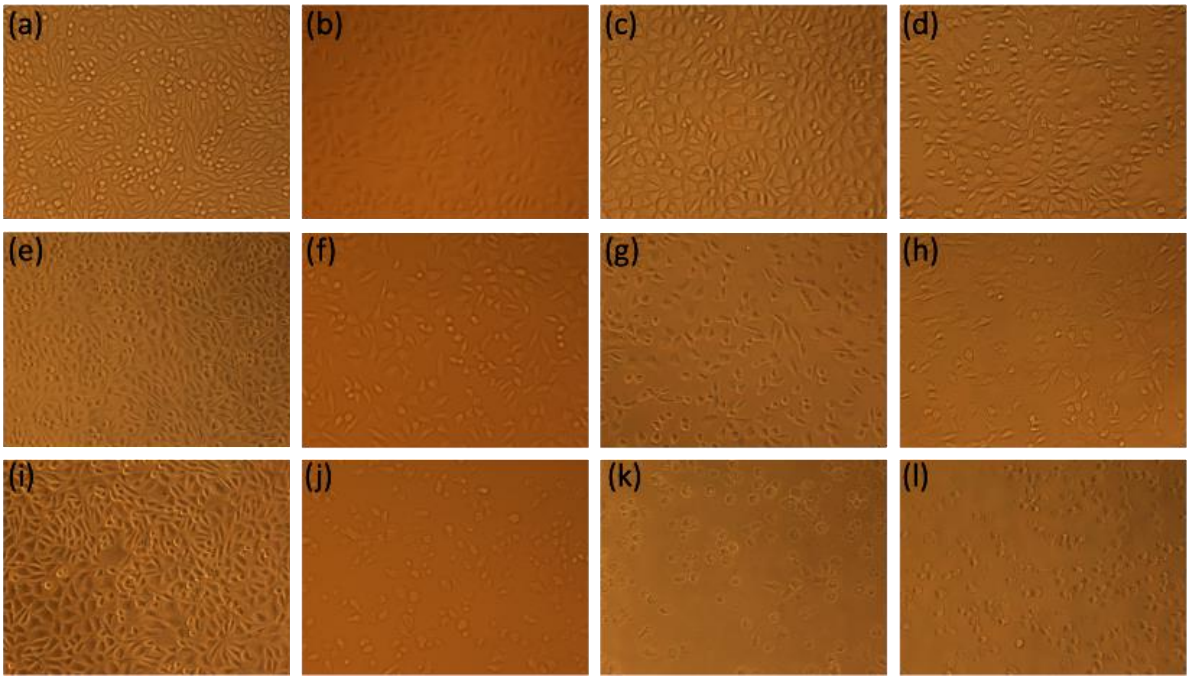

Figure 39. Effect of CHXD; CHX-$SrCl_2$ and CHX-$ZnCl_2$ particle on cellular viability. The Fibroblast like cell lines (L929) were treated with a), e) and i) 0 (untreated) b) 0.00025% CHX-$SrCl_2$ particles, c) 0.00025% CHX-$ZnCl_2$ particles, d) 0.00025% CHXD particle for 48 hours, f) 0.0005% CHX-$SrCl_2$ particles, g) 0.0005% CHX-$ZnCl_2$ particles, h) 0.0005% CHXD particle for 48 hours. j) 0.001% CHX-$SrCl_2$ particles, k) 0.001% CHX-$ZnCl_2$ particles, l) 0.001% CHXD particle for 48 hours. (n=3).

4.3.4 Results of the Tissue Adherence Study

Figure 40 demonstrated the morphology of the gingiva surface before and after coating with CHX particles as well as the influence of different drying methods. The gingiva had a clean and smooth surface before coating the CHX particles. Figure 40 b, d, f confirmed particles could be synthesised by using the prepared solutions on the separate SEM stubs. However, if the gingiva was rinsed using human saliva (Figure 40 a, c, e), no CHX particles (CHX-$CaCl_2$, CHX-$ZnCl_2$, CHX-$SrCl_2$) could be retained on the surface, leaving a clean surface similar to the control group (38, g). Synthesis of these particles in conjunction with moist pig's tissue illustrates these particles do not bind to moist tissue (Figure 40c, e).

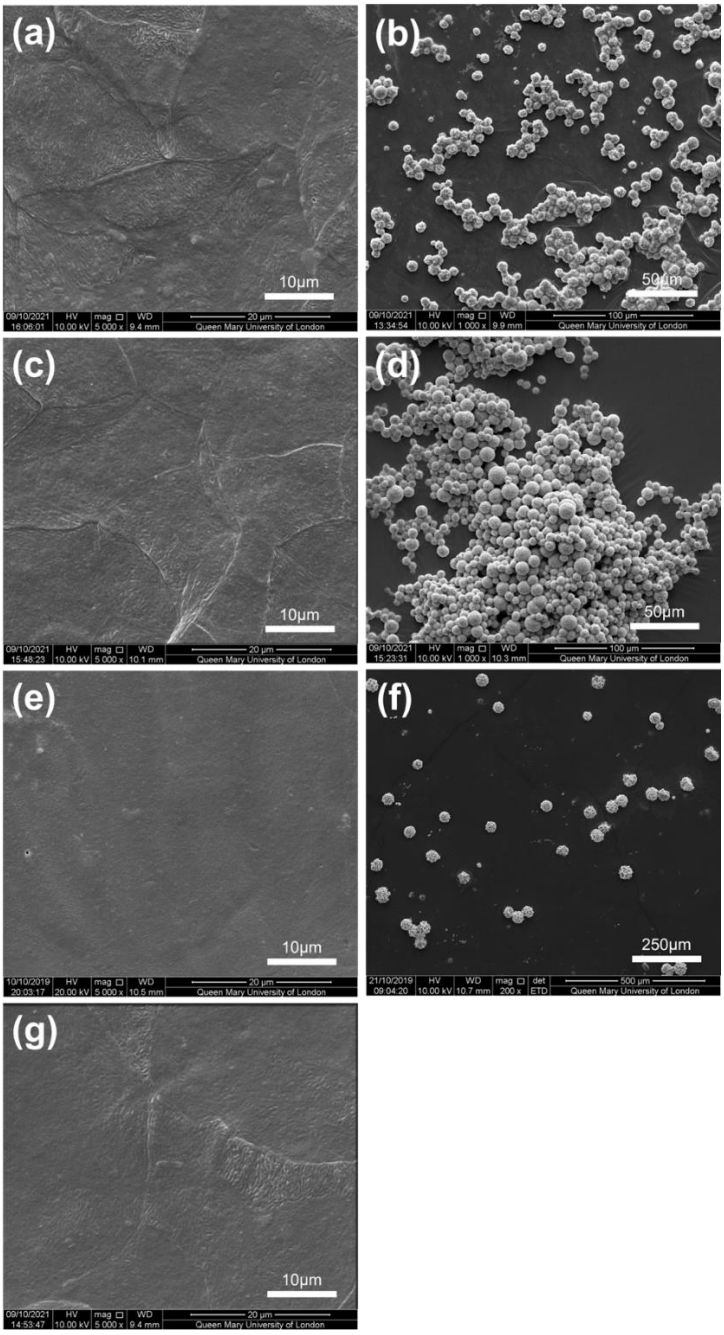

Figure 40. a) CHX-$SrCl_2$ particles coating on the moisturized pig's tissue after rinsing, b) CHX-$SrCl_2$ particles formed on separate SEM stub, c) CHX-$ZnCl_2$ particle coating on the moisturized pig's tissue after rinsing, d) CHX-$ZnCl_2$ particles formed on the on the separate SEM stub, e) CHX-$CaCl_2$ particle coating on the moisturized pig's tissue after rinsing, f) CHX-$CaCl_2$ particles formed on the on the separate SEM stub. g) SEM images for pig's tissue without any coating.

4.3.5 Results of ALP Activity

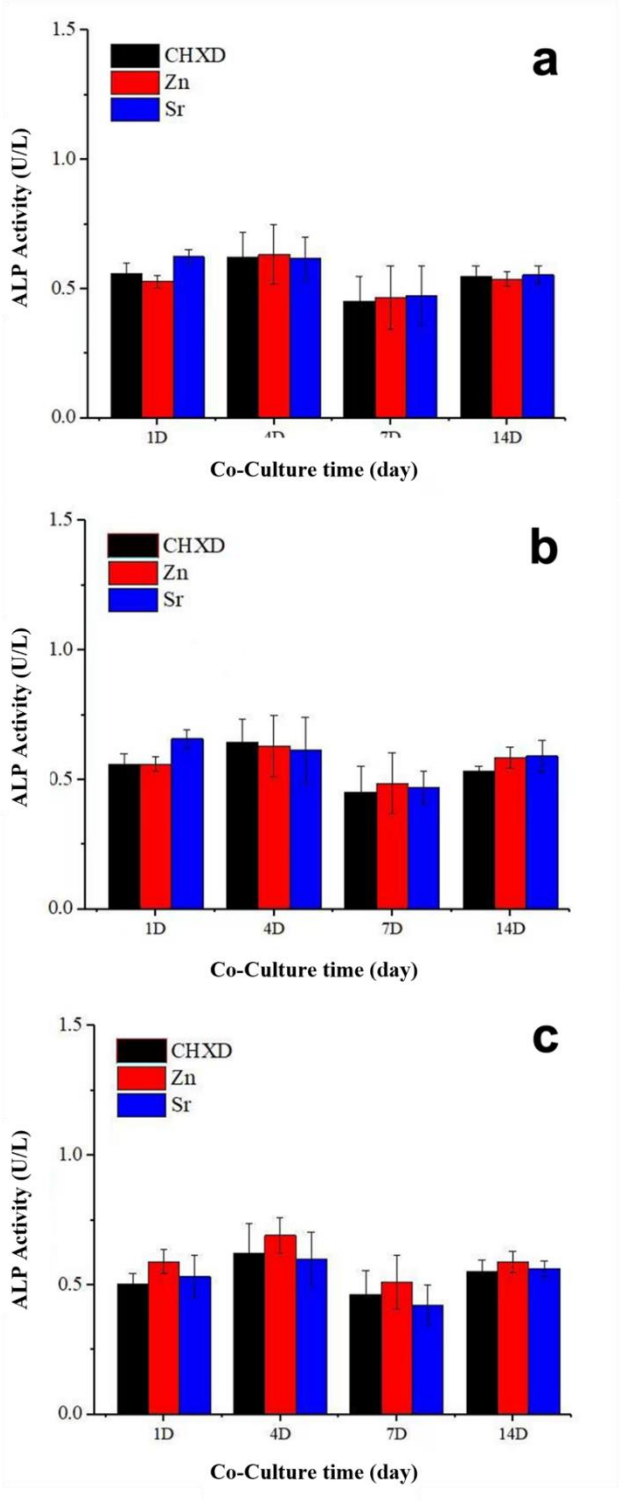

Figure 41. The ALP activity of CHXD, zinc or strontium containing CHX particles treatment. a, under concentration at 0.0000625%, b, under concentration at 0.000125%, c, under concentration at 0.00025%. (n=3)

ALP activity was assessed to identify the early-stage differentiation of EC3T3-E1 cells with strontium or zinc treatment. CHX-$SrCl_2$ and CHX-$ZnCl_2$ particles treated cells which enhanced cell ALP activity were shown in Figure 41 a-c. The ALP activity assay revealed that low concentrations of Sr or Zn did not promote cell viability and proliferation rate.

4.3.6 Results of Alizarin Red S Staining

The deposition of the inorganic mineral was measured by Alizarin Red S staining as it binds Ca. Consistent with ALP results, there is no significant increase in the staining compared with cell only group over 4 weeks period (Figure 43). The CHX-$SrCl_2$ and CHX-$ZnCl_2$ particles in the concentration range from 0.0000625% to 0.000125% induced an increase in the staining from day 14, day 21 to day 28 (Figure 42). However, when the cells exposed to the CHX solutions concentration at 0.00025% for more than 14 days, the shape of the cell became more rounded and less prolific (Figure 42). The cell indicated a significant influence on cellular viability and morphology at concentration of 0.00025% of CHX.

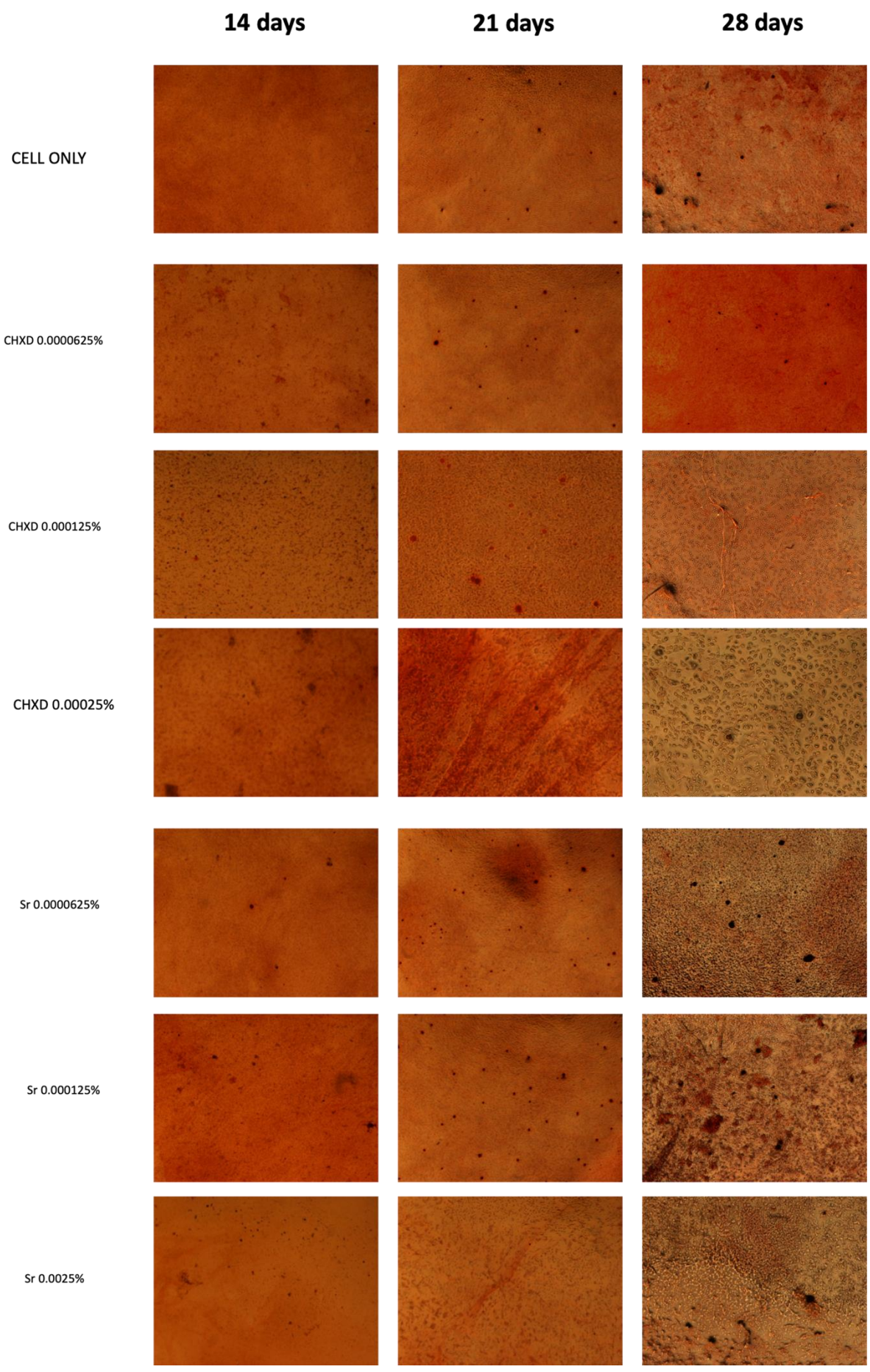
14 days
21 days
28 days
CELL ONLY
CHXD 0.0000625%
CHXD 0.000125%
CHXD 0.00025%
Sr 0.0000625%
Sr 0.000125%
Sr 0.0025%

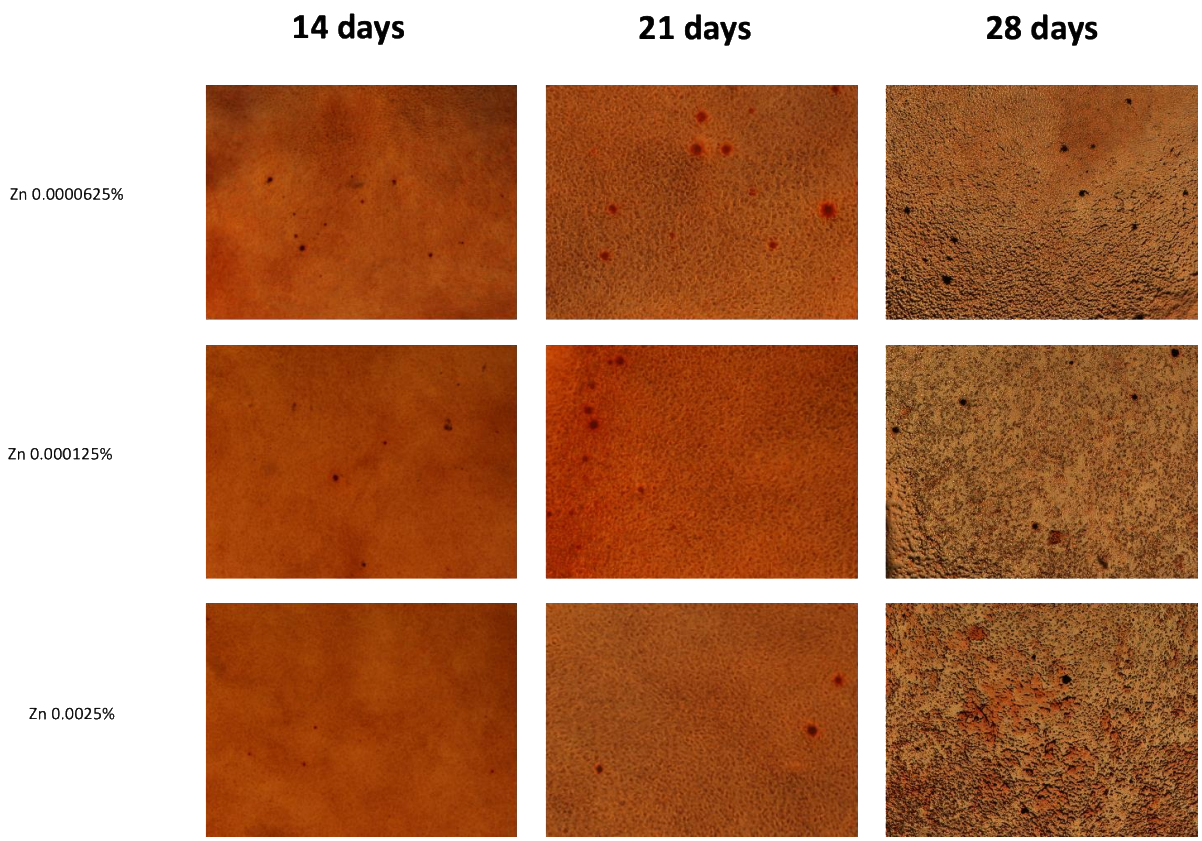

Figure 42. Alizarin Red S staining of mineralisation in EC3T3-E1 cell following CHXD, CHX-$SrCl_2$ and CHX-$ZnCl_2$ particles treatment (n=3).

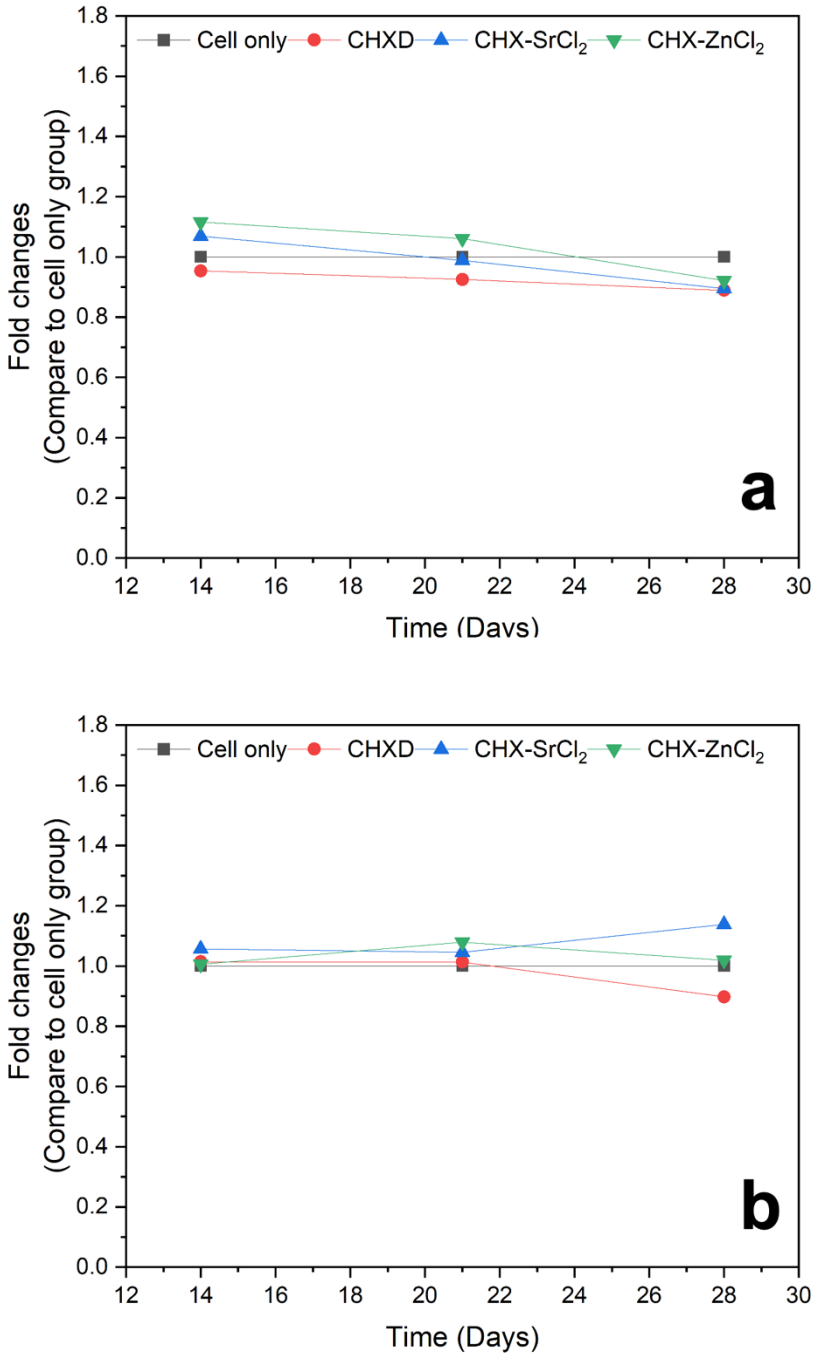

Figure 43. Quantification of Alizarin Red S staining of mineralisation in EC3T3-E1 cell following CHXD, CHX-$SrCl_2$ and CHX-$ZnCl_2$ particles treatment. a, under concentration at 0.0000625%, b, under concentration at 0.000125%. (n=3)

Chapter 5. Efficacy of CHX particles on antimicrobial release profile using a gel and medical device model

5.1 Introduction

One of the main limitations of CHX formulations and delivery methods currently being used is the difficulty in maintaining bacteriostatic concentrations in the mouth for effective time periods [257,310]. Especially for periodontal disease treatment, the CHX have to reach and remain in the deep of the periodontal/peri-implant pocket [311]. The clinical studies demonstrated that after scaling and root planning (SRP), the subgingival microflora may continuously changes [146,312]. Thus, the antibacterial agent like CHX containing gels can be used to reduce the limitations in deep inaccessible periodontal pockets after surgical intervention [313].

Many sustained release delivery mechanisms for CHX have been attempted including degradable gelatine chips [157] and gels [314], with varied but limited evidence of their efficacy in the treatment of both periodontitis and peri-implantitis [315]. Various gels including cellulose gel forming polymers and xanthan gum [171,172] are used as carriers for CHX, all showing muco-adhesive properties. The commercial CHX gels include the cellulose based Corsodyl® (containing 1% CHX digluconate); a xanthan gum gel containing 0.5% CHX digluconate and 1% CHX dihydrochloride. Gels have the advantage that they can carry much higher concentrations of CHX (1%- 2% in Dentistry) than liquids and their higher viscosity reduces the clearance of CHX from the periodontal pocket. The ease with which gels can be clinically placed and avoidance of tissue damage, make them much easier to administer than the more technique sensitive chip carriers.

The bacterial aetiology of periodontal and peri-implant diseases is clear [16,19]. There are specific situations where antimicrobials are beneficial, particularly as an adjunct to root surface debridement. The development of a novel CHX-$CaCl_2$, CHX-$ZnCl_2$ and CHX-$SrCl_2$ particles that have exhibited sustained CHX release, good wetting abilities [86] and reduced cytotoxicity [303], may therefore be good candidates for new CHX gel products. Especially, Strontium would be beneficial to perform the dual action of bone stimulation and bone resorption suppression [208,316] , and zinc is able to release during bacterial infections at low pH value (pH = 4.5) [232,303]. A gel carrier for the novel CHX-$CaCl_2$, CHX-$ZnCl_2$ and CHX-$SrCl_2$ particles, with muco-adhesive properties, that is easy to inject into deep periodontal and peri-implant pockets, may resolve many of the shortcomings of existing CHX products and offer extra functional ions. This study therefore aims to incorporate novel CHX-$CaCl_2$, CHX-$ZnCl_2$ and CHX-$SrCl_2$ particles into injectable gel carrier systems and test the release kinetics and antibacterial efficacy against *P. gingivalis.*

Therefore, this work proposed a simple and cost-effective way to use low-cost reagents and energy-saving synthesis to develop novel CHX drug particles, which take advantage of the therapeutic functions of the additionally released metal ions. Their further incorporation into an injectable gel was to provide a vehicle or delivery system in high demand for dental and medical applications.

The CHX-$CaCl_2$ particles have a unique surface crystallisation mechanism which may provide an intriguing option to treat white spot lesions and caries for patients. This controlled coating method will also allow the clinician to apply the drug precisely onto the desired area such as implant, tooth, or orthodontics brackets without disrupting the reagent and simultaneously, avoiding excess CHXD in the oral cavity. Avoiding an

excess of the CHX will prevent any mucosal irritations or allergic effects. This will also not interrupt the nitrogen cycle of the oral microbiome. Thus, the CHX-$CaCl_2$ particles as a mouthwash were also explored.

5.2 Methods and materials

5.2.1 Synthesis CHX Particle Containing Gels

Hydroxypropyl methyl cellulose (HPMC) was used in the current study and prepared as carriers for the CHX-$CaCl_2$, CHX-$SrCl_2$, CHX-$ZnCl_2$ particles. To prepare HPMC gel, 100ml deionized water was filled into a glass beaker and placed on a hot plate (UC152D, Stuart, UK) at 85°C. Then stirring the hot water at 400 rpm using an overhead mechanical stirrer (RW20 digital, IKA®, Germany) while gently adding 3g HPMC (viscosity 2,600-5,600 cP, 2% in H_2O, Lot: MKBV9071V, Sigma, UK) powder until all the power was fully dissolved (around 15 minutes). The mixture was then removed from the hot plate followed with the addition of 50 ml of cold deionised water. Afterwards, the gel was stirred for another 15 minutes at 600rpm. The gel was transferred into a 50 ml centrifuged tube and stored in the 4°C refrigerator for 24 hours before the next step.

In order to incorporate CHX particles into the gel, 100 mg of CHX-$CaCl_2$, CHX-$SrCl_2$ or CHX-$ZnCl_2$ particles was weighed and sprinkled over 20 ml of the pre-made HPMC gel independently. The mixture was then gently folded by a stainless-steel spatula for 4 minutes. After that, the gel was mixed in a vacuum mixer (Iris 2 Evolution, Mestra®, Spain) for 1 minute at 200rpm before sprinkling another 100mg of CHX-$CaCl_2$, CHX-$SrCl_2$ or CHX-$ZnCl_2$ particles over the gel and repeated the same step. CHX digluconate (Sigma-Aldrich, UK, Lot bcbz5940) was also introduced into a separate

HPMC gel using the same method in above as a comparison material. Further, Corsodyl (1% CHX digluconate, GSK, UK, lot 5144707) was used as a commercial comparison group in this study.

5.2.2 Release Assay for the CHX Particle Containing Gels

Thirteen test groups of gel (Table 13) were prepared and performed in this study and each group contained 3 replicates (n=3). For each group, three 150 mm dialysis tubes (Ref: 300806888, Membra-CEL MD10 14X100 CLR, USA) were prepared and each tube was filled with 1 ml of the designated gel by using a 2 ml syringe (Ref 307727; Lot: 1605, BD Emerald, UK) and a 21G needle (Lot: E03723, Sabre®, Luer, UK). After loading the gel, the filled dialysis tube was inserted into a 5ml micro-centrifuge tube (Eppendorf, Germany) which contained 4 ml of deionized water, PBS, or artificial saliva pH=7. The tube then was placed into the 37°C incubators. Following the designed time points (Table 4), the dialysis tubes were removed from the centrifuge tubes to a new 5 ml microcentrifuge tube which contained 4 ml fresh solutions (deionized water, PBS or AS). These steps were repeated until 24 weeks. The HPMC gel only was run for a week as a control group and the media was changed at 5 minutes, 24 hours, and 7 days.

The gel samples from the release study were collocated and analysed using UV-Vis spectrometry as described in section 3.4.5.2. The fresh deionized water, PBS or AS were used as a reference in order to remove the background environment during the experiment.

Table 13. Gel release assay groups

Group	Gel in dialysis tube	Medium in Eppendorf tube
A	CHX$CaCl_2$/HPMC	Deionised water
B	CHX$CaCl_2$/HPMC	PBS
C	CHX$CaCl_2$/HPMC	AS
D	CHX$ZnCl_2$/HPMC	Deionised water
E	CHX$ZnCl_2$/HPMC	PBS
F	CHX$ZnCl_2$/HPMC	AS
G	CHX$SrCl_2$/HPMC	Deionised water
H	CHX$SrCl_2$/HPMC	PBS
I	CHX$SrCl_2$/HPMC	AS
J	CHX digluconate/HPMC	Deionised water
K	CHX digluconate/HPMC	PBS
L	Corsodyl® (1% CHX digluconate) hydroxypropyl cellulose, isopropyl, alcohol, peppermint oil.	Deionised water
M	Corsodyl® (1% CHX digluconate) hydroxypropyl cellulose, isopropyl, alcohol, peppermint oil.	PBS
N	HPMC alone	Deionised water
O	HPMC alone	PBS
P	HPMC alone	AS

5.2.3 Antibacterial Study for the CHX Particle Containing Gels

P. gingivalis strain W50 was cultured as described in section 4.2.1.1. After overnight incubation, the bacterial suspensions were diluted in pure BHI, to achieve an optical density of 0.1. This gave approximately $6.36*10^7$ colony-forming units (CFU) per ml, in order to standardise the bacterial inoculum used in these experiments.

Samples were collected from 5 minutes, 2 hours, 24 hours, 7 days and 14 days from the release assay and used in the antimicrobial study. 100 µl strain *P. gingivalis* strain W50 suspension was spread by sterile hockey stick spreader onto each plate. A 10 mm diameter borer (Lot; Z165220, Sigma Aldrich, UK) was used to cut wells in each agar plate for samples.

The CHXD standard solutions were prepared at concentrations of 1, 3, 5, 10, 20, 30, 40, 50, 60, 70, 80, 90, 100 µg/ml which were tested for antibacterial activity. The deionized water, PBS, AS were used as comparison groups in the antibacterial test. Three wells were punched into each plate and 150 µl of the selected solution was placed into each well using a 200p micro pipette (Eppendorf, Germany). Plates were examined at 24h and 48h for the presence of a zone of inhibition. Each well was then measured by a vernier calliper (Mitutoya, UK) across the whole diameter which was inclusive of the well (Figure 44).

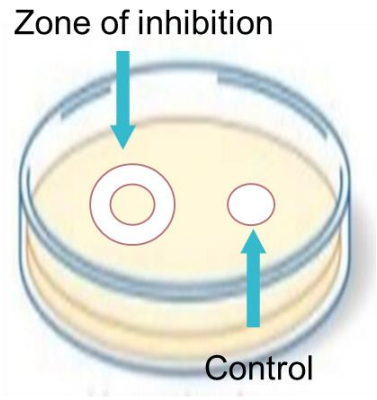

Figure 44. An example showing a zone of inhibition of sample and control group.

5.2.4 Synthesis of CHX-$CaCl_2$ Mouthwash

To explore the potential surface crystallization of the CHX-$CaCl_2$ crystal system, this section was proposed to experiment with the deposition of the CHXD and $CaCl_2$ reagents used in the previous section (3.3.1), when in contact with different material surfaces and medical devices. To achieve this, a simple mouthwash was created and used to coat the surface of dentures, titanium implants, teeth and orthodontic brackets. The final part of this work demonstrated the CHX-$CaCl_2$ release from a medical device (orthodontic bracket) as a proof of concept.

5.2.4.1 Application of CHX-$CaCl_2$ to the Glass Slide Surface

In order to assess the effects of CHX-$CaCl_2$ crystallization, the solutions were first applied to a glass slide to assess the mechanism without the effect of processing flaws. Two solutions were prepared for this study including 0.024M CHXD solution and 0.33 M $CaCl_2$ solution. The 20 µl CHXD solution was added onto glass slides (VWR, USA) and left for 1 minute, 20 µl of $CaCl_2$ was further added and reacted for 60 seconds. Then the excess liquid was carefully removed with fuzz-free lab wipes. The sample

was next prepared for SEM following the same steps in section 3.4.1 whose morphologies were observed using SEM.

5.2.4.2 Application to Medical Devices-Dentures and Implants

To demonstrate the effects of CHX-$CaCl_2$ crystallisation on the surface of medical devices, sections (2 cm × 2cm) were cut from a polymethyl methacrylate denture base. A regular neck implant (Ø3.3mmRN, 8mm, lot RA221, Straumann) with an SLActive® surface was also selected for this study.

The samples (denture base sections, implant) were coated using the following emersion technique when positioned on carbon tape on an SEM holder inside of a custom tube. 8 ml of a 0.024M CHX diacetate solution was syringed into the tube and left for 1 minute (covering the sample). Then, 8ml of the $CaCl_2$ solution (0.33 M) was applied using a syringe into the tube and left for another minute before removal of the solution. The prepared samples were then transferred to an incubator at 37°C for 10 minutes. The morphology of the samples was checked with SEM following the steps in section 3.4.1.

5.2.4.3 Application of CHX-$CaCl_2$ to Teeth and Orthodontic Brackets

Preliminary investigations were carried out using human teeth (premolars) which were collected from the QM teeth bank (QMREC 2014/17) as substrates for CHX-$CaCl_2$ particle deposition. Teeth were coated by applying 8 ml of 0.024M CHXD (left for 1 minute), followed by 8 ml of $CaCl_2$ solution (0.33 M) left for 1 minute, using the method/processes described in section 5.9.2. The specimens were next gold coated and viewed using SEM.

Human teeth with orthodontic brackets *in situ* were also coated using the novel CHX-$CaCl_2$ rinse. The preparation methods were as follows. Each labial tooth surface was air-dried (20 seconds) and etched using etching gel (phosphonic acid, super etch SDI, Australia) for 10 seconds. Then, the gel was rinsed using DI water for 20 seconds and blow-dried for 10 seconds with an airline. A bonding agent (Ortho Solo™, USA) was applied using a micro-brush, followed by 10 seconds of air-drying and then light-cured for 20 seconds using a light gun (3 Tech Led-1007 Curing light, UK) in the gradual mode. An orthodontic bracket (Victory Series, 3M Unitek, Monrovia, Calif) was next placed on the labial tooth surface, and excess bonding cement removed using a dental probe. Curing was carried out using a light gun in the gradual mode, illuminating the top and bottom sides of the bracket for 20 seconds, respectively. Finally, the wires (Nitinol Super-Elastic, USA) and elastics (Elast-O loop Ligatures, DB03-0040, Dbortho, UK) were placed on the brackets (Figure 17).

To coat CHX-$CaCl_2$ particles on the tooth /bracket surface, 0.024M CHXD solution was syringed onto the brackets on three individual teeth and left for 1 minute using a 1 ml syringe (Terumo, Japan) and 30ga bendy-tip (Schottlander, UK). The coating of CHX-$CaCl_2$ particles on brackets was achieved by further syringing 20 ul of 0.33M $CaCl_2$ solutions onto the bracket to react with CHXD solutions for a further 1 minute. In addition, the surface morphology of the coated bracket was examined using SEM. After release experiments (section 5.2.5), the sample was further examined using SEM in order to check for remaining particles.

Figure 45. Image of the tooth with bracket after CHX-$CaCl_2$ coating.

5.2.5 Release Assay for the Coated Bracket

The release studies were conducted in artificial saliva (AS), prepared by dissolving 0.4411g $CaCl_2$, 0.245g KH_2PO_4(P3786, Lot #BCBC2041), 9.532g Hepes (lot SLBW8459) and 19.386g KCl (Lot BCBZ4557) in 800 ml of DI water. The prepared AS was then diluted to a volume of 2 L and the pH adjusted to pH 7 by adding 0.5 M KOH diluted with DI water. The AS solution was stored at 4°C in a fridge. One day before the release experiments, it was preheated in an incubator (Benchmark Scientific, Inc., New Jersey, USA) at 37°C.

The prepared teeth with coated bracket (n=3) were submerged into 7 ml tubes (Starlab Ltd, Milton Keynes, UK) filled with 2 ml AS at 37°C, to guarantee the full immersion of the teeth. Every 12 hours, the AS was replaced by transferring the samples to tubes containing fresh AS, while the original tubes and AS samples were collected for CHX concentration measurement by UV/Vis spectrometry. All sample tubes were stored in

an incubator at 37℃ throughout the release experiment. The CHX release of each tooth /bracket sample was run parallel and repeated three times.

5.3 Results of Containing Gels

5.3.1 Results of the Release Kinetics of the Gels

The results of the CHX release study in water and PBS are shown in Figure 46 and Figure 47. The data for Corsodyl and CHX digluconate gels was contributed by Dr Yavar Khan (Dclin Dent Periodontology, QMUL). Although the novel CHX-$CaCl_2$, CHX-$SrCl_2$ and CHX-$ZnCl_2$ particles HPMC gel released the lowest amount of CHX in water, it showed sustained release behaviour compared with the other two comparison groups (Figure 46). However, the comparison groups (Corsodyl and CHX digluconate gels) demonstrated a burst release in the beginning from 7 to 48 hours. The second plateau commenced at 102 hours and no further burst release was observed. The CHX release from Corsodyl dropped below 6 μg/ml after week 9 and the CHX digluconate HPMC gel dropped below 6 μg/ml after 3 weeks. In contrast, the experimental CHX-$CaCl_2$, CHX-$ZnCl_2$ and CHX-$SrCl_2$ HPMC gels showed a more controlled steady release from the 7-hour point till the end of the release study (24 weeks). The novel CHX-$CaCl_2$, CHX-$ZnCl_2$ and CHX-$SrCl_2$ HPMC gels took 11 weeks for the CHX release to cease exceeding 6 μg/ml.

There were no distinct peaks observed at the 254 nm wavelength at any of the time points for HPMC gel only. It further confirms that no CHX was present in the HPMC gel.

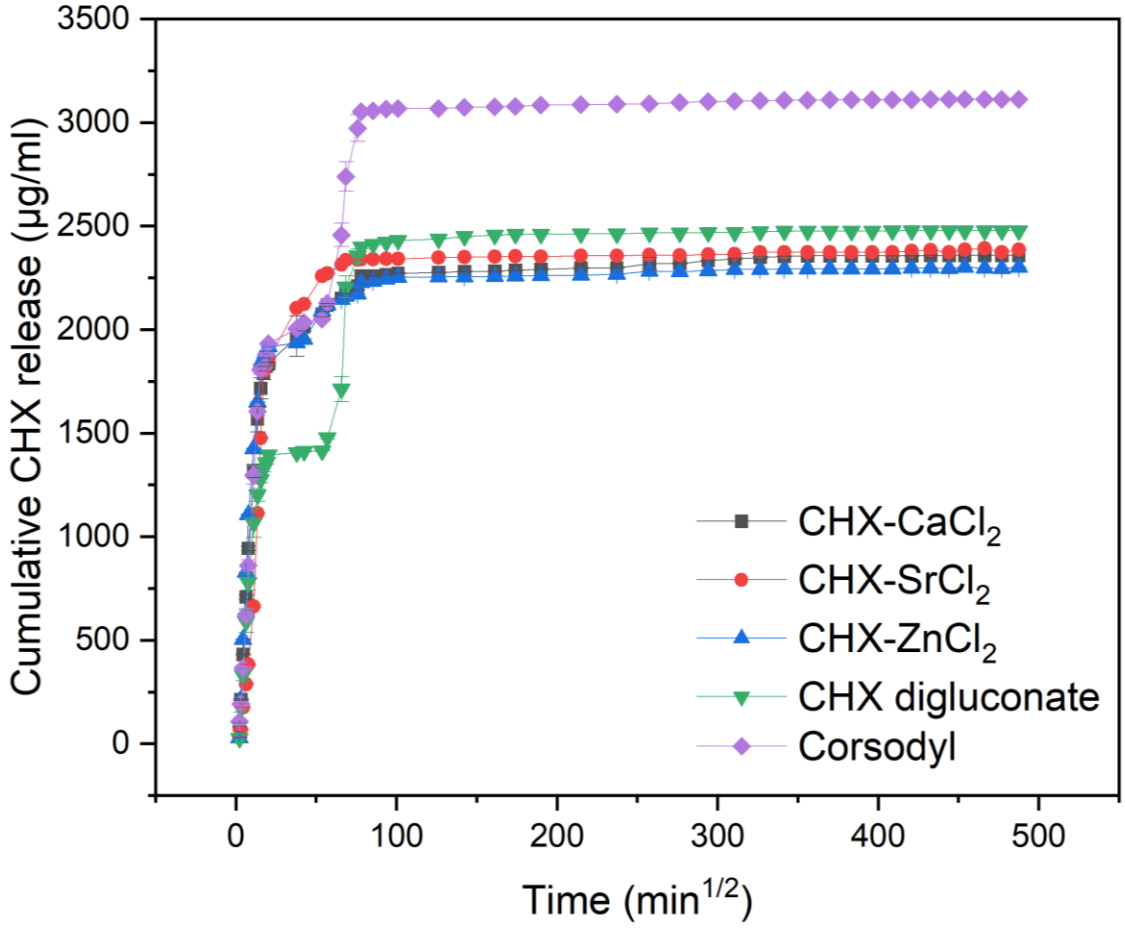

Figure 46. Cumulative CHX release over time for gels in deionized water (n=3).

Figure 47 showed the gel release results in PBS. Corsodyl demonstrated a sustained-release behaviour while the CHX digluconate HPMC gel was released in multiple stages, with three distinct plateau periods. The cumulative CHX release from the novel CHX-$CaCl_2$, CHX-$SrCl_2$ and CHX-$ZnCl_2$ particle HPMC gels was nearly double that of the Corsodyl and CHX digluconate gels at week 24. In this release experiment, the CHX-$CaCl_2$, CHX-$SrCl_2$ and CHX-$ZnCl_2$ particle HPMC gels demonstrated a sustained release until week 22, before the CHX concentration was below 5 µg/ml. Corsodyl ceased to release above 5 µg/ml by 16 weeks, and the CHX digluconate HPMC gel by just 9 weeks. Interestingly a similar CHX release behaviour to PBS was also found

when the experimental HPMC gels (Groups C, F, and I) were evaluated in artificial saliva (Figure 48).

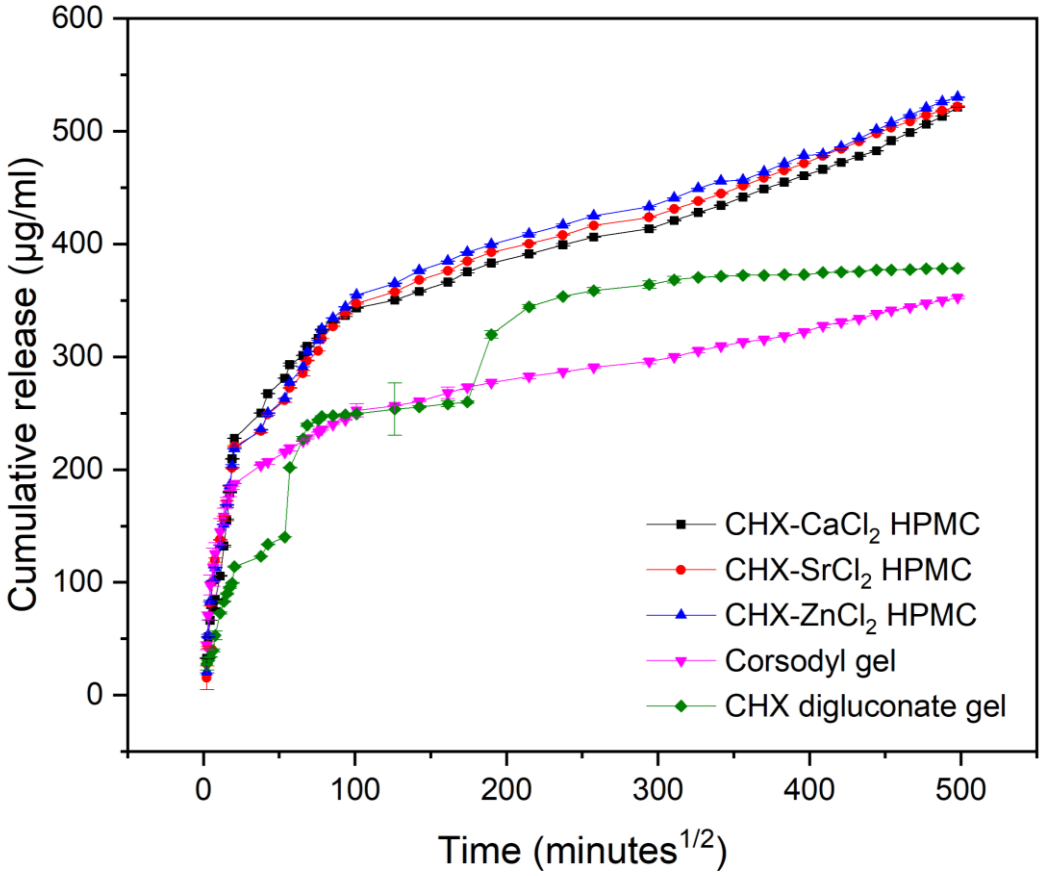

Figure 47. Cumulative CHX release over time for gels in PBS (n=3).

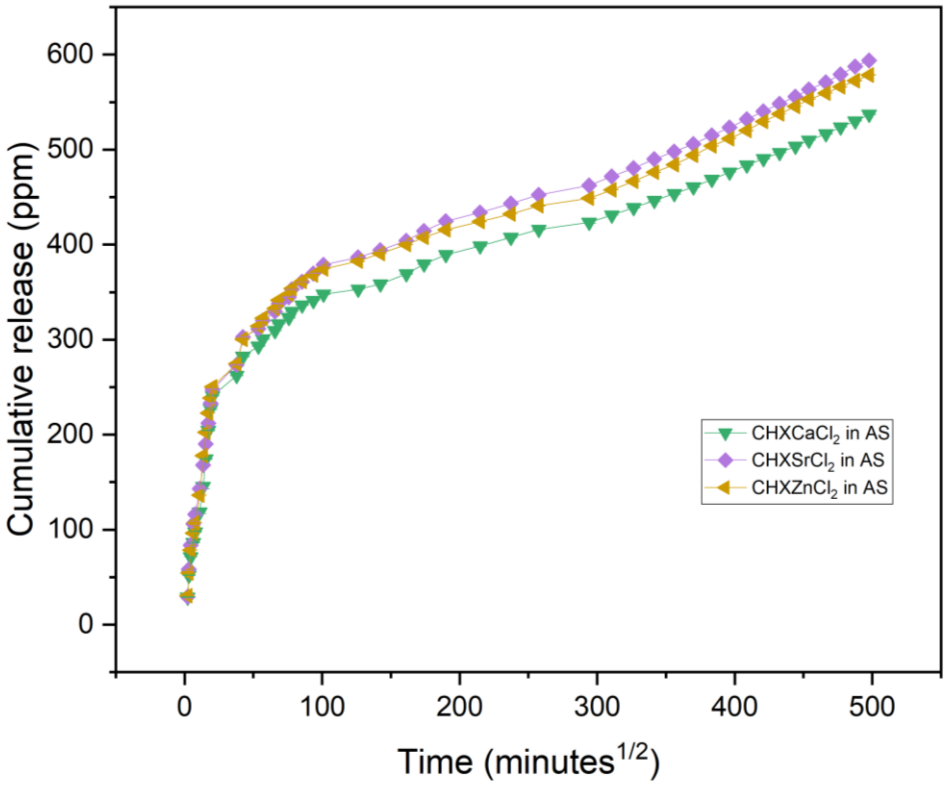

Figure 48. Cumulative CHX release over time for gels in AS (n=3).

5.3.2 Results of Antimicrobial Assay of the Gels

The results of the zone of inhibition experiments from different CHXD concentration standards were shown in Figure 49. The antimicrobial activity of the CHXD standard solution in water were tested 3 times. The mean (SD) zone of inhibition diameter around the wells was calculated (n=3). There was no inhibition observed in the PBS only group which confirms that any inhibition of *P. gingivalis* in the test and comparison samples was due to the released CHX in the dialysate.

It is shown in Figure 49 that an increase in inhibition of *P. gingivalis* was observed with raising concentrations of CHXD. There was no inhibition from 1µg/ml to 5µg/ml concentrations.

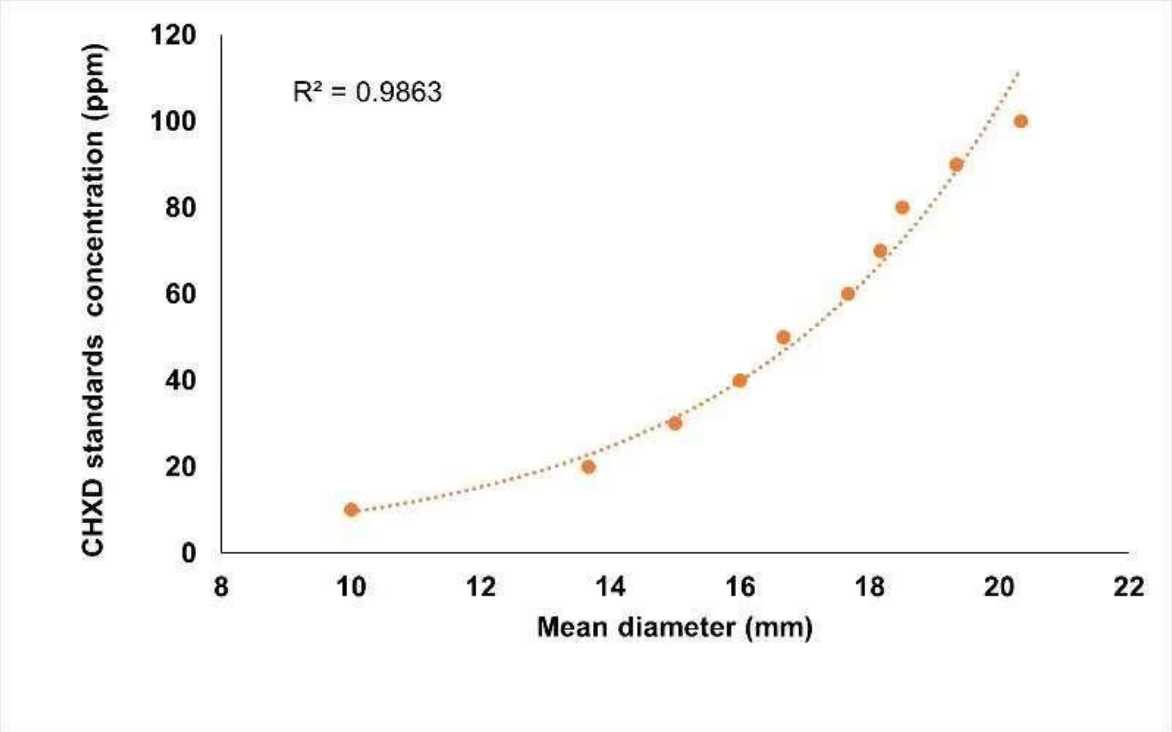

Figure 49. The zone of inhibition for each concentration of CHX diacetate solution.

The graph in Figure 50 showed the results for the antibacterial testing (zone of inhibition) for the dialysates from the release assay for CHX-$CaCl_2$, CHX-$SrCl_2$, CHX-$ZnCl_2$ HPMC gels in PBS, and compared with the commercial comparison gel Corsodyl (Figure 50).

The Corsodyl group showed a higher zone of inhibition at 5 minutes, then the CHX$CaCl_2$, CHX$ZnCl_2$, CHX$SrCl_2$ cellulose gel groups maintained a higher level of inhibition of against P. gingivalis for the remainder of the 2 weeks (Figure 50). The Corsodyl groups had no detectable zone of inhibition at 14 days while a clear zone was found in the CHX$CaCl_2$, CHX$ZnCl_2$, CHX$SrCl_2$ HPMC gel groups (Figure 50).

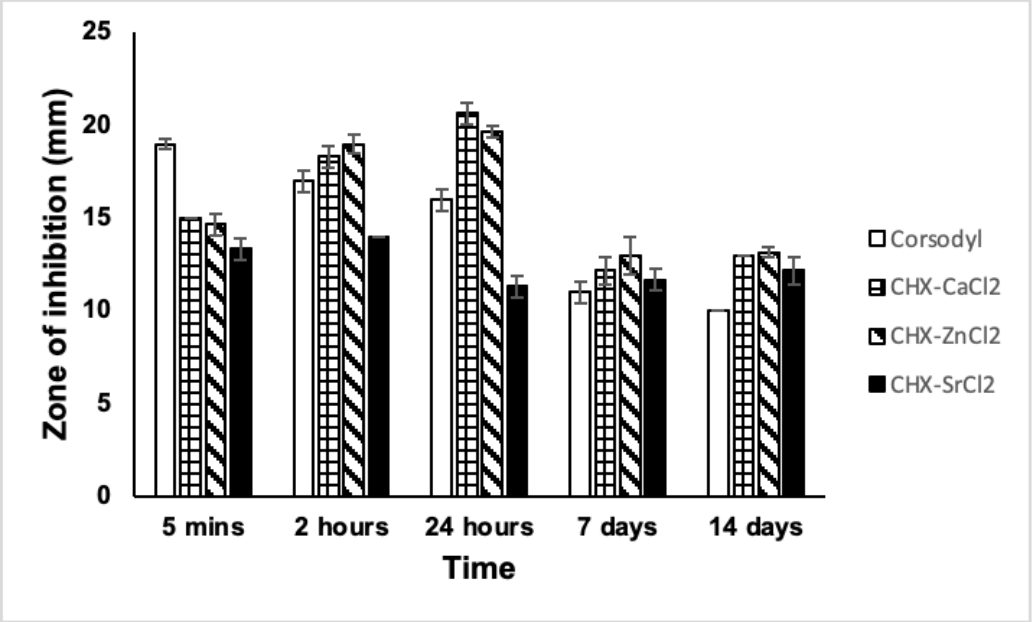

Figure 50. Results of the zone of inhibition for the gel dialysates released in PBS (n=3).

5.4 Results of the CHX-$CaCl_2$ Mouth Wash

5.4.1 Results of SEM of CHX-$CaCl_2$ Coating of the Glass Slide

Both CHX-$CaCl_2$ particles demonstrated unique morphologies of a porous and interconnected dendritic structure, grown from a nucleation site centre to the sphere (Figure 51 a-c). For the CHX-$CaCl_2$ particles prepared in the bulk solution, free-standing spherical dendritic structures harvested were shown in Figure 51 a-c. In contrast, the CHX particles would attach and grow on the surface dendritically, demonstrating a hemispherical structure but a smaller size when directly synthesized on the substrate (Figure 51 d-e).

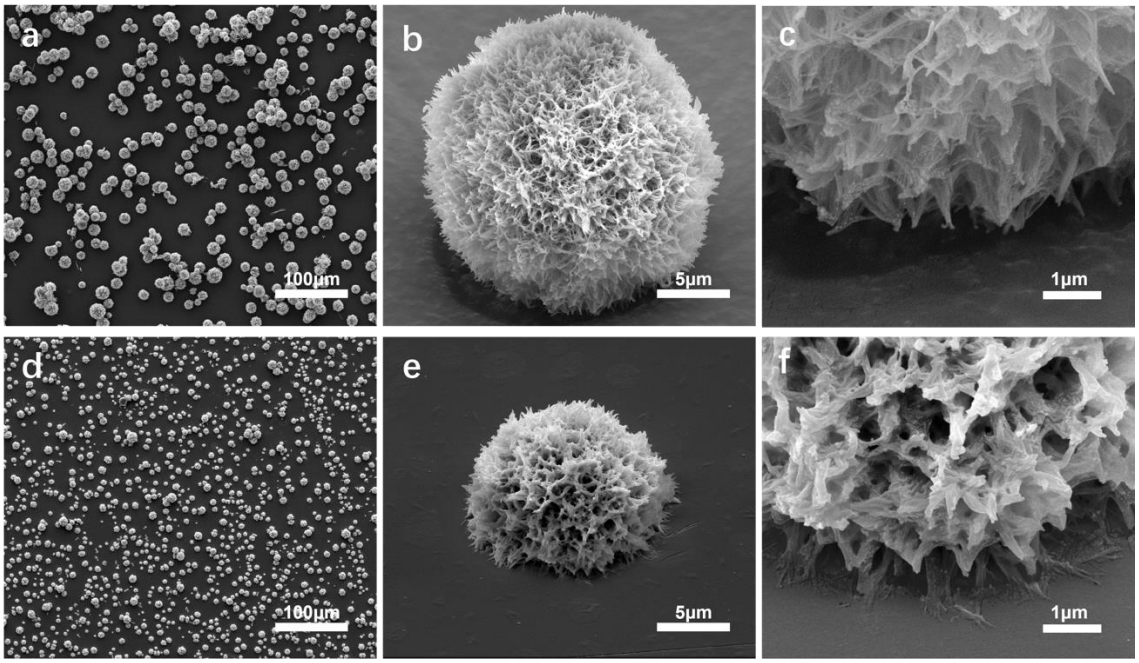

Figure 51. CHX-$CaCl_2$ particles synthesized (a-c) in bulk solution and (d-f) on a glass slide.

5.4.2 Results of SEM of CHX-$CaCl_2$ Coating of Medical Devices

The results of the SEM analysis for CHX-$CaCl_2$ coating on the implant and denture base surface were shown in Figure 52 a-f. Figure 52 a indicates that CHX-$CaCl_2$ particles were fully coated on the implant surface, while Figure 52 b, c showed the particles were able to be coated both rough (implant SLA rough surface) and smooth surfaces (abutments). Figure 52 c demonstrated the CHX-$CaCl_2$ particles could bind and grow onto the implant surface. Similarly, Figure 52 d showed the CHX-$CaCl_2$ particles fully coated the denture base surfaces. Figure 52 e illustrated the bi-modal distribution of the CHX-$CaCl_2$ particles on the polymer surface, while the Figure 52 f demonstrated the CHX-$CaCl_2$ particles growth and binding dendritically to the polymer surface.

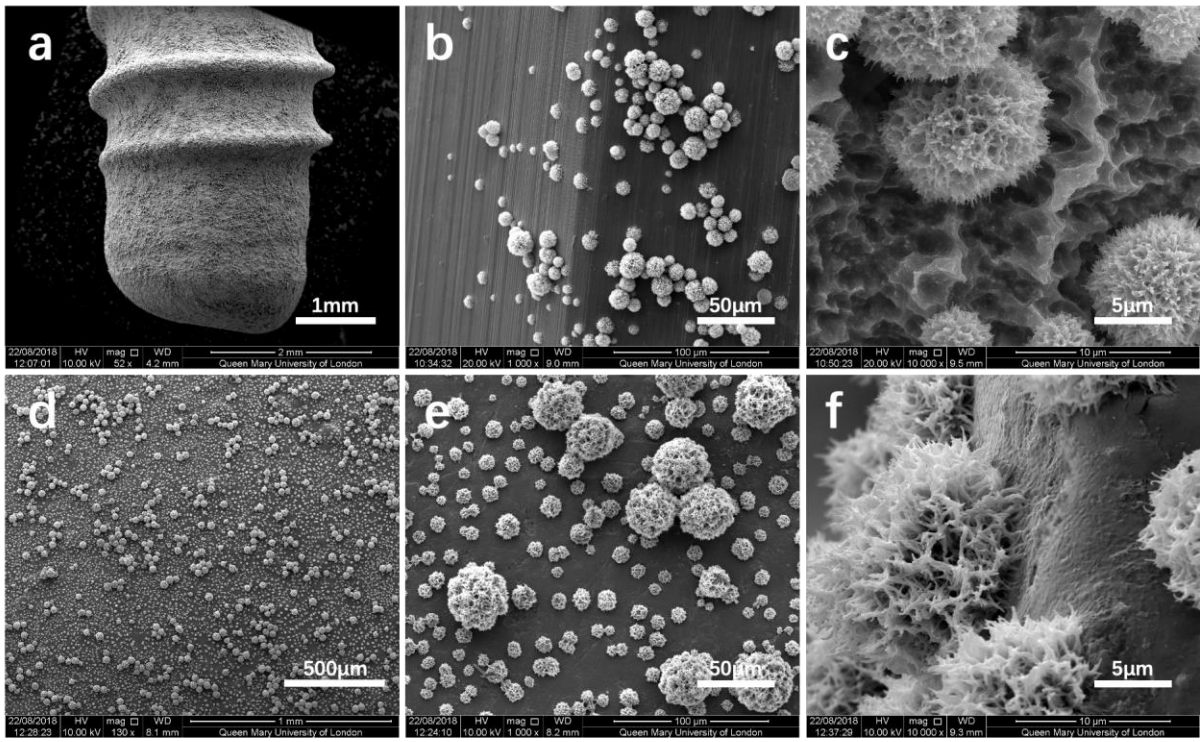

Figure 52. CHX-$CaCl_2$ particles coated on; (a-c) the implant surface and (d-f) the denture base.

5.4.3 Results of SEM of CHX-$CaCl_2$ Coating of Teeth and Orthodontic Brackets

Figure 53 indicated the crystallisation action of the novel CHX-$CaCl_2$ coating on the molar tooth. Figure 53 illustrated an even distribution of the CHX-$CaCl_2$ particles and especially at the pits and fissures on the occlusal surface. A bi-modal particle distribution was observed in Figure 53 b, with both spherical and dendritic morphologies. Figure 53 c demonstrated the novel CHX-$CaCl_2$ particles were binding dendritically to the tooth surface like tree roots.

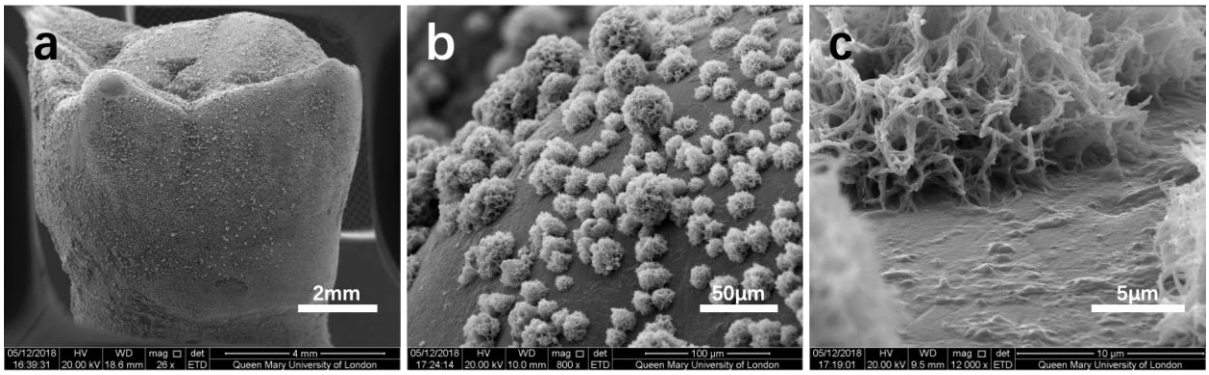

Figure 53. CHX-$CaCl_2$ particles coated on a) labial and occlusal tooth surface; b) distribution of CHX-$CaCl_2$ particles on the enamel surface; c) CHX-$CaCl_2$ particles binding to the tooth surface.

To take the advantage of the surface attaching properties of the particles, orthodontic brackets were employed to be coated with CHX-$CaCl_2$ particles, whose morphology both before and after the release experiment was evaluated via SEM with the results shown in Figure 54. An overview of the CHX-$CaCl_2$ particle coated bracket was demonstrated in Figure 54 a, showing a large amount of CHX particles successfully deposited on the surface of the bracket, rubber bands and wire, covering most of the surface areas. A magnified view of coated wire was shown in Figure 54 b, showing the CHX-$CaCl_2$ particles were physically attached to the wire. In addition to the metal surface, the CHX-$CaCl_2$ particles also grew on the rough surface of rubber bands (Figure 54 c). Figure 54 d showed the CHX-$CaCl_2$ particles can be formed on both the top and sloping sides of the bracket. Moreover, a small portion of CHX-$CaCl_2$ particles also coated on the surface of resin and tooth surface (Figure 55 a, b). In contrast, the surface morphology of the bracket after the release experiment of 21 days was demonstrated in Figure 54 e-h), where the majority of the CHX had been released from the bracket surface, leaving some remnants on the surface of the brace, rubber

band and wire. In addition, some dried salts also are observed on the bracket surface, which may result from the AS incubation solutions while preparing the samples.

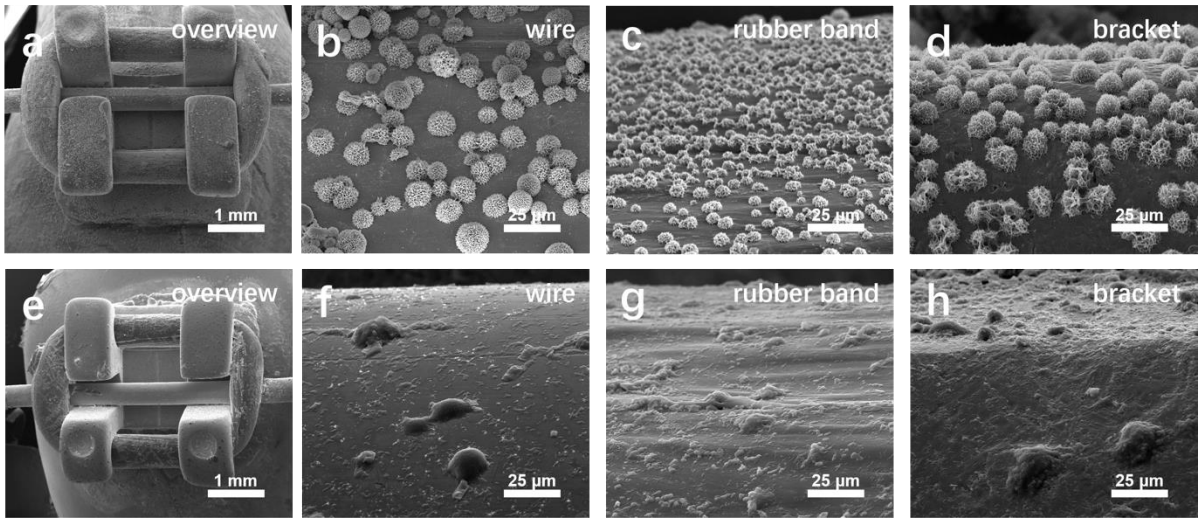

Figure 54. Bracket coated with CHX-$CaCl_2$ particles (a-d) before and (e-h) after 21 days incubation in AS solution.

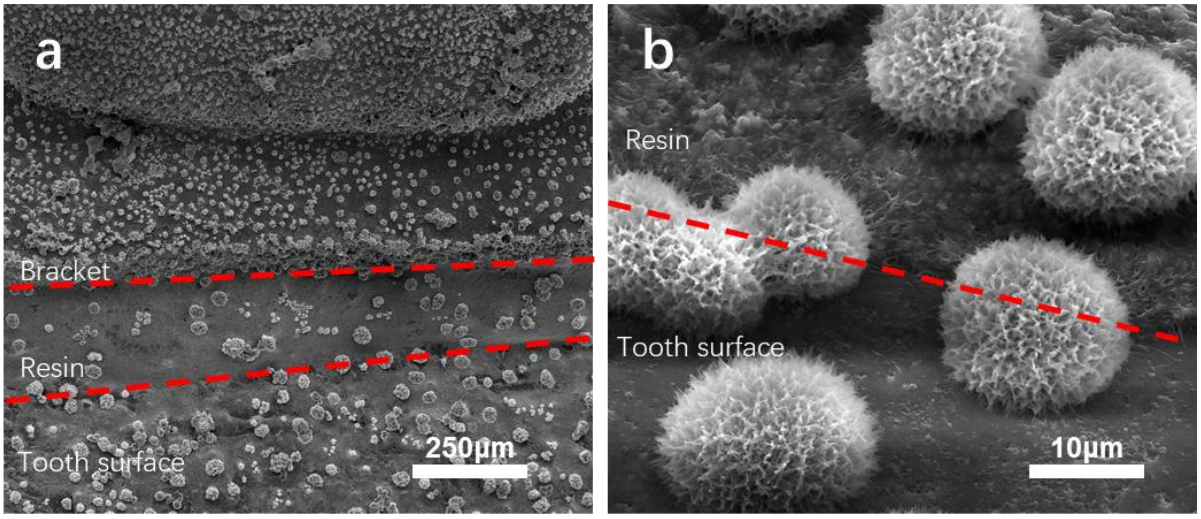

Figure 55. The SEM images of CHX particles coated on the surface of bracket, resin and tooth surface.

5.4.4 Results of UV-Vis of the CHX-$CaCl_2$ Particle-Coated Brackets

The results of CHX-$CaCl_2$ particle coated brackets immersed in artificial saliva (AS) pH 7 were demonstrated in Figure 56. When employing the CHX- $CaCl_2$ solutions for bracket coating, the cumulative CHX released reached 101 μg/ml over 21 days.

Figure 57 provided the quantitative amount of CHX used for coating, the coating efficiency and the amount released from the bracket after 21 days. Overall, 300μg CHX was used for bracket coating with the loading efficiency of 76.97% for 0.024M CHXD solution. On day 21, it is calculated that around 86.25% of the CHX was released from the bracket.

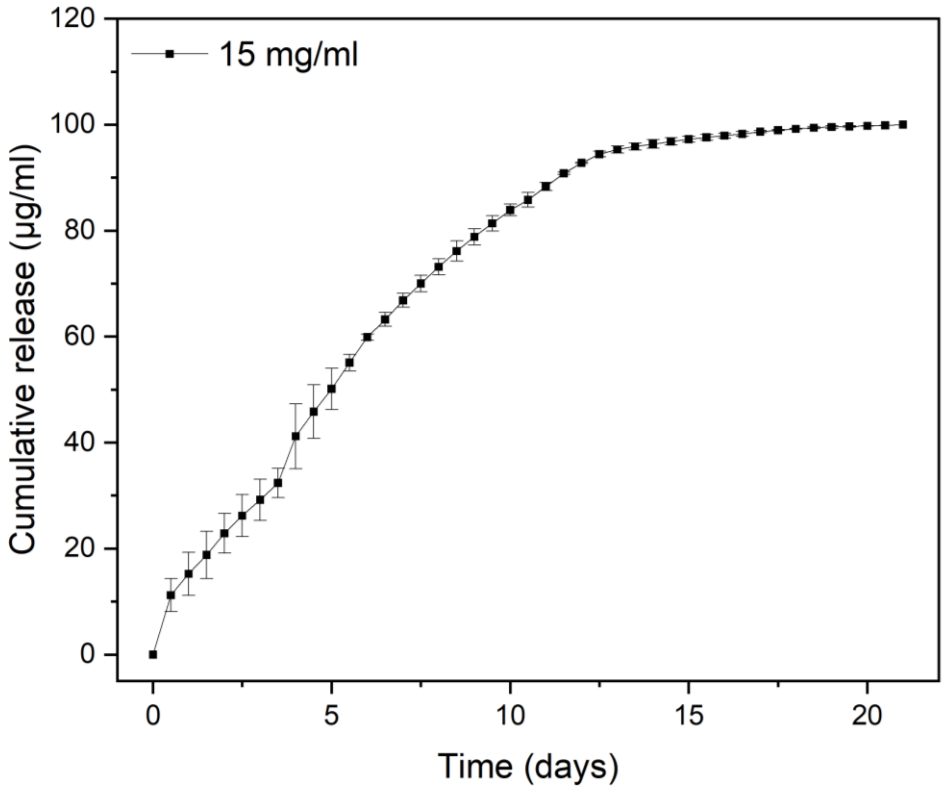

Figure 56. The release kinetics of CHX-$CaCl_2$ particles in artificial saliva (n=3).

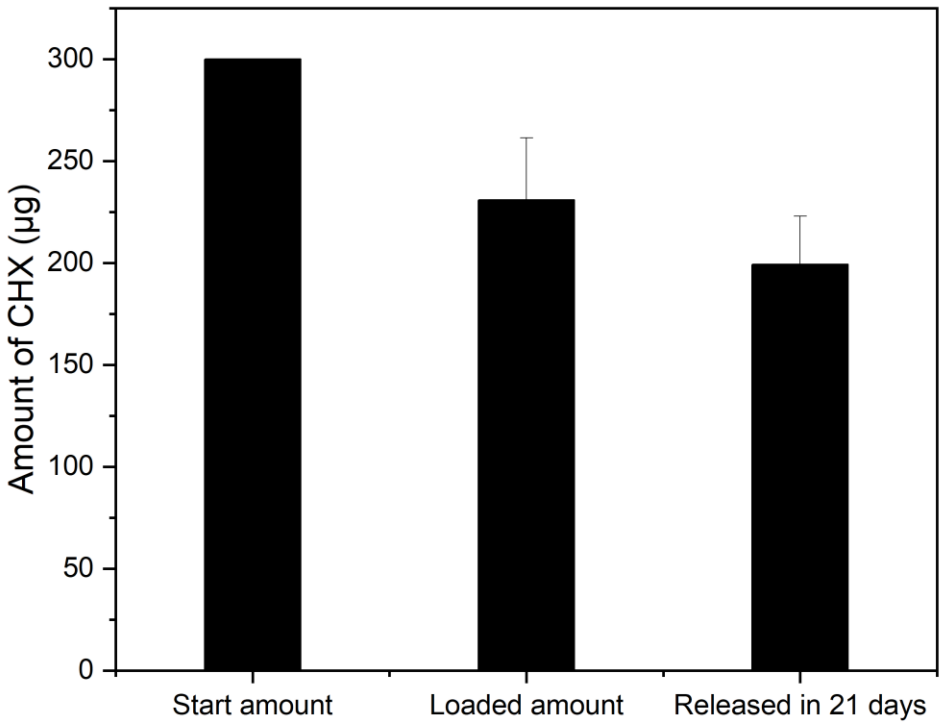

Figure 57. The comparison among the overall amount of CHX applied for the synthesis, coating on the bracket surface and release from the bracket in 21 days. (n=3)

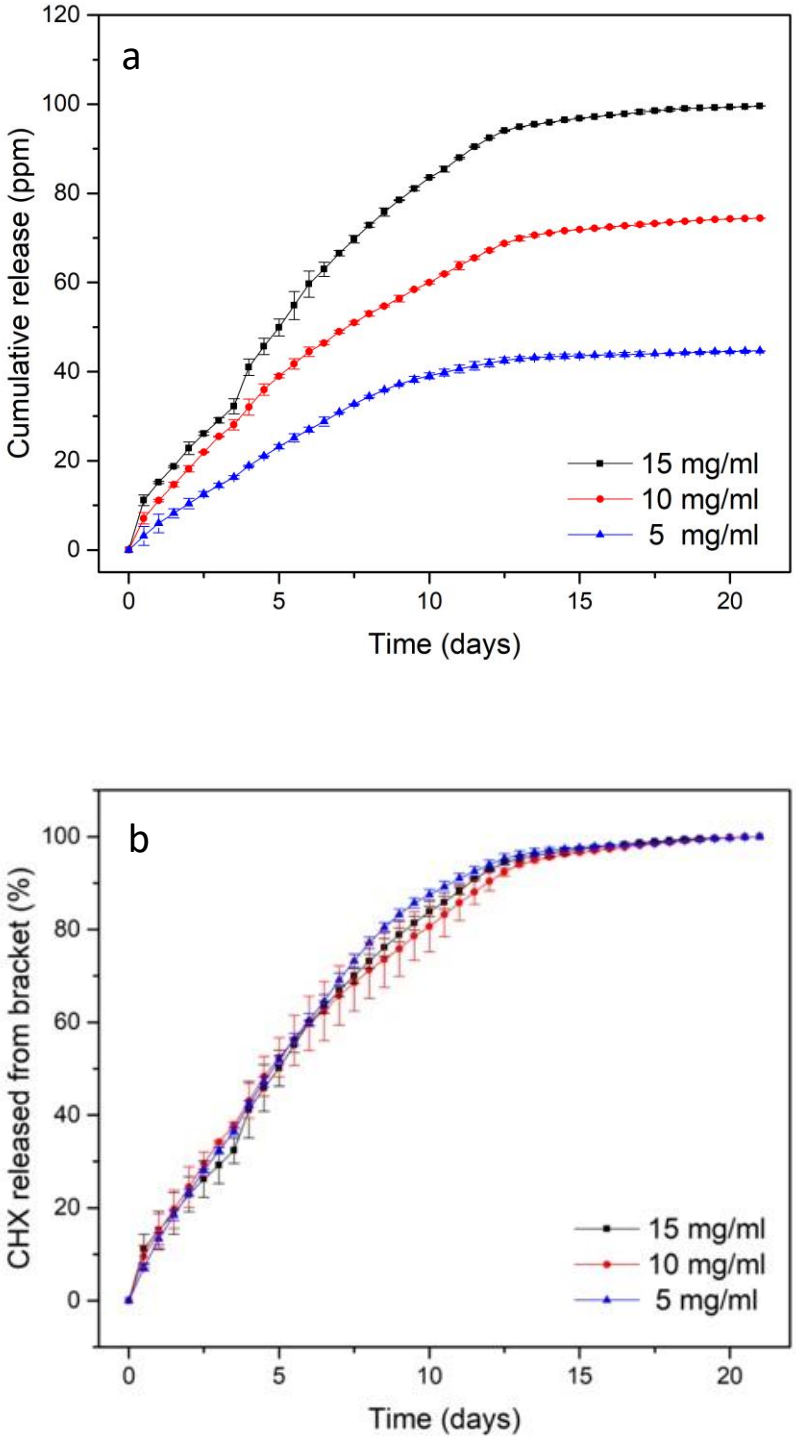

Figure 58. The release kinetics of CHX-$CaCl_2$ particles prepared with; a) different CHX solution concentrations and; b) then applied to orthodontic brackets. (n =3 in each group)

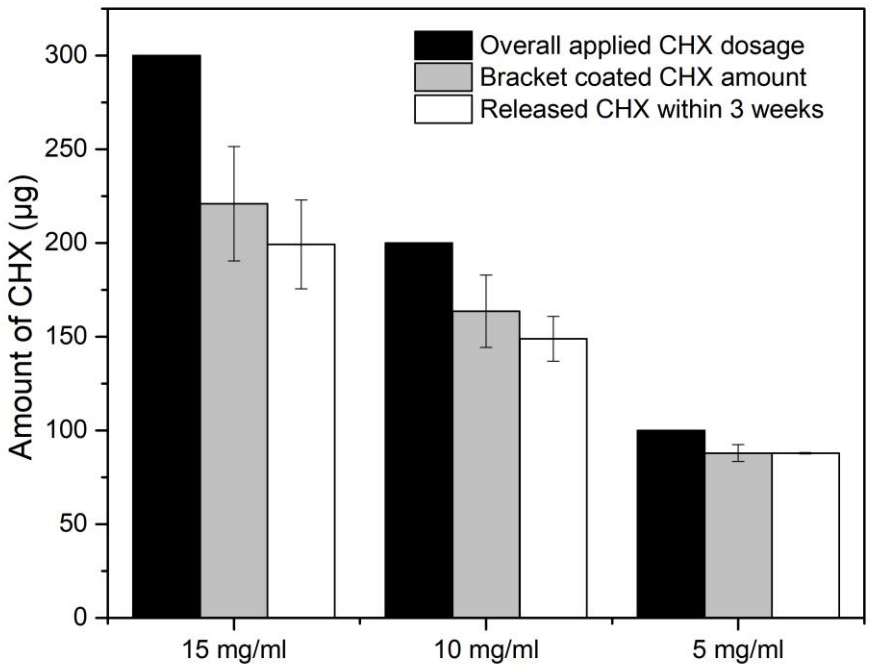

Figure 59. Comparation among the overall amount of CHX applied for the synthesis, coating on the bracket surface and that released from the bracket in 21 days, using different CHX concentrations (n=3).

Chapter 6. Final Discussion

6.1 Synthesis and characterisation of CHX antimicrobial agents

Gingivitis, periodontitis and peri-implantitis are common diseases in oral health clinics. Periodontal disease may be confined to the gingiva (gingivitis) or extend to the deeper supporting structures. Specifically, the periodontal ligament and the alveolar bone that supports the teeth (periodontitis) can be deconstructed. In addition, the associated periodontal pocket would form and ultimately lead to loosening and loss of the affected teeth. CHXD and chlorhexidine di-gluconate are the common components of antibacterial drugs, that have been extensively applied in the field of Medicine and Dentistry [317,318]. Chlorhexidine is widely used for the treatment of gingivitis, periodontitis, and peri-implantitis. There are some works focused on the modification of CHX formulations. For example, it has been reported that when new copper (II) complex compounds were utilized, the biguanidine of chlorhexidine coordinated with Cu^{2+} to produce a new CHX formulation with comparable antibacterial properties [66]. Therefore, sustained CHX release vehicles that can prolong the release time as well as lower the release concentration is needed.

Previously work proposed a novel method for the preparation of spherical CHX-$CaCl_2$ particles, using CHXD to coordinate with $CaCl_2$ [86]. The incorporated calcium ions, however, may hold less significant antibacterial and therapeutic functions. In the previous work, novel CHX-$CaCl_2$ particles can be synthesized by coprecipitation of CHX and $CaCl_2$ solutions. It shows great potential in the sustained release of CHX and in clinic applications. After those antibacterial ions can be used and introduced into

CHX particles by the same process. Therefore, additional or ions substitution is needed.

6.1.1 CHX-Ca/Sr/$ZnCl_2$ Particles

Similar to Calcium, strontium and zinc ions are both divalent metal ions with ionic radii (Sr=1.16 Å, Zn=0.74 Å) close to calcium (0.94 Å) [319,320] facilitating the substitution. Moreover, the substitution of calcium by strontium and zinc has become a feasible route, especially in the application of bioactive glasses [209,321]. Therefore, in the present work, a novel method of producing functionalized spherical CHX particles was demonstrated by substituting zinc and strontium ions into the particle structure to enhance antibacterial effects.

The synthesized CHX-$SrCl_2$ and CHX-$ZnCl_2$ particles had a similar spherical morphology and inter-connected dendritic microstructure to the CHX-$CaCl_2$ particles, which grew dendritically from a nucleation site central to the structure, however it was extremely different to the angular original CHXD platelets (Figure 11). Furthermore, as the reaction time and temperature were key factors affecting the crystallization processes, the structure and size of the particles were additionally evaluated with SEM. Crystallization of the current CHX-$SrCl_2$ and CHX-$ZnCl_2$ particles required a limited reaction time (0.05 secs) and energy input to produce spherical particles. This reactive crystallization may in part be due to the differing pH of the solutions used (pH 7.42 for CHXD-15 mg/mL, pH 5.03 for $SrCl_2$ and pH 5.31 for $ZnCl_2$), producing the formation of a lower solubility solute with higher concentration and allowing crystallization [322]. These pH differences are significant since the pH scale is logarithmic and therefore a 1 pH unit increase leads to tenfold increases in H^+

concentration. Jiang et al. 2005 [323] indicated the particle size of SnO_2 nanoparticles via colloids could similarly be controlled from 6 to 12 nm by varying pH values from 2 to 6. This co-precipitation process requires much higher nucleation and growth times/temperatures and mechanical agitation [324], to control particle size and distribution [322]. The crystallization reaction of the CHXD and $SrCl_2$/$ZnCl_2$ solutions appeared to be extremely rapid (turbidity in 0.05 secs, Figure 14), with a systematic increase in Mean particle diameter with increased reaction time (Figure 12). Both particles showed dendritic and spherical structures and differences in mean particle diameter between all reaction time groups. The Mean diameter of the CHX-$SrCl_2$ and CHX-$ZnCl_2$ particles was correlated (r^2=0.96, r^2=0.99) with reaction time (15s to 60s).

Additionally, temperature plays an essential role in the nucleation and crystal growth process which is also shown in the CHX-$CalCl_2$ study [86]. The novel CHX-$SrCl_2$ and CHX-$ZnCl_2$ particles were produced at different temperatures with the results shown in Figure 14. The novel CHX particle diameters demonstrated an overall increase in size with the increase of the synthesis temperature. Specifically, increased temperature will not only encourage the movement of ions, thereby speeding up the rate of crystal growth, but also decrease nucleation centres, increasing the critical size of the nucleus, resulting in the formation of particles of larger size [325,326]. At lower temperatures, both the molecular movement and the critical nucleus size will be reduced, which may facilitate molecules binding and attaching impurities in their structure, forming a large number of smaller crystals [322]. This may partly explain the results in Figure 15, as at 0°C where the novel CHX-$SrCl_2$ and CHX-$ZnCl_2$ particles exhibited the formation and agglomeration of smaller crystallites, whereas crystal growth increased in response to higher temperatures.

Crystallization of the current CHX-$SrCl_2$ and CHX-$ZnCl_2$ particles required a limited reaction time and energy input to produce spherical particles. The present work provides a simple method to control particle size/surface area, so structure-property particle relations can be tailored for applications, such as electro spinning, coating or incorporation in micro chamber arrays for drug delivery [327,328].

To confirm the presence of metal ions, quantitative elemental analysis of CHX-$CaCl_2$, CHX-$SrCl_2$ and CHX-$ZnCl_2$ particles was performed using EDS (Figure 17 - Figure 19). The results confirm the structural presence and homogeneous distribution of the metal cations and chloride. It can be assumed that the coordination of chlorhexidine to the divalent metal (Ca, Zn and Sr) ions happened during particle formation. Consequently, both the negatively charged chloride ions and the counterpart divalent metal ions are responsible for the formation of novel chlorhexidine particles. Specifically, the additional chloride ions may reduce the solubility of the chlorhexidine as well as influence the rate of structural formation, whilst the metal ions may contribute to the production of the compactness of spherical microstructure as previously proposed [86]. Additionally, it is noteworthy to mention that the CHX-$SrCl_2$ and CHX-$ZnCl_2$ particles were washed with DI water to remove unreacted elements and any physically absorbed divalent metal ions as much as possible. The zinc and strontium ions were therefore confirmed evenly incorporated into the particle structures. Moreover, EDS results in Table 5 - Table 7 also revealed a higher ratio (25.4 -28.3 at%) of Cl^- ions compared to cations distributed within the particles, where the weight percentage of divalent ions incorporated in the CHX particles was 3.95wt% and 7.66wt% for strontium and zinc, respectively.

The chemical structural information of synthesized novel CHX particles was further characterized using FTIR and XRD. In the FTIR spectrum of chlorhexidine diacetate (CHXD), three absorption peaks appeared at high wave numbers, at 3325 cm^{-1}, 3120 cm^{-1}, 3180 cm^{-1} which may have contributed to the stretching vibrations N-H of the groups $(Alkyl)_2$ NH, Alkyl-NH-Aryl and to the group =NH, respectively [329]. Besides, a typical band at 1612 cm^{-1} can be assigned to the stretching vibration of the imine group C=N [330,331]. While in the IR spectrum of the chlorhexidine particles, the band of the imine group displays a positive shift from 1612cm^{-1} to 1623 cm^{-1}(Figure 21). In addition, after forming the novel CHX-$SrCl_2$ and CHX-$ZnCl_2$ particles, the stretching vibrations N-H of the groups $(Alkyl)_2$ NH and the group =NH showed a significant shift as well.

According to the XRD results, CHX-$SrCl_2$ and CHX-$ZnCl_2$ particles indicated they had missing peaks, which were compared with the CHXD XRD plot (Figure 21). There were also slight deviations in the 2 theta positions, changes in intensity for similar peaks for the CHXD and the novel particles, and signs of peak broadening (Figure 21). Crystal lattice strain and crystal size can affect XRD peak broadening, the intensity of the peaks and shifts in 2 theta positions [332]. XRD peak broadening has been previously associated with smaller crystallite size and changes to the lattice parameters, due to zinc incorporation into hydroxyapatite structure [333]. The CHX-$SrCl_2$ and CHX-$ZnCl_2$ particles also displayed new peak positions (not in the CHXD plot). The CHX-$SrCl_2$ and CHX-$ZnCl_2$ particles displayed almost the same 2 theta positions, indicating the formation of a similar particle structure after the incorporation of divalent metal ions (Sr, Zn). It is clear the new particle complexes displayed structural differences with CHXD which were confirmed by differences both in polymorph structure and crystallite size (Figure 15).

6.1.2 CHX-NaF-NaCl and CHX-NaF Particles

In addition to the cation substitution of Sr and Zn in novel CHX particles, the anion can also be replaced by beneficial functional ions. Chlorhexidine mouth wash and NaF mouth wash are currently used for patients having orthodontic and periodontal treatments [334]. Daily use of fluoridated mouth rinses (0.05% NaF) shows significantly reduced lesion formation and is the best method to prevent enamel demineralization [335] and WSLs [336]. High concentrations of fluoride (10-100μg/ml) in local applications can contribute to enamel remineralization especially for those patients with a higher risk of caries [337]. Thus, the introduction of fluoride into novel CHX particles may potentially improve remineralization and enhance the antibacterial effect without affecting their original particle properties.

When CHXD was mixed with either NaBr or K, some fibrous structures or individual clusters were observed. Thus, it is assumed that the halogen elements may have the potential to help produce novel chlorhexidine particles [86]. However, what is different from the previous study is that NaBr, Kl and $CaCl_2$ can react with CHXD in one minute to produce precipitation [86], when CHX was reacted with NaF, it took more than 40 minutes to start to form novel CHX-NaF particles in the current study (Figure 26 a, b).

This slow novel CHX-NaF particle formation process was evaluated with SEM. When the reaction time was less then 20 minutes, the reaction was minor and unreacted NaF formed cubic crystal precipitation when drying the reaction solutions (Figure 25). After 40 minutes reaction time there was agglomeration, signs of NaF crystallites and the first signs of precipitation of spherical CHX-NaF particles (Figure 26 a, b). After 60-80 minutes reaction there was a higher volume fraction of spherical CHX-NaF particles and some NaF remnants (Figure 26 c-f). When the reaction time was increased to

100-120 minutes the reaction appeared completed, and CHX-NaF spheres were produced and signs of partially formed crystallites appearing as wheat sheaves (Figure 27). It is assumed that compared with Cl, Br, and I, fluoride will generate hydrogen bonds in the solution, so that more energy is required for precipitation [338]. As the result, CHXD reacted with NaF at a lower reaction rate than other halogen elements.

For the purpose of accelerating the synthesis process, a mixture of NaF and NaCl solution was therefore used to encourage a more rapid particle synthesis, since the presence of Cl^- in solution was expected to accelerate precipitation [86]. A previous study demonstrated that CHX solubility was highly dependent on salt type and solution concentration [339]. Thus, the crystallization rate and mechanism of the CHX may be expected to be dependent on Cl^- [86].

To investigate the influence of different NaF concentration on the particle formation, the novel CHX-NaCl-NaF particles were synthesized by mixing CHXD solution with increased concentrations of NaF (0,125M, 0.33M, 0,5M and 0,66M) while maintaining NaCl content constant at 0.66M. Here, a 0.66M NaCl was adopted to allow adequate chloride available for the reaction while keeping a constant chloride concentration as previously used (0.33M $CaCl_2$ solutions).

Figure 28 and Figure 29 showed different morphologies and particle sizes of CHX-NaCl-NaF crystals. With the increase of NaF concentration, the novel CHX particles showed an increased crystallite size and a more open morphology. It has been pointed out that that the introduction of other ions such as F^-, Cu^{2+}, Zn^{2+} or Ag^+ to CHX salts, changes the metal / ligand molar ratio and the anion of the metal salt due to the transitional metals [267]. These ion transitions lead to the development of new CHX structures with alternating crystal sizes and morphologies. Both the size and

morphology of the particles can affect the crystallisation process as it proposes the number of atoms that are required in the crystalline cluster and hence, they enhance the crystallisation rate [340].

The EDS elemental analysis also confirmed the presence of F^- in the structure (Figure 30). As DI water was used to remove the unreacted solution, it was assumed that the F^- was bound in the particle structure instead of physically absorbed on the surface. Figure 33 showed that the 0.66M NaF group demonstrated the highest release of F^-. Studies conducted by Marinho (2016) [240] showed that local applications of high concentrations of F^- (10-100 µg/ml) can contribute to the enamel remineralisation and hence its recommended for patients with a high risk of caries. Thus, these particles provide advantageous release of F^- (136.9 µg/ml available fluoride, Figure 33), which may enhance the process of enamel remineralisation [341] and the F^- concentration can be adjusted by the NaF concentration during the particle preparation.

The structure of the CHX-NaF-NaCl particles and the CHX-NaF particles were further analysed with XRD (Figure 31). The unique peaks of synthesized CHX fluoride containing particles were different to the pattern of either CHXD, NaF or NaCl, which indicates that the fluoride-containing CHX particles have a different crystalline structure compared with the original reagents.

Using fluoride alone does not totally prevent caries lesions [342]. However, when using CHX and fluoride rinses together, it has been shown to reduce both lesion depth and mineral loss [343]. A combination antibacterial effect of CHX and fluoride-containing mouthwash on dental caries have also been reported [344]. Thus, the combination of chlorhexidine and fluoride has a positive effect on the prevention of white spot lesions in orthodontic patients and in maintaining better oral hygiene [345]. Since the CHX-NaF-

NaCl particles afford this unique combination in a single vehicle this will provide some unique clinical advantages.

6.2 In Vitro Studies on Novel CHX Particles

There are several bacteria associated with periodontitis. Porphyromonas gingivalis is highly associated with chronic periodontitis and can be detected in up to 85% of the disease-affected sites [135]. Aggregatibacter actinomycetemcomitans is also detected in aggressive periodontitis and often starts at an early age[17]. Therefore, in order to investigate the antibacterial effects of the novel CHX particles, an antibacterial study was carried out. Additionally, when the CHX concentration in the infection area is too high, both tissue cells and bacteria can be eliminated. Thus, in order to measure the living cell activity, cytotoxicity testing was conducted. Moreover, synthesis of these particles in conjunction with moist pig's tissue was conducted in order to illustrate the particles' binding ability to moist tissue.

6.2.1 Antibacterial Study of Novel CHX-Sr/$ZnCl_2$ Particles

For an antimicrobial agent to be efficacious in the treatment of a disease, it must be effective against the involved pathogens. In this study, we used *P. gingivalis (strain-381)*, *A. actinomycetemcomitans (strain-Y4)* and *F. nucleatum subsp. polymorphum (strain- ATCC10953)* are grouped as the red complex because of their shared strong association in the aetiology of periodontitis (i.e., high numbers of these usually means periodontal disease is active). The confirmation of MIC/MBC of CHX-$SrCl_2$ and CHX-$ZnCl_2$ particles against the bacteria tested provided an effective concentration range when conducting release experiments (Figure 36 - Figure 37 and Table 9 -Table 12).

To inhibit bacterial growth, a sufficient dosage for an effective duration is required locally at the infection site to prevent secondary infections [346]. When the CHX concentration in the infection area is however too high, both tissue cells and bacteria can be eliminated [170]. CHX digluconate mouth rinses (0.12-0.2%) indicate a substantivity < 12 hours, requiring multiple daily applications to be effective [347]. The novel particles offered an effective CHX release up to 8 days for CHX-$SrCl_2$ and 12 days for CHX-$ZnCl_2$ particles (Figure 22), which may be particularly beneficial in the prevention of recurrent infections and maintenance of oral hygiene. Sustained release delivery systems also allow a better antibacterial efficacy against bacteria [170,348]. The calculated chlorhexidine content in the CHX-$SrCl_2$ and CHX-$ZnCl_2$ particles was around 98.6wt% and 99.1wt%, respectively, which was higher than many reported carriers [349]. The CHX-$SrCl_2$ or CHX-$ZnCl_2$ particles were able to release additional antibacterial ions which gave the potential function for bone regeneration. However, the mineralization study of CHX-$SrCl_2$ or CHX-$ZnCl_2$ particles did not show a positive result in bone regeneration, as there was no significant difference between the cell-only group and the test samples group (Figure 43). It is inferred that this result was caused by the low concentration of Sr or Zn ions in the releasing solution, which may be improved by increasing the ion loading amount. CHX-$SrCl_2$ particles contained strontium which can potentially be an antibacterial agent, whose antibacterial effects can be further enhanced by the presence of fluoride [198].

During the caries and tissue inflammation process, there is a pH reduction due to the activity of *mutans streptococci* and *lactobacilli* [350], which triggers the local acidification processes, encouraging acid-tolerant pathogenic bacteria to colonize [351]. However, an acid environment can favour the dissolution of chlorhexidine [352], as CHX consists of two ionizable guanidine moieties [353] that demonstrate alkalinity [354]. The enhanced

release rate of CHX will also affect the zinc release behaviour thus, the Zn from the CHX-$ZnCl_2$ particles will give rise to accelerated dissolution under acidic conditions compared with neutral conditions (Figure 23). The smart and rapid release of CHX and Zn demonstrated in the current technology may efficiently eliminate caries related bacteria when the oral environment becomes acidic, avoiding the further development of caries or inflammation. The drug release of the novel CHX-$ZnCl_2$ particles can therefore vary with the surrounding pH conditions, enabling a responsive and controlled release of CHX and Zn, as demonstrated in Figure 24. This is especially useful in the treatment of patients who are susceptible to caries or bacterial infections, so early-stage disease effects are arrested or reversed. In particular, a reduction in oral bacterial load in Covid -19 patients may prevent pneumonia and acute respiratory distress syndrome, which can exacerbate patient morbidity [355]. It is noteworthy to mention that CHX-$SrCl_2$ and CHX-$ZnCl_2$ particles may have multiple applications including antibacterial mouth rinses, gels, cement, or coatings to take advantage of the sustained/ smart release, or possible additional functions such as promoting bone proliferation [356].

6.2.2 Cytotoxicity Study of Novel CHX-Sr/$ZnCl_2$ Particles

Tissue exposed to high CHX concentrations (> 0.5-2%) [95] for long periods may have adverse effects on the oral tissues [357,358]. The potential cytotoxic effects and safe concentration levels of the novel particles were, therefore, evaluated. Application of the CHXD, CHX-$CaCl_2$, CHX-$SrCl_2$ and CHX-$ZnCl_2$ particles reduced the viability of the L929 cells in a dose-dependent manner, but to different degrees. Relative cellular viability was reduced to approximately 40% when 0.001% of CHX-$SrCl_2$, and CHX-

$ZnCl_2$ particles were used for 24 h, which was further decreased to around 2% after 48 h treatment (Figure 38).

Similar results were reported for human gingival fibroblast cells indicating decreased cell proliferation and division when exposed to 0.01%- 0.02% CHX for 15 minutes [359]. When evaluating the cell structure of the fibroblast cells exposed to the current CHXD solutions (>0.01%), the shape of the cell became more rounded and less prolific (Figure 39). The characteristics of fibroblast spindle-shaped morphology was previously shown to lack filopodia and presented a more oval or rounded shape at 0.002-0.04% CHX concentration, indicating a significant influence of CHX concentration on cellular viability and morphology [359–361]. Similar results were also found in the mineralisation study (Figure 42).

Lower concentrations of CHX-$SrCl_2$ and CHX-$ZnCl_2$ particles ranging from 0.0000625% to 0.00025% showed around 90% and 60% cellular viability at 24 h and 48 h, respectively. However, when the concentration increased to 0.005%, the cellular viability dropped to around 40% at 48 h. Similar viability was observed in CHXD treated cultures (Figure 38). Interestingly, a CHX concentration of 0.00025% caused no reported apoptosis and necrosis in L929 fibroblasts [362], and no necrosis at 0.125% CHX [360]. Current commercial products contain 0.12%-0.3% [140,263] CHX for mouthwashes and up to 4% for burns [363,364] which could significantly reduce cell viability. Furthermore, 0.05% CHX was reported as non-toxic to wound healing and granulation tissue [262], with no suggested bioaccumulation after repeated exposure at higher CHX levels [365]. Therefore, the current CHX-$SrCl_2$, CHX-$ZnCl_2$ particles have the potential as safe and effective antimicrobials.

In the current cell studies, all the treated groups were normalized to the control groups at 24 and 48 hours respectively as is standard practice (Figure 38). It should however be taken into account that the stated 100% cell viability may not be possible during cell expansion in 2D monolayer culture for up to 2 weeks.

6.2.3 Tissue Adhesive Study of Novel CHX-$CaCl_2$ Particles

In practice, it is unavoidable that the synthesis solutions would contact the gingiva during the coating process. Given the CHX would have an adverse influence on the cells, it is necessary to investigate the attachment properties of CHX particles on gingiva.

In this study, a gingival tissue cut from a pig was employed to mimic the human gingiva. All the gingiva samples were rinsed with 1 ml human saliva before and after the coating process to mimic the clinical conditions. When the gingiva was rinsed with saliva according to clinical dental treatment practice, no CHX particles were observed on the gingiva, indicating the CHX particles were not attached (Figure 40). Therefore, synthesis of these particles in conjunction with moist pig's tissue illustrates these particles did not bind to moist tissue, making local CHX absorption less likely. The novel CHX particle coating technique can also avoid the undesired harmful effect on the oral environment when compared with current CHX mouthwashes [134].

6.3 Clinical Applications of Novel CHX Particles

It is well known that periodontitis is a chronic inflammatory process brought about by the accumulation of plaque [146]. Therefore, a local antimicrobial agent must be effective against the complex biofilm found in the plaque [226].

For a CHX gel product to succeed in the treatment of periodontal disease it must display sustained-release properties [366,367]. Effective concentrations of CHX released in a controlled manner allow successful control of microbial levels during key phases of healing [368,369], following conventional mechanical periodontal therapy.

The current study evaluated novel CHX-$CaCl_2$, CHX-$SrCl_2$ and CHX-$ZnCl_2$ particles dispersed in a series of gels and versus commercial comparisons. The hydrophilic nature of these unique particles, their different dissolution mechanisms [303] and unique morphology (Figure 11) and sustained release properties [86], were thought useful in this application.

6.3.1 Novel CHX particle Containing Gels

DI water is firstly adopted as the media for the CHX release experiment. The natural release mechanism for chlorhexidine digluconate gels in DI water (Table 13 Groups J, L) was that of a burst release mechanism, whereas the experimental novel CHX particle containing HPMC gels (A, D, G) was released in a more sustained manner (Figure 46). There was no CHX detected from HPMC gel only (N). The solubility of CHX diacetate and digluconate differs significantly [339,370], with CHX digluconate having a higher solubility than the diacetate form (>70 vs 0.8% w/v). It has been proposed that this solubility is related to the ability of CHX digluconate to undergo self-association [371], influencing the resultant CHX concentration in solution. This explains the rapid and burst drug release episodes demonstrated by the digluconate gels in DI water (Figure 46). The commercial comparison gel (Group L, Corsodyl®) contains additional ingredients (Table 13) [372] and the DW results suggest these additives enabled a heightened CHX release while maintaining a similar release pattern to the

Group J gel (CHX digluconate only). One of these additional ingredients is isopropyl alcohol (IPA), which is miscible in water and can dissolve ethyl cellulose [373], thus, potentially playing a role in gel release kinetics.

The release kinetic of all the gel samples were then compared in the PBS environment. Generally, the commercial comparison gel showed a burst release pattern in DI water (Group L, cumulative CHX release = 3067.05 µg/ml/ 1 week), but a lower-level sustained release in PBS (Group M, cumulative CHX release = 252.5 µg/ml / 1 week, Figure 47). Similar behaviours were also observed in the other groups of gels (Groups J, K, Table 13) which demonstrated that the PBS composition affected the diffusion of CHX across the dialysis tube. The salt content and pH of PBS (pH=7.4) however more closely imitates the natural physiological environment and ions encountered in the mouth. The comparison HPMC gel Group K (CHX digluconate) nevertheless released CHX in multiple waves in PBS, with three distinct plateau periods (Figure 47). Here again, no CHX was detected from HPMC gel itself (Group O). The difference in dissolution with the HPMC gel group M could be again attributed to the presence of IPA, which is not miscible in salt solutions [374]. The presence of salt in a solution leads to the separation of IPA into a distinct layer, a process known as salting out [339]. The released drug from the HPMC gel delivery system involves the absorption of water into the gel. The HPMC gels are hydrophilic matrices that swell in water, and release the drug through spaces in the gel network by dissolution and disintegration [374]. The gel's viscosity also enhances its firmness in the periodontal pocket. Although the release patterns for the comparison gels (Groups M and K) in PBS were different, the cumulative CHX amounts released were similar over 24 weeks (352.6 µg/ml and 378.42 µg/ml). In contrast, the experimental HPMC gels in PBS (Groups B, E, H) not only displayed a sustained release but released higher amounts of CHX during all

release periods compared to the comparison gels (Groups M and K) after 1 week. This may be due to the hydrophilic nature of the novel CHX particles [86]; the ability to be wet by the gel, and their release behaviour associated with the unique interconnected structure of the novel particles, whose dissolution process initiates from the particle interior [88].

The different release kinetics of CHX diacetate and CHX digluconate are also believed caused by the solubility differences. Basically, the solubility properties of CHX salts were investigated by the addition of sodium chloride and sodium gluconate to form various CHX formulations [339]. The results confirmed that the solubility of the CHX salts increased when mixing with sodium gluconate, while the addition of sodium chloride resulted in the precipitation of a reduced solubility product (CHX-Cl_2). This precipitation thus reduced the CHX concentration in the low solubility CHX solution. As CHXD was reacted with $SrCl_2$, $ZnCl_2$ and $CaCl_2$ to form novel particle formulations, it will have reduced dissolution compared to other CHX salts, contributing to sustained release behaviour. The presence of salts within the PBS and AS mediums used in our assays may also affect the dissolution characteristics, through binding of salt ions with the available CHX [375]. High concentrations of chloride ions were available in the PBS (KCl;2.02%, NaCl; 80.93%) and AS (KCl;31.96%, NaCl;10.85%) used in this study. Therefore, by submerging the novel CHX-$CaCl_2$, CHX-$SrCl_2$ and CHX-$ZnCl_2$ HPMC gels into PBS or AS, there may exist a common ion effect [376]. Therefore, submerging the CHX gel in PBS medium, the ions such as $Na^{+,}$ Cl^-, K^+, HPO_4^{2-}, $H_2PO_4^{2-}$ in PBS may bind with the available CHX. This may reduce the CHX concentrations in the solution. Interestingly a similar CHX release behaviour to PBS was also found when the experimental HPMC gels (Groups C, F, and I) were evaluated in artificial saliva (Figure 48).

The antibacterial effect was tested by the inhibitory capabilities of the dialysates from the release assays against *P. gingivalis*. The experimental CHX gels were able to maintain a sustained release of inhibitory concentrations of CHX against *P. gingivalis* during the critical stages of wound healing, which the comparison gel (Group M, Corsodyl® gel) did not (Figure 50). However, the experimental limitations in this technique should be noted as the CHXD standards failed to demonstrate a zone of inhibition at concentrations below 10 µg/ml. Additionally, the novel CHX particles have nevertheless demonstrated antibacterial efficacy against a range of periodontal pathogens at low CHX concentration including *A. actinomycetemcomitan* and *F. nucleatum* [303]. As for clinical applications, it may not be necessary to continue releasing CHX for 20 - 22 weeks from the experimental HPMC gels (Groups B, E and H). This is because periodontal treatment requires regular re-evaluation intervals employed to assess the response to root surface debridement (6 and 12 weeks), which will remove the gel to repeat non-surgical therapy [146]. However, this technology can be adapted as needed to fit into clinical practice. The experimental CHX HPMC gels however, indicated the ability for sustained release at effective concentrations during the whole healing period to the re-evaluation appointment. Thus, this confirmed the experimental CHX gels with sustained and effective CHX release may have the potential to be used in the treatment of periodontitis, preventing proliferation of bacteria during the initial stages of healing.

6.3.2 Novel CHX Particle Coated Medical Devices

Here, a novel synthesis method to coat and release CHX onto implant, denture, tooth and orthodontic bracket surfaces is for the first time introduced. The controlled coating method may allow the clinician to apply the drug precisely onto the selected surface,

avoiding excess CHX into the oral cavity. Therefore, this will not interrupt the nitrogen cycle of the oral microbiome [132]. The CHX-$CaCl_2$ particle is selected as a representative to show the coating properties of novel CHX particles.

The surface coating of CHX-$CaCl_2$ particles was initially tested on a glass slide. Compared with CHX-$CaCl_2$ particles synthesized in the bulk solution, which have a dendritic and spherical interconnected structure (20 - 50 μm diameter) (Figure 51 a, b), the CHX-$CaCl_2$ particles directly coated on the glass slide surfaces had a hemispherical dendritic structure, with a smaller size (5 - 10 μm, Figure 51 d, e). These structure and size differences are believed related to the nucleation processes.

Nucleation, in general, is a process that initiates a phase transition from a metastable phase to a more stable phase. Seeds or templates for the more stable phase can induce nucleation; otherwise, nucleation is an activated process that is associated with a stochastic induction time. The formation mechanism of CHX-$CaCl_2$ particles has been discussed in previous work, where the chloride anions reduced the solubility of CHX, while the calcium served as counterpart cations responsible for the assembly of a more compact spherical structure.[86] Generally, ignoring the container walls, the precipitation of CHX-$CaCl_2$ particles in bulk solutions could be considered as homogeneous nucleation, where the nuclei can occur with equal probability in any part of the solution and resulted in a spherical morphology [377].

While for the precipitation and crystallization on the selected material surfaces, such as implant, denture base, teeth and brackets, the nucleation may be characterized as heterogeneous, because the differing surfaces produced differing crystal distributions, (Figure 52 - Figure 54), which indicates the crystallization is reactive to the different material surface flaws and sites available for nucleation. CHX-$CaCl_2$ particle growth

was reactive to both the machined implant head and the course acid etched /sandblasted surface of the implant thread (Figure 52 a, b, c), producing finer CHX-$CaCl_2$ particles. The polymer denture base however had a bimodal particle distribution and signs of increased particle growth (Figure 52 d, e) in comparison, which may be associated with its processing, smoother surface profile allowing dendritic growth and particle ripening. This was also in evidence on the smoother tooth coated surface (Figure 53 b, c). Therefore these sites may have taken part in catalyzing nucleation and the presence of an existing interface reduced the free-energy barrier for nucleation [378]. It is clear that different biomaterial surface morphology and chemistry may affect the CHX-$CaCl_2$ crystallization (Figure 52 b-e, Figure 53 b and Figure 54 a-d).

Based on the classical spherical-cap model for heterogeneous nucleation [379], the CHX-$CaCl_2$ particles grow on the flaws on the surface and in the shape of a hemisphere and allowing a wetting angle on the surface. Additionally, the spherical cap nucleation process on a substrate is a stochastic process with similar overall kinetic behavior to homogeneous nucleation [380]. Moreover, much less driving force is needed for nucleation in heterogeneous conditions compared with homogeneous nucleation.

One of the most important parameters for nucleation control is the distribution of the heterogeneities. Additionally, the surface coated CHX-$CaCl_2$ particles had a large number of “roots” that grew on and attached to the interface (Figure 51 f, Figure 52 b, e and Figure 53 b), enabling a strong binding between the CHX-$CaCl_2$ particles and the material surface, which was distinct from the CHX particles that were synthesized from the bulk solutions (Figure 51 c, Figure 52 c, f and Figure 53 c). The above surface

attaching properties offered a great opportunity to form and coat CHX-$CaCl_2$ particles on different material surfaces at the desired location.

One of the promising applications of CHX-$CaCl_2$ particle coating would be the prevention of white spot lesions during the orthodontic treatment, where the antibacterial agent CHX can be site-specifically released in a sustained manner (Figure 54) around the brackets. The surface of the metal bracket, wire and the rubber band were quickly and efficiently coated with a high-volume fraction of CHX-$CaCl_2$ particles (Figure 54 a-d). The differing surface and tension in the rubber band induced crystals which were a third of the size of that on the wire and bracket indicating a surface crystallization effect. The calculated CHX drug loading efficiency of the coated bracket was 76.97% (Figure 57), but with the residual unbound crystallites available in the solution for antibacterial activity. The release from the brackets was 85.25% (Figure 57) at 21 days, so it appears there were still remnants which could potentially release CHX (Figure 54). 0.024M was chosen as the CHX concentration for the CHX-$CaCl_2$ rinse, as release experimentation on brackets using different CHX concentrations (Figure 58), indicated increasing duration of CHX release was associated with the increasing concentration. The highest concentration group (0.024M) had the longest MIC duration (11 days, Figure 58). This provides a longer sustained and effective CHX release than current mouth rinses (less than one day) [105].

The proposed CHX-$CaCl_2$ coating technique using a syringe allowed a precise application of CHX to the area of tooth (Figure 53) or prosthesis avoiding an excess of the CHX and preventing potential mucosal irritations or allergic effects [351]. In addition, the prolonged release of CHX around the bracket can help the patient to maintain oral hygiene, especially in the areas around the bracket that were difficult to

clean, preventing the development of WSL and caries. The ability to rapidly apply the CHX-$CaCl_2$ coating to implant, and denture and tooth surfaces could also give the potential to treat periodontal disease, peri-implantitis [20] and denture stomatitis [289].

Chapter 7. Conclusions and Future Work

7.1 Conclusions

Antibacterial ions Sr and Zn containing novel CHX particles were successfully synthesized in a cost-effective and efficient route, whose size could be manipulated by adjusting synthesis time and temperature. CHX-$SrCl_2$ and CHX-$ZnCl_2$ particles showed sustained release behaviours for 8 and 12 days, respectively. The CHX-$ZnCl_2$ particles also performed a smart pH-responsive drug/ ion release. The antibacterial and cytotoxicity studies confirm that both novel CHX-$SrCl_2$ and CHX-$ZnCl_2$ particles were effective against a range of oral pathogens with reduced cytotoxicity and extended duration. These particles show great potential for a new responsive treatment modality for the prevention or reversal of caries and infections in Medicine and Dentistry.

In addition, fluoride containing CHX-NaF particles were prepared, but showing slower particle synthesis. The co-precipitation process of CHX and NaF salts was accelerated by the addition of NaCl to form CHX-NaF-NaCl particles with high (136.9μg/ml) fluoride content. These particles show great potential as an enamel remineralisation agent and bringing additional antibacterial effects for the prevention of infections.

The novel CHX-$SrCl_2$ and CHX-$ZnCl_2$ particles were incorporated into commercial HPMC gel giving a sustained drug release. When compared to a commercial product (Corsodyl®) the novel CHX particle-containing gels had a longer and safer CHX release. Preliminary experiments suggest they may be useful in a sustained release local antimicrobial device in the treatment of periodontitis alongside traditional non-surgical treatment, for the maintenance of oral hygiene and prevention of infections.

The CHX-$CaCl_2$ particles could be directly coated onto implant, denture base, tooth, and orthodontic bracket surfaces in a simple and quick fashion. The CHX-$CaCl_2$ coating allowed the prolonged release of CHX near to orthodontic brackets, potentially avoiding excess CHX in the mouth. Thus, preventing mucosal irritations or allergic effects and interruption in the nitrogen cycle of the oral microbiome. In addition, the prolonged release of CHX around a medical device could help patients to maintain oral hygiene, especially in areas that are difficult to clean, preventing the development of caries and other dental diseases.

7.2 Future Work

In this thesis, the CHX-$ZnCl_2$ and CHX-$SrCl_2$ particles showed good biocompatibility and in vitro antibacterial activity. However, these particles did not show significant bone proliferation in the antibacterial range due to Sr or Zn concentrations. An increase in the loaded ion content is necessary, which could be achieved by the reformulation of the novel particle.

The fluoride-containing CHX particles was successfully synthesized and characterized in this study, however further experiments are required to assess their biocompatibility and antibacterial activity.

Additionally, the crystal structure of novel chlorhexidine particles has been studied in this thesis. The chemical interactions between chlorhexidine molecules and ions were demonstrated by FTIR and XRD. However, the mechanism of how this interconnected structure formed may not be fully explored. To explain how the bonding between chlorhexidine and ions XPS or other techniques could help to analyse this special crystal structure.

Although the cell studies for safety evaluation and the antibacterial assay were carried out in this study, only single cell or single species bacteria were used. Further studies are required to analyse the antibacterial efficacy of CHX novel particles or novel CHX particle gels against mixed planktonic bacteria or biofilms. *In vivo* animal studies could then be the next step.

Chapter 8. References

1. Socransky, S. S., Haffajee, A. D., Cugini, M. A., Smith, C. & Kent, R. L. Microbial complexes in subgingival plaque. *J. Clin. Periodontol.* **25**, 134–144 (1998).

2. Preshaw, P. M. *et al.* Periodontitis and diabetes: A two-way relationship. *Diabetologia* **55**, 21–31 (2012).

3. Mager, D. L., Ximenez-Fyvie, L. A., Haffajee, A. D. & Socransky, S. S. Distribution of selected bacterial species on intraoral surfaces. *J. Clin. Periodontol.* **30**, 644–654 (2003).

4. Ismail, A. D. Oral bacterial interactions in periodontal health and disease. *J. Dent. Oral Hyg.* **6**, 51–57 (2014).

5. Leys, E. J., Lyons, S. R., Moeschberger, M. L., Rumpf, R. W. & Griffen, A. L. Association of Bacteroides forsythus and a novel Bacteroides phylotype with periodontitis. *J. Clin. Microbiol.* **40**, 821–825 (2002).

6. Rüdiger, S. G., Carlén, A., Meurman, J. H., Kari, K. & Olsson, J. Dental biofilms at healthy and inflamed gingival margins. *J. Clin. Periodontol.* **29**, 524–530 (2002).

7. Genco, R. J. & Slots, J. Host Responses Host Responses in Periodontal Diseases. *J. Dent. Res.* **63**, 441–451 (1984).

8. Bostanci, N. & Belibasakis, G. N. Porphyromonas gingivalis: An invasive and evasive opportunistic oral pathogen. *FEMS Microbiol. Lett.* **333**, 1–9 (2012).

9. Pihlstrom, B. L., Michalowicz, B. S. & Johnson, N. W. Periodontal diseases. *Lancet* **366**, 1809–1820 (2005).

10. Inaba, H. & Amano, A. Roles of oral bacteria in cardiovascular diseases - From molecular mechanisms to clinical cases: Implication of periodontal diseases in development of systemic diseases. *J. Pharmacol. Sci.* **113**, 103–109 (2010).

11. Madigan, M. T., Martinko, J. M., Dunlap, P. V & Clark, D. P. Brock biology of microorganisms. *Int. Microbiol* **11**, 65–73 (2008).

12. Biology, B. & Microbes, O. Basic Biology of Oral Microbes. *Atlas Oral Microbiol.* 1–14 (2015) doi:10.1016/b978-0-12-802234-4.00001-x.

13. Beveridge, T. J. Use of the Gram stain in microbiology. *Biotech. Histochem.* **76**, 111–118 (2001).

14. Smith, A. C. & Hussey, M. A. Gram stain protocols. *Am. Soc. Microbiol.* **1**, 14 (2019).

15. Marsh, P. D. Dental plaque as a microbial biofilm. *Caries Res.* **38**, 204–211 (2004).

16. Loe, H., Theilade, E. & Jensen, S. B. Experimental Gingivitis in Man. *J. Periodontol.* **36**, 177–187 (1965).

17. Spormann, A. M., Thormann, K., Saville, R., Shukla, S. & Entcheva, P. Microbial biofilms. *Nanoscale Technol. Biol. Syst.* 341–357 (2004) doi:10.1201/9780203500224.

18. Kinane, D. F., Attstrom, R. & European Workshop Periodontology, g. Advances in the pathogenesis of periodontitiss - Group B consensus report of the fifth European workshop in periodontology. *J. Clin. Periodontol.* **32**, 130–131 (2005).

19. Pontoriero, R. *et al.* Experimentally induced peri-implant mucositis. A clinical study in humans. *Clinical Oral Implants Research* vol. 5 254–259 (1994).

20. Lang, N. P. & Berglundh, T. Periimplant diseases: Where are we now? - Consensus of the Seventh European Workshop on Periodontology. *J. Clin. Periodontol.* **38**, 178–181 (2011).

21. Socransky, S. S. *et al.* The microbiota of the gingival crevice area of man-I. Total microscopic and viable counts and counts of specific organisms. *Arch. Oral Biol.* **8**, 275–280 (1963).

22. Rawlinson, A., Duerden, B. I. & Goodwin, L. Microbiology of periodontal disease. *Dent. Health* **30**, 3–6 (1991).

23. Soskolne, W. A. *et al.* An in vivo study of the chlorhexidine release profile of the PerioChip™ in the gingival crevicular fluid, plasma and urine. *J. Clin. Periodontol.* **25**, 1017–1021 (1998).

24. Oncul, B., Karakis, D. & Al, F. D. The effect of two artificial salivas on the adhesion of Candida albicans to heatpolymerized acrylic resin. *J. Adv. Prosthodont.* **7**, 93–97 (2015).

25. Socransky, S. S. & Haffajee, A. D. Periodontal microbial ecology. Periodontol 38: 135–187. (2005).

26. Kornman, K. S. *et al.* The interleukin-1 genotype as a severity factor in adult periodontal disease. *J. Clin. Periodontol.* **24**, 72–77 (1997).

27. Ximénez-Fyvie, L. A., Haffajee, A. D. & Socransky, S. S. Comparison of the microbiota of supra- and subgingival plaque in health and periodontitis. *J. Clin. Periodontol.* **27**, 648–657 (2000).

28. Mandell, R. L. & Socransky, S. S. A Selective Medium for Actinobacillus actinomycetemcomitans and the Incidence of the Organism in Juvenile Periodontitis . *J. Periodontol.* **52**, 593–598 (1981).

29. Zambon, J. J. Actinobacillus actinomycetemcomitans in human periodontal disease. *J. Clin. Periodontol.* **12**, 1–20 (1985).

30. Fine, D. H., Markowitz, K., Furgang, D. & Velliyagounder, K. Aggregatibacter actinomycetemcomitans as an early colonizer of oral tissues: Epithelium as a reservoir? *J. Clin. Microbiol.* **48**, 4464–4473 (2010).

31. Haubek, D. & Johansson, A. Pathogenicity of the highly leukotoxic JP2 clone of Aggregatibacter actinomycetemcomitans and its geographic dissemination and role in aggressive periodontitis. *J. Oral Microbiol.* **6**, (2014).

32. Raja, M., Ummer, F. & Dhivakar, C. P. Aggregatibacter Actinomycetemcomitans - A Tooth Killer. *J. Clin. Diagnostic Res.* **8**, 13–17 (2014).

33. Duncan, M. J. Genomics of oral bacteria. *Crit. Rev. Oral Biol. Med.* **14**, 175–187 (2003).

34. Darveau, R. P. The oral microbial consortium's interaction with the periodontal innate defense system. *DNA Cell Biol.* **28**, 389–395 (2009).

35. Baehni, P. & Takeuchi, Y. Anti-plaque agents in the prevention of biofilm-associated oral diseases. *Oral Dis.* **9**, 23–29 (2003).

36. van der Ouderaa, F. J. G. Anti-plaque agents. Rationale and prospects for prevention of gingivitis and periodontal disease. *J. Clin. Periodontol.* **18**, 447–454 (1991).

37. Allaker, R. P. & Ian Douglas, C. Non-conventional therapeutics for oral infections. *Virulence* **6**, 196–207 (2015).

38. Mengel, R., Behle, M. & Flores-de-Jacoby, L. Osseointegrated Implants in Subjects Treated for Generalized Aggressive Periodontitis: 10-Year Results of a Prospective, Long-Term Cohort Study. *J. Periodontol.* **78**, 2229–2237 (2007).

39. Mengel, R. & Flores-de-Jacoby, L. Implants in Patients Treated for Generalized Aggressive and Chronic Periodontitis: A 3-Year Prospective Longitudinal Study. *J. Periodontol.* **76**, 534–543 (2005).

40. Reijden, W. A. Van Der & Raghoebar, G. Microbiota around root-form endosseous implants: A review of the literature. *J. Prosthet. Dent.* **89**, 517 (2003).

41. Hultin, M., Gustafsson, A. & Klinge, B. Long-term evaluation of osseointegrated dental implants in the treatment of partly edentulous patients. *J. Clin. Periodontol.* **27**, 128–133 (2000).

42. Kidd, E. A. M. & Beighton, D. Prediction of secondary caries around tooth-colored restorations: a clinical and microbiological study. *J. Dent. Res.* **75**, 1942–1946 (1996).

43. Okada, M. *et al.* PCR detection of Streptococcus mutans and S. sobrinus in dental plaque samples from Japanese pre-school children. *J. Med. Microbiol.* **51**, 443–447 (2002).

44. Kidd, E. A. M. Essentials of Dental Caries. Thirds Edition. (2005).

45. Selwitz, R. H., Ismail, A. I. & Pitts, N. B. Dental caries. *Lancet* **369**, 51–59 (2007).

46. Doychinova, M., Kussovski, V., Tonchev, T. & Dimitrov, S. Photodynamic Inactivation of Human Dental Biofilm Isolated Streptococcus Mutans With 2 Photosensitizers – an In Vitro Study. *Scr. Sci. Medica* **47**, 32 (2015).

47. Ehrlich, H., Koutsoukos, P. G., Demadis, K. D. & Pokrovsky, O. S. Principles of demineralization: Modern strategies for the isolation of organic frameworks. Part II. Decalcification. *Micron* **40**, 169–193 (2009).

48. Association, C. D.-J.-C. D. & 2003, U. Are Modern Dentin Adhesives Too Hydrophilic? Critical pH Revisited Measuring Normal Mouth Opening Unusual Root Canal Anatomy. *Cda-Adc.Ca* **69**, (2003).

49. Anderson, P., Hector, M. P. & Rampersad, M. A. Critical pH in resting and stimulated whole saliva in groups of children and adults. *Int. J. Paediatr. Dent.* **11**, 266–273 (2001).

50. Hanes, P. J. & Purvis, J. P. Local anti-infective therapy: Pharmacological agents. A systematic review. *Ann. Periodontol.* **8**, 79–98 (2003).

51. Bjarnsholt, T. *et al.* Why chronic wounds will not heal: A novel hypothesis. *Wound Repair Regen.* **16**, 2–10 (2008).

52. Slots, J. Selection of antimicrobial agents in periodontal therapy. *J. Periodontal Res.* **37**, 389–398 (2002).

53. BG, S. J. R. Suppression of the periodontopathic microflora in localized juvenile. *J Clin Periodontol* **10**, 465–486 (1983).

54. Novak, M. J., Polson, A. M. & Adair, S. M. Tetracycline therapy in patients with early juvenile periodontitis. *J. Periodontol.* **59**, 366–372 (1988).

55. Herrera, D., Alonso, B., León, R., Roldán, S. & Sanz, M. Antimicrobial therapy in periodontitis: The use of systemic antimicrobials against the subgingival biofilm. *J. Clin. Periodontol.* **35**, 45–66 (2008).

56. Feres-Filho, E. J. *et al.* Treatment of chronic periodontitis with systemic antibiotics only. *J. Clin. Periodontol.* **33**, 936–937 (2006).

57. Ünsal, E., Walsh, T. F. & Akkaya, M. The effect of a single application of subgingival antimicrobial or mechanical therapy on the clinical parameters of juvenile periodontitis. *J. Periodontol.* **66**, 47–51 (1995).

58. Kaner, D., Bernimoulin, J. P., Hopfenmüller, W., Kleber, B. M. & Friedmann, A. Controlled-delivery chlorhexidine chip versus amoxicillin/metronidazole as adjunctive antimicrobial therapy for generalized aggressive periodontitis: A randomized controlled clinical trial. *J. Clin. Periodontol.* **34**, 880–891 (2007).

59. Xiong, M. H., Bao, Y., Yang, X. Z., Zhu, Y. H. & Wang, J. Delivery of antibiotics with polymeric particles. *Adv. Drug Deliv. Rev.* **78**, 63–76 (2014).

60. Rai, M., Yadav, A. & Gade, A. Silver nanoparticles as a new generation of antimicrobials. *Biotechnol. Adv.* **27**, 76–83 (2009).

61. Hoque, S. *et al.* Water uptake of modified pem/thfm systems. in *JOURNAL OF DENTAL RESEARCH* vol. 82 529 (INT AMER ASSOC DENTAL RESEARCHI ADR/AADR 1619 DUKE ST, ALEXANDRIA, VA 22314 …, 2003).

62. Wade, W. G. & Addy, M. In vitro Activity of a Chlorhexidine–Containing Mouthwash Against Subgingival Bacteria. *J. Periodontol.* **60**, 521–525 (1989).

63. McDonnell, G. & Russell, A. D. Antiseptics and disinfectants: activity, action, and resistance. *Clin. Microbiol. Rev.* **14**, 227 (2001).

64. Al-Tannir, M. A. & Goodman, H. S. A review of chlorhexidine and its use in special populations. *Spec. Care Dent.* **14**, 116–122 (1994).

65. Davies, G. E., Martin, J. F. a R., Rose, F. L. & Swain, G. (" HIBITANE "*). LABORATORY INVESTIGATION OF A NEW IkH N1H. *Brit. J. Pharmacol.* **9**, 192–196 (1954).

66. Călinescu, M., Negreanu-Pîrjol, T., Georgescu, R. & Călinescu, O. Synthesis and characterization of new copper(II) complex compounds with chlorhexidine. Part I. *Cent. Eur. J. Chem.* **8**, 543–549 (2010).

67. Zanatta, F. B., Antoniazzi, R. P. & Rösing, C. K. The Effect of 0.12% Chlorhexidine Gluconate Rinsing on Previously Plaque-Free and Plaque-Covered Surfaces: A Randomized, Controlled Clinical Trial. *J. Periodontol.* **78**, 2127–2134 (2007).

68. Foulkes, D. M. Some toxicological observations on chlorhexidine. *J. Periodontal Res.* **8**, 55–60 (1973).

69. Stabholz, A., Sela, M. N., Friedman, M., Golomb, G. & Soskolne, A. Clinical and microbiological effects of sustained release chlorhexidine in periodontal pockets. *J. Clin. Periodontol.* **13**, 783–788 (1986).

70. Genuit, T., Bochicchio, G., Napolitano, L. M., McCarter, R. J. & Roghman, M. C. Prophylactic chlorhexidine oral rinse decreases ventilator-associated pneumonia in surgical icu patients. *Surg. Infect. (Larchmt).* **2**, 5–18 (2001).

71. Silveira, C. F. D. M. *et al.* Assessment of the antibacterial activity of calcium hydroxide combined with chlorhexidine paste and other intracanal medications against bacterial pathogens. *Eur. J. Dent.* **5**, 1–7 (2011).

72. Bassett, D. C. The effect of pH on the multiplication of a pseudomonad in chlorhexidine and cetrimide. *J. Clin. Pathol.* **24**, 708–711 (1971).

73. Baliga, S., Muglikar, S. & Kale, R. Salivary pH: A diagnostic biomarker. *J. Indian Soc. Periodontol.* **17**, 461 (2013).

74. Winkler, F. Practical Absorption Spectrometry. Hg. von A. KNOWLES und C. BURGESS. vol. 3 of Techniques in Visible and Ultraviolet Spectrometry. ISBN 0-412-24390-3. London/New York: Chapman and Hall 1984. XXII, 234 S., geb. £ 19.25. *Acta Polym.* **37**, 398–398 (1986).

75. Moermann, J. E. & Muehlemann, H. R. Synergistic inhibitory effect of zinc and hexetidine on in vitro growth and acid production of Streptococcus mutans. *J. Dent. Res.* **62**, 135–137 (1983).

76. Minor, H. & Technology, C. General procedure for evaluating amorphous scattering and crystallinity from X-ray diffraction scans of semicrystalline polymers. *Polymer (Guildf).* **31**, 996–1002 (1989).

77. Călinescu, M., Negreanu-Pîrjol, T., Georgescu, R. & Călinescu, O. Synthesis and characterization of new copper(II) complex compounds with chlorhexidine. Part I. *Cent. Eur. J. Chem.* **8**, 543–549 (2010).

78. Calinescu, M., Negreanu-Pirjol, T., Calinescu, O. & Georgescu, R. Spectral and biological characterization of some copper(II) complex compounds with chlorhexidine. *Rev. Chim.* **63**, 682–687 (2012).

79. Barbour, M. E., Maddocks, S. E., Wood, N. J. & Collins, A. M. Synthesis, characterization, and efficacy of antimicrobial chlorhexidine hexametaphosphate nanoparticles for applications in biomedical materials and consumer products. *Int. J. Nanomedicine* **8**, 3507 (2013).

80. Garner, S. & Barbour, M. E. Nanoparticles for controlled delivery and sustained release of chlorhexidine in the oral environment. *Oral Dis.* **21**, 641–644 (2015).

81. Wood, N. J. *et al.* Chlorhexidine hexametaphosphate nanoparticles as a novel antimicrobial coating for dental implants. *J. Mater. Sci. Mater. Med.* **26**, 1–10 (2015).

82. Garner, S. J., Nobbs, A. H., McNally, L. M. & Barbour, M. E. An antifungal coating for dental silicones composed of chlorhexidine nanoparticles. *J. Dent.* **43**, 362–372 (2015).

83. Bellis, C. A. *et al.* Glass ionomer cements with milled, dry chlorhexidine hexametaphosphate filler particles to provide long-term antimicrobial properties with recharge capacity. *Dent. Mater.* **34**, 1717–1726 (2018).

84. Wood, N. J., Maddocks, S. E., Grady, H. J., Collins, A. M. & Barbour, M. E. Functionalization of ethylene vinyl acetate with antimicrobial chlorhexidine hexametaphosphate nanoparticles. *Int. J. Nanomedicine* **9**, 4145 (2014).

85. Barbour, M. E. *et al.* Chlorhexidine hexametaphosphate as a wound care material coating: Antimicrobial efficacy, toxicity and effect on healing. *Nanomedicine* **11**, 2049–2057 (2016).

86. Luo, D., Shahid, S., Wilson, R. M., Cattell, M. J. & Sukhorukov, G. B. Novel Formulation of Chlorhexidine Spheres and Sustained Release with Multilayered Encapsulation. *ACS Appl. Mater. Interfaces* **8**, 12652–12660 (2016).

87. Luo, D. *et al.* Gold Nanorod Mediated Chlorhexidine Microparticle Formation and Near-Infrared Light Induced Release. *Langmuir* **33**, 7982–7993 (2017).

88. Luo, D., Shahid, S., Sukhorukov, G. B. & Cattell, M. J. Synthesis of novel chlorhexidine spheres with controlled release from a UDMA–HEMA resin using ultrasound. *Dent. Mater.* **33**, 713–722 (2017).

89. Luo, D. *et al.* Electrospun poly(lactic acid) fibers containing novel chlorhexidine particles with sustained antibacterial activity. *Biomater. Sci.* **5**, 111–119 (2017).

90. Hugo, W. B. & Longworth, A. R. Some aspects of the mode of action of chlorhexidine. *J. Pharm. Pharmacol.* **16**, 655–662 (1964).

91. BOWEN, R. L. Properties of a silica-reinforced polymer for dental restorations. *J. Am. Dent. Assoc.* **66**, 57–64 (1963).

92. Block, S. S. *Disinfection, sterilization, and preservation*. (Lippincott Williams & Wilkins, 2001).

93. Cheung, H.-Y. *et al.* Differential Actions of Chlorhexidine on the Cell Wall of Bacillus subtilis and Escherichia coli. *PLoS One* **7**, e36659 (2012).

94. Giannopoulou, I., Saïs, F. & Thomopoulos, R. Linked data annotation and fusion driven by data quality evaluation. *Rev. des Nouv. Technol. l'Information* **E.28**, 257–262 (2015).

95. Cline, N. V. & Layman, D. L. The Effects of Chlorhexidine on the Attachment and Growth of Cultured Human Periodontal Cells. *J. Periodontol.* **63**, 598–602 (1992).

96. Hugo, W. *Inhibition and destruction of the microbial cell*. (Elsevier, 2012).

97. CHAWNER, J. A. & GILBERT, P. A comparative study of the bactericidal and growth inhibitory activities of the bisbiguanides alexidine and chlorhexidine. *J. Appl. Bacteriol.* **66**, 243–252 (1989).

98. Jones, C. G. Chlorhexidine: Is it still the gold standard? *Periodontol. 2000* **15**, 55–62 (1997).

99. HUGO, W. B. & LONGWORTH, A. R. The effect of chlorhexidine on the electrophoretic mobility, cytoplasmic constituents, dehydrogenase activity and cell walls of Escherichia coli and Staphylococcus aureus. *J. Pharm. Pharmacol.* **18**, 569–578 (1966).

100. Kuyyakanond, T. & Quesnel, L. B. The mechanism of action of chlorhexidine. *FEMS Microbiol. Lett.* **100**, 211–215 (1992).

101. Athanassiadis, B., Abbott, P. & Walsh, L. The use of calcium hydroxide, antibiotics and biocides as antimicrobial medicaments in endodontics. *Aust. Dent. J.* **52**, S64–S82 (2007).

102. P. Bonesvoll, P. Lokken, G. R. and P. N. P. Retention of Chlorhexidine. *Arch. Oral Biol.* **19**, 209–212 (1974).

103. Welk, A. *et al.* The effect of a polyhexamethylene biguanide mouthrinse compared with a triclosan rinse and a chlorhexidine rinse on bacterial counts and 4-day plaque re-growth. *J. Clin. Periodontol.* **32**, 499–505 (2005).

104. Shapiro, S., Giertsen, E. & Guggenheim, B. An in vitro oral biofilm model for comparing the efficacy of antimicrobial mouthrinses. *Caries Res.* **36**, 93–100 (2002).

105. Loe, H. & Rindom Schiott, C. The effect of mouthrinses and topical application of chlorhexidine on the development of dental plaque and gingivitis in man. *J. Periodontal Res.* **5**, 79–83 (1970).

106. Rolla, G. & Melsen, B. On the mechanism of the plaque inhibition by chlorhexidine. *J. Dent. Res.* **54**, 57–62 (1975).

107. Mohammadi, Z. & Abbott, P. V. The properties and applications of chlorhexidine in endodontics. *Int. Endod. J.* **42**, 288–302 (2009).

108. Rindom-Schiöutt, C., Löue, H. & Briner, W. W. Two year oral use of chlorhexidine in man: IV. Effect on various medical parameters. *J. Periodontal Res.* **11**, 158–164 (1976).

109. Addy, M. & Moran, J. Mechanisms of Stain Formation on Teeth, in Particular Associated with Metal Ions and Antiseptics. *Adv. Dent. Res.* **9**, 450–456 (1995).

110. Addy, M. & Roberts, W. R. Comparison of the bisbiguanide antiseptics alexidine and chlorhexidine. II. Clinical and in vitro staining properties. *J. Clin. Periodontol.* **8**, 220–230 (1981).

111. Scully, C. & Felix, D. H. Oral medicine - Update for the dental practitioner. Orofacial pain. *Br. Dent. J.* **200**, 75–83 (2006).

112. Vishnu Prasanna, S. G. & Lakshmanan, R. Characteristics, Uses and Side effects of Chlorhexidine-A Review. *IOSR J. Dent. Med. Sci. e-ISSN* **15**, 57–59 (2016).

113. Sheen, S., Owens, J. & Addy, M. The effect of toothpaste on the propensity of chlorhexidine and cetyl pyridinium chloride to produce staining in vitro: A possible predictor of inactivation. *J. Clin. Periodontol.* **28**, 46–51 (2001).

114. Vu, M., Rajgopal Bala, H., Cahill, J., Toholka, R. & Nixon, R. Immediate hypersensitivity to chlorhexidine. *Australas. J. Dermatol.* **59**, 55–56 (2018).

115. Timsit, J. F. *et al.* Randomized controlled trial of chlorhexidine dressing and highly adhesive dressing for preventing catheter-related infections in critically ill adults. *Am. J. Respir. Crit. Care Med.* **186**, 1272–1278 (2012).

116. Pemberton, M. N. & Gibson, J. Chlorhexidine and hypersensitivity reactions in dentistry. *Br. Dent. J.* **213**, 547–550 (2012).

117. Odedra, K. M. & Farooque, S. Chlorhexidine: an unrecognised cause of anaphylaxis. *Postgrad. Med. J.* **90**, 709–714 (2014).

118. Opstrup, M. S., Jemec, G. B. E. & Garvey, L. H. Chlorhexidine allergy: on the rise and often overlooked. *Curr. Allergy Asthma Rep.* **19**, 1–10 (2019).

119. Liippo, J., Kousa, P. & Lammintausta, K. The relevance of chlorhexidine contact allergy. *Contact Dermatitis* **64**, 229–234 (2011).

120. Opstrup, M. S., Johansen, J. D., Zachariae, C. & Garvey, L. H. Contact allergy to chlorhexidine in a tertiary dermatology clinic in Denmark. *Contact Dermatitis* **74**, 29–36 (2016).

121. Cieplik, F. *et al.* Resistance toward chlorhexidine in oral bacteria-is there cause for concern? *Front. Microbiol.* **10**, (2019).

122. Horner, C., Mawer, D. & Wilcox, M. Reduced susceptibility to chlorhexidine in staphylococci: Is it increasing and does it matter? *J. Antimicrob. Chemother.* **67**, 2547–2559 (2012).

123. Maynard, J. H. *et al.* A 6-month home usage trial of a 1% chlorhexidine toothpaste: (II). Effects on the oral microflora. *J. Clin. Periodontol.* **20**, 207–211 (1993).

124. Kulik, E. M. *et al.* Development of resistance of mutans streptococci and Porphyromonas gingivalis to chlorhexidine digluconate and amine fluoride/stannous fluoride-containing mouthrinses, in vitro. *Clin. Oral Investig.* **19**, 1547–1553 (2015).

125. Wang, S. *et al.* Do quaternary ammonium monomers induce drug resistance in cariogenic, endodontic and periodontal bacterial species? *Dent. Mater.* **33**, 1127–1138 (2017).

126. Li, M. *et al.* Elastin Blends for Tissue Engineering Scaffolds. *J. Biomed. Mater. Res. Part A* **79**, 963–73 (2006).

127. Priyadarshini, B. M. *et al.* Chlorhexidine Nanocapsule Drug Delivery Approach to the Resin-Dentin Interface. *J. Dent. Res.* **95**, 1065–1072 (2016).

128. Morelli, L., Cappelluti, M. A., Ricotti, L., Lenardi, C. & Gerges, I. An Injectable System for Local and Sustained Release of Antimicrobial Agents in the Periodontal Pocket. *Macromol. Biosci.* **17**, (2017).

129. Tsioufis, C., Kasiakogias, A., Thomopoulos, C. & Stefanadis, C. Periodontitis and blood pressure: The concept of dental hypertension. *Atherosclerosis* **219**, 1–9 (2011).

130. Bryan, N. S., Tribble, G. & Angelov, N. Oral microbiome and nitric oxide: the missing link in the management of blood pressure. *Curr. Hypertens. Rep.* **19**, 1–8 (2017).

131. Lundberg, J. O., Weitzberg, E., Cole, J. A. & Benjamin, N. Nitrate, bacteria and human health. *Nat. Rev. Microbiol.* **2**, 593–602 (2004).

132. Blot, S. Antiseptic mouthwash, the nitrate–nitrite–nitric oxide pathway, and hospital mortality: a hypothesis generating review. *Intensive Care Med.* **47**, 28–38 (2021).

133. Shapiro, K. B., Hotchkiss, J. H. & Roe, D. A. Quantitative relationship between oral nitrate-reducing activity and the endogenous formation of N-nitrosoamino acids in humans. *Food Chem. Toxicol.* **29**, 751–755 (1991).

134. Bondonno, C. P. *et al.* Antibacterial mouthwash blunts oral nitrate reduction and increases blood pressure in treated hypertensive men and women. *Am. J. Hypertens.* **28**, 572–575 (2015).

135. Tribble, G. D. *et al.* Frequency of Tongue Cleaning Impacts the Human Tongue Microbiome Composition and Enterosalivary Circulation of Nitrate. *Front. Cell. Infect. Microbiol.* **9**, 1–16 (2019).

136. Oggioni, C. *et al.* Dietary nitrate does not modify blood pressure and cardiac output at rest and during exercise in older adults: a randomised cross-over study. *Int. J. Food Sci. Nutr.* **69**, 74–83 (2018).

137. Preshaw, P. M. Mouthwash use and risk of diabetes. *Br. Dent. J.* **225**, 923–926 (2018).

138. Oliveira-Paula, G. H., Pinheiro, L. C. & Tanus-Santos, J. E. Mechanisms impairing blood pressure responses to nitrite and nitrate. *Nitric Oxide - Biol. Chem.* **85**, 35–43 (2019).

139. Yue, I. C. *et al.* A novel polymeric chlorhexidine delivery device for the treatment of periodontal disease. *Biomaterials* **25**, 3743–3750 (2004).

140. Lang, N. *et al.* Plaque formation and gingivitis after supervised mouthrinsing with 0.2% delmopinol hydrochloride, 0.2% chlorhexidine digluconate and placebo for 6 months. *Oral Diseases* vol. 4 105–113 (2010).

141. Balagopal, S. & Arjunkumar, R. Chlorhexidine: The gold standard antiplaque agent. *J. Pharm. Sci. Res.* **5**, 270–274 (2013).

142. Jaidka, S., Somani, R., Singh, D. J. & Shafat, S. Comparative evaluation of compressive strength, diametral tensile strength and shear bond strength of GIC type IX, chlorhexidine-incorporated GIC and triclosan-incorporated GIC: An in vitro study. *J. Int. Soc. Prev. Community Dent.* **6**, S64 (2016).

143. Padois, K. *et al.* Chlorhexidine salt-loaded polyurethane orthodontic chains: In vitro release and antibacterial activity studies. *AAPS PharmSciTech* **13**, 1446–1450 (2012).

144. Storhaug, K. Hibitane in oral disease in handicapped patients. *J. Clin. Periodontol.* **4**, 102–107 (1977).

145. Kasetsuwan, C., Sirirat, M. & Prachyabrued, W. Effect of scaling and root planing on the composition of microorganisms in human periodontal pockets. *J. Dent. Assoc. Thai.* **33**, 250–263 (1983).

146. Cugini, M. A., Haffajee, A. D., Smith, C., Kent, R. L. & Socransky, S. S. The effect of scaling and root planing on the clinical and microbiological parameters of periodontal diseases: 12-month results. *J. Clin. Periodontol.* **27**, 30–36 (2000).

147. Mousquéegs, T., Listgarten, M. A. & Stoller, N. H. Effect of sampling on the composition of the human subgingival microbial flora. *J. Periodontal Res.* **15**, 137–143 (1980).

148. Baehni, P. C. & Takeuchi, Y. Anti-plaque agents in the prevention of biofilm-associated oral diseases. in *Oral Diseases* vol. 9 23–29 (2003).

149. Tallury, P., Alimohammadi, N. & Kalachandra, S. Poly(ethylene-co-vinyl acetate) copolymer matrix for delivery of chlorhexidine and acyclovir drugs for use in the oral environment: Effect of drug combination, copolymer composition and coating on the drug release rate. *Dent. Mater.* **23**, 404–409 (2007).

150. Mendieta, C., Vallcorba, N., Binney, A. & Addy, M. Comparison of 2 chlorhexidine mouthwashes on plaque regrowth in vivo and dietary staining in vitro. *J. Clin. Periodontol.* **21**, 296–300 (1994).

151. Legéňová, K., Kovalčíková, M., Černáková, L. & Bujdáková, H. The Contribution of Photodynamic Inactivation vs. Corsodyl Mouthwash to the Control of Streptococcus mutans Biofilms. *Curr. Microbiol.* **77**, 988–996 (2020).

152. Sanz, M. *et al.* Clinical Enhancement of Post-Periodontal Surgical Therapy by a 0.12% Chlorhexidine Gluconate Mouthrinse. *J. Periodontol.* **60**, 570–576 (1989).

153. Grossman, E. *et al.* Chlorhexidine Mouthrinse on Gingivitis in Aduits. *J. Feriodontal Res. Suppl.* 33–43 (1986).

154. Zanatta, F. B., Antoniazzi, R. P. & Rösing, C. K. The Effect of 0.12% Chlorhexidine Gluconate Rinsing on Previously Plaque-Free and Plaque-Covered Surfaces: A Randomized, Controlled Clinical Trial. *J. Periodontol.* **78**, 2127–2134 (2007).

155. Faveri, M. *et al.* Scaling and root planing and chlorhexidine mouthrinses in the treatment of chronic periodontitis: A randomized, placebo-controlled clinical trial. *J. Clin. Periodontol.* **33**, 819–828 (2006).

156. Feres, M., Gursky, L. C., Faveri, M., Tsuzuki, C. O. & Figueiredo, L. C. Clinical and microbiological benefits of strict supragingival plaque control as part of the active phase of periodontal therapy. *J. Clin. Periodontol.* **36**, 857–867 (2009).

157. Quirynen, M., Teughels, W., Soete, M. De & Sreenberghe, D. Van. Topical antiseptics and antibiotics in the initial therapy of chronic adult periodontitis: microbiological aspects. *Periodontol. 2000* **28**, 72–90 (2002).

158. Fenwick, J., Needleman, I. G. & Moles, D. R. The effect of bias on the magnitude of clinical outcomes in periodontology: A pilot study. *J. Clin. Periodontol.* **35**, 775–782 (2008).

159. Renvert, S., Roos-Jansåker, A. M. & Claffey, N. Non-surgical treatment of peri-implant mucositis and peri-implantitis: A literature review. *J. Clin. Periodontol.* **35**, 305–315 (2008).

160. Heitz-Mayfield, L. J. A. *et al.* Anti-infective treatment of peri-implant mucositis: A randomised controlled clinical trial. *Clin. Oral Implants Res.* **22**, 237–241 (2011).

161. Gimeno, M. *et al.* A controlled antibiotic release system to prevent orthopedic-implant associated infections: An in vitro study. *Eur. J. Pharm. Biopharm.* **96**, 264–271 (2015).

162. Matesanz-Pérez, P. *et al.* A systematic review on the effects of local antimicrobials as adjuncts to subgingival debridement, compared with subgingival debridement alone, in the treatment of chronic periodontitis. *J. Clin. Periodontol.* **40**, 227–241 (2013).

163. Sahm, N., Becker, J., Santel, T. & Schwarz, F. Non-surgical treatment of peri-implantitis using an air-abrasive device or mechanical debridement and local application of chlorhexidine: a prospective, randomized, controlled clinical study. *J. Clin. Periodontol.* **38**, 872–878 (2011).

164. Renvert, S., Lessem, J., Dahlén, G., Renvert, H. & Lindahl, C. Mechanical and Repeated Antimicrobial Therapy Using a Local Drug Delivery System in the Treatment of Peri-Implantitis: A Randomized Clinical Trial. *J. Periodontol.* **79**, 836–844 (2008).

165. Rams, T. E. & Slots, J. Local delivery of antimicrobial agents in the periodontal pocket. *Periodontol. 2000* **10**, 139–159 (1996).

166. Heasman, P. A., Heasman, L., Stacey, F. & McCracken, G. I. Local delivery of chlorhexidine gluconate (PerioChipTM) in periodontal maintenance patients. *J. Clin. Periodontol.* **28**, 90–95 (2008).

167. MacNeill, S. R., Johnson, V. B., Killoy, W. J., Yonke, M. & Ridenhour, L. The time and ease of placement of the chlorhexidine chip local delivery system. *Compend. Contin. Educ. Dent. (Jamesburg, NJ 1995)* **19**, 1158–1162 (1998).

168. Jeffcoat, M. K. *et al.* Adjunctive Use of a Subgingival Controlled-Release Chlorhexidine Chip Reduces Probing Depth and Improves Attachment Level Compared With Scaling and Root Planing Alone. *J. Periodontol.* **69**, 989–997 (1998).

169. Soskolne, W. A. *et al.* Sustained Local Delivery of Chlorhexidine in the Treatment of Periodontitis: A Multi-Center Study. *J. Periodontol.* **68**, 32–38 (1997).

170. Mai *et al.* A New Antibacterial Agent-Releasing Polydimethylsiloxane Coating for Polymethyl Methacrylate Dental Restorations. *J. Clin. Med.* **8**, 1831 (2019).

171. Fini, A., Bergamante, V. & Ceschel, G. C. Mucoadhesive gels designed for the controlled release of chlorhexidine in the oral cavity. *Pharmaceutics* **3**, 665–675 (2011).

172. Gupta, R., Pandit, N., Aggarwal, S. & Verma, A. Comparative evaluation of subgingivally delivered 10% doxycycline hyclate and xanthan-based chlorhexidine gels in the treatment of chronic periodontitis. *J. Contemp. Dent. Pract.* **9**, 025–032 (2008).

173. Cavallari, C., Brigidi, P. & Fini, A. Ex-vivoand in-vitro assessment of mucoadhesive patches containing the gel-forming polysaccharide psyllium for buccal delivery of chlorhexidine base. *Int. J. Pharm.* **496**, 593–600 (2015).

174. Kharenko, E. A., Larionova, N. I. & Demina, N. B. Mucoadhesive drug delivery systems (Review). *Pharm. Chem. J.* **43**, 200–208 (2009).

175. Rossi, S., Bonferoni, M. C., Ferrari, F. & Caramella, C. Drug release and washability of mucoadhesive gels based on sodium carboxymethylcellulose and polyacrylic acid. *Pharm. Dev. Technol.* **4**, 55–63 (1999).

176. ISHIDA, M., NAMBU, N. & NAGAI, T. Highly viscous gel ointment containing Carbopol for application to the oral mucosa. *Chem. Pharm. Bull.* **31**, 4561–4564 (1983).

177. Deshmukh, K. *et al.* Biopolymer composites with high dielectric performance: interface engineering. in *Biopolymer composites in electronics* 27–128 (Elsevier, 2017).

178. Dorożyński, P. *et al.* The macromolecular polymers for the preparation of hydrodynamically balanced systems—methods of evaluation. *Drug Dev. Ind. Pharm.* **30**, 947–957 (2004).

179. Fu, X. C., Wang, G. P., Liang, W. Q. & Chow, M. S. S. Prediction of drug release from HPMC matrices: Effect of physicochemical properties of drug and polymer concentration. *J. Control. Release* **95**, 209–216 (2004).

180. Caraballo, I. Factors affecting drug release from hydroxypropyl methylcellulose matrix systems in the light of classical and percolation theories. *Expert Opin. Drug Deliv.* **7**, 1291–1301 (2010).

181. Siepmann, J. & Peppas, N. A. Modeling of drug release from delivery systems based on hydroxypropyl methylcellulose (HPMC). *Adv. Drug Deliv. Rev.* **64**, 163–174 (2012).

182. Williams, R. O., Sykora, M. A. & Mahaguna, V. Method to recover a lipophilic drug from hydroxypropyl methylcellulose matrix tablets. *AAPS PharmSciTech* **2**, (2001).

183. Vazquez, M. J. *et al.* Influence of technological variables on release of drugs from hydrophilic matrices. *Drug Dev. Ind. Pharm.* **18**, 1355–1375 (1992).

184. Miyazaki, S. *et al.* Oral mucosal bioadhesive tablets of pectin and HPMC: In vitro and in vivo evaluation. *Int. J. Pharm.* **204**, 127–132 (2000).

185. Do, M. P. *et al.* In situ forming implants for periodontitis treatment with improved adhesive properties. *Eur. J. Pharm. Biopharm.* **88**, 342–350 (2014).

186. Do, M. P. *et al.* Mechanistic analysis of PLGA/HPMC-based in-situ forming implants for periodontitis treatment. *Eur. J. Pharm. Biopharm.* **94**, 273–283 (2015).

187. Jain, M. *et al.* Efficacy of xanthan based chlorhexidine gel as an adjunct to scaling and root planing in treatment of the chronic periodontitis. *J. Indian Soc. Periodontol.* **17**, 439 (2013).

188. Frentzen, M., Ploenes, K. & Braun, A. Clinical and microbiological effects of local chlorhexidine applications. *Int. Dent. J.* **52**, 325–329 (2002).

189. Dudic, V. B., Lang, N. P. & Mombelli, A. Microbiological and clinical effects of an antiseptic dental varnish after mechanical periodontal therapy. *J. Clin. Periodontol.* **26**, 341–346 (1999).

190. Galganny-Almeida, A., Rocha, C. T., Neves, B. G. & Rebouças, B. R. The use of chlorhexidine varnishes in children: what is out there? *IJD. Int. J. Dent.* **9**, 142–147 (2010).

191. Sachdeva, S., Grover, V., Malhotra, R., Kapoor, A. & Mohanty, K. Comparison of clinical effectiveness of single and multiple applications of 1% chlorhexidine varnish (Cervitec Plus) along with scaling and root planing in patients with chronic periodontitis. *J. Indian Soc. Periodontol.* **22**, 523 (2018).

192. Hugoson, A. & Norderyd, O. Has the prevalence of periodontitis changed during the last 30 years? *J. Clin. Periodontol.* **35**, 338–345 (2008).

193. Drebenstedt, S., Zapf, A., Rödig, T., Mausberg, R. F. & Ziebolz, D. Efficacy of two different CHX-containing desensitizers: A controlled double-blind study. *Oper. Dent.* **37**, 161–171 (2012).

194. Petersson, L. G., Edwardsson, S. & Arends, J. Antimicrobial effect of a dental varnish, in vitro. *Swed. Dent. J.* **16**, 183–189 (1992).

195. Silla, M. P., Company, J. M. M. & Almerich-Silla, J. M. Use of chlorhexidine varnishes in preventing and treating periodontal disease. A review of the literature. *Med. Oral Patol. Oral Cir. Bucal* **13**, 257–260 (2008).

196. Pors Nielsen, S. The biological role of strontium. *Bone* **35**, 583–588 (2004).

197. Bonnelye, E., Chabadel, A., Saltel, F. & Jurdic, P. Dual effect of strontium ranelate: Stimulation of osteoblast differentiation and inhibition of osteoclast formation and resorption in vitro. *Bone* **42**, 129–138 (2008).

198. Guida, A., Towler, M. R., Wall, J. G., Hill, R. G. & Eramo, S. Preliminary work on the antibacterial effect of strontium in glass ionomer cements. *J. Mater. Sci. Lett.* **22**, 1401–1403 (2003).

199. Johnson, A. R., Armstrong, W. D. & Singer, L. The incorporation and removal of large amounts of strontium by physiologic mechanisms in mineralized tissues of the rat. *Calcif. Tissue Res.* **2**, 242–252 (1968).

200. Verbeeck, R. M. H., Lassuyt, C. J., Heijligers, H. J. M., Driessens, F. C. M. & Vrolijk, J. W. G. A. Lattice parameters and cation distribution of solid solutions of calcium and lead hydroxyapatite. *Calcif. Tissue Int.* **33**, 243–247 (1981).

201. WALSER, M. Renal Excretion of Alkaline Earths**These studies have been supported by the National Institutes of Health (AM-02306 and GM-K3-2583). in *Calcium Physiology* 235–320 (Elsevier, 1969). doi:10.1016/B978-1-4832-2743-6.50010-8.

202. Zhao, Y. *et al.* Porous Allograft Bone Scaffolds: Doping with Strontium. *PLoS One* **8**, 1–10 (2013).

203. Buehler, J., Chappuis, P., Saffar, J. L., Tsouderos, Y. & Vignery, A. Strontium ranelate inhibits bone resorption while maintaining bone formation in alveolar bone in monkeys (Macaca fascicularis). *Bone* **29**, 176–179 (2001).

204. Meunier, P. J. *et al.* Effects of long-term strontium ranelate treatment on vertebral fracture risk in postmenopausal women with osteoporosis. *Osteoporos. Int.* **20**, 1663–1673 (2009).

205. Meunier, P. J. *et al.* Strontium ranelate: Dose-dependent effects in established postmenopausal vertebral osteoporosis - A 2-year randomized placebo controlled trial. *J. Clin. Endocrinol. Metab.* **87**, 2060–2066 (2002).

206. Marie, P. J., Ammann, P., Boivin, G. & Rey, C. Mechanisms of action and therapeutic potential of strontium in bone. *Calcif. Tissue Int.* **69**, 121–129 (2001).

207. Hidalgo, E. & Dominguez, C. Mechanisms underlying chlorhexidine-induced cytotoxicity. *Toxicol. Vitr.* **15**, 271–276 (2001).

208. Dahl, S. G. *et al.* Incorporation and distribution of strontium in bone. *Bone* **28**, 446–453 (2001).

209. Matsunaga, K. & Murata, H. Strontium substitution in bioactive calcium phosphates: A first-principles study. *J. Phys. Chem. B* **113**, 3584–3589 (2009).

210. Henrotin, Y. *et al.* Strontium ranelate increases cartilage matrix formation. *J. Bone Miner. Res.* **16**, 299–308 (2001).

211. Pearce, N. X., Addy, M. & Newcombe, R. G. Dentine hypersensitivity: a clinical trial to compare 2 strontium densensitizing toothpastes with a conventional fluoride toothpaste. *J. Periodontol.* **65**, 113–119 (1994).

212. Hill, R. & Gillam, D. G. Future strategies for the development of desensitising products. in *Dentine Hypersensitivity* 157–179 (Springer, 2015).

213. Davies, D. R., Bassingthwaighte, J. B. & Kelly, P. J. Transcapillary exchange of strontium and sucrose in canine tibia. *J. Appl. Physiol.* **40**, 17–22 (1976).

214. Koletsi-Kounari, H., Mamai-Homata, E. & Diamanti, I. An in vitro study of the effect of aluminum and the combined effect of strontium, aluminum, and fluoride elements on early enamel carious lesions. *Biol. Trace Elem. Res.* **147**, 418–427 (2012).

215. Curzon, M. E. J. The Relation Between Caries Prevalence and Strontium Concentrations in Drinking Water, Plaque, and Surface Enamel. *J. Dent. Res.* **64**, 1386–1388 (1985).

216. Meyerowitz, C., Spector, P. C. & Curzon, M. E. J. Pre- or Post-Eruptive Effects of Strontium Alone or in Combination with Fluoride on Dental Caries in the Rat. **210**, 203–210 (1979).

217. Curzon, M. E. J., Ashrafi, M. H. & Spector, P. C. Effects of strontium administration on rat molar morphology. *Arch. Oral Biol.* **27**, 667–671 (1982).

218. Featherstone, J. D. B., Shields, C. P., Khademazad, B. & Oldershaw, M. D. Acid Reactivity of Carbonated Apatites with Strontium and Fluoride Substitutions. *J. Dent. Res.* **62**, 1049–1053 (1983).

219. Lippert, F. & Hara, A. T. Strontium and Caries: A Long and Complicated Relationship. *Caries Res.* **47**, 34–49 (2013).

220. Luo, J., Billington, R. W. & Pearson, G. J. Kinetics of fluoride release from glass components of glass ionomers. *J. Dent.* **37**, 495–501 (2009).

221. Maret, W. Zinc biochemistry: From a single zinc enzyme to a key element of life. *Adv. Nutr.* **4**, 82–91 (2013).

222. Bettger, W. J. & O'Dell, B. L. Physiological roles of zinc in the plasma membrane of mammalian cells. *J. Nutr. Biochem.* **4**, 194–207 (1993).

223. Yamaguchi, M., Oishi, H. & Suketa, Y. Effect of zinc on bone formation. **36**, (1987).

224. Saino, E. *et al.* In vitro calcified matrix deposition by human osteoblasts onto a zinc-containing bioactive glass. *Eur. Cells Mater.* **21**, 59–72 (2011).

225. Lansdown, A. B. G., Mirastschijski, U., Stubbs, N., Scanlon, E. & Ågren, M. S. Zinc in wound healing: Theoretical, experimental, and clinical aspects. *Wound Repair Regen.* **15**, 2–16 (2007).

226. Sevinç, B. A. & Hanley, L. Antibacterial activity of dental composites containing zinc oxide nanoparticles. *J. Biomed. Mater. Res. - Part B Appl. Biomater.* **94**, 22–31 (2010).

227. Primosch, R. E., Ahmadi, A., Setzer, B. & Guelmann, M. A retrospective assessment of zinc oxide-eugenol pulpectomies in vital maxillary primary incisors successfully restored with composite resin crowns. *Pediatr. Dent.* **27**, 470–477 (2005).

228. He, G., Pearce, E. I. F. & Sissons, C. H. Inhibitory effect of ZnCl2 on glycolysis in human oral microbes. *Arch. Oral Biol.* **47**, 117–129 (2002).

229. Cummins, D. Zinc citrate/Triclosan: a new anti-plaque system for the control of plaque and the prevention of gingivitis: short-term clinical and mode of action studies. *J. Clin. Periodontol.* **18**, 455–461 (1991).

230. Tronstad, L., Andreasen, J. O., Hasselgren, G., Kristerson, L. & Riis, I. pH changes in dental tissues after root canal filling with calcium hydroxide. *J. Endod.* **7**, 17–21 (1981).

231. Periodontol, C. Zinc citrate / Triclosan : a new anti- plaque system for the control of plaque and the prevention of gingivitis : short-term clinical and mode of action studies. (1991).

232. Chen, X. *et al.* ‘ Smart ’ acid-degradable zinc-releasing silicate glasses. *Mater. Lett.* **126**, 278–280 (2014).

233. Glass, B., Engineering, T., Ranga, N., Gahlyan, S. & Duhan, S. Antibacterial Efficiency of Zn , Mg and Sr Doped. **20**, 2465–2472 (2020).

234. Aaseth, J., Shimshi, M., Gabrilove, J. L. & Birketvedt, G. S. Fluoride: A Toxic or Therapeutic Agent in the Treatment of Osteoporosis? *J. Trace Elem. Exp. Med.* **17**, 83–92 (2004).

235. Dogan, S., Günay, H., Leyhausen, G. & Geurtsen, W. Chemical-biological interactions of NaF with three different cell lines and the caries pathogen Streptococcus sobrinus. *Clin. Oral Investig.* **6**, 92–97 (2002).

236. Ten Gate, J. M. Review on fluoride, with special emphasis on calcium fluoride mechanisms in caries prevention. *Eur. J. Oral Sci.* **105**, 461–465 (1997).

237. Fawell, J. *et al. Flouride in Drinking-water*. (2001).

238. Satoh, R. *et al.* Changes in fluoride sensitivity during in vitro senescence of normal human oral cells. *Anticancer Res.* **25**, 2085–2090 (2005).

239. Beltrán-Aguilar, Eugenio D.; Barker, Laurie K. ; Canto, María Teresa; Dye, Bruce A.; Gooch, Barbara F.; Griffin, Susan O.; Hyman, Jeffrey Jaramillo, Freder; Kingman, Albert; Nowjack-Raymer, Ruth; Selwitz, Robert H.; Wu, T. Centers for Disease Control and Prevention. Surveillance for dental caries, dental sealants, tooth retention, edentulism, and enamel fluorosis — United States, 1988–1994 and 1999–2002. *Morb. Mortal. Wkly. Rep. Surveill. Summ.* **54**, 1–48 (2005).

240. Bidwell, J. Fluoride mouthrinses for preventing dental caries in children and adolescents. *Public Health Nurs.* **35**, 85–87 (2018).

241. Grynpas, M. D. Fluoride effects on bone crystals. *J. Bone Miner. Res.* **5**, 169–175 (1990).

242. Dorozhkin, S. V. Dissolution mechanism of calcium apatites in acids: A review of literature. *World J. Methodol.* **2**, 1 (2012).

243. Burke, F. M., Ray, N. J. & McConnell, R. J. Fluoride-containing restorative materials. *Int. Dent. J.* **56**, 33–43 (2006).

244. Marquis, R. E. Antimicrobial actions of fluoride for oral bacteria. *Can. J. Microbiol.* **41**, 955–964 (1995).

245. Marquis, R. E., Clock, S. A. & Mota-Meira, M. Fluoride and organic weak acids as modulators of microbial physiology. *FEMS Microbiol. Rev.* **26**, 493–510 (2003).

246. Chen, W., Cao, Q., Li, S., Li, H. & Zhang, W. Impact of daily bathing with chlorhexidine gluconate on ventilator associated pneumonia in intensive care units: A meta-analysis. *J. Thorac. Dis.* **7**, 746–753 (2015).

247. Mullany, L. C., Darmstadt, G. L. & Tielsch, J. M. Safety and impact of chlorhexidine antisepsis interventions for improving neonatal health in developing countries. *Pediatr. Infect. Dis. J.* **25**, 665–675 (2006).

248. Lawn, J. E., Cousens, S., Zupan, J. & Team, L. N. S. S. 4 million neonatal deaths: when? Where? Why? *Lancet* **365**, 891–900 (2005).

249. Vincent JL, Rello J, Marshall J, Silva E, Anzueto A, Martin CD, Moreno R, Lipman J, Gomersall C, Sakr Y, R. K. E. I. G. of I. International Study of the Prevalence and Outcomes of Infection in Intensive Care Units. *Jama* **302**, 2323–2329 (2009).

250. Jeansonne, M. J. & White, R. R. A comparison of 2.0% chlorhexidine gluconate and 5.25% sodium hypochlorite as antimicrobial endodontic irrigants. *J. Endod.* **20**, 276–278 (1994).

251. Salim, N., Moore, C., Silikas, N., Satterthwaite, J. & Rautemaa, R. Chlorhexidine is a highly effective topical broad-spectrum agent against Candida spp. *Int. J. Antimicrob. Agents* **41**, 65–69 (2013).

252. Herrera, D. Chlorhexidine mouthwash reduces plaque and gingivitis. *Evid. Based. Dent.* **14**, 17–18 (2013).

253. Farrugia, C. & Camilleri, J. Antimicrobial properties of conventional restorative filling materials and advances in antimicrobial properties of composite resins and glass ionomer cements - A literature review. *Dent. Mater.* **31**, e89–e99 (2015).

254. Zhang, J. F. *et al.* Antibacterial dental composites with chlorhexidine and mesoporous silica. *J. Dent. Res.* **93**, 1283–1289 (2014).

255. Swan, J. T. *et al.* Effect of chlorhexidine bathing every other day on prevention of hospital-acquired infections in the surgical ICU: a single-center, randomized controlled trial. *Crit. Care Med.* **44**, 1822–1832 (2016).

256. Biggar, R. J. Vaginal cleansing and the gold standard. *J. Women's Heal.* **14**, 531–533 (2005).

257. Bonesvoll, P. & Gjermo, P. A comparison between chlorhexidine and some quaternary ammonium compounds with regard to retention, salivary concentration and plaque-inhibiting effect in the human mouth after mouth rinses. *Arch. Oral Biol.* **23**, 289–294 (1978).

258. Lang, N. P. & Brecx, M. C. Chlorhexidine digluconate–an agent for chemical plaque control and prevention of gingival inflammation. *J. Periodontal Res.* **21**, 74–89 (1986).

259. Pluss, E. M., Engelberglr, P. R. & Ratehcschak, K. H. Effect of chlorhexidine on dental plaque formation under periodontal pack. *J. Clin. Periodontol.* **2**, 136–142 (1975).

260. Baehni, P. & Takeuchi, Y. Anti-plaque agents in the prevention of biofilm-associated oral diseases. *Oral Dis.* **9**, 23–29 (2003).

261. Kamolnarumeth, K. *et al.* Effect of mixed chlorhexidine and hydrogen peroxide mouthrinses on developing plaque and stain in gingivitis patients: a randomized clinical trial. *Clin. Oral Investig.* 1–8 (2020) doi:10.1007/s00784-020-03470-7.

262. Edmiston, C. E. *et al.* Reducing the risk of surgical site infections: Does chlorhexidine gluconate provide a risk reduction benefit? *Am. J. Infect. Control* **41**, S49–S55 (2013).

263. Pilloni, A. *et al.* A preliminary comparison of the effect of 0.3% versus 0.2% chlorhexidine mouth rinse on de novo plaque formation: A monocentre randomized double-blind crossover trial. *Int. J. Dent. Hyg.* **11**, 198–202 (2013).

264. Hiraishi, N., Yiu, C. K. Y., King, N. M. & Tay, F. R. Chlorhexidine release and antibacterial properties of chlorhexidine- incorporated polymethyl methacrylate-based resin cement. *J. Biomed. Mater. Res. - Part B Appl. Biomater.* **94**, 134–140 (2010).

265. Gjermo, P. Some aspects of drug dynamics as related to oral soft tissue. *J. Dent. Res.* **54**, 44–56 (1975).

266. Ravi, N. D., Balu, R. & Sampath Kumar, T. S. Strontium-Substituted Calcium Deficient Hydroxyapatite Nanoparticles: Synthesis, Characterization, and Antibacterial Properties. *J. Am. Ceram. Soc.* **95**, 2700–2708 (2012).

267. Badea, M., Olar, R., Iliş, M., Georgescu, R. & Călinescu, M. Synthesis, characterization, and thermal decomposition of new copper (II) complex compounds with chlorhexidine. *J. Therm. Anal. Calorim.* **111**, 1763–1770 (2013).

268. Tenovuo, J., Häkkinen, P., Paunio, P. & Emilson, C. G. Effects of chlorhexidine-fluoride gel treatments in mothers on the establishment of mutans streptococci in primary teeth and the development of dental caries in children. *Caries Res.* **26**, 275–280 (1992).

269. Burlet, N. & Reginster, J.-Y. Strontium Ranelate. *Clin. Orthop. Relat. Res.* **443**, 55–60 (2006).

270. Canalis, E., Hott, M., Deloffre, P., Tsouderos, Y. & Marie, P. J. The divalent strontium salt S12911 enhances bone cell replication and bone formation in vitro. *Bone* **18**, 517–523 (1996).

271. Braux, J. *et al.* A new insight into the dissociating effect of strontium on bone resorption and formation. *Acta Biomater.* **7**, 2593–2603 (2011).

272. Hoppe, A., Mouriño, V. & Boccaccini, A. R. Therapeutic inorganic ions in bioactive glasses to enhance bone formation and beyond. *Biomater. Sci.* **1**, 254–256 (2013).

273. Haja Hameed, A. S. *et al.* Impact of alkaline metal ions Mg2+, Ca2+, Sr2+ and Ba2+ on the structural, optical, thermal and antibacterial properties of ZnO nanoparticles prepared by the co-precipitation method. *J. Mater. Chem. B* **1**, 5950 (2013).

274. Lynch, R. J. M. Zinc in the mouth, its interactions with dental enamel and possible effects on caries; a review of the literature. *Int. Dent. J.* **61**, 46–54 (2011).

275. Fischer, E. R., Hansen, B. T., Nair, V., Hoyt, F. H. & Dorward, D. W. *Scanning electron microscopy*. *Current Protocols in Microbiology* (2012). doi:10.1002/9780471729259.mc02b02s25.

276. Van De Leemput, L. E. C. & Van Kempen, H. Scanning tunnelling microscopy. *Reports Prog. Phys.* **55**, 1165–1240 (1992).

277. Reimer, L. *Scanning electron microscopy: physics of image formation and microanalysis*. vol. 45 (Springer, 2013).

278. Britain, G. The general principles of scanning electron microscopy. *Philos. Trans. R. Soc. London. B, Biol. Sci.* **261**, 45–50 (1971).

279. Goldstein, J. I. *et al. Scanning electron microscopy and X-ray microanalysis*. (Springer, 2017).

280. Kotula, P. G., Keenan, M. R. & Michael, J. R. Automated analysis of SEM X-ray spectral images: A powerful new microanalysis tool. *Microsc. Microanal.* **9**, 1–17 (2003).

281. Parish, C. M. & Brewer, L. N. Multivariate statistics applications in phase analysis of STEM-EDS spectrum images. *Ultramicroscopy* **110**, 134–143 (2010).

282. Scherer, P. A. & Bochem, H.-P. Energy-Dispersive X-ray Microanalysis. *Ec. Polytech. Fed. Lausanne* **9**, 187–193 (1983).

283. Gaffney, J. S., Marley, N. A. & Jones, D. E. Fourier transform infrared (FTIR) spectroscopy. *Charact. Mater.* 1–33 (2002).

284. Chai, F., Wang, C., Wang, T., Ma, Z. & Su, Z. L-cysteine functionalized gold nanoparticles for the colorimetric detection of Hg2+ induced by ultraviolet light. *Nanotechnology* **21**, (2010).

285. Antonov, L., Gergov, G., Petrov, V., Kubista, M. & Nygren, J. UV-Vis spectroscopic and chemometric study on the aggregation of ionic dyes in water. *Talanta* **49**, 99–106 (1999).

286. Owen, T. Fundamentals of Modern UV-Visible Spectroscopy: A Primer. edit. *Agil. Technol. Ger.* (2000).

287. Perkampus, H.-H. *UV-VIS Spectroscopy and its Applications*. (Springer Science & Business Media, 2013).

288. Mark, H. *Principles and practice of spectroscopic calibration*. vol. 167 (John Wiley & Sons, 1991).

289. Bertolini, M. M. *et al.* Resins-based denture soft lining materials modified by chlorhexidine salt incorporation: An in vitro analysis of antifungal activity, drug release and hardness. *Dent. Mater.* **30**, 793–798 (2014).

290. Salim, N., Moore, C., Silikas, N., Satterthwaite, J. & Rautemaa, R. Candidacidal effect of fluconazole and chlorhexidine released from acrylic polymer. *J. Antimicrob. Chemother.* **68**, 587–592 (2013).

291. Hiraishi, N., Yiu, C. K. Y., King, N. M., Tay, F. R. & Pashley, D. H. Chlorhexidine release and water sorption characteristics of chlorhexidine-incorporated hydrophobic/hydrophilic resins. *Dent. Mater.* **24**, 1391–1399 (2008).

292. Anusavice, K. J., Zhang, N.-Z. & Shen, C. Controlled release of chlorhexidine from UDMA-TEGDMA resin. *J. Dent. Res.* **85**, 950–954 (2006).

293. Clark, B. J., Frost, T. & Russell, M. A. *UV Spectroscopy: Techniques, instrumentation and data handling*. vol. 4 (Springer Science & Business Media, 1993).

294. Kneipp, J., Lasch, P., Baldauf, E., Beekes, M. & Naumann, D. Detection of pathological molecular alterations in scrapie-infected hamster brain by Fourier transform infrared (FT-IR) spectroscopy. *Biochim. Biophys. Acta - Mol. Basis Dis.* **1501**, 189–199 (2000).

295. Imai, N. Multielement Analysis of Rocks with the Use of Geological Certified Reference Material by Inductively Coupled Plasma Mass Spectrometry. *Anal. Sci.* **6**, 389–395 (1990).

296. Nielsen, A. H. Inductively coupled plasma mass spectrometry analyzer. (2016).

297. Amadasi, A. *et al.* The survival of gunshot residues in cremated bone: An inductively coupled plasma optical emission spectrometry study. *J. Forensic Sci.* **58**, 964–966 (2013).

298. Wang, Z. *et al.* Model and experimental investigations of aluminum oxide slurry transportation and vaporization behavior for nebulization inductively coupled plasma optical emission spectrometry. *Talanta* **107**, 338–343 (2013).

299. Bao, N. *et al.* Novel synthesis of plasmonic Ag/AgCl@TiO2 continues fibers with enhanced broadband photocatalytic performance. *Catalysts* **7**, (2017).

300. Eigen, N. *et al.* Reversible hydrogen storage in NaF-Al composites. *J. Alloys Compd.* **477**, 76–80 (2009).

301. Kołodziejska, B., Stępień, N. & Kolmas, J. The influence of strontium on bone tissue metabolism and its application in osteoporosis treatment. *Int. J. Mol. Sci.* **22**, (2021).

302. Li, H. *et al.* The Role of Zinc in Bone Mesenchymal Stem Cell Differentiation. *Cell. Reprogram.* **24**, 80–94 (2022).

303. Sun, R., Zhang, J., Whiley, R. A., Sukhorukov, G. B. & Cattell, M. J. Synthesis, drug release, and antibacterial properties of novel dendritic chx-srcl2 and chx-zncl2 particles. *Pharmaceutics* **13**, 1–16 (2021).

304. Vignoletti, F., Nunez, J. & Sanz, M. Soft tissue wound healing at teeth, dental implants and the edentulous ridge when using barrier membranes, growth and differentiation factors and soft tissue substitutes. *J. Clin. Periodontol.* **41**, S23–S35 (2014).

305. Kamaruddin, N. M. *et al.* Cytotoxicity of pharma grade zno with higher surficial oxygen on l929 mouse cell. *Solid State Phenom.* **290 SSP**, 286–291 (2019).

306. Jeong, M. J. *et al.* Effect of rosmarinic acid on differentiation and mineralization of MC3T3-E1 osteoblastic cells on titanium surface. *Animal Cells Syst. (Seoul).* **25**, 46–55 (2021).

307. Strober, W. Monitoring cell growth. *Curr. Protoc. Immunol.* **21**, A-3A (1997).

308. Harrison, G., Shapiro, I. M. & Golub, E. E. The phosphatidylinositol-glycolipid anchor on alkaline phosphatase facilitates mineralization initiation in vitro. *J. Bone Miner. Res.* **10**, 568–573 (1995).

309. Sun, N. *et al.* Effect of advanced oxidation protein products on the proliferation and osteogenic differentiation of rat mesenchymal stem cells. *Int. J. Mol. Med.* **32**, 485–491 (2013).

310. Gjermo, P., Bonesvoll, P., Hjeljord, L. G. & Rölla, G. Influence of variation of pH of chlorhexidine mouth rinses on oral retention and plaque-inhibiting effect. *Caries Res.* **9**, 74–82 (1975).

311. Flötra, L. Different modes of chlorhexidine application and related local side effects. *J. Periodontal Res.* **8**, 41–44 (1973).

312. Mousquéegs, T., Listgarten, M. A. & Phillips, R. W. Effect of scaling and root planing on the composition of the human subgingival microbial flora. *J. Periodontal Res.* **15**, 144–151 (1980).

313. Caffesse, R. G., Sweeney, P. L. & Smith, B. A. Scaling and root planing with and without periodontal flap surgery. *J. Clin. Periodontol.* **13**, 205–210 (1986).

314. Cosyn, J. & Wyn, I. A systematic review on the effects of the chlorhexidine chip when used as an adjunct to scaling and root planing in the treatment of chronic periodontitis. *J. Periodontol.* **77**, 257–264 (2006).

315. Machtei, E. E. *et al.* Treatment of peri-implantitis using multiple applications of chlorhexidine chips: A double-blind, randomized multi-centre clinical trial. *J. Clin. Periodontol.* **39**, 1198–1205 (2012).

316. Ammann, P. Strontium ranelate: A physiological approach for an improved bone quality. *Bone* **38**, 15–18 (2006).

317. Lin, S. C. *et al.* Formulation and stability of an extemporaneous 0.02% chlorhexidine digluconate ophthalmic solution. *J. Formos. Med. Assoc.* **114**, 1162–1169 (2015).

318. Boaro, L. C. C. *et al.* Antibacterial resin-based composite containing chlorhexidine for dental applications. *Dent. Mater.* **35**, 909–918 (2019).

319. Rajabnejadkeleshteri, A., Kamyar, A., Khakbiz, M., Bakalani, Z. L. & Basiri, H. Synthesis and characterization of strontium fluor-hydroxyapatite nanoparticles for dental applications. *Microchem. J.* **153**, 104485 (2020).

320. Garley, A. *et al.* Adsorption and Substitution of Metal Ions on Hydroxyapatite as a Function of Crystal Facet and Electrolyte pH. *J. Phys. Chem. C* **123**, 16982–16993 (2019).

321. Murphy, S., Wren, A. W., Towler, M. R. & Boyd, D. The effect of ionic dissolution products of Ca-Sr-Na-Zn-Si bioactive glass on in vitro cytocompatibility. *J. Mater. Sci. Mater. Med.* **21**, 2827–2834 (2010).

322. Joop, H. & Sefcik, J. *The Handbook of Continuous Crystallization*. *The Handbook of Continuous Crystallization* (Royal Society of Chemistry, 2020). doi:10.1039/9781788013581.

323. Jiang, L. *et al.* Size-controllable synthesis of monodispersed SnO 2 nanoparticles and application in electrocatalysts. *J. Phys. Chem. B* **109**, 8774–8778 (2005).

324. Manzoor, U., Tuz Zahra, F., Rafique, S., Moin, M. T. & Mujahid, M. Effect of Synthesis Temperature, Nucleation Time, and Postsynthesis Heat Treatment of ZnO Nanoparticles and Its Sensing Properties. *J. Nanomater.* **2015**, 1–6 (2015).

325. Shedam, M. R. & Venkateswara Rao, A. Effect of temperature on nucleation and growth of cadmium oxalate single crystals in silica gels. *Mater. Chem. Phys.* **52**, 263–266 (1998).

326. Haas, I., Shanmugam, S. & Gedanken, A. Pulsed sonoelectrochemical synthesis of size-controlled copper nanoparticles stabilized by poly(N-vinylpyrrolidone). *J. Phys. Chem. B* **110**, 16947–16952 (2006).

327. De Geest, B. G. *et al.* Layer-by-layer coating of degradable microgels for pulsed drug delivery. *J. Control. Release* **116**, 159–169 (2006).

328. Zhang, J., Sun, R., Desouza-Edwards, A. O., Frueh, J. & Sukhorukov, G. B. Microchamber arrays made of biodegradable polymers for enzymatic release of small hydrophilic cargos. *Soft Matter* **16**, 2266–2275 (2020).

329. Woo, L. C. Y., Yuen, V. G., Thompson, K. H., McNeill, J. H. & Orvig, C. Vanadyl-biguanide complexes as potential synergistic insulin mimics. *J. Inorg. Biochem.* **76**, 251–257 (1999).

330. Holešová, S., Samlíková, M., Pazdziora, E. & Valášková, M. Antibacterial activity of organomontmorillonites and organovermiculites prepared using chlorhexidine diacetate. *Appl. Clay Sci.* **83**–**84**, 17–23 (2013).

331. Bharatam, P. V, Patel, D. S. & Iqbal, P. Pharmacophoric Features of Biguanide Derivatives: An Electronic and Structural Analysis. *J. Med. Chem.* **48**, 7615–7622 (2005).

332. Yogamalar, R., Srinivasan, R., Vinu, A., Ariga, K. & Bose, A. C. X-ray peak broadening analysis in ZnO nanoparticles. *Solid State Commun.* **149**, 1919–1923 (2009).

333. Mardziah, C. M. *et al.* Effect of zinc ions on the structural characteristics of hydroxyapatite bioceramics. *Ceram. Int.* **46**, 13945–13952 (2020).

334. Benson, P. E. *et al.* Fluorides, orthodontics and demineralization: A systematic review. *J. Orthod.* **32**, 102–114 (2005).

335. Benson, P. E., Pender, N. & Higham, S. M. Quantifying enamel demineralization from teeth with orthodontic brackets - A comparison of two methods. Part 2: Validity. *Eur. J. Orthod.* **25**, 159–165 (2003).

336. Geiger, A. M., Gorelick, L., Gwinnett, A. J. & Griswold, P. G. The effect of a fluoride program on white spot formation during orthodontic treatment. *Am. J. Orthod. Dentofac. Orthop.* **93**, 29–37 (1988).

337. Petersen, P. E. & Lennon, M. A. Effective use of fluorides for the prevention of dental caries in the 21st century: The WHO approach. *Community Dent. Oral Epidemiol.* **32**, 319–321 (2004).

338. Čech Barabaszová, K. *et al.* Antimicrobial PVDF nanofiber composites with the ZnO - vermiculite - chlorhexidine based nanoparticles and their tensile properties. *Polym. Test.* **103**, (2021).

339. Zeng, P., Zhang, G., Rao, A., Bowles, W. & Wiedmann, T. S. Concentration dependent aggregation properties of chlorhexidine salts. *Int. J. Pharm.* **367**, 73–78 (2009).

340. Sosso, G. C. *et al.* Crystal Nucleation in Liquids: Open Questions and Future Challenges in Molecular Dynamics Simulations. *Chem. Rev.* **116**, 7078–7116 (2016).

341. Horst, J. A. Silver Fluoride as a Treatment for Dental Caries. *Adv. Dent. Res.* **29**, 135–140 (2018).

342. Liu, B. Y., Mei, L., Chu, C. H. & Lo, E. C. M. Effect of Silver Fluoride in Preventing the Formation of Artificial Dentinal Caries Lesions in vitro. *Chin. J. Dent. Res.* **22**, 273–280 (2019).

343. Ullsfoss, B. N. *et al.* Effect of a combined chlorhexidine and NaF mouthrinse: an in vivo human caries model study. *Eur. J. Oral Sci.* **102**, 109–112 (1994).

344. Karuna, Y. M., Nayak, A. P., Pralhad, S., Mutalik, S. & Padya, B. S. Intraoral slow-releasing polymeric patches containing sodium fluoride and chlorhexidine: Development and evaluation. *J. Appl. Pharm. Sci.* **10**, 30–35 (2020).

345. Anderson, G. B., Bowden, J., Morrison, E. C. & Caffesse, R. G. Clinical effects of chlorhexidine mouthwashes on patients undergoing orthodontic treatment. *Am. J. Orthod. Dentofacial Orthop.* **111**, 606–612 (1997).

346. Shapur, N. K. *et al.* Second Prize: Sustained Release Varnish Containing Chlorhexidine for Prevention of Biofilm Formation on Urinary Catheter Surface: In Vitro Study. *J. Endourol.* **26**, 26–31 (2012).

347. Tomás, I. *et al.* Substantivity of a single chlorhexidine mouthwash on salivary flora: Influence of intrinsic and extrinsic factors. *J. Dent.* **38**, 541–546 (2010).

348. Steinberg, D. & Friedman, M. Development of sustained-release devices for modulation of dental plaque biofilm and treatment of oral infectious diseases. *Drug Dev. Res.* **50**, 555–565 (2000).

349. Priyadarshini, B. M. *et al.* PLGA nanoparticles as chlorhexidine-delivery carrier to resin-dentin adhesive interface. *Dent. Mater.* **33**, 830–846 (2017).

350. Hahn, C. Lo & Liewehr, F. R. Relationships between Caries Bacteria, Host Responses, and Clinical Signs and Symptoms of Pulpitis. *J. Endod.* **33**, 213–219 (2007).

351. Pitts, N. B. *et al.* Dental caries. *Nat. Rev. Dis. Prim.* **3**, 17030 (2017).

352. Bonesvoll, P., Lökken, P. & Rölla, G. Influence of concentration, time, temperature and pH on the retention of chlorhexidine in the human oral cavity after mouth rinses. *Arch. Oral Biol.* **19**, 1025–1029 (1974).

353. Zeng, P., Rao, A., Wiedmann, T. S. & Bowles, W. Solubility properties of chlorhexidine salts. *Drug Dev. Ind. Pharm.* **35**, 172–176 (2009).

354. Hiller, H. *et al. Ullmann's Encyclopedia of Industrial Chemistry*. *Ullmann's Encyclopedia of Industrial Chemistry* (Wiley, 2000). doi:10.1002/14356007.

355. Sampson, V., Kamona, N. & Sampson, A. Could there be a link between oral hygiene and the severity of SARS-CoV-2 infections? *Br. Dent. J.* **228**, 971–975 (2020).

356. Schumacher, M., Lode, A., Helth, A. & Gelinsky, M. Acta Biomaterialia A novel strontium (II) - modified calcium phosphate bone cement stimulates human-bone-marrow-derived mesenchymal stem cell proliferation and osteogenic differentiation in vitro. *Acta Biomater.* **9**, 9547–9557 (2013).

357. Pucher, J. J. & Daniel, C. The Effects of Chlorhexidine Digluconate on Human Fibroblasts In Vitro. *J. Periodontol.* **63**, 526–532 (1992).

358. Giannelli, M., Chellini, F., Margheri, M., Tonelli, P. & Tani, A. Effect of chlorhexidine digluconate on different cell types: A molecular and ultrastructural investigation. *Toxicol. Vitr.* **22**, 308–317 (2008).

359. Wyganowska-Swiatkowska, M. *et al.* Clinical implications of the growth-suppressive effects of chlorhexidine at low and high concentrations on human gingival fibroblasts and changes in morphology. *Int. J. Mol. Med.* **37**, 1594–1600 (2016).

360. Faria, G. *et al.* Evaluation of Chlorhexidine Toxicity Injected in the Paw of Mice and Added to Cultured L929 Fibroblasts. *J. Endod.* **33**, 715–722 (2007).

361. Tsourounakis, I., Palaiologou-Gallis, A. A., Stoute, D., Maney, P. & Lallier, T. E. Effect of Essential Oil and Chlorhexidine Mouthwashes on Gingival Fibroblast Survival and Migration. *J. Periodontol.* **84**, 1211–1220 (2013).

362. Faria, G., Cardoso, C. R. B., Larson, R. E., Silva, J. S. & Rossi, M. A. Chlorhexidine-induced apoptosis or necrosis in L929 fibroblasts: A role for endoplasmic reticulum stress. *Toxicol. Appl. Pharmacol.* **234**, 256–265 (2009).

363. Abdel-Sayed, P. *et al.* Implications of chlorhexidine use in burn units for wound healing. *Burns* **46**, 1150–1156 (2020).

364. Edmiston, C. E., Okoli, O., Graham, M. B., Sinski, S. & Seabrook, G. R. Evidence for Using Chlorhexidine Gluconate Preoperative Cleansing to Reduce the Risk of Surgical Site Infection. *AORN J.* **92**, 509–518 (2010).

365. Lee, A. *et al.* Blood concentrations of chlorhexidine in hospitalized children undergoing daily chlorhexidine bathing. *Infect. Control Hosp. Epidemiol.* **32**, 395–397 (2011).

366. Kornman, K. S. Controlled-release local delivery antimicrobials in periodontics: Prospects for the future. *J. Periodontol.* **64**, 782–791 (1993).

367. Southard, G. L. & Godowski, K. C. Subgingival controlled release of antimicrobial agents in the treatment of periodontal disease. *Int. J. Antimicrob. Agents* **9**, 239–253 (1998).

368. Clark, R. A. F. Wound repair. Overview and general considerations. *Mol. Cell. Biol. wound repair* (1994).

369. Goodson, J. M. Pharmacokinetic principles controlling efficacy of oral therapy. *J. Dent. Res.* **68**, 1625–1632 (1989).

370. Farkas, E., Zelko, R., Török, G., Rácz, I. & Marton, S. Influence of chlorhexidine species on the liquid crystalline structure of vehicle. *Int. J. Pharm.* **213**, 1–5 (2001).

371. Heard, D. D. & Ashworth, R. W. The colloidal properties of chlorhexidine and its interaction with some macromolecules. *J. Pharm. Pharmacol.* **20**, 505–512 (1968).

372. Brookes, Z. L. S., Bescos, R., Belfield, L. A., Ali, K. & Roberts, A. Current uses of chlorhexidine for management of oral disease: a narrative review. *J. Dent.* 103497 (2020).

373. Doolittle, A. K. *technology of solvents and plasticizers*. (Wiley, 1954).

374. Kim, S. W., Bae, Y. H. & Okano, T. Hydrogels: swelling, drug loading, and release. *Pharm. Res.* **9**, 283–290 (1992).

375. Leach, A. On the nature of interactions associated with aggregation phenomena in the mouth. 149–160 (1979).

376. Annunziata, O., Payne, A. & Wang, Y. Solubility of lysozyme in the presence of aqueous chloride salts: Common-ion effect and its role on solubility and crystal thermodynamics. *J. Am. Chem. Soc.* **130**, 13347–13352 (2008).

377. Lei, Y. G. *et al.* Growth process of homogeneously and heterogeneously nucleated spherulites as observed by atomic force microscopy. *Polymer (Guildf).* **44**, 4673–4679 (2003).

378. Agarwal, V. & Peters, B. Solute Precipitate Nucleation: A Review of Theory and Simulation Advances. *Adv. Chem. Phys.* **155**, 97–160 (2014).

379. Lee, D.-W., Hopke, P. K., Rasmussen, D. H., Wang, H.-C. & Mavliev, R. Comparison of Experimental and Theoretical Heterogeneous Nucleation on Ultrafine Carbon Particles. *J. Phys. Chem. B* **107**, 13813–13822 (2003).

380. Kelton, K. F. & Greer, A. L. Heterogeneous Nucleation. in *New York* vol. Volume 15 165–226 (2010).

Chapter 9. Publications

1. **Sun R**, Zhang J, Whiley RA, Sukhorukov GB, Cattell MJ. Synthesis, Drug Release, and Antibacterial Properties of Novel Dendritic CHX-$SrCl_2$ and CHX-$ZnCl_2$ Particles. Pharmaceutics. 2021 Nov;13(11):1799.
2. Zhang J, **Sun R**, DeSouza-Edwards AO, Frueh J, Sukhorukov GB. Microchamber arrays made of biodegradable polymers for enzymatic release of small hydrophilic cargos. Soft matter. 2020;16(9):2266-75.
3. **Sun R**, Gould, D. J, Sukhorukov GB, Cattell MJ. Novel chlorhexidine particles for antibacterial application in orthodontic treatment. Dental material. (in progress)
4. Khan Y[1], **Sun R**[1], Duminis.T, Shahid.S, Whiley. R, Sukhorukov GB, Cattell. MJ, Donos N. Synthesis of injectable gels containing novel chlorhexidine particles for use in Periodontology. Dental materials. (in progress)